QUANTITATIVE MODELS AND FRAMEWORK FOR EVALUATING COMMUNITY RESILIENCE ACCOUNTING FOR ITS INTERDEPENDENT SYSTEMS

A Dissertation

by

MOHAMMAD AGHABABAEI

Submitted to the Graduate and Professional School of
Texas A&M University
in partial fulfillment of the requirements for the degree of

DOCTOR OF PHILOSOPHY

Chair of Committee,	Maria Koliou
Committee Members,	John Michael Niedzwecki
	Walter Gillis Peacock
	Arash Noshadravan
Head of Department,	Zachary Grasley

May 2022

Major Subject: Civil Engineering

ABSTRACT

The main objective of this dissertation is to advance the models and methods utilized to model a community as a system of systems (SoS) accounting for their interdependencies. In line with this objective, this dissertation contributes to the disaster resilience literature by, first, developing a set of probabilistic models for the business recovery and residential building stock restoration, and second, proposing a modeling approach based on agent-based modeling (ABM) to develop a SoS model of a community. The model developed using the proposed approach can ultimately be used to assess the resilience of a community and make decisions to enhance its resilience. The next few paragraphs summarize the main steps in this dissertation to achieve the proposed objective.

First, a modeling approach based on Bayesian linear regression is proposed to develop predictive models for different attributes of business recovery, including cease operation days, revenue recovery, customer retention, and employee retention. This stepwise modeling approach includes three main steps namely data collection, development of model forms, and model selection. This modeling approach is applied on the data collected from Lumberton, NC, after the 2016 Hurricane Matthew and predictive models were developed for the business recovery in this community. The developed models can be further used in risk analysis studies on businesses in communities with similar characteristics as the Lumberton community. One of the notable findings of this study was the significance of housing recovery on customer retention of the businesses.

Second, an existing analytical framework to generate distributions for the recovery time of different building archetypes subject to tornado hazard was validated and calibrated in this dissertation. Because of the lack of empirical restoration time data, researchers developed an analytical framework based on the performance-based engineering (PBE) approach to develop time distributions for the restoration of different building archetypes damaged in tornado events. In this dissertation, an empirical dataset was developed using the observations from a longitudinal field study in the city of Joplin, MO, after the 2011 Joplin tornado. Time distributions developed using this dataset were compared to the outcomes from the analytical framework, and a number of modifications were proposed to calibrate the analytical framework to better represent the real-world conditions in the aftermath of tornado events.

Third, a modeling approach based on ABM is presented to develop a quantitative model of a community accounting for its interdependent systems. Agents in this context are discretized entities making their decisions based on a set of micro-behaviors, while their internal interactions form different systems in the community model and external interactions between different systems shape the complex behavior of the community. The application of this study is presented in the virtual community of Centerville by defining different agent types for its various entities, including the Electric Power Network (EPN), Water Supply Network (WSN), education system, businesses, healthcare system, households, and people. A broad review of the literature was conducted to define agents and their interactions, while verification and validation were performed to assure the credibility of the outcomes. The developed agent-based model

was first utilized to assess the resilience of the education system, which was one of the least-studied components in the quantitative disaster literature. Ultimately, resilience measures were proposed for the community as well as its systems. The proposed community resilience measure, which needs input from decision makers of a community in order to be calculated, is employed to assess the resilience of Centerville in its current condition, while the effect of different mitigation strategies on the resilience of the community was evaluated using the calculated resilience measures after implementing such decisions into the quantitative community model.

DEDICATION

To my wife, Shima

And to my parents

ACKNOWLEDGEMENTS

I would like to thank my committee chair, Dr. Maria Koliou, and my committee members, Dr. Niedzwecki, Dr. Peacock, and Dr. Noshadravan for their guidance and support throughout the course of this research.

Thanks also go to my friends and colleagues and the department faculty and staff for making my time at Texas A&M University a great experience.

Finally, thanks to my mother and father for their encouragement and to my wife for her patience and love.

CONTRIBUTORS AND FUNDING SOURCES

Contributors

This work was supervised by a dissertation committee consisting of my doctoral advisor, Dr. Maria Koliou, from the Department of Civil and Environmental Engineering, and doctoral committee members Dr. Niedzwecki and Dr. Noshadravan of the Department of Civil and Environmental Engineering and Dr. Peacock of the Department of Landscape Architecture and Urban Planning.

Business recovery dataset for Chapter 2 of this dissertation was provided by Dr. Maria Watson and Dr. Yu Xiao. The raw spatial data from the City of Joplin after the 2011 Joplin tornado in Chapter 3 was provided by Dr. Andrew Curtis and Dr. Jayakrishnan Ajayakumar. The analysis in Chapter 3 was supported by Dr. John W. van de Lindt, Dr. Stephanie Pilkington, Dr. Maria Watson, Dr. Steve Smith, and Dr. Hussam Mahmoud.

All other work conducted for the dissertation was completed by the student independently.

Funding Sources

My graduate study was supported by financial support provided by the Zachry Department of Civil and Environmental Engineering at Texas A&M University and O.H. Ammann Research fellowship by American Society of Civil Engineers (ASCE).

This work was also made possible in part by NIST-funded Center for Risk-Based Community Resilience Planning (Grant Numbers 70NANB15H044 and

70NANB20H008). The contents in this dissertation are solely the responsibility of the authors and do not necessarily represent the official views of the funding agencies.

TABLE OF CONTENTS

Page

LIST OF FIGURES

Page

LIST OF TABLES

Page

1. INTRODUCTION

1.1. Problem Statement

The frequency of natural disasters and their resulting impacts have been increasing during recent years. According to National Oceanic and Atmospheric Administration (NOAA, 2020), frequency of weather related disasters in the recent decade had a significant increase compared to the previous decades. This caused communities to suffer from not only the direct consequences of the disasters, but also long duration of recovery. Studies in the disaster literature indicated that longer period of recovery intensifies the severity of the post-disaster socio-economic impacts (Kates, Colten, Laska, & Leatherman, 2006; Smith & Sutter, 2013b). Due to these massive consequences, governments and decision makers started to make plans and take mitigation actions to enhance the resilience of the communities. Koliou et al. (2018) presented a comprehensive review of the definition of resilience and its evolution in the literature through time from its initial introduction by Holling (1973). According to this review, one of the most notable definitions of resilience was provided by the Presidential Policy Directives (PPD) in PPD-21: “the ability to prepare for and adapt to changing conditions and to withstand and recover rapidly from disruptions” (PPD 21, 2013).

A large number of studies in the literature have focused on the direct and indirect losses of disasters in the impacted communities and methods to mitigate those losses. A large portion of these studies utilized risk analysis tools to quantify such consequences considering the uncertainties inherent in these problems. One prominent risk analysis approach for these purposes was the one proposed by the Pacific Earthquake

Engineering Research (PEER) Center (Cornell & Krawinkler, 2000; Moehle & Deierlein, 2004), known as Performance Based Earthquake Engineering (PBEE). Various other studies utilized risk analysis approaches which were based on the structural reliability methods, such as First Order Reliability Method (FORM), Second Order Reliability Method (SORM), and Monte Carlo sampling. Mahsuli and Haukaas (2013a) presented three levels of refinement in conducting risk analysis using structural reliability methods, namely, region, building, and component. One of the advantages of a number of risk analysis methods based on the structural reliability, such as FORM, over PBEE methods is their potential in quantitative decision making. However, there are some drawbacks as well, such as the need to have continuously differentiable models.

Various studies employed different methods to account for the losses due to long period of recovery in addition to the direct physical losses. Aghababaei and Mahsuli (2018) conducted a seismic risk analysis for a building located in a high seismic area. In this study, in addition to the physical losses, long-term socio-economic consequences due to inoperability of the building were accounted for using downtime estimates computed using the existing probabilistic downtime models. Various studies in the disaster literature with a wide range of different focuses used the concept of downtime to implicitly account for the socio-economic losses due to loss of function of infrastructures during the recovery phase (Han, Li, & Van De Lindt, 2017; Kammouh, Cimellaro, & Mahin, 2018; Yazdi-Samadi & Mahsuli, 2018). Another approach in the literature to account for the recovery phase of a community and associating losses was using simulation methodologies, such as Markov Chain process (Nariman L Dehghani,

Fereshtehnejad, & Shafieezadeh, 2020; Lin & Wang, 2017a; Sutley & Hamideh, 2020) and agent-based modeling (Esmalian, Wang, & Mostafavi, 2021; Nasrazadani & Mahsuli, 2020; Sun, Stojadinovic, & Sansavini, 2019). Nasrazadani and Mahsuli (2020) employed agent-based modeling to simulate the response of a community subject to seismic events and its recovery afterwards. They also utilized risk analysis methods to accumulate the socio-economic costs due to various consequences in the face of a disaster and during its recovery.

Among studies on the disaster resilience, a large portion of them focused on a single component of a community, such as transportation networks (e.g. Adams et al. (2012)), Electrical Power Networks (EPN) (e.g. Ouyang and Dueñas-Osorio (2012)), or hospitals and healthcare facilities (e.g. Cimellaro et al. (2010a)), due to their significance in the case of a disaster occurrence. In these studies, the response and recovery of the component were modeled and studied to find its resistance against disaster loads, its vulnerabilities, the extent of disruption in the cases of disaster occurrence, and its recovery pace afterwards. Additionally, one main outcome of such studies was decision actions to improve the current state of the component to make it more resilient against future events. Although these studies are of great importance due to the critical role of such components in the aftermath, it is essential to account for the interdependencies of all main components of a community in studies of community resilience. One common approach in the literature for this purpose is modeling the recovery process as a Markov Chain of events from the disaster occurrence to the recovery of the infrastructure. Lin and Wang (2017a) proposed a continuous time Markov Chain for the recovery of

building portfolio accounting for its dependence on the utility access. This method is typically useful to model a few interconnected components interacting with one another during the recovery.

Despite the growing resilience literature, additional research is needed in order to develop appropriate quantitative frameworks capable of comprehensively simulating the response of a community in the aftermath accounting for its interdependencies. Such framework is essential to quantify the current resilience level of a community and enable decision-making to enhance its resilience. According to the review provided above, a comprehensive framework of a community to be used in quantitative disaster resilience studies should have the following features: (i) it should span from the event occurrence to the community recovery (or the control time in the aftermath), (ii) all major systems contributing to the restoration of the community should be included, and (iii) interactions between the systems should be sufficiently accounted for. In addition to a comprehensive framework, appropriate models are required to simulate the response of the components and their interactions in the community.

Having a comprehensive model of a community facilitates studying the resilience of the community as a whole as well as focusing on the resilience of each system within the community. A number of systems within communities are also less studied compared to other well-studied components (e.g., electric power network). One of the least studied components is the education system. Education system has interdependencies with various other players in a community, especially in the case of a disaster occurrence. After a disaster occurs, performance of the education system depends on schools,

lifelines (e.g., power and water), transportation, school district, households, and construction companies, among others. There exist a number of studies in the literature investigating the effect of major natural disasters on schools and students (RAND, 2006; The Boston Consulting Group, 2012). However, there is virtually no study in the quantitative disaster resilience literature to quantify the resilience of the education systems.

1.2. Theoretical Framework

A community can be described as a complex system of interconnected systems (e.g., households, businesses, lifelines, schools, etc.). Each system is composed of one or more interconnected components working together to achieve the performance goals of the system. The interactions between these systems, although may be simple, result in a complex behavior at the community level, and this is escalated when a disruption occurs in the community due to major natural disasters. In order to assess the resilience of a community and systems within it as well as enable decision making, a quantitative framework accounting for these components and their interactions is proposed in this study.

Figure 1 presents the theoretical framework of a community with its main components and simple schematic interactions between them. As Figure 1 shows, a number of models are required to characterize the behavior of each system within the community. These models simulate the direct impact of the disruptions on the system and its restoration afterwards. Additionally, for illustration purposes, this figure presents simple descriptions for interactions between each two interacting systems. Quantitative

models are required to implement these interactions and micro-behaviors into the model of the community. The proposed framework starts with a model characterizing the disaster and its extent throughout the community. Appropriate consequence models determine the extent of impact on each system within the community, and the defined interactions between different systems determine the cascading consequences on other interacting systems. Afterwards, each decentralized system initiates its recovery by allocating its resources based on their specific prioritization rules. Additionally, a number of systems may communicate with one another when making restoration decisions. The functionality state of each system through the simulation time has cascading effects on the rest of systems within the community, which are defined using the interaction rules between each two interacting systems as schematically presented in Figure 1. The proposed quantitative framework to model the community enables assessing the current resilience level of the community and each of its systems against its threatening hazards, identifying vulnerabilities in the community, and making quantitative decisions to enhance the resilience of the community.

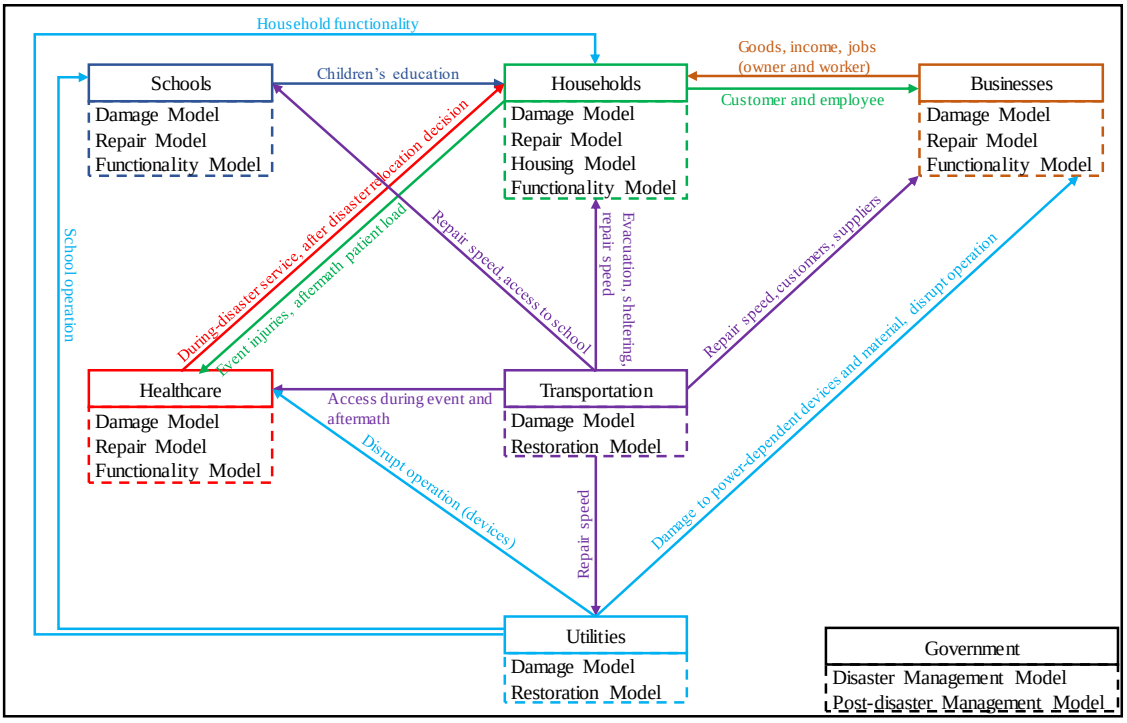

Figure 1: Main components and systems of the community, required models for each of them, and their potential interactions.

1.3. Research Methodology

This study is divided into two main parts: (i) developing models to be used in community resilience studies, and (ii) developing an approach to model a community with its interdependent components. Two sets of models were developed as the first part of this study for businesses and residential buildings, and one quantitative framework was proposed to model the community. In the next three subsections, each is discussed with more details.

1.3.1. Probabilistic modeling approach based on Bayesian linear regression to develop business recovery models

In this study, four recovery attributes were defined to comprehensively characterize the recovery of businesses in the aftermath, namely, cease operation days, revenue recovery, customer retention, and employee retention. A probabilistic modeling approach based on Bayesian linear regression was proposed to develop business recovery models for each of these four attributes. Bayesian linear regression is an appealing approach to develop predictive models accounting for the uncertainties inherent in the problem. Two key components in developing a predictive model using Bayesian linear regression are having a thorough knowledge of the problem and having relevant data. The former identifies the factors affecting the model outputs, and hence, determines the model variables and the model form. In this study, a thorough review of the literature on business recovery after natural disasters helped identifying the variables (and their combinations) influencing the recovery of the businesses in the aftermath of natural disasters. The latter component (i.e., relevant data) is necessary to calibrate the resulting models based on the real-world observations. This modeling approach provides the opportunity to utilize the observations collected after major disasters from a large number of reconnaissance studies to develop appropriate predictive models. Another desirable feature of Bayesian linear regression is its ability to characterize the uncertainties in prediction through random variables input to the model. This ability is bolded specifically in the application of this study due to the highly uncertain nature of recovery of businesses in the cumbersome after disasters.

A comprehensive review of the business recovery literature was conducted in this study, and seven sets of information were identified as critical to be collected to develop predictive business recovery models: (i) direct and indirect impacts (e.g., damage to the building and content, and utility disruption), (ii) recovery status measures, (iii) business characteristics (e.g., ownership structure, sector, business age, etc.), (iv) pre-disaster state of the business (e.g., total annual sales), (v) geographical characteristics of the business (e.g., its location relative to hazard sources, customer and supplier range of the business, etc.), (vi) loss containment measures (e.g., financial resources and the business has), and (vii) neighborhood characteristics and condition (e.g., damage incurred by nearby households, their socio-economic characteristics, etc.). This broad literature review paved the way to understand the problem, and hence, to develop candidate Bayesian linear regression model forms. A longitudinal dataset collected in the community of Lumberton, NC, after the 2016 Hurricane Matthew was employed to develop predictive models for each of the four business recovery attributes. This modeling approach also provided insights about factors affecting the recovery of the businesses using the empirical data used.

1.3.2. Repair-based functionality fragility models for residential building stock

Functionality fragility models are suitable probabilistic tools to predict the time needed to return a damaged building back to its pre-disaster functionality. An analytical framework was proposed by Koliou and van de Lindt (2020) to develop repair fragility models for a wide range of archetypes. This simulation-based approach starts from hazard models, structural analysis models, and damage models, and then characterizes

repair of each building at the component level, and finally aggregates all repair procedures into the building level. By conducting a Monte Carlo sampling, a desirable number of samples are obtained for the time it takes for the building to evolve from a lower functionality level to a higher/better level. Using these values, repair-based functionality fragility models are developed similar to the approach used in the damage fragility literature. Koliou and van de Lindt (2020) also utilized this framework to develop repair fragility models for the community of Joplin, MO, subject to tornado hazards.

The current study utilized an empirical longitudinal dataset of residential buildings collected after the 2011 Joplin tornado to calibrate the analytical framework developed by Koliou and van de Lindt (2020). For this purpose, first, empirical repair fragilities were developed for each residential building archetype using the collected dataset. Afterwards, these models were compared to the analytical fragilities developed for Joplin based on the method proposed by Koliou and van de Lindt (2020). A number of discrepancies were identified between the two sets of fragility models leading to modifications of the analytical framework to better represent the real-world observations collected after the 2011 Joplin tornado. These modifications included changes in the approach used by Koliou and van de Lindt (2020) to calculate the time to reach each level of functionality, and adopting more representative distributions for impeding factors delaying the repair procedure. Finally, using the collected data and the modified framework, repair-based functionality fragility models were developed for various

building archetypes, especially for residential buildings that can be further adopted for evaluating the recovery process of a typical US community subjected to tornado loads.

1.3.3. Agent-based modeling approach to develop quantitative model of communities

A simulation approach is adopted in this study to model the community with its interdependent components, which enables building the computational framework for quantifying the response of a community to disruptions. This will allow quantifying the direct effect of disruptions on the community, identifying the vulnerable components, assessing the response of each component of the community to the disruption, quantifying the resilience of the community, and finally evaluating the effectiveness of the mitigation strategies on the resilience of the community. A number of steps are needed to be taken in order to develop the simulation approach for the purpose of this study: (i) develop the conceptual framework of the community, (ii) select a community and collect sufficient information to effectively model its components and interdependencies, (iii) collect appropriate models from the disaster resilience literature to model components and their interactions, or develop appropriate ones if no suitable model exists in the literature, (iv) create the community model based on the conceptual framework and the collected information and models and validate its performance, and (v) conduct simulation experiments and explore findings/insights out of the results and validate them with the literature. Using the calibrated and validated community model, it is possible to answer the research questions, such as the resilience level of the community, its vulnerabilities, and the effect of mitigation actions on its resilience.

This study adopted agent-based modeling (ABM) to effectively and comprehensively simulate the response of the components of a community and their interplay in the restoration phase in the aftermath. In ABM, a system is modeled as a set of decentralized entities (called agents) functioning all together while specific relationships among them form and govern the complex system (Nasrazadani & Mahsuli, 2020; Rasoulkhani & Mostafavi, 2018). Agents are defined by specific rules and micro-behaviors which determine their objectives and priorities based on the environment characteristics through time. According to Ouyang (2014), agent-based approach is suitable for modeling the complex behavior of interconnected infrastructures since it works with bottom-up methods and aggregates the simple micro-level interactions of agents into complex macro-level responses of the system/community. ABM is able to account for the response of each agent to the environment changes through time, behavioral decision making within each agent, and reactions of the agent to the decisions made by other agents, which all make this approach desirable to model a community with its complexities. The computational framework in this study is implemented in an object-oriented modeling platform called AnyLogic.

Although application of ABM in the disaster resilience literature is a new topic, this simulation approach has been widely used in other research areas to study complex behaviors of infrastructure systems and the effect of different policies on the outcomes. In 1998, Sandia National Laboratory (SNL) (Basu, Pryor, & Quint, 1998) developed its first agent-based model of interdependent infrastructures of US economy called Aspen in order to simulate the response of the community to a number of financial policies. This model

contained various types of agents including households, banks, federal reserve, four types of firms, realtor, capital goods producer, and a financial market place agent. They modeled complex behavior of each agent and their interactions with one another by assuming multiple interaction rules. After using Monte Carlo sampling to account for the uncertainties in the problem, this study compared different policies using the results. SNL developed Aspen-EE agent-based model (Barton, Eidson, Schoenwald, Stamber, & Reinert, 2000) which was an extension of Aspen but more comprehensive and included power market as well. This model had various agents, including hazard agent (which simulated the power outage occurrences), household, industry, weather, and government agents among others. For each agent, multiple detailed simple rules were determined which defined agent's behavior and interactions. In another study, Rasoulkhani et al. (2020) utilized ABM to assess the resilience of the water supply infrastructures in coastal areas subject to the sea-level rise threats.

A few studies utilized ABM for the purpose of studying disaster resilience and recovery of communities. Eid and El-adaway (2017) presented a decision-making framework to model the affected communities using ABM. Their framework accounted for the needs of the impacted residents, their wealth recovery, social vulnerabilities, governmental aids, and various insurance plans available. Nejat and Damnjanovic (2012) employed ABM to model the dynamic interaction between homeowners and their neighbors and its effect on the homeowner's reconstruction decision in the recovery process. Nasrazadani & Mahsuli (2020) combined risk analysis methods and ABM to study disaster resilience of a community subject to seismic hazards. These few studies

paved the way to conduct quantitative disaster resilience assessment using ABM. However, much more efforts are needed to take the full advantage of the ABM potentials to comprehensively model a community and utilize it in decision making.

1.4. Research Overview and Contributions

Three research thrusts are defined in this study, each focusing on specific topics which are in line with the objectives of this study. This dissertation includes five chapters. The current chapter (Chapter 1) provided an introduction to the problem, the theoretical framework proposed in this study, and the research methodology adopted. The last chapter (Chapter 5) discusses the conclusions and future work. Thrusts A, B, and C of this study are presented in Chapters 2, 3, and 4. In the following, a brief overview of each chapter, and their contribution to the objectives of this study, and in overall, to the quantitative disaster literature is discussed.

1.4.1. Overview of Chapter 2

Chapter 2 presents Thrust A of this study, which describes the methodology proposed in this study to probabilistically model the recovery of businesses after natural disasters. A comprehensive review of the business recovery literature is presented in this chapter along with the modeling approach and its application on a longitudinal dataset collected in Lumberton, NC, after the 2016 Hurricane Matthew. The main contributions of this chapter are:

- A stepwise modeling approach is proposed which can be utilized to develop predictive business recovery models. This stepwise approach discusses the data

categories that are essential to be collected for this purpose, the model development methodology, and the method to select the appropriate model.

- An application of this approach is presented using the business recovery data collected from the community of Lumberton, NC, after the 2016 Hurricane Matthew. Although the developed models in this application may not be generalized to communities with significantly different characteristics, it is possible to update the models using Bayes theorem when new data merges.
- The developed business recovery models in this study can be used along with other probabilistic models for risk analysis studies. The outcomes of such studies would be evaluation of current condition of the businesses in the community and decision making to enhance their condition.
- This study indicated the significant interaction between the recovery of households and businesses. One of the significant predictors of the business customer retention was found to be the average damage incurred by housing units in the nearby areas around the business. The customer retention rate had opposite relationship with this predictor, meaning that the more impacted the residential neighborhood around the business, the less the business is able to retain its customers.

1.4.2. Overview of Chapter 3

Chapter 3 presents Thrust B of this study, which describes the method proposed in this study to modify an existing analytical approach to develop repair-based functionality fragilities. A number of functionality fragilities were developed using the modified

approach for various residential building archetypes. The main contributions of this chapter are:

- Before this study, there was no empirical recovery time distributions for buildings damaged due to tornado events. Researchers overcame this lack of empirical data by developing restoration time distributions for 19 building archetypes using an analytical framework which was based on the Performance Based Engineering (PBE) approach. However, this analytical framework was not validated using empirical data. In Chapter 3 of this dissertation, empirical restoration time distributions are developed using data collected through a longitudinal study after the 2011 Joplin tornado, while comparisons are made with the outcomes from the analytical framework, and finally, an updated version of the analytical framework is proposed by calibrating it to the empirical data.
- The updated analytical framework included the impeding factors which typically exist in the aftermath of major disasters in addition to the repair time of the buildings. Using the updated framework, it is possible to develop restoration time distributions for building archetypes in any community by knowing their specific characteristics.
- The empirical distributions developed in this chapter are applicable in quantitative studies as variables representing the restoration time of a building damaged in a tornado. These distributions are utilized in the quantitative model developed for the community of Centerville in Chapter 4 of this dissertation.

1.4.3. Overview of Chapter 4

Chapter 4 presents Thrust C, which itself is divided into two consecutive subchapters, named Thrust C-A and Thrust C-B. In Thrust C-A, the ABM approach to model a community with its interdependent components is presented. To better demonstrate the approach, it is presented along with its application to the virtual community of Centerville subject to tornado hazard. The proposed ABM approach in this subchapter is first utilized to study education system, which was one of the least studied components of the communities in quantitative disaster literature. In the next subchapter of Chapter 4, Thrust C-B is presented which is an extension to the community model developed in Thrust C-A to include additional community players after natural disasters. Resilience measures are proposed to quantify resilience of the community and its systems. The community resilience measure is computed for Centerville using its quantitative community model to assess its resilience. In addition, this model is used to evaluate various decision actions and their effect on the resilience of the community. The main contributions of this chapter are:

- This study contributed to the disaster resilience literature by developing a comprehensive modeling approach to model a community and its interdependent systems, which enables studying the short- and long-term resilience of the community subject to its threatening hazards. To this end, this study developed a simulation approach based on agent-based modeling (ABM), which is capable of modeling a system of systems (SoS) model with all their interdependencies.

- To model the systems within a community (e.g., lifelines, households, businesses, schools, etc.), a thorough understanding of their behavior in cases of disruption is required, which is attained in this study by a detailed review of the existing literature and past disasters. This understanding is used to develop decision rules, prioritization rules, and micro-behaviors which define an agent (e.g., one household, a component of electric power network, utility company, etc.) and interplay between agents in the restoration process. ABM is capable of implementing these micro-behaviors and rules effectively to simulate the responses of and interactions between different agents in the community.
- Resilience measures were proposed for the community and its individual systems. In addition, this study demonstrated the application of these measures to evaluate the resilience of the community and to compare different mitigation strategies. The outcomes can be utilized for decision making under uncertainties.
- The application of this study is presented for the community of Centerville subject to tornado hazard. Agent types are developed for Schools, households, Electric Power Network (EPN), Water Supply Network (WSN), construction companies, businesses, hospitals, and people. In addition, interactions between these agents are defined and implemented based on the broad review of the literature and past events. Various types of analysis are conducted on the developed community model, including Monte Carlo sampling analysis. The community model is capable of accounting for the uncertainties in its response and restoration to a tornado event.

2. THRUST A: QUANTIFYING POST-DISASTER BUSINESS RECOVERY THROUGH BAYESIAN METHODS [*]

Business recovery after a disaster plays an important role in the socioeconomic recovery of a community. This chapter focuses on the development of a probabilistic modeling approach for quantifying and predicting business recovery through Bayesian linear regression. The proposed modeling approach consists of three steps including data collection, development of model forms, and model selection through rigorous evaluation and elimination steps. Four attributes, namely business cease operation days, revenue recovery, customer retention, and employee retention, which describe the post-disaster recovery state of a business, are considered. One of the main contributions of this study is incorporating the interplay between household and businesses in a community in developing predictive business recovery models. Towards that direction, different methods to account for the effect of household recovery into the customer retention rate of a business are investigated and proposed. As an application, the proposed modeling approach is applied on the results of a longitudinal field study at the community of Lumberton, NC, which was heavily impacted by the 2016 Hurricane Matthew, focusing on business recovery. The predictive models proposed in this study may be further applicable in risk-based resilience assessment of communities following disastrous events.

---

[*]This is an **Author's Original Manuscript** of an article published by Taylor & Francis Group in **Structure and Infrastructure Engineering** available online at https://doi.org/10.1080/15732479.2020.1777569 (Mohammad Aghababaei, Koliou, Watson, & Xiao, 2020)

2.1. Introduction

The frequency of weather-related disasters and their resulting losses have been increasing significantly in recent years (Aghababaei, Koliou, & German Paal, 2018; NOAA, 2017) and communities suffer not only from the direct physical consequences of disasters, but also the long duration of recovery. It has been observed that the longer the restoration period lasts, the more severe the post-disaster consequences, such as socio-economic impacts, are for the community (Kates, Colten, Laska, & Leatherman, 2006; Smith & Sutter, 2013).

Business recovery after a disaster, which is the focus of this chapter, plays a significant role in the larger socioeconomic recovery of a community. Post-disaster recovery is not only the recovery of the physical infrastructure, but also the rebuilding of livelihoods, which requires all groups and members of the community—including businesses and households—to make decisions for the path of their recovery (Marshall & Schrank, 2014). Previous studies have shown that recovery of businesses and households throughout a community are correlated (Xiao & van Zandt, 2012) where household recovery affects the business recovery through the retention of customers and employees (Xiao, Wu, Finn & Chandrasekhar, 2018; Y. Zhang, Lindell, & Prater, 2004, 2009;). Furthermore, because households depend on businesses for employment, goods, and services, businesses need to be recovered for households to achieve their own recovery and sense of normalcy (Liu, Black, Lawrence, & Garrison, 2012). Therefore, recovery of the businesses after a disaster contributes significantly to a community's

recovery trajectory, and consequently understanding and predicting their recovery can help communities become more resilient to future disaster events.

A vast majority of empirical studies focusing on business recovery have utilized statistical modeling techniques, such as ordinary least squares (OLS) regression for the purpose of identifying various significant factors on business recovery and their relationships, but without focusing on the development of predictive models (e.g., Orhan (2016), Wasileski, Rodríguez, & Diaz (2011), Webb, Tierney, & Dahlhamer (2002), Xiao & Nilawar (2013), Xiao & Peacock (2014), and Y. Zhang et al. (2009)). The outcome of such studies is finding the most significant factors in the post-disaster recovery of businesses. These findings were considered in the current study to identify the most critical factors in business recovery and collect data accordingly, as discussed in detail in the next sections (Step 1: Data collection). The core objective of this study is to develop predictive probabilistic business recovery models that are applicable in risk-based resilience assessment studies, while this approach also reveals the significant factors in business recovery during the modeling procedure as discussed in this Chapter. Developed predictive business recovery models should be able to incorporate uncertainties inherent in such predictions. Towards that direction, a Bayesian linear regression methodology is proposed to quantify business recovery herein accounting for uncertainties related to the problem posed. One of the advantages of the developed models is being continuously differentiable which is the requirement of being employed in a number of risk analysis methods. Two examples of such methods are first order reliability method (FORM) and second order reliability method (SORM) which are two

computationally efficient risk analysis methods capable of handling uncertainties in complex problems (Der Kiureghian, 2005).

Recovery after a disaster cannot be simply characterized by a dichotomy of recovered or not recovered (Karatani & Hayashi, 2007) due to the multiscale nature of recovery. The current study considers and makes use of different quantitative dimensions of business recovery after a disaster to achieve a comprehensive snapshot of the status of businesses following natural disasters. The measures considered in this study are: (i) cease operation days, i.e., the duration after the disaster that the business was out of operation, (ii) revenue recovery, i.e., the change in the business revenue compared to its pre-disaster status, (iii) customer retention, i.e., the percent of customers compared to pre-disaster conditions, and (iv) employee retention, i.e., the change in the number of employees compared to pre-disaster.

The proposed modeling methodology is applied to the community of Lumberton, NC which was severely impacted by the 2016 Hurricane Matthew. A survey dataset of business recovery, collected during a field study performed by the NIST-funded Centre of Excellence on Risk-Based Community Resilience Planning about a year following Hurricane Matthew, is utilized for the purpose of model development herein (van de Lindt et al., 2018). Using this dataset, Bayesian linear regression was conducted to predict each of the aforementioned metrics of business recovery.

One of the innovations of this study is incorporating the interplay between household and business recovery trajectories. In a realistic model, the recovery state of the housing units throughout the community affects business recovery (Y. Zhang et al.,

2009), while household recovery, especially in terms of the reestablishment of livelihood and daily routines, might also be affected by business recovery (Xiao & van Zandt, 2012). To account for such interdependencies in the recovery trajectory quantification, this study focuses on addressing the effect of household recovery on businesses.

2.2. Background

Business recovery is complex due to the various spatial and transactive factors that affect business performance after a disastrous event. It is not simply a function of physical damage to the business itself, but also encompasses interruptions of various suppliers, households, and governmental inputs that may affect a business's ability to operate since these critical inputs may also originate from within the impact area (Xiao & Nilawar, 2013; Y. Zhang et al., 2009). Business recovery can be measured by various indicators. For example, Webb, Tierney, and Dahlhamer (2002) in their study of business recovery, considered four factors representing recovery, including present state of the business compared to just before the event, change in number of employees, change in number of customers, and change in profits.

Characteristics of the business itself that affect recovery include business age, sector, and ownership status of business premises (owned or rented). Older, established businesses are thought to be more stable as well as more likely to engage in preparedness actions which help them before and after an event (Dahlhamer & Tierney, 1996; Webb et al., 2002). In contrast, some studies suggest that businesses in a better financial condition prior to the disaster take longer to recoup their losses since they may have had

more to lose (G. R. Webb et al., 2002). The sector of the business is also important because it can capture information on the characteristics of the business's contents and inventory as well as how the demand for the business's goods or services might change after a disaster. Businesses' contents are not uniform across sectors and can be more or less perishable, heavy, and/or mobile (Gissing & Blong, 2004), which makes them to be affected differently subject to hazards. Moreover, different business offerings may become more or less desirable after a disaster (Alesch, Holly, Mittler, & Nagy, 2001). Orhan (2016) studied the most significant factors in the long-term recovery of the businesses after the 1999 earthquake in Adapazari, Turkey, and concluded that businesses in finance, insurance, real-state, and construction sectors tend to recovery faster, while the lowest recovery rate was observed for the trade sector. Lastly, whether a business owns or rents the building out of which it operates may have consequences for recovery. If the business owns the property then they are in full control of the property; however, businesses that rent do not have control of mitigation of the property before the disaster and the timeline of repairs after the disaster which might postpone the business recovery (Alesch et al., 2001). Businesses renting their premises are more vulnerable because they are more likely to face debt issues after a disaster since they will be required to pay rent even if they cannot recover their full revenue stream (W. Zhang, Lin, Wang, Nicholson, & Xue, 2018).

The management of the business is important to be considered as it relates to decision-making, adaptability, and flexibility in response to hazard events. Khan and Sayem (2013) found that institutional education reduces recovery time; more experience

may also indicate a higher likelihood of having experienced a disaster previously, which was also negatively correlated with recovery time (Asgary, Anjum, & Azimi, 2012). In addition, navigating insurance coverage and the claim process can be difficult after disaster (Brown, Seville, & Vargo, 2017), therefore having more experience may be helpful.

Insurance as its own factor helps replace damaged assets and allows a business more flexibility in its recovery (Alesch et al., 2001). A business' physical capital is vulnerable to the hazard, and higher amount of non-liquid assets will make a business more exposed to damage (Y. Zhang et al., 2009). This is not limited to the structure out of which the business operates, but also the contents and machinery within the building. However, even if the business itself is not impacted, external inputs crucial to the operation of the business, especially utilities (e.g., electricity and telecommunications), might have been damaged or disrupted. Literature has suggested that the loss of these utilities, and the resulting temporary closure of the business, may be just as—if not more—disruptive to business functionality as the physical damage (Tierney & Nigg, 1995). Other input-related disruptions include accessibility and transportation issues, which limit the flow of products, labor and customers.

In order to develop predictive recovery models that consider all aforementioned factors and are capable of incorporating the high uncertainty inherent in their nature, a Bayesian linear regression modeling approach is proposed in this study. Bayesian linear regression (which is based on the Bayesian inference) has been well represented in the literature (e.g., Box & Tiao, 1992) and is selected for this study among the prediction

methods available in the literature for a number of reasons. First, this modeling approach is based on the mechanics of the problem (here the business characteristics and the condition during the aftermath) as well as the available data (Aghababaei, 2017; Aghababaei & Mahsuli, 2019). Particularly for this study, the literature on the most significant factors affecting the business recovery determines the model form and its variables. Additionally, various datasets available from multiple reconnaissance and/or longitudinal studies (existing or future ones) can be employed to calibrate the developed recovery models. Bayesian linear regression is a powerful tool for prediction purposes to characterize the uncertainties by means of variables input to the model. The probability distribution of these variables is updated as new data merges through Bayesian updating. A detailed description on how those advantages of using Bayesian linear regression are accomplished in the predictive business recovery models is provided later in this chapter. Gardoni, Der Kiureghian, and Mosalam (2002) initiated the use of Bayesian linear regression in the structural engineering field with application on earthquake hazard, as they utilized it to predict the capacity of reinforced concrete columns using experimental data. The Bayesian approach was later utilized by other researchers on a variety of applications including the development of fragility functions or for prediction purposes, such as the seismic demand in different structural members, the material properties, and the disaster direct and indirect impacts (Bazli, Ashra, Jafari, Zhao, & Gholipour, 2019; Khaneghahi, Alembagheri, & Soltani, 2019; Li, Spencer Jr, & Elnashai, 2012; Mishra, Vanli, Alduse, & Jung, 2017; Najafabadi, Khaneghahi, Amiri, Estekanchi, & Ozbakkaloglu, 2019; Tamhidi et al., 2021). More recently, Aghababaei and Mahsuli

(2019) proposed a stepwise approach to apply Bayesian linear regression to the real-world data in order to predict the damage incurred by building components, based on the component demand (e.g., inter-story drift ratio) and component characteristics.

There is a strong interaction between the recovery of households and businesses in a community after a disaster. Thus, business recovery has a crucial role in community recovery, and hence, the community resilience. Koliou et al. (2018) recently performed a broad literature review on the research related to community resilience focusing on identifying the challenges and needs to be addressed for risk-informed decision-making of communities. One aspect of the work by Koliou et al. (2018) focused on presenting the evolution of the meaning of the term "resilience" since its first introduction in 1973 (Holling, 1973), and stated that the prevalent parts among all definitions presented since then are: (i) reducing consequences, (ii) accelerating the recovery process, and (iii) reducing vulnerability against disasters. Risk-informed decision-making is a reliable tool for enhancing community resilience with focus on these three aspects. In the past decades, a large number of studies (Aghababaei & Mahsuli, 2018; Cornell & Krawinkler, 2000; Ganji, Alembagheri, & Khaneghahi, 2019; Koliou, van de Lindt, & Filiatrault, 2016; Mahsuli & Haukaas, 2013; Moehle & Deierlein, 2004) have focused on risk-based simulations accounting for uncertainties with the ultimate objective being to comprehend the state of the infrastructure systems following a disastrous hazard as well as reducing the disaster consequences through proposed solutions. Furthermore, various studies utilized risk-based decision-making for enhancing resilience following a disaster. For instance, Lounis and McAllister (2016) proposed a risk-informed framework for

infrastructure performance which considers sustainability and resilience, with an example application on highway bridges resilient design by means of the conventional damage states and their associated loss and downtime estimates. In that same direction, the current study introduces a modeling methodology based on Bayesian linear regression models which are applicable in risk-based resilience analysis. As shown in Figure 2, a generic framework for risk-based resilience analysis requires occurrence models to generate random events based on the hazards threatening the community, hazard intensity models to generate random intensities for the occurred hazard, response models to estimate the structural performance of all infrastructure systems within a community during the hazard occurrence, direct impact models to predict the physical damage incurred by the infrastructure systems, indirect impact models to predict other adverse impacts on the community in addition to the physical impacts (such as unemployment, economy failure, business interruption, household displacement etc.), and recovery models to simulate the recovery trajectory of the community and its systems (social, economic) during the aftermath. The predictive recovery models proposed in the current study may be applicable in such a generic framework to model the recovery of businesses. By employing a risk analysis method along with the sequence of models presented in Figure 2, it is possible to predict the consequences as well as recovery measures, and give recommendations towards making a community more robust to future events, while decreasing the consequences and recovery time which all constitute the tripartite view of resilience.

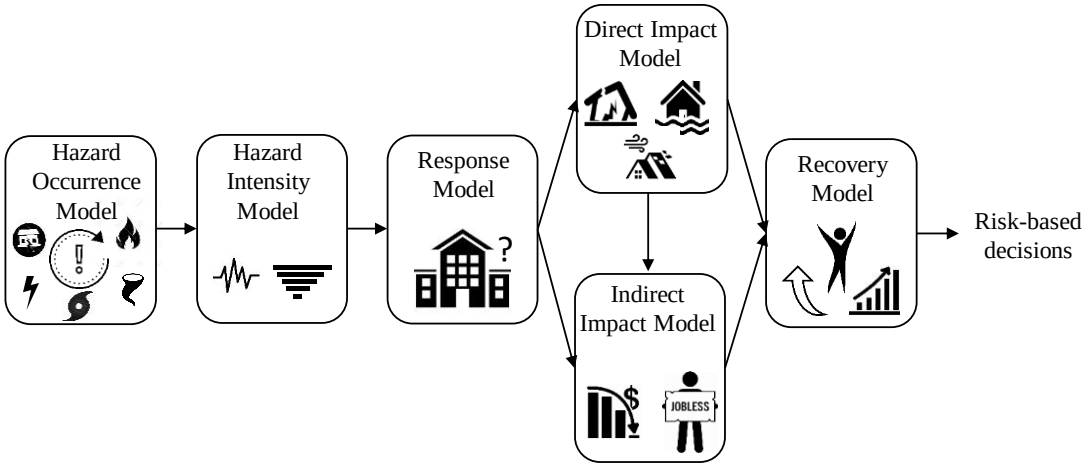

Figure 2: Representation of a generic framework for risk-based resilience analysis.

2.3. Modeling Approach

In this section, the steps to model a recovery measure/attribute are explained in detail including steps on data collection, development of candidate model forms as well as the model selection process. A schematic representation of the proposed approach to model recovery measures is provided in Figure 3. In the first step, an appropriate dataset to calibrate the model is collected, while a set of initial candidate model forms containing the most important predictors of the measure of interest—named initial candidate model form basket—are developed in the second step. In part one and two of the third step, each initial candidate model form transforms to a new model form, herein called the "*upgraded*" candidate model form, after accounting for model diagnostics and elimination of inconclusive terms. Finally, the most desirable model from the upgraded candidate model form basket is selected and high correlation between model parameters is eliminated in part three of step three. Each step is discussed in detail in the following sections of this chapter.

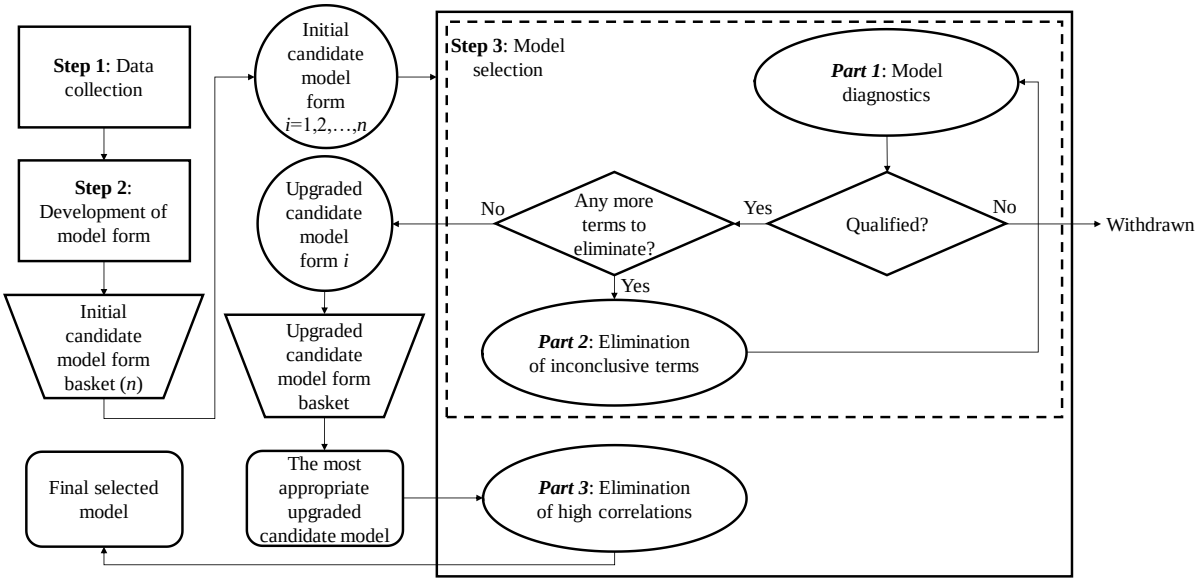

Figure 3: Schematic overview of the proposed methodology to develop predictive business recovery models.

2.3.1. Step 1: Data collection

Real-world data are commonly used for modeling and calibration purposes in order to generate realistic predictive business recovery models. Therefore, survey information from field studies following natural disasters focusing on the most important factors affecting business recovery are valuable resources. Such information can be collected by directly interviewing business managers and business owners as well as conducting paper-based, email-based, and/or phone-based surveys.

Based on these studies (e.g., Corey & Deitch (2011), Dahlhamer & Tierney (1998), Marshall & Schrank (2014), Runyan (2006), Wasileski, Rodríguez, & Diaz (2011), Webb et al. (2002), Xiao & van Zandt (2012), and Zhang Y. et al. (2004)), seven sets of information are identified as critical to be collected for modeling business recovery: (i) *Direct and indirect impacts* accounting for the extent of physical damage

the business incurred, including building damage, machinery damage, content damage, and utility disruption, (ii) *Recovery status measures* including cease operation days, customer retention, employee retention, and revenue recovery, (iii) *Business characteristics* including ownership structure (e.g., single owner, partnership, and franchise), sector (e.g., manufacturing, construction, and retail), business age, renter or owner status, as well as manager age, education, and race, (iv) *Business pre-disaster state* including pre-disaster profitability level of the business, total annual sales range of the business, and pre-disaster number of employees, (v) *Geographical characteristics of the business* referring to whether or not the business is located in an inundation area, close to an active fault, coastline etc., whether or not the business is location-dependent, as well as the customer and supplier range of the business, (vi) *Loss containment measures* accounting for different types of insurance policies the business have (all available financial resources and aids the business has, and preparedness pre-disaster), and (vii) *Neighborhood characteristics and condition aftermath* referring to the damage incurred by households nearby accounting for the amount of vacant households in near proximity, the amount of households nearby that are rental, as well as other socio-economic household characteristics such as income, race, etc.

2.3.2. Step 2: Development of model forms

After developing the necessary datasets, appropriate candidate model forms are developed to predict the recovery measures using Bayesian linear regression. The general form of the Bayesian linear regression per Box & Tiao (1992) is as follows:

$$y = \boldsymbol{\Theta} \cdot \mathbf{h}\left(\mathbf{x}\right) + \varepsilon \quad (1)$$

where y is model dependent variable (i.e. regressand), $\boldsymbol{\Theta}=\{\theta_1, \theta_2, \ldots, \theta_n\}$ is the vector of model parameters, $\mathbf{h}(\mathbf{x})=\{h_1(\mathbf{x}), h_2(\mathbf{x}), \ldots, h_n(\mathbf{x})\}$ where h_i, $1\leq i\leq n$, is i^{th} explanatory function (i.e. regressor), n is the number of explanatory functions, $\mathbf{x}$ is the vector of independent variables (also called explanatory variables), and ε is the model error assumed as a normal random variable with mean zero and standard deviation σ.

The key point in developing appropriate business recovery models is the rational selection of explanatory functions. Each explanatory function, $h_i(\mathbf{x})$, consists of one or more explanatory variables which are considered important in predicting the recovery measure of interest. Furthermore, explanatory variables should be combined in a way that results in a meaningful/realistic explanatory function. For example, combining explanatory variables representing the building damage, δ_b, and manager's age, $n_{m,age}$, in an explanatory function is not a rational combination for a proper predictor of the business recovery. On the other hand, combining certain explanatory variables might result in a more meaningful explanatory function and better prediction. For example, a model containing one explanatory function summing all utility disruptions (e.g., electricity, gas, etc.) may result in a meaningful model and provide accurate and realistic predictions. This is mainly attributed to the fact that restoration of all utilities is needed for a business to return to normal operations, and summation of all utility disruptions in a single explanatory is an effective way to take this fact into account.

Different transformations, such as logarithmic and exponential, may be applied to the explanatory functions ($h_i(\mathbf{x})$) in the right-hand side of Equation (1). These

transformations control the range and trend of the explanatory function to be conclusive and associated with a higher degree of certainty. For instance, in the cases that the value of an explanatory function changes significantly through the dataset, it is more challenging to capture the effect of the explanatory function in the modeling, whereas using logarithmic or similar functions narrows down the range and helps to better identify the impact of the value of the explanatory function in the predictive models. Additionally, in order to control the range of the output, it is necessary to introduce the link functions (F(.)) in the predictive models as shown in the following equation.

$$\mathrm{F}\left(y\right) = \boldsymbol{\Theta} \cdot \mathbf{h}\left(\mathbf{x}\right) + \varepsilon \tag{2}$$

A wide variety of link functions (F(.)) may be used in predictive models depending on the requirements and needs of the respective models. For example, in order to restrict the output between 0 and 1, various functions including probit function ($\Phi^{-1}(y)$), log-log function ($-\ln(-\ln(y))$), complementary log-log function ($-\ln(-\ln(1-y))$), and logit function ($\ln(y/(1-y))$) may be considered. In the cases that the output should be positive and there is no associated upper limit, the log function ($\ln(y)$) and square root function ($y^{1/2}$) may be incorporated in the model form. Different combinations of link functions (on the left-hand side of Equation (2)) as well as different transformation functions (on the right-hand side of Equation (2)) will lead to a set of candidate model forms, called the "initial candidate model form basket" in Figure 3, amongst which the best one will be selected.

2.3.3. Step 3: Model selection

In this section, the process of selecting the most appropriate predictive model among the set of developed candidate model forms is discussed. The procedure starts with performing two iterative parts including model diagnostics (part 1) and elimination of inconclusive terms (part 2), as presented in a dashed box in Figure 3. After conducting Bayesian linear regression, each candidate from the basket of the initial model forms goes through this iterative process in order to be evaluated through part 1 and to eliminate the inconclusive terms through part 2, which finally results in the upgraded candidate model form. As shown in Figure 3, if the candidate is not qualified based on the outcome of part 1 of this methodology, the candidate is removed from the basket, while if it is qualified, it goes through part 2 until no inconclusive terms are left in the model form, and therefore, the upgraded model form is added to the upgraded candidate model form basket. Part 2 starts with the elimination of the first most inconclusive term from the model form, and afterwards, the new model goes through diagnostics again to determine whether or not this elimination is accepted. As presented in Figure 3, if the new model is qualified, it goes to part 2 again if there are more inconclusive terms to be eliminated. If the new model is not qualified, it either goes back to part 2 to eliminate the next inconclusive term or is removed from the basket. The reasons for a model not to be qualified include unsuitable diagnostics, large number of inconclusive terms, or inconsistency in the model interpretation with the literature and expert judgement. Ultimately, after conducting the aforementioned two steps for all the candidate model forms, the "*best*"—or more representative model amongst the upgraded candidate model

forms basket—is selected based on the diagnostics of each model, the posterior statistics of the model parameters as well as the desirability of the remaining regressors and the findings out of them (according to the sign and value of their model parameters). The final selected model then progresses to part 3, which involves the elimination of high correlation between model parameters.

There are a number of measures widely used (Aghababaei & Mahsuli, 2019; Box & Tiao, 1992; Gardoni et al., 2002) to qualify a candidate model form in Bayesian linear regression as the ***first part (diagnostics)*** of the model selection process (step three of Figure 3). To evaluate the candidate model form, various diagnostic tool/quantities are considered including the model scatter prediction, coefficient of determination (R^2) and standard deviation of model error (σ), quantile-quantile (Q-Q) plots, as well as plots of residuals versus regressors and regressand values. The most imperative examination of the mean candidate model form is the observation versus model prediction scatter. A good fit appears when the scatter is aligned along the 45° line. To prevent the over-fit, it is recommended to divide the data into training and testing sets, e.g., with a ratio of 85 to 15. If the developed model predicts accurately the testing data (i.e., the scatter of testing data and their corresponding prediction are aligned along 45° line) no over-fit is observed in the predictive model. The coefficient of determination and standard deviation of model error are used to quantitatively evaluate the accuracy of the model where higher values of R^2 and lower values of σ represent a more representative and accurate model. The quantile-quantile (Q-Q) plot demonstrates whether or not there is non-normality of residuals by plotting the residuals (referring to the difference between

observed and predicted values, versus the normal theoretical quantiles). If the Q-Q plot aligns along the 45° line, the assumption of the normal distribution in the modeling process is validated. The heteroscedasticity and autocorrelation of residuals are examined through the plots of residuals versus regressors and regressand values. Heteroscedasticity appears if the points are unequally distributed along the x-axes (i.e., regressors or regressand values) while autocorrelation appears if there is a visible pattern in the plot.

When eliminating inconclusive terms (part 2), the measure used to find inconclusive terms is the posterior Coefficient of Variation (CoV) of the model parameters. The explanatory function associated with the largest CoV is the least informative among all explanatory functions in the model form (Gardoni et al., 2002) and therefore, it should be eliminated. After eliminating the explanatory function from the model form, the Bayesian linear regression is conducted again to calculate the posterior statistics of the model, including model parameters as well as model error. Sudden jump in the CoV of the standard deviation of the model error indicates that the eliminated term was not inconclusive and is essential in the model prediction, and thus, it should not be eliminated. Elimination of the inconclusive terms continues until no model parameter associated with a large CoV is included in the model.

Finally, after selecting the most desirable model among the set of upgraded candidate model form basket, high correlation between model parameters ($\rho_{\theta i \theta j}$) should be eliminated by evaluating the largest absolute value between model parameters θ_i and θ_j ($\max_{i \neq j} |\rho_{\theta i \theta j}|$). A high correlation (e.g., $|\rho_{\theta i \theta j}|>0.7$) indicates close relation between θ_i

and θ_j, and thus, those parameters should be combined (Gardoni et al., 2002). By so doing, not only is the high correlation eliminated, but also the model uncertainty is decreased by avoiding repeating uncertainties in two separate model parameters. If the correlation is low (e.g., $|\rho_{\theta i \theta j}|<0.5$), it indicates that there is no close relation between θ_i and θ_j. For high correlations, per Gardoni et al. (2002), θ_i ($\theta_i \geq \theta_j$) can be replaced by θ_i as described in Equation (3).

$$\theta_i = \mu_i + \rho_{ij} \frac{\sigma_i}{\sigma_j}\left(\theta_j - \mu_j\right) \tag{3}$$

where μ_i and σ_i are the mean and standard deviation of θ_i. Elimination of high correlation between model parameters is performed one by one until no correlation above 0.5 is observed (i.e., $|\rho_{\theta i \theta j}|<0.5$ for all $i \neq j$). It should be noted that if the quality of the model through diagnostics of the new model after elimination of high correlation between each two model parameters (e.g., θ_i and θ_j) drops significantly or if the posterior statistics show a sudden increase in the model error or the CoV of model parameters, the elimination is declined. In addition, in some cases, since the observation values for the explanatory function associated with one of the model parameters, for instance $h_i(\mathbf{x})$, is large, after elimination of high correlations using Equation (3), one large value at the left-hand side of the Equation (2), $F\left(y\right)-\left(\mu_i-\rho_{\theta_i\theta_j}\cdot\sigma_i\cdot\mu_i/\sigma_j\right)\cdot h_i\left(\mathbf{x}\right)$, and one large value at the right-hand side of the Equation (2), $\theta_j\cdot\left(h_j\left(\mathbf{x}\right)+\left(\rho_{\theta_i\theta_j}\cdot\sigma_i/\sigma_j\right)\cdot h_i\left(\mathbf{x}\right)\right)$, appear. By conducting the Bayesian linear regression between the left-hand side of the Equation (2) and the explanatory functions in the right-hand side, the effect of other

terms of the model form becomes negligible compared to the large values of the new explanatory function, $\left(h_j(\mathbf{x})+\left(\rho_{\theta_i\theta_j}\cdot\sigma_i/\sigma_j\right)\cdot h_i(\mathbf{x})\right)$, which is not correct and desirable. Hence, in these cases, elimination of high correlation should be avoided.

2.4. Business recovery measures/attributes

Four attributes and their corresponding measures are proposed and explained in this section to comprehensively capture the recovery of the businesses after a disaster. Figure 4 presents these four recovery attributes and their interactions as well as their prospective explanatory variables to develop predictive models. The description of each explanatory variable is provided in Table 1. Each model is shown by a rectangle, arrows entering vertically to the model are the prospective explanatory variables, and arrows entering horizontally in the left-side of the models are inputs from upstream models.

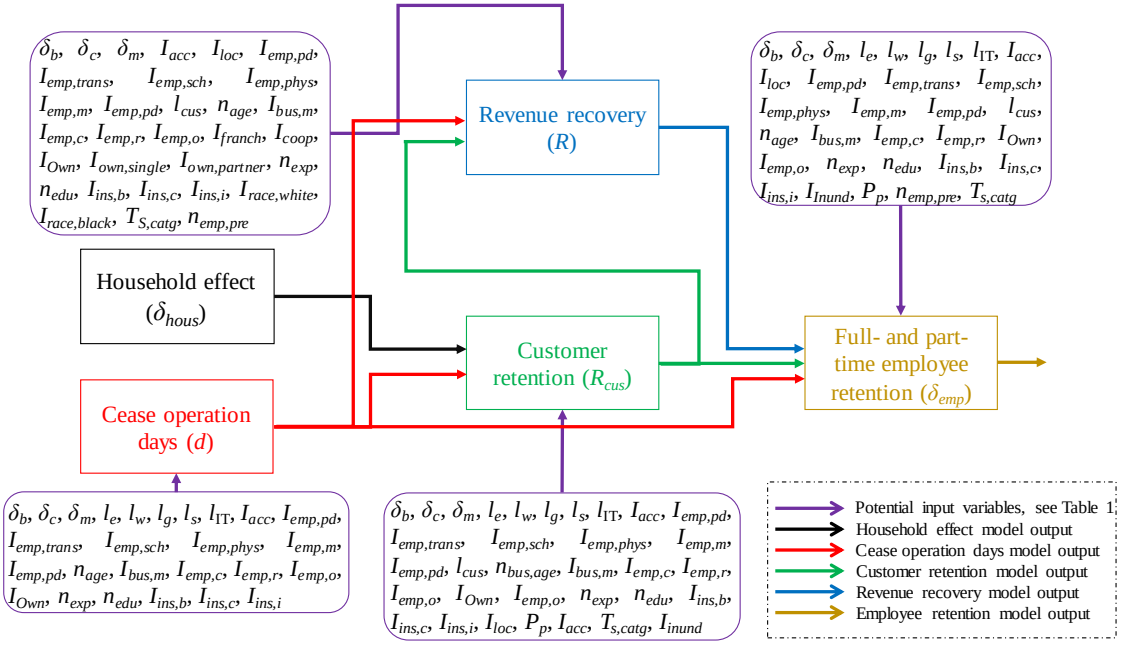

Figure 4: Schematic representation of the interaction between the recovery attributes considered in this study and their prospective inputs.

Table 1: Description of the explanatory variables in Figure 4.

Description of variable	Symbol
Revenue change (from 1 to 5 as increases)	R
Customer percentage loss (%)	l_{cus}
Number of employees the business had at the time of the survey	$n_{emp,now}$
Cease operation (days)	d
Profitability before the disaster (from 1 to 5 as decreases)	P_p
Damage to the building (from 1 to 5 as increases from none to complete)	δ_b
Damage to the content (from 1 to 5 as increases from none to complete)	δ_c
Damage to the machinery (from 1 to 5 as increases from none to complete)	δ_m
Electricity loss (days)	l_e
Water loss (days)	l_w
Gas loss (days)	l_g
Sewer loss (days)	l_s
Internet loss (days)	l_{IT}
Accessibility problems (1 if yes, 0 otherwise)	I_{acc}
Employee transportation problem (1 if yes, 0 otherwise)	$I_{emp,trans}$
Employee personal damage (1 if yes, 0 otherwise)	$I_{emp,pd}$
Employee children/school problem (1 if yes, 0 otherwise)	$I_{emp,sch}$
Employee physical health problem (1 if yes, 0 otherwise)	$I_{emp,phys}$
Employee mental problems (1 if yes, 0 otherwise)	$I_{emp,m}$
Physical location dependency (1 if yes, 0 otherwise)	I_{loc}
Single owner or not (1 if yes, 0 otherwise)	$I_{own,single}$
Partnership or not (1 if yes, 0 otherwise)	$I_{own,partner}$
Corporation or franchise or not (1 if yes, 0 otherwise)	I_{franch}
Cooperative or not (1 if yes, 0 otherwise)	I_{coop}
Is the line of business construction? (1 if yes, 0 otherwise)	$I_{bus,c}$
Is the line of business manufacturing? (1 if yes, 0 otherwise)	$I_{bus,m}$
Is the line of business retail? (1 if yes, 0 otherwise)	$I_{bus,r}$
Is the line of business other than these three? (1 if yes, 0 otherwise)	$I_{bus,o}$
Owned or rent (1 if owned, 0 otherwise)	I_{Own}
Had building insurance? (1 if yes, 0 otherwise)	$I_{ins,b}$
Had content flood insurance? (1 if yes, 0 otherwise)	$I_{ins,c}$
Had interruption flood insurance? (1 if yes, 0 otherwise)	$I_{ins,i}$
Business age	n_{age}
Years worked as business manager	n_{exp}
Numbers of years of education of the manager	n_{edu}
White racial makeup (1 if white, and 0 otherwise)	$I_{race,white}$
Black racial makeup (1 if white, and 0 otherwise)	$I_{race,black}$
Inside or outside the inundation area (1 if inside, 0 otherwise)	I_{inund}
Number of employees the business had pre-disaster	$n_{emp,pre}$
The catalog at which the total sale places; 1 (<$500k), 2 (>$500k,<$1 million), 3 (>$1 million,<$2.5 million), 4 (>$2.5 million,<$5 million), 5 (>$5 million,<$10 million), 6 (>$10 million,<$20 million), 7 (>$20 million,<$50 million) , 8 (>$50 million,<$100 million)	$T_{s,catg}$

2.4.1. Cease operation days

This measure refers to how many days are needed for the business to restore its operation, which is the most essential measure showing the initial operational recovery. As presented in Figure 4 using the color red, its prediction is the prospective input to downstream recovery models (i.e., customer retention, employee retention, and revenue recovery).

2.4.2. Revenue recovery

Revenue recovery is the most influential descriptor of the business status following a disruptive event. If the business is back to operation but its revenue has not yet returned back to the pre-disaster level or higher, it is not considered to have reached a certain recovery stage. A measure showing the change in the business revenue (i.e., how much revenue it lost or gained compared to pre-disaster status) can represent business financial recovery. As presented using the color blue in Figure 4, it is expected that two upstream models (cease operation days and customer retention) affect this recovery measure and, their prediction models are inputs into the revenue recovery model.

2.4.3. Customer retention

Customer retention can be an indicator of the business as well as an indicator of the status of community recovery after the disaster. If the business gains its pre-disaster customers, it does not only show that the business is recovering, but also shows that the whole community is recovering and be an indication of household recovery as well (Xiao & van Zandt, 2012). Since customer retention is closely related to household recovery, this relation should be taken into account in any effort to predict the customer retention. Four different approaches to determine the housing units affecting the recovery of a business unit in a community are proposed in this study. The damage sustained by these housing units, their vacancy status, and any other socio-economic characteristics, such as income, can affect the recovery of the business and its customer retention trajectory. Each of the aforementioned characteristics of the affecting housing

units may be incorporated in the customer retention predictive model via explanatory variables representing them. Each proposed approach is presented in detail in the following sections.

2.4.3.1. r-method

This method assumes that the customer retention of each business is affected by the condition of the adjacent housing units within a distance of *r*-kilometers (or miles) from that business. Figure 5 illustrates the proposed concept of this method showing the effective areas around each business as a circle of radius *r*. In order to take into account the interactions between the business and household recovery, the condition and characteristics of the housing units (such as the extent of damage they incurred and their income level) in the effective area of each business unit (shown in Figure 4) should be included in the business customer retention predictive model.

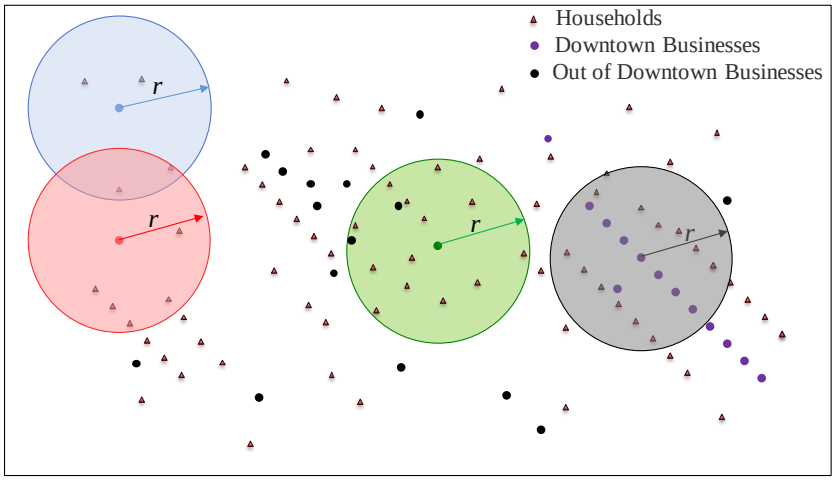

Figure 5: Conceptual representation of the proposed *r*-method to account for the interplay of household and business recovery.

2.4.3.2. k-method

Similarly to the mindset behind the *r*-method, in the proposed *k*-method it is assumed that the trajectory of the business recovery is affected by the *k*-nearest housing units. This approach may be more applicable to communities with non-uniformly distributed buildings around business locations. As shown in Figure 5, the *r*-method accounts for a greater number of affected household units in dense areas (see the business denoted by green) compared to the businesses in sparse populated areas or under-sampled areas (see the business denoted by blue). On the other hand, the *k*-method is not dependent on the density of the neighborhood housing units, as shown in Figure 6.

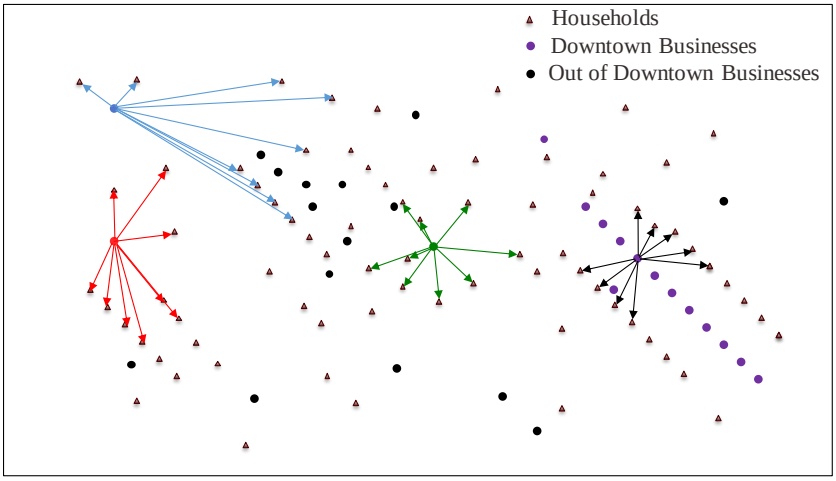

Figure 6: Illustrative example of the proposed *k*-method for *k*=9 housing units nearby certain businesses to account for the interplay of household and business recovery.

2.4.3.3. Weighted method

The weighted method assumes that all housing units across the city affect each business with a specified weight computed as the ratio of number of units versus the distance between the business and housing units. Therefore, if a residential building is located

further away from the business units, its damage, vacancy status, and recovery will influence the recovery of business units less than a residential building located in a closer proximity to the business unit.

2.4.3.4. Downtown district effect method

This proposed method assumes that the businesses located in the downtown area of the community cover wider areas of the city (i.e., have customers from larger areas around the business) (King, 1985; Murphy, 2017; Runyan & Huddleston, 2006). Therefore, if the *r*-method is used a larger distance (r_d) should be considered for businesses located within the downtown business district compared to the distance (r_{nd}) for businesses that are not within the downtown area (i.e., $r_d > r_{nd}$ as shown by an example in Figure 7). Similarly, when the *k*-method is utilized, a larger number of nearest household units should be assumed for businesses within the downtown (k_d) compared to businesses (k_{nd}) located further away from the downtown district (i.e., $k_d > k_{nd}$ as shown by an example in Figure 8). As illustrated by a grey shadow in Figure 7 and black arrows in Figure 8, the businesses in downtown areas, shown by purple circles, may have customers from a wider area and therefore, their recovery trajectory may be influenced by a larger number of housing units located in that area compared to other businesses in the same community.

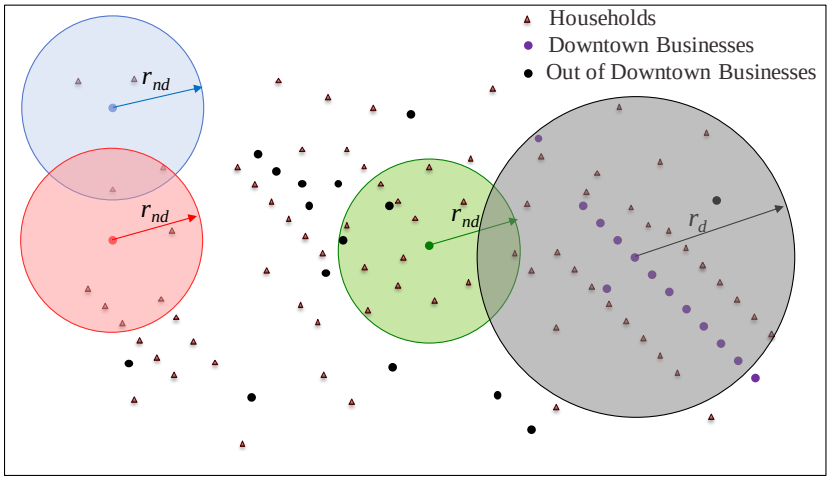

Figure 7: The proposed *r*-method modified to account for the effect of the downtown business district.

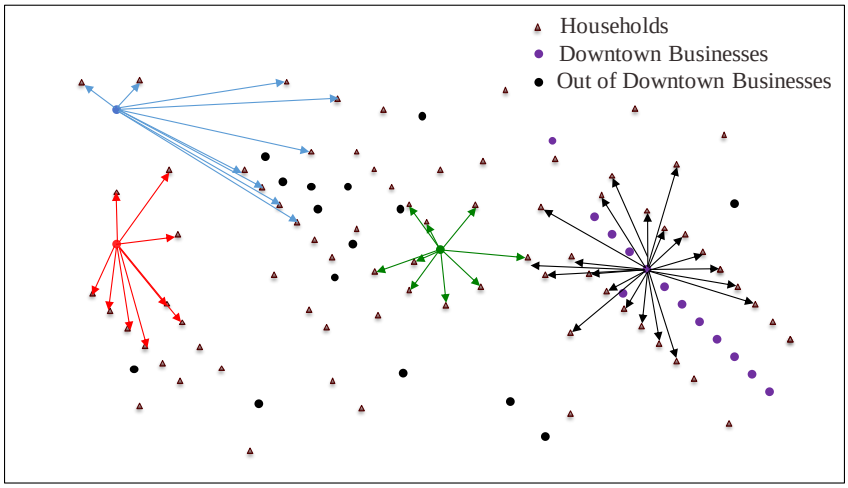

Figure 8: The proposed *k*-method modified to account for the effect of the downtown business district, with k_{nd}=9 and k_d=21 nearest housing units.

2.4.4. Employee retention

The employee retention measure reflects the retention rates of the full- and part-time employees in businesses after a disaster compared to their pre-disaster status. This particular recovery attribute is an indicator of the level of operation of a business compared to its pre-disaster status because as the operation level increases it will require more employees. As presented in Figure 4, the model for predicting the employee

retention requires the predicted values of all upstream models (as input), including revenue recovery, cease operation days, and customer retention in addition to other explanatory variables.

2.5. Application

The proposed modeling approach for quantifying business recovery is applied on a set of data collected through a longitudinal field study in the community of Lumberton, NC. Lumberton was heavily impacted due to historic flooding of the Lumber river caused by heavy raining during 2016 Hurricane Matthew, which crested at approximately 6.7 meters (22 feet) (North Carolina Emergency Management, 2017; U.S. Geological Survey [USGS], 2018). Aggravating this effect was the fact that Lumberton is amongst the most economically disadvantaged counties in the state prior to the hurricane (Centers for Disease Control and Prevention, 2018) with a 10% unemployment rate and a 35% poverty rate according to 2012-2016 American Community Survey 5-Year Estimates, making the application of business recovery models to this case particularly pertinent. Data for the models were collected through in-person surveys to the business owner or manager over a 10-day period in January 2018 (13 months after the disaster). Questions were related to larger themes such as damage and utility interruption, recovery status, business characteristics, owner or manager demographics as well as financial assistance. The sample was drawn from ReferenceUSA, a business database, using ArcGIS to identify and select all businesses in the predicted inundation area as well as a set of randomly selected businesses from the FEMA 100-year floodplain in the northern part of the city (unflooded area as a comparison to the inundation area). It should be noted that

medical professionals were under-sampled due to their limited walk-in availability and specialized operational strategy. Such businesses were included in the sample selected from the predicted inundation area but excluded them from the floodplain sample. Of the 380 businesses selected for inclusion in the study, 164 responses were completed, yielding to a response rate of 43%. This database contains a wide variety of information including most of the potential explanatory variables as presented in Figure 4. For each of the attributes towards the business recovery introduced in the previous section, a model was developed to predict the associated recovery measure using the modeling methodology introduced in this study.

As illustrated in Figure 3, the first step towards model development is data collection. In this study, the database developed for the Lumberton community is utilized, which contains the seven sets of general information discussed in the Modeling Approach section. In Step 2 of the modeling approach, the initial candidate model form basket is generated using various initial candidate model forms using the instruction in the previous sections (Step 2: Development of model forms), accounting for different combinations of explanatory functions as well as various transformation and link functions. After conducting Bayesian linear regression using a computer program called Rt (Mahsuli & Haukaas, 2012), each of the candidates went through Step 3 to generate the upgraded candidate model form basket. Ultimately, the best upgraded candidate was selected from the basket in accordance with the quality of the models determined by diagnostics, posterior statistics, and consistency with the engineering judgements and the available literature. As an illustration of the model diagnostics, the associated plots are

presented and discussed for the cease operation days recovery attribute. Afterwards, the high correlation between its model parameters was eliminated. To illustrate the three-stage process of Step 3 presented in Figure 3, this procedure is discussed for the final selected model, from its initial form to upgraded form, and ultimately after elimination of high correlations between its model parameters.

2.5.1. Cease operation days

As discussed previously, this recovery measure indicates the time required for the business to recover its operational status. The initial form of the selected candidate model to predict the cease operation days of a business is presented in Equation (4), accounting for various explanatory variables that can affect business recovery.

$$\begin{aligned} -\ln\left(-\ln\left(\frac{d}{3\times 365}\right)\right) &= \theta_1 + \theta_2 \cdot \left(\delta_b + \delta_c + \delta_m\right) + \theta_3 \cdot \ln\left(l_e + l_w + l_g + l_s + l_i + 1\right) + \theta_4 \cdot I_{acc} \\ &+ \theta_5 \cdot \left(I_{emp,pd} + I_{emp,sch} + I_{emp,phys} + I_{emp,m}\right) + \theta_6 \cdot n_{age} + \theta_7 \cdot I_{bus,c} + \theta_8 \cdot I_{bus,m} + \theta_9 \cdot I_{bus,r} \\ &+ \theta_{10} \cdot I_{bus,o} + \theta_{11} \cdot I_{Own} + \theta_{12} \cdot I_{ins,b} + \theta_{13} \cdot I_{ins,c} + \theta_{14} \cdot I_{ins,i} + \theta_{15} \cdot n_{\exp} + \theta_{16} \cdot n_{edu} + \varepsilon \end{aligned} \quad (4)$$

The description of each explanatory variable (**x**) can be found in Table 1. A link function was used (as shown in Equation (4)) on the left-hand side of the proposed model form to restrict the values of predicted cease operation days (d) between zero days and three years (3×365 days) assuming that if a business has not recovered after three years (3×365 days), it can be concluded that it will not return back to operation. The log-log function ($-\ln(-\ln(y))$) that was considered here as the link function ($F(y)$) predicts y in Equation (2) between 0 and 1, and since $y=d/(3\times365)$, the predicted value for d will be between 0 and 3×365. Equation (4) includes almost all the potential explanatory

variables presented in Figure 4 to predict cease operation days. Different explanatory variables are combined to form more representative explanatory functions (e.g., sustained physical damage and utility disruptions).

This initial candidate model then goes through the first two parts of model selection (step 3), namely diagnostics and elimination of inconclusive terms. After 13 iterations between these two parts, illustrated by the dashed box in Figure 3, only three explanatory functions are retained and are informative enough not to be eliminated from the model. The upgraded model form then becomes:

$$-\ln\left(-\ln\left(\frac{d}{3\times 365}\right)\right)=\theta_1+\theta_2\cdot\left(\delta_b+\delta_c+\delta_m\right)+\theta_3\cdot\ln\left(l_e+l_w+l_g+l_s+l_i+1\right)+\varepsilon \quad (5)$$

For the upgraded model presented in Equation (5), CoVs of all remaining model parameters (θ_i) are below 30% as summarized in Table 2, with a coefficient of determination (R^2) equal to 0.53.

Table 2: Posterior statistics summary for cease operation days model of Equation (5).

Parameter	Mean	CoV	Correlation Coefficient		
			θ_1	θ_2	θ_3
θ_1	−2.0536	0.030	1		
θ_2	0.0523	0.010	−0.08	1	
θ_3	0.0716	0.273	−0.83	−0.42	1
σ	0.2346	0.057			

As shown in Figure 3, the upgraded model goes through the elimination of high correlations procedure (part 3). Based on the posterior statistics presented in Table 2, it is observed that the correlation between the model parameters θ_1 and θ_3 is high (equal to −0.83), which can be eliminated using Equation (3). The elimination of high correlation results in a new upgraded model form as presented in Equation (6).

$$-\ln\left(-\ln\left(\frac{d}{3\times 365}\right)\right)=\theta_1\left(1-0.263\ln\left(l_e+l_w+l_g+l_s+l_i+1\right)\right)+\theta_2\cdot\left(\delta_b+\delta_c+\delta_m\right) \quad (6)$$
$$-0.47\ln\left(l_e+l_w+l_g+l_s+l_i+1\right)+\varepsilon$$

This new model has a higher R^2 (equal to 0.89), and also a lower mean of σ (equal to 0.2339), with posterior statistics presented in Table 3. Per Table 3, the model parameters, θ_1 and θ_2, in the new model have low correlation (−0.15), and thus, the procedure is stopped and the final model is Equation (6).

Table 3: Posterior statistics summary for cease operation days model of Equation (6).

Parameter	Mean	CoV	Correlation Coefficient	
			θ_1	θ_2
θ_1	−2.0536	0.030	1	
θ_2	0.0529	0.049	−0.15	1
σ	0.2339	0.057		

Figure 9 shows diagnostics plots for the final model. Figure 9a presents the prediction versus observation scatter that is well aligned along the 45° line, which indicates an appropriate prediction. The Q-Q plot in Figure 9b validates the normality assumption in this model since points are aligned along the 45° line. In order to avoid an over-fit, the developed model using the training dataset (85% of the initial dataset) is used to predict the testing dataset and the combined results are shown in Figure 9c. The testing data, illustrated by triangles, are along the 45° line through the training scatter which indicates no over-fit. Figure 9d, e, and f present the residuals versus the first regressor, the second regressor, and regressand, respectively. Points in all of these three plots are distributed almost equally along the x-axes, which indicates homoscedasticity. Furthermore, there is no visible pattern in the scatter and therefore, there is no autocorrelation of residuals.

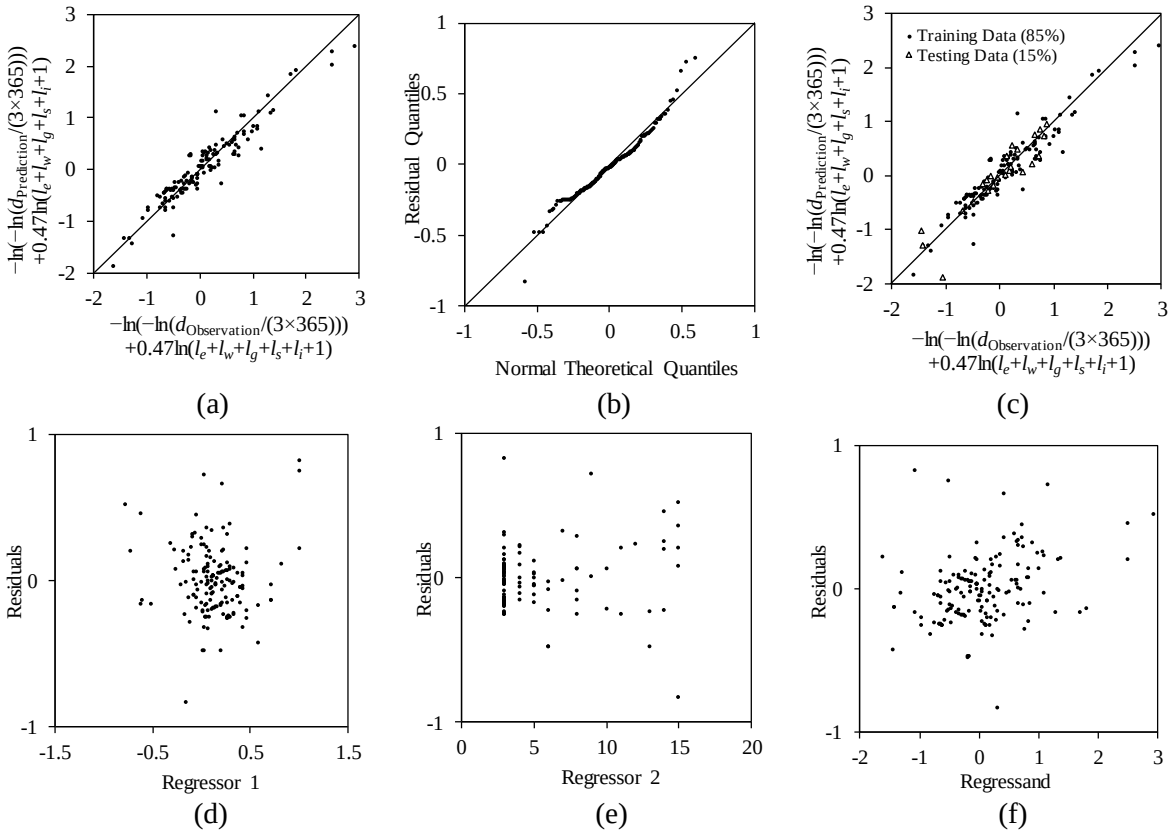

Figure 9: Diagnostics of the final model for the cease operation days recovery attribute, in Equation (6); (a) model prediction vs. model observation plot, (b) Q-Q plot, (c) model prediction vs. model observation plot for training and testing sets, (d) residuals vs. the first regressor, (e) residuals vs. the second regressor, (f) residuals vs. regressand.

One of the advantages of the proposed approach to develop Bayesian linear regression models is that it determines the most significant factors in the model prediction. By comparing the initial and upgraded model forms in Equations (4) and (6), it can be concluded that the 13 eliminated explanatory functions were not significant enough to be included in the model form for the prediction/quantification of the cease operation days recovery measure. Three terms remained in the upgraded model form, i.e., intercept, summation of damage to the building, content, and machinery, as well as the summation of different utility disruptions, which indicates that the business cease

operation days is governed mainly by the physical damage to the business and infrastructure systems of the community. Based on the final upgraded model of Equation (5) for predicting cease operation days (d), the contributing explanatory functions and their effects considering the effect of other regression terms are as follows:

(1) *Summation of damage to the building, contents, and machinery*: increase in the damage incurred by the business results in higher predictions for cease operation days and longer duration of recovery.

(2) *The summation of different utility disruptions*: increase in the length of utility disruptions results in higher predictions for cease operation days and longer duration of recovery, which is in line with findings of other studies in the literature (e.g., Tierney (1997)).

2.5.2. Revenue recovery

A predictive model was also developed for the revenue recovery attribute. Likert scaling was used to describe the revenue recovery of the business during the field study at Lumberton, NC, in a way that this recovery attribute describes the revenue change by one of the following levels: "*decreased greatly, decreased, stayed the same, increased, or increased greatly*". In order to quantitatively model this recovery measure an integer number from one to five was assigned to each level such that predictions close to five indicate significant revenue increase while predictions close to one indicate significant revenue decrease. The selected model to predict the revenue recovery (13 months after the disaster) has the initial form as provided in Equation (7).

$$\Phi^{-1}\left(\frac{R-1}{4}\right)=\theta_1+\theta_2\cdot P_p+\theta_3\cdot\ln\left(d+1\right)+\theta_4\cdot\delta_c+\theta_5\cdot\ln\left(\delta_b+\delta_m\right)+\theta_6\cdot I_{acc}$$
$$+\theta_7\cdot\left(I_{emp,trans}+I_{emp,pd}+I_{emp,sch}+I_{emp,phys}+I_{emp,m}\right)+\theta_8\cdot\left(\frac{100-R_{cus}}{100}\right)+\theta_9\cdot I_{loc}+\theta_{10}\cdot I_{Own}$$
$$+\theta_{11}\cdot I_{bus,c}+\theta_{12}\cdot I_{bus,m}+\theta_{13}\cdot I_{own,single}+\theta_{14}\cdot I_{own,partner}+\theta_{15}\cdot I_{franch}+\theta_{16}\cdot I_{coop} \quad (7)$$
$$+\theta_{17}\cdot I_{cus,geo}+\theta_{18}\cdot I_{sup,out}+\theta_{19}\cdot\ln\left(n_{\exp}\right)+\theta_{20}\cdot n_{edu}+\theta_{21}\cdot I_{race,white}+\theta_{22}\cdot I_{race,black}$$
$$+\theta_{23}\cdot I_{Inund}+\theta_{24}\cdot n_{emp}+\theta_{25}\cdot T_S+\theta_{26}\cdot T_{S,catg}+\varepsilon$$

Explanatory variables of Equation (7) and their associated description are summarized in Table 1. In order to restrict the predictions of *R* between one and five, a link function $\Phi^{-1}(.)$ was utilized in the left-hand side of the equation to restrict the predicted value inside the parentheses $\left(\left(R-1\right)/4\right)$ between zero and one (value of *y* in Equation (2)), and as a result, restrict the predicted *R* between one and five. In the right-hand side of the equation, different combinations of explanatory functions with different transformations were considered in order to achieve the most realistic model form.

The initial candidate model form of Equation (7) was further evaluated through the diagnostics and elimination of inconclusive terms processes, and after 21 iterations and 21 uninformative terms elimination, the upgraded model form of Equation (8) was derived accounting for the explanatory variables representing the profitability of the business before the disaster (*Pp*), damage to the business contents (δ_c), customer retention (R_{cus}), number of employees pre-disaster (n_{emp}), and the total annual sale category ($T_{S,catg}$) of the business (per Table 1).

$$\Phi^{-1}\left(\frac{R-1}{4}\right)=\theta_1\cdot P_p+\theta_2\cdot\delta_c+\theta_3\cdot\left(\frac{100-R_{cus}}{100}\right)+\theta_4\cdot\ln\left(n_{emp}\right)+\theta_5\cdot T_{S,catg}+\varepsilon \quad (8)$$

The posterior statistics of the upgraded model of Equation (8) are summarized in Table 4. The largest observed CoV of the model parameters is 33% for parameter θ_4, which is desirable. The coefficient of determination for this model (R^2) is around 0.36, which although relatively low, it may be acceptable for a complex predictive model as the one considered here.

Table 4: Posterior statistics summary for revenue recovery model of Equation (8).

Parameter	Mean	CoV	Correlation Coefficient				
			θ_1	θ_2	θ_3	θ_4	θ_5
θ_1	0.3378	0.266	1				
θ_2	−0.2413	0.218	−0.40	1			
θ_3	−2.4824	0.152	−0.25	−0.21	1		
θ_4	0.3425	0.333	−0.10	−0.26	0.04	1	
θ_5	−0.2697	0.297	−0.27	0.13	−0.06	−0.80	1
σ	1.1000	0.060					

As shown in Table 4, two model parameters θ_4 and θ_5 are highly correlated with $\rho_{45} = -0.80$. This high correlation can be addressed by expressing one of these parameters as a function of the other using Equation (3). The resulting model again has high correlation between two of its new model parameters (θ_1 and θ_2) with $\rho_{12} = -0.65$, and hence, the elimination process is repeated. The resulting model form is as follows:

$$\Phi^{-1}\left(\frac{R-1}{4}\right) = \theta_1 \cdot \left(\delta_c - 0.982P_p\right) + \theta_2 \cdot \left(\frac{100-R_{cus}}{100}\right) + \theta_3 \cdot \left(T_{S,catg} - 1.139\ln\left(n_{emp}\right)\right) + 0.035\ln\left(n_{emp}\right) + 0.101P_p + \varepsilon \quad (9)$$

Per the posterior statistics of the model form of Equation (9) shown in Table 5, no correlation with an absolute value of more than 0.5 appears in the resulting model, and therefore, no further elimination of high correlations is required. Based on the results of Table 5, it is observed that the mean of the error is slightly lower in the model form of Equation (9) than in its prior model form of Equation (8), while the overall uncertainty

of the problem is decreased, and the coefficient of determination (R^2) remained almost the same (0.36). Thus, the model in Equation (9) is the final selected form.

Table 5: Posterior statistics summary for revenue recovery model of Equation (9).

Parameter	Mean	CoV	Correlation Coefficient		
			θ_1	θ_2	θ_3
θ_1	−0.2413	0.209	1		
θ_2	−2.4823	0.122	−0.28	1	
θ_3	−0.2697	0.281	0.14	−0.31	1
σ	1.0925	0.059			

Based on the final upgraded model of Equation (8) for predicting revenue recovery (R), the contributing explanatory variables and their effects considering the effect of other regression terms are as follows:

(1) *Profitability of the business before the disaster*: the more profitable the business is before the disaster, the slower the revenue recovery trajectory appears after the disaster. This suggests that it is harder for a highly profitable business to reach that level of high profitability quickly, similar to the findings by Webb et al. (2002) stating that larger businesses have more to lose and it is harder for them to reach their pre-disaster state.

(2) *Content damage*: the greater the extent of content damage in the business, the slower the revenue recovery is.

(3) *Customer retention rate*: higher customer retention results in faster revenue recovery. Customer loss was identified as one of the main factors adversely affecting the businesses after the disasters occur in prior studies (e.g., Corey & Deitch (2011) and Tierney (1997)).

(4) *Annual sales category*: if the business is classified in a higher category of

annual sales, the revenue recovery is slower, which is in agreement with the findings by Webb et al. (2002) for large businesses.

(5) *Number of employees before the disaster*: if the business had a larger number of employees before the disaster, its post-disaster recovery is faster.

2.5.3. Customer retention

The measure for this recovery attribute is defined as the ratio of the number of customers the business has compared to its pre-disaster number in a percentage form. In order to develop this model, two databases from the longitudinal field study conducted in the Lumberton community were used, accounting not only for business surveys but for household surveys as well. A two-stage non-proportional random cluster sampling was conducted in the household survey in order to obtain a valid sample representing the community, including the areas impacted directly by the flooding and areas not impacted directly by flooding loads adopting a 3 to 1 ratio for high and low probability flooding areas, respectively. A box named "*household effect*" in Figure 4 represents the outcomes of the household unit surveys which are used as input in the customer retention predictive model. Different methods to include the effect of the recovery of households in the customer retention of the businesses, which were introduced in the previous sections, are examined here to develop a representative model. Based on a sensitivity study conducted (which is not presented herein due to space limitations), it was found that the modified *r*-method (with r_d=2.5 and r_{nd}=0.7 kilometres) accounting for the effect of the downtown business district is more representative for the community of

Lumberton, NC. The finally selected candidate model to predict the customer retention has the initial form of Equation (10).

$$\Phi^{-1}\left(\frac{R_{cus}}{100}\right)=\theta_1\cdot\exp\left(\delta_{hous}\right)+\theta_2\cdot\frac{\exp\left(\delta_b+\delta_m\right)}{100}+\theta_3\cdot\ln\left(d+1\right)+\theta_4\cdot I_{loc}$$
$$+\theta_5\cdot\ln\left(n_{age}\right)+\theta_6\cdot I_{bus,v}+\theta_7\cdot I_{bus,s}+\theta_8\cdot I_{bus,c}+\theta_9\cdot I_{bus,m}+\theta_{10}\cdot I_{bus,o} \quad (10)$$
$$+\theta_{11}\cdot\ln\left(P_p\cdot T_{s,catg}\right)+\theta_{12}\cdot n_{exp}+\varepsilon$$

The description of each explanatory variable is provided in Table 1. After five iterations of the diagnostics and elimination processes, five uninformative explanatory functions (d, I_{loc}, n_{age}, P_p, $T_{s,catg}$, n_{exp}) were eliminated from the initial candidate model form and the upgraded candidate form of Equation (11) was formed.

$$\Phi^{-1}\left(\frac{R_{cus}}{100}\right)=\theta_1\cdot\exp\left(\delta_{hous}\right)+\theta_2\cdot\frac{\exp\left(\delta_b+\delta_m\right)}{100}+\theta_3\cdot I_{bus,v}+\theta_4\cdot I_{bus,s} \quad (11)$$
$$+\theta_5\cdot I_{bus,c}+\theta_6\cdot I_{bus,m}+\theta_7\cdot I_{bus,o}+\varepsilon$$

The posterior statistics associated with the upgraded model in Equation (11) are presented in Table 6. The largest CoV is around 34% which is within acceptable ranges, while the coefficient of determination (R^2) is 0.23. Future business and household field studies would be beneficial for updating the proposed Bayesian regression models using the merged datasets. Furthermore, the non-proportional random cluster sampling (in the Lumberton field study) might be a reason for the imperfect prediction since in some low probability flooding areas there are not enough housing data points surveyed around the business units.

Table 6: Posterior statistics summary for customer retention model of Equation (11).

Parameter	Mean	CoV	Correlation Coefficient						
			θ_1	θ_2	θ_3	θ_4	θ_5	θ_6	θ_7
θ_1	−0.2433	0.214	1						
θ_2	−0.0351	0.345	−0.07	1					
θ_3	2.3524	0.137	−0.79	−0.14	1				
θ_4	2.4419	0.164	−0.69	−0.05	0.56	1			
θ_5	2.5199	0.143	−0.68	−0.05	0.55	0.48	1		
θ_6	2.6445	0.173	−0.11	−0.05	0.10	0.08	0.08	1	
θ_7	2.3506	0.109	−0.93	−0.01	0.74	0.65	0.64	0.11	1
σ	0.9066	0.061							

Based on the posterior statistics shown in Table 6, there are high correlations between various model parameters which should be further addressed through the elimination of high correlations process per Equation (3). The largest correlation observed is between parameters θ_1 and θ_7, with ρ_{17}=−0.93, and hence, the procedure starts with the elimination of high correlation between these two parameters. After using Equation (3) to eliminate the high correlation, the Bayesian regression was reconducted with the new model resulting in the model of Equation (12).

$$\Phi^{-1}\left(\frac{R_{cus}}{100}\right)=\theta_1\cdot\frac{\exp\left(\delta_b+\delta_m\right)}{100}+\theta_2\cdot I_{bus,v}+\theta_3\cdot I_{bus,s}+\theta_4\cdot I_{bus,c}$$
$$+\theta_5\cdot I_{bus,m}+\theta_6\cdot\left(I_{bus,o}-0.189\exp\left(\delta_{hous}\right)\right)+0.2\exp\left(\delta_{hous}\right)+\varepsilon \quad (12)$$

Per the posterior statistics of Equation (12) in Table 7, the mean of the error is slightly lower in Equation (12) compared to Equation (11), while it has a higher R^2 (0.43). According to Table 7, a correlation coefficient higher than 0.7 (ρ_{26}=0.77) exists between θ_2 and θ_6, indicating that the elimination of high correlations between model parameters should be continued. However, by eliminating this correlation, a model form results (although its R^2 is higher) the CoV of model parameters of which are significantly

increased, except for its last term. As discussed previously, if after elimination of high correlation between two model parameters, there is a significant jump in the CoV of the new model parameters, this elimination should be rejected. Therefore, the model of Equation (12) is selected herein as the final model form.

Table 7: Posterior statistics summary for customer retention model of Equation (12).

Parameter	Mean	CoV	Correlation Coefficient					
			θ_1	θ_2	θ_3	θ_4	θ_5	θ_6
θ_1	−0.0350	0.337	1					
θ_2	2.3563	0.132	−0.21	1				
θ_3	2.4465	0.158	−0.10	0.53	1			
θ_4	2.5240	0.138	−0.10	0.52	0.45	1		
θ_5	2.6452	0.172	−0.06	0.09	0.08	0.08	1	
θ_6	2.3506	0.109	−0.01	0.77	0.67	0.66	0.11	1
σ	0.9033	0.061						

According to Equation (12) for predicting customer retention, the contributing explanatory variables and their effects are as follows:

(1) *Average damage in household units within r kilometers* (or miles) around the identified business unit accounting for a larger *r* if the business is located in the downtown district to account for servicing areas outside that district as well: If the average damage in household units nearby increases, the customers of the business recover slower (lower retention rate) according to the sign of the associated model parameter in Table 6. Local population has been proven to be a critical source of customers for the businesses, and hence, severe damage to the houses causing the population displacement is an important factor in the customer loss (Corey & Deitch, 2011; Tierney, 1997).

(2) *Building and machinery damage*: If the damage of the building in which the business operates and damage to the machinery is more severe, the customer

retention rates are lower.

(3) *Various explanatory functions representing the sector of the business*: the order of the business sectors with the highest rate of customer retention is manufacturing, construction, supermarkets, vehicle-related businesses, and other types of businesses, which aligns well with findings of previous studies focusing on business recovery attributes (Durkin, 1984; Kroll, Landis, Shen, & Stryker, 1991; Webb, Tierney, & Dahlhamer, 2000).

2.5.4. Employee retention

This model predicts the retention rates of the business's employees compared to before the disaster, as a ratio of change in the number of employees (lumped full- and part-time) divided by the total number of employees before the disaster. Figure 4 presents a number of potential input variables to predict employee retention, which also includes the outputs of upstream models (i.e., cease operation days, revenue recovery, and customer retention). Various candidate models were examined using the Lumberton database which amongst all the following initial candidate model form was selected as presented in Equation (13):

$$\delta_{emp} = \frac{n_{emp,now} - n_{emp,pre} - 1}{n_{emp,pre}} = \theta_1 \cdot \ln(\delta_b) + \theta_2 \cdot \ln(\delta_c) + \theta_3 \cdot \sqrt{d} + \theta_4 \cdot \sqrt{l_{cus}} + \theta_5 \cdot I_{loc} + \theta_6 \cdot n_{age} + \theta_7 \cdot I_{bus,c} + \theta_8 \cdot I_{bus,m} + \theta_9 \cdot I_{bus,r} + \theta_{10} \cdot I_{bus,o} + \theta_{11} \cdot I_{own} + \theta_{12} \cdot R + \theta_{13} \cdot P_p + \theta_{14} \cdot n_{\exp} + \theta_{15} \cdot n_{edu} + \theta_{16} \cdot I_{Inund} + \theta_{17} \cdot T_{s,catg} + \theta_{18} \cdot \ln(n_{emp,pre}) + \varepsilon \quad (13)$$

where $n_{emp,now}$ is the number of employees of the business after the disaster (around 13 months after the disaster). This initial model goes through model selection and after

eliminating the 11 most uninformative terms, the upgraded candidate model is described by Equation (14), where the explanatory variables representing cease operation days (d), different business sectors ($I_{bus,c}$, $I_{bus,m}$, $I_{bus,r}$, and $I_{bus,o}$), revenue recovery percentage (R), and number of employees before the disaster ($n_{emp,pre}$) are included.

$$\frac{n_{emp,now}-n_{emp,pre}-1}{n_{emp,pre}}=\theta_1\cdot\sqrt{d}+\theta_2\cdot I_{bus,c}+\theta_3\cdot I_{bus,m}+\theta_4\cdot I_{bus,r}+\theta_5\cdot I_{bus,o}+\theta_6\cdot R +\theta_7\cdot\ln(n_{emp,pre})+\varepsilon \quad (14)$$

The posterior statistics of this model are summarized in Table 8, where the largest CoV is approximately 48% while the coefficient of determination (R^2) is around 0.48 which are also within acceptable ranges.

Table 8: Posterior statistics summary for employee retention model of Equation (14).

Parameter	Mean	CoV	Correlation Coefficient						
			θ_1	θ_2	θ_3	θ_4	θ_5	θ_6	θ_7
θ_1	−0.0170	0.400	1						
θ_2	−0.9251	0.182	−0.26	1					
θ_3	−1.0567	0.127	−0.32	0.34	1				
θ_4	−0.7331	0.113	−0.45	0.47	0.57	1			
θ_5	−0.7045	0.115	−0.59	0.51	0.61	0.83	1		
θ_6	0.0451	0.482	0.27	−0.48	−0.45	−0.71	−0.74	1	
θ_7	0.1813	0.100	0.08	−0.18	−0.42	−0.37	−0.40	−0.12	1
σ	0.2453	0.060							

According to the results of Table 8, the largest correlation is observed between parameters θ_4 and θ_5 (ρ_{45}=0.83). After repeating the high correlation elimination process two times, the final upgraded model form of Equation (15) is derived as:

$$\frac{n_{emp,now}-n_{emp,pre}-1}{n_{emp,pre}}=\theta_1\cdot\sqrt{d}+\theta_2\cdot I_{bus,c}+\theta_3\cdot I_{bus,m}+\theta_4\cdot\left(I_{bus,r}+0.809I_{bus,o}-0.187R\right) +\theta_5\cdot\ln(n_{emp,pre})-0.112I_{bus,o}-0.092R+\varepsilon \quad (15)$$

The final model has five model parameters with posterior statistics summarized in Table 9. Since there is no correlation coefficient above 0.7 in this table, there is no need to continue the elimination process. The resulting model has larger coefficient of determination (R^2=0.58), which is more suitable, as well as lower mean of standard deviation of the model error (σ).

Table 9: Posterior statistics summary for employee retention model of Equation (15).

Parameter	Mean	CoV	Correlation Coefficient				
			θ_1	θ_2	θ_3	θ_4	θ_5
θ_1	−0.0170	0.357	1				
θ_2	−0.9247	0.176	−0.25	1			
θ_3	−1.0572	0.122	−0.24	0.31	1		
θ_4	−0.7331	0.112	−0.51	0.49	0.59	1	
θ_5	0.1817	0.073	−0.22	−0.32	−0.49	−0.50	1
σ	0.2436	0.060					

Based on the final upgraded model of Equation (15) for predicting employee retention, the contributing explanatory variables and their effects (considering the effects of the other regression terms) are as follows:

(1) *Cease operation days*: if the business gets back to operation faster, it has higher ability to retain its number of employees.

(2) *Various explanatory functions describing the business sector*: the sector orders with the highest rate of employee retention is sectors other than construction, manufacturing, and retail, retail, construction, and manufacturing.

2.6. Concluding Remarks

This chapter proposed a modeling approach for quantifying the recovery trajectory of businesses after a disaster using different recovery attributes. A probabilistic modeling approach is proposed based on Bayesian linear regression modeling to develop

predictive recovery models for businesses after disastrous events. Since such predictions are associated with a high degree of uncertainty, it is necessary to quantify this uncertainty in the prediction. The Bayesian approach is a suitable modeling methodology for modeling business recovery given the associated high degree of uncertainty since it inherently accounts for the aleatory and epistemic uncertainties. The proposed modeling methodology utilizes real-world observations to calibrate the model parameters using data collected from businesses following a disastrous event. The modeling methodology consists of three steps, including data collection, development of model forms, and model selection. The most desirable model among the basket of candidates is selected as the predictive model of the recovery measure of interest. This model is selected based on its appropriate diagnostics, posterior statistics, and compatibility with the available literature and expert judgment.

Four business recovery attributes along with their measures are presented in this study, including: cease operation days, revenue recovery, customer retention, and employee retention. The potential inputs to each of these four recovery measures include direct and indirect impacts that account for the extent of physical damage the business incurred (e.g., building, machinery, and content damage and utility disruptions), business characteristics (e.g., ownership, sector, business age, etc.), business geographical characteristics as well as neighborhood characteristics and aftermath condition. One of the advantages of the proposed approach is taking into account the interplay between household and business recovery after a disaster, which is incorporated into the model through different proposed methods.

As an application of the proposed modeling approach, this study considers the community of Lumberton, NC, that was severely affected after Hurricane Matthew, 2016. Through a longitudinal field study conducted in this community after Hurricane Matthew by the NIST-funded Centre of Excellence on Risk-Based Community Resilience Planning, a large dataset containing the most significant factors affecting business recovery was generated using in-person surveys. A predictive Bayesian linear regression model for each of the four business recovery attributes is developed in this chapter using the proposed approach. It was observed that the extent of utility disruptions as well as damage to the building, its contents, and machinery are the most significant predictors of cease operation days of a business aftermath. Furthermore, the most significant factors in predicting revenue recovery of a business after a disaster are the profitability of the business before the disaster, the extent of its content damage, the business customer retention rate, the business annual sales category, and the number of employees of the business pre-disaster. Moreover, the final model for customer retention revealed that the damage to the business's building and machinery, the average of extent of damage to the households within *r*-kilometres from the business (considering a larger value for *r* if the business is in downtown district) as well as the business sector are the most significant predictors. Lastly, it was concluded that the business cease operation days and the business sector are the most effective factors in predicting employee retention rate after a disaster.

The developed Bayesian models using the approach presented in this study are applicable in risk-based resilience analysis frameworks to enhance community

resilience. As these models quantify recovery trajectories in the aftermath of a disaster, they are capable of being utilized in any decision-making effort using risk-based resilience assessment methods. In addition, since these models are continuously differentiable, they are suitable to be used in resilience assessments using structural reliability methods, like first order (FORM) and second order (SORM) reliability methods. Another advantage of this approach is identifying the most efficient predictors of recovery measures of interest through the Bayesian regression. Additionally, the Bayesian method can update the posterior statistics of the model as new data merges from future survey studies. Hence, if it is needed, it is possible to decrease the uncertainties of the developed models using this approach by collecting more real-world observations through survey field studies after disasters, for instance by directly interviewing business managers and business owners as well as conducting paper-based, email-based, and/or phone-based surveys.

Although the proposed business recovery models are capable of inherently capturing the uncertainties associated with predictive models, there are limitations associated with their applicability. The application of the developed models is limited to the communities the data of which was utilized to calibrate the models (in this case Lumberton, NC). However, since it is not feasible to collect data from all communities impacted by a variety of hazard intensities throughout a year given the time and resource allocation needed for such longitudinal study efforts, the developed models can be used for communities with similar socio-economic characteristics subjected to similar hazard types and intensities to predict business recovery trajectories and make risk-informed

decisions to enhance their resilience in terms of pre-disaster preparedness as well as post-disaster resource allocations. This may also be applicable to a large number of communities that are prone to hazards (such as flooding as considered in this study) but have not recently been impacted by a natural disaster, in order to make risk-informed decisions to enhance their resilience. The developed business recovery models can also be further generalized using datasets from other communities subject to various levels of flooding in order to be applicable to a wider range of communities for the utmost goal of resilience-based risk analysis.

3. THRUST B: VALIDATION OF TIME-DEPENDENT REPAIR RECOVERY OF THE BUILDING STOCK FOLLOWING THE 2011 JOPLIN TORNADO [*]

Damage fragilities are among the most commonly used models in the literature to predict damage to the physical infrastructures and their components. The concept of fragility is used in the literature to model functionality recovery of the affected infrastructures as well. This chapter seeks to calibrate an existing analytical framework to develop building repair fragility models using a restoration dataset collected through a longitudinal field study in the city of Joplin, MO, after the catastrophic 2011 Enhanced Fujita 5 tornado. First, an existing recovery data set from Joplin is documented and the main findings pertaining to the observed recovery trajectory of the buildings are highlighted. In the next step, various empirical functionality fragilities conditioned on the initial functionality level (and associated damage) of the building are generated and compared to the analytical repair time/functionality fragilities. Results revealed moderate to significant differences between empirical and analytical functionality fragilities depending on the extent of the initial damage and the initial associated functionality state of the buildings. This was anticipated and one of the goals of this study was to quantify this discrepancy that is caused by not including the delay time resulting from cumbersome circumstances during the aftermath. A number of methods

[*] This chapter is published in the "Journal of Natural Hazards Review" as an individual paper (Aghababaei, M., Koliou, M., Pilkington, S., Mahmoud, H., van de Lindt, J.W., Curtis, A., Smith, S., Ajayakumar, J. and Watson, M., 2020. Validation of Time-Dependent Repair Recovery of the Building Stock Following the 2011 Joplin Tornado. *Natural Hazards Review*, *21*(4), p.04020038.) With permission from ASCE.

available in the literature are first explored in this study to address these differences by introducing the various sources of initial delays into the repair time, and further be modified to realistically represent the associated delay factors. The modification employed included: (i) changing the formulations used to aggregate different types of delays to calculate the initial delay of the buildings, and (ii) using more representative distributions for various types of delays based on available real-world datasets. The main delays included are inspection delay, time to obtain adequate financial resources, delays in finding and hiring contractors, and construction permitting delays. The proposed methodology was integrated with the analytical framework to generate updated repair time/functionality fragilities. The updated analytical fragilities result into a more realistic prediction of the recovery trajectory of the building stock when compared with the empirical ones.

3.1. Introduction

Tornadoes are one of the most devastating natural disasters that occur frequently each year in the United States (U.S.) and around the world. The largest number of tornadoes worldwide occur in the U.S. with an average of 1,300 tornadoes each year (NOAA, 2019). Some of the most severe tornadoes exhibit wind speeds exceeding 321.9km/h (200mph) and leaving a damaged path of 1.6km (one mile) wide and 80.5 km (50 miles) long.

The impact of a tornado may result in both direct and indirect losses to the local economy. Direct losses are mainly associated with the destruction of assets caused by

the initial impact of the tornado hazard including loss of human lives (casualties), damage to lifelines (e.g., roads, power and phone lines), crops, businesses (e.g., factories), homes, and natural resources. Indirect losses to the local economy, which can be harder to estimate, occur from the destruction of physical assets for households and businesses, loss in production and sales, lost income and labor time, as well as increased commute time and utility disruption (Rose, Benavides, Chang, Szczesniak, & Lim, 1997). Long periods of recovery after disasters intensify such indirect consequences for the communities.

Over the last decade, studies have focused on evaluating and/or predicting recovery and restoration progress/trajectory of the building stock in communities impacted by tornadoes. A number of studies reported in the literature have focused on the 2011 Joplin, Missouri EF-5 tornado (Attary, van de Lindt, Mahmoud, & Smith, 2019; Attary et al., 2018; Kuligowski, Lombardo, Phan, Levitan, & Jorgensen, 2014; Masoomi & van de Lindt, 2018b; Prevatt et al., 2012; Ramachandran, Long, Shoberg, Corns, & Carlo, 2015). Ramachandran et al. (2015) proposed a probabilistic framework to compute the restoration time of urban communities following tornado events and applied this framework to the city of Joplin, while Attary et al. (2018) and Attary et al. (2019) performed community-level building damage assessment and combined building-electrical network damage assessment for the city of Joplin. Restoration and functionality probabilistic frameworks incorporating aspects of performance-based engineering have also been developed and used to quantify various levels of restoration and functionality both at the building level (Koliou & van de Lindt, 2020) and

community level (Farokhnia, van de Lindt, & Koliou, 2020; Masoomi & van de Lindt, 2018b). Furthermore, studies have focused on quantifying the post-disaster recovery of communities subjected to tornado events using field studies and data collected through a period of time after the hazard occurrence (e.g. Kikitsu and Sarkar (2014) and Pilkington et al. (2019)). However, the available literature on computational recovery and restoration models has not been validated with the real-world data related to long-term recovery patterns and trajectory of communities. It is of great importance to validate recovery and restoration models which may be later used to predict recovery trajectories associated with various forms of pre-disaster preparedness and post-disaster decision making actions. Unlike studies focusing on the structural response of the built infrastructure, where experimental studies can easily be used to validate and evaluate the efficiency of numerical models, for studies concerned with the recovery of communities impacted by natural hazards, data collected from "living laboratories" (i.e., impacted communities) are needed to validate recovery models. Such data may take a long period of time to be collected due to the nature of the community recovery process, but there is a need to identify a systematic approach of using them for the numerical model validation process.

Towards that direction, the current study focuses on validating and calibrating a probabilistic methodology for quantifying restoration time of built infrastructure subjected to tornado loads through functionality/repair time fragility models developed by Koliou and van de Lindt (2019) and using long-term recovery data collected for the city of Joplin, Missouri, following the 2011 tornado. The May 22, 2011 Joplin tornado in

Missouri, has been classified as the deadliest and costliest single tornado in the U.S. which resulted in approximately $3 billion in economic losses (Kuligowski et al., 2014). This tornado event was a catastrophic EF-5 multiple-vortex tornado that reached a maximum width of 1.6 km (1 mile) along its path, as shown in Figure 1. A total of 7,964 buildings were damaged including 7,411 residential and 553 non-residential buildings (Kuligowski et al., 2014). Approximately 43% of the residential buildings were classified as destroyed with extensive or complete damage states resulting in significant economic losses and contributing to 59% of the total building related fatalities. Non-residential buildings, including major regional hospitals, public schools, churches, fire stations as well as commercial buildings, were also severely damaged (Kuligowski et al., 2014).

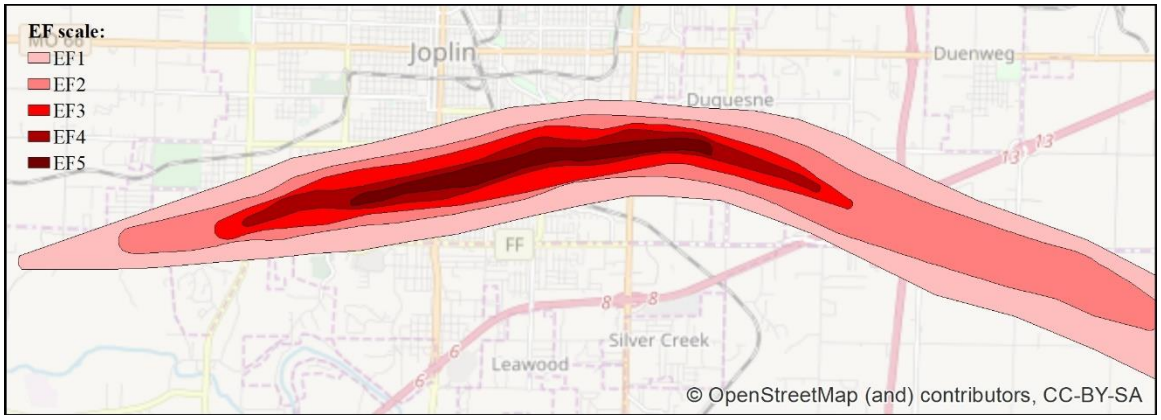

Figure 10: Path of 2011 Joplin tornado

A summary of the analytical framework to generate repair time fragility models is first presented in this study for a set of archetypes designed to represent the building stock of the city of Joplin. Then, the dataset of spatial videos documenting the recovery of Joplin in a five-year period after the catastrophic tornado collected through a

longitudinal field study is described along with the main findings associated with the linkage between the video recordings and recovery/functionality states. Empirical functionality fragility curves are also developed using the collected dataset to be compared with the analytical fragilities. Given that the analytical fragilities developed by Koliou and van de Lindt (2019) did not include the effect of any impeding factors (i.e., any factor which impedes the initiation of the building repair, such as construction permitting delays) on the recovery process, an approach is proposed in this study to further account for such factors and combine them with the analytical models for a more realistic representation/prediction of the recovery path of the building stock subjected to tornado loads.

The resulting functionality fragility models in this study may be applicable in other studies focusing on evaluating the recovery time of communities subject to different tornado scenarios. A large number of studies in the literature have utilized impact models (e.g., damage fragility functions Bayesian damage ratio models) in risk analysis frameworks, including performance-based engineering (PBE) and structural reliability-based studies, to perform risk-based analysis for decision making. The goal of these studies was to decrease the extent of impacts and enhance the reliability of the systems subject to natural hazards (M. Aghababaei & Mahsuli, 2019; Mohammad Aghababaei & Mahsuli, 2018; Attary, Unnikrishnan, van de Lindt, Cox, & Barbosa, 2017; Cornell & Krawinkler, 2000; Han et al., 2017). The functionality fragility models developed in this study provide additional information beyond direct impacts to include functional recovery of buildings, which is a pre-requisite for risk-based community

recovery studies. The outcomes of such studies may be strategies to mitigate the direct consequences as well as strategies to speed up the restoration process.

3.2. Probabilistic models for building restoration and recovery time predictions

Metrics meaningful to stakeholders and building owners (dollars, death, and downtime (Cornell & Krawinkler, 2000)) already accounted for in the existing studies are not sufficient or useful to fully evaluate the recovery trajectory of the built infrastructure and propose risk-informed decisions in terms of retrofit strategies or emergency response. Although downtime is a reflection of the repair time of the building, it does not fully capture the recovery trajectory of the building considering its different sequential functionality levels; rather, it only represents the time it takes for a damaged building to be completely repaired. To address this, a post-disaster building repair time methodology that incorporates the basic principles of PBE, and combines them with repair and functionality analyses to allow quantification of building functionality through a series of probabilistic simulations was introduced (Koliou and van de Lindt (2019)). The outcome of the methodology is repair time fragility curves, which define the probability of achieving a specified level of building functionality after a certain time period following the event occurrence and given the initial damage state of the buildings. Although the methodology is generic and could be applied to any hazard, it was applied to a minimum size community building portfolio based on the city of Joplin that was developed by Memari et al. (2018) subject to tornado hazard. This building portfolio is comprised of 19 building types of different occupancies and construction practices

representative of the city of Joplin, as tabulated in Table 1. Tornado fragility curves were developed by Memari et al. (2018), Masoomi and van de Lindt (2016), Masoomi et al. (2018), and Koliou et al. (2017), and were considered for the 19 building types of the proposed portfolio.

This methodology, which consists of four discrete steps, namely, (i) performance-based engineering analyses (e.g., hazard characterization, structural analysis, and damage analysis), (ii) repair characterization, (iii) functionality analysis for each building component, and (iv) functionality analysis/evaluation of the building system, was used to assess the risk and vulnerability of the Joplin community subjected to tornado loads. Four damage states (minor, moderate, extensive and extreme) were considered as described in Table 11 for building type T4 (residential) and were associated with performance levels (i.e., safe and operational, safe and usable during repairs, safe and not usable, and unsafe/partial or complete collapse) as well as business status (i.e., fully open, partially open, and fully closed) per NIST (2015) in order to associate structural damage to certain post-disaster functionality levels and recovery trajectory.

Table 10: Summary of community building portfolio (after Memari et al. 2018)

Building Type	Building Description	Area (m^2)	Occupancy Class
T1	Wood residential bldg. - small rectangular plan - gable roof - 1 story	125.51	
T2	Wood residential bldg. - small square plan - gable roof - 2 stories	169.74	
T3	Wood residential bldg. - medium rectangular plan - gable roof - 1 story	216.25	Residential
T4	Wood residential bldg. - medium rectangular plan - hip roof - 2 stories	146.51	
T5	Wood residential bldg. - large rectangular plan - gable roof - 2 stories	291.81	
T6	Business and retail building (strip mall)	2,787	Commercial
T7	Light industrial building	465	Industrial
T8	Heavy industrial building	3,716	
T9	Elementary/middle school (unreinforced masonry)	9,290	Education
T10	High school (reinforced masonry)	23,226	
T11	Fire/Police station	110	Government
T12	Hospital	10,220	Commercial
T13	Community center/Church	1,394	Religion/ Non-profit
T14	Government building	8,175	Government
T15	Large big-box	14,865	Commercial
T16	Small big-box	929	Commercial
T17	Mobile home	68	Residential
T18	Shopping center	3,716	Commercial
T19	Office building	446	Commercial

Table 11: Summary of damage combination, performance level, business status and functionality level for T4 (residential) (after Koliou and van de Lindt 2019)

Functionality Level (FL)	Performance Level	Business Status	Damage combination	Description of damage combination			
				Roof Cover Failure	Window/Door Failures	Roof Sheathing Failure	Roof Truss Failure
FL0	Safe & operational	Fully open	--	--	--	--	--
FL1	Safe & operational	Partially open	DM1	> 2% and ≤ 15%	1	No	No
FL2	Safe & usable during repair	Partially open	DM2	> 15% and ≤ 50%	2 or 3	1-3	No
FL3	Safe & not usable	Fully closed	DM3	> 50%	> 3	>3 and ≤ 35%	No
FL4	Unsafe – partial or complete collapse	Fully closed	DM4	Typically > 50%	Typically > 3	> 35%	Yes

Repair time fragility curves for reaching various levels of functionality based on the initial functionality (and associated damage state) as well as through the

reconstruction/repair process advancing from one functionality level to the next were computed based on the study by Koliou and van de Lindt (2019). All of the parameters for generating the cumulative distribution functions following a lognormal distribution were considered for the purpose of the current study. A sample of a repair time fragility curve reaching a full functionality of FL0 for the residential archetypes T1-T5, conditioned on initial functionality levels (FL1, FL2, FL3, or FL4) is shown in Figure 11. It should be noted that the results of this study did not include the effect of impeding factors on the recovery time but focused solely on the repair/reconstruction based on the initial damage and associated functionality level.

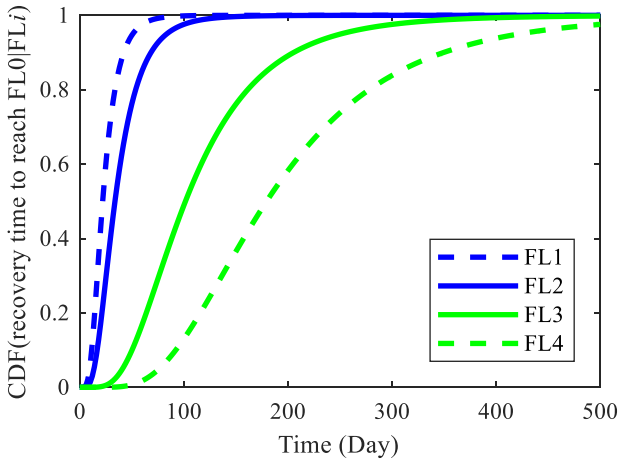

Figure 11: Functionality fragility curves for reaching FL0 for residential archetypes (T1-T5) conditioned on different levels of functionality (FLs)

3.3. Joplin tornado building damage and recovery assessment – Documented data

For the purpose of the current study, a dataset collected from a longitudinal field study conducted in the city of Joplin, MO, after the Joplin Tornado was utilized (Pilkington et al., 2019). The aim of this longitudinal field study was to capture the recovery evolution

throughout the city from 2011 to 2017. For this purpose, spatial videos were recorded to capture an appropriate view of the approximate environment along with geospatial information. This was accomplished with a Global Positioning System (GPS) receiver and a video camera working simultaneously. By syncing the videos and GPS data in an appropriate software, a certain GPS coordinate was assigned to each video frame. This method was applied in a number of studies to capture damage as well as restoration after disasters (Curtis et al., 2015; Curtis & Fagan, 2013; Curtis & Mills, 2012; Mills, Curtis, Kennedy, Kennedy, & Edwards, 2010).

The first run of observations was conducted on June 14, 2011, to have an appropriate overview of the damage in the community (Curtis & Fagan, 2013) shortly after the tornado occurrence. In this run as well as the following observations between 2011 and 2012, a set-up of separate video cameras (three Panasonic PV-GS500) and a GPS receiver (Red Hen Systems GPS receiver) were utilized to capture the data. The resulting videos were processed through an extension of ArcGIS called Red Hen's MediaMapper that shows the video frames and locations as points in Geographical Information System (GIS) at the same time. After the upgrade in this technology, the previous set-up was replaced with Contour +2 video cameras (Curtis et al., 2015), which were smaller, easier to operate, and had an internal GPS receiver. The videos were recorded by driving through the pre-determined routes in the city, and the resulting videos were displayed in bespoke software, and locations were extracted (Ajayakumar, Curtis, Smith, & Curtis, 2019).

According to Attary et al. (2018), the total number of buildings located within the Joplin tornado path was 7,912, out of which 3,058 buildings were included in this longitudinal study to record their recovery trajectory over a five year period. In order to describe the recovery of the community through time, each building at each run was labeled with a recovery state score proposed by Pilkington et al. (2019) using the descriptions in Table 12 (see first four columns) based on the physical observations from the videos. Two scores were used to describe the recovery state of the buildings: *Score 1* that indicates the overall recovery state by six states: (i) uninhabited, (ii) cleared, (iii) rebuilding, (iv) rebuilt and occupied, (v) no rebuild/new structure, and (vi) new archetype built; and *Score 2* that indicates the sub-category of the recovery states that require further classification (namely, uninhabited and rebuilding states).

Table 12: Recovery states per Pilkington et al. (2019) and corresponding functionality levels per Koliou and van de Lindt (2019)

Recovery State (Score1)	**Description**	**Sub-Category (Score 2)**	**Elaboration**	**Functionality Level** (Koliou and van de Lindt (2019))
		2	Livable: unoccupied	FL1
1	Uninhabited	5	Blighted	FL3
		10	Non-livable: extreme	FL4
2	Cleared		Lot empty due to destroyed home or clear for reconstruction	FL4
3	Rebuilding	1	Frame skeleton is up. This would only appear for homes needing a complete rebuild.	FL3
		2	Walls are enclosed	FL3
		3	Non-structural components have been added. Likely that DS 2&3 would not require more than this level of construction.	FL2
		4	Cosmetic finishes being applied	FL1
4	Rebuilt and Occupied		"Good as new"	FL0
5	No rebuild/new structure		Abandoned lot	FL4
6	New archetype built		New structure of different zoning designation	FL0

At this stage, in order to employ the resulting dataset into validating and calibrating the functionality fragility functions proposed by Koliou and van de Lindt (2019), it was necessary to correlate the recovery states presented in Table 12 with functionality levels of Table 11. To do so, a column was added to the table proposed by Pilkington et al. (2019), as shown by the last column in Table 12, correlating the relative functionality levels (FL) per Koliou and van de Lindt (2019) by comparing the descriptions in Table 12 and Table 11.

Error! Reference source not found. demonstrates the Functionality Level (FL) of the inspected buildings throughout Joplin during a five-year period as recorded for six

time intervals: (a) one year, (b) one and a half years, (c) two years, (d) three years, (e) four years, and (f) five years after the tornado occurrence. Five shades of red are used to represent the five functionality levels - FLs (FL0 to FL4), such that more intense red indicates a worse condition, i.e., lower level of functionality close to FL4, and lighter red indicates a better condition, i.e., close to FL0. Gray color indicates buildings which were not inspected in that specific inspection time. As **Error! Reference source not found.**a shows, a large portion of the buildings are classified as FL4 which is the lowest level of functionality, i.e., they are fully closed. **Error! Reference source not found.** clearly shows the gradual decrease in the number of buildings classified as FL4 through time and increase of buildings moving to a higher functionality level. A sudden significant decrease in the percentage of buildings labeled as FL4 in the third run of inspection (24 months) compared with the year before it can be observed in **Error! Reference source not found.**c. However, the gradual increase in the functionality of the buildings in the city slowed down in the next inspections (see **Error! Reference source not found.**d, e, and f for three, four and five years, respectively, after the 2011 tornado), and in the last inspection (60 months) there remained a considerable portion of damaged and not recovered buildings. This could mainly be attributed to the fact that those buildings were abandoned, and no recovery effort was initiated by the time they were inspected and hence, no recovery progress was observed within the five-year period.

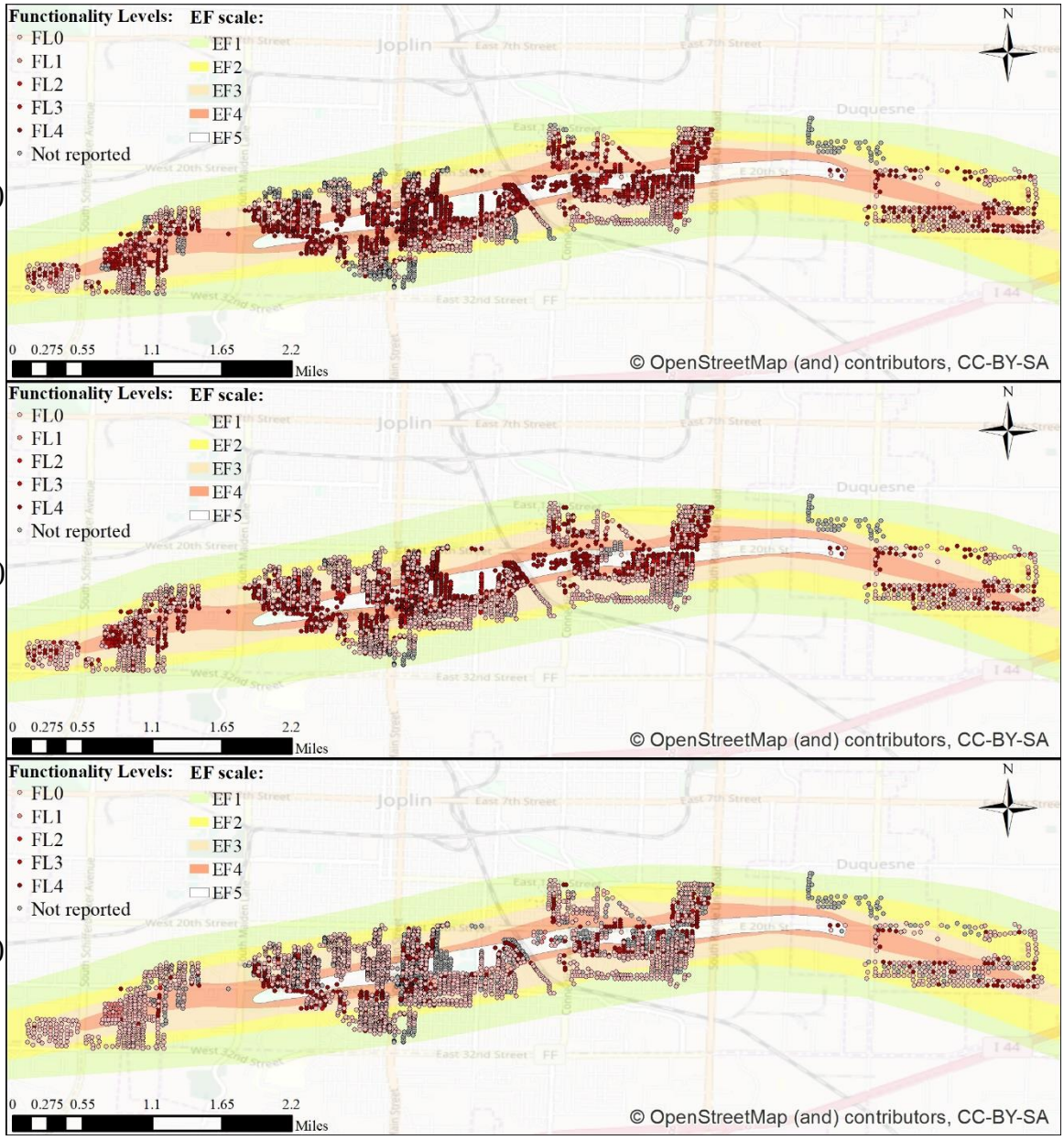

Figure 12: Spatial distribution of the functionality level of the inspected buildings after (a) one year, (b) one and a half years, (c) two years, (d) three years, (e) four years, and (f) five years from the Joplin tornado.

(d)

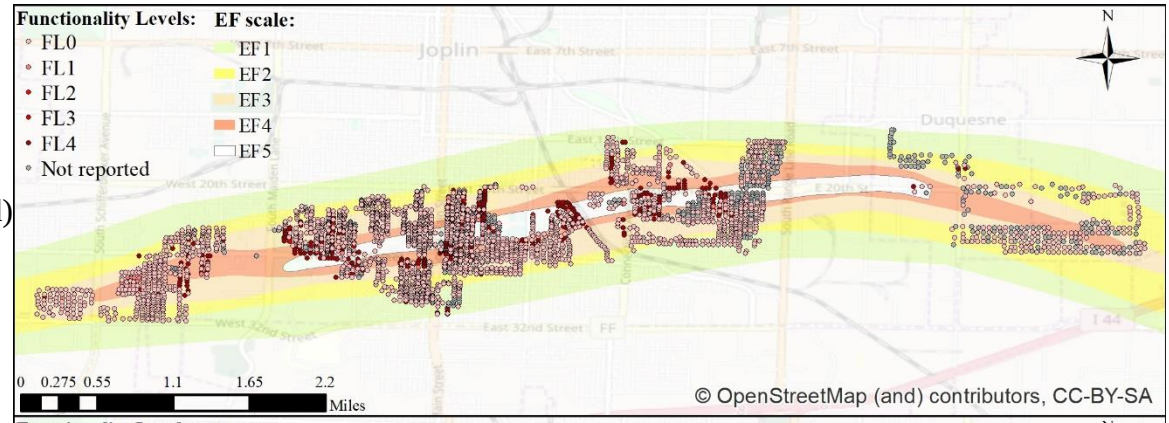

(e)

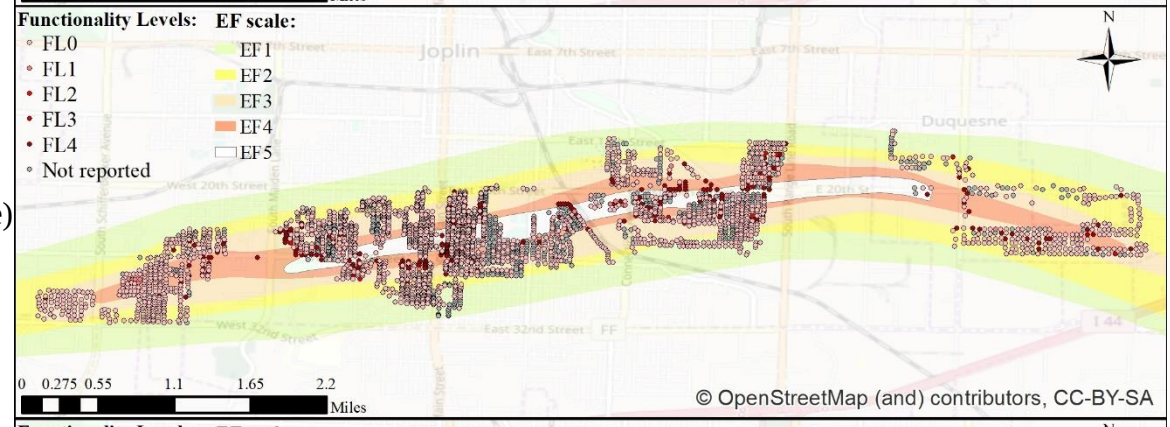

(f)

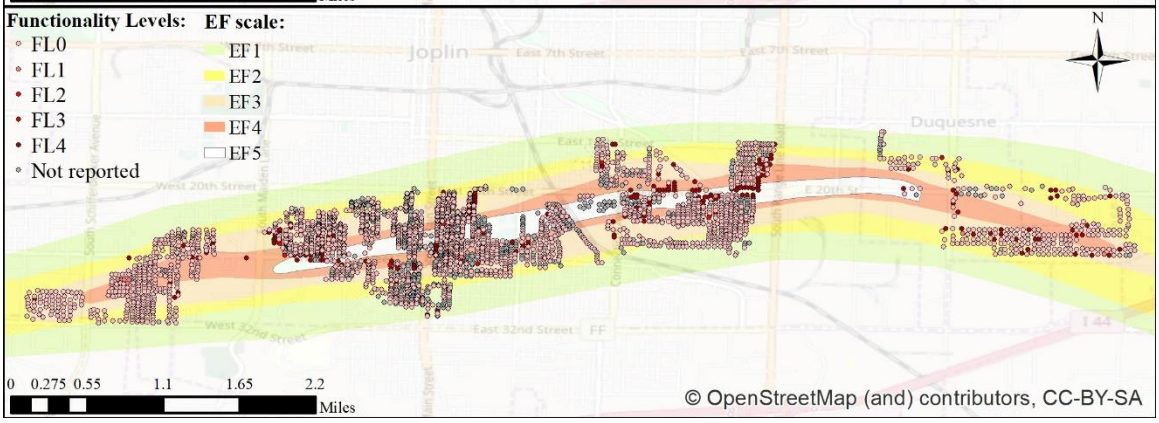

Figure 12 Continued.

Figure 13a presents the distribution of the initial damage state throughout the city of Joplin, and as it shows a considerable portion of the buildings (>41%) were classified as DS4 right after the tornado. Figure 13b shows the distribution of recovery time of the inspected buildings through time (from year 1 to year 5+). It is observed that only 151

buildings out of 3,058 were fully functional (FL0) right after the tornado, while the largest amount of recovered buildings was identified during the first year, such that 854 other buildings went back to full operation within a year after the tornado. A large portion of the inspected buildings (>64%) returned to full operation within the first two years after the tornado. However, the recovery pace slowed down after two years, and a total of 433 buildings (>14%) did not recover at all within the first five years after the tornado. Figure 13c demonstrates the percentage of the recovered buildings at each year after they are classified based on their initial damage state. As this figure shows, a considerable portion of the buildings classified as DS1, DS2, and DS3 were fully recovered during the first year, and the recovery pace decreased in the following years, while a small percentage (4%, 6%, and 7% for DS1, DS2 and DS3, respectively) of them were not fully recovered within the five years aftermath. On the contrary, the recovery of the buildings initially classified as DS4 spreads widely between the years with approximately 53% of them to be recovered within the first two years. More specifically, based on the results of Figure 13c, the largest percentage of the buildings classified as DS4 were recovered between 18 and 24 months following the disaster, while approximately 19% of those buildings were not recovered at all within the first five years.

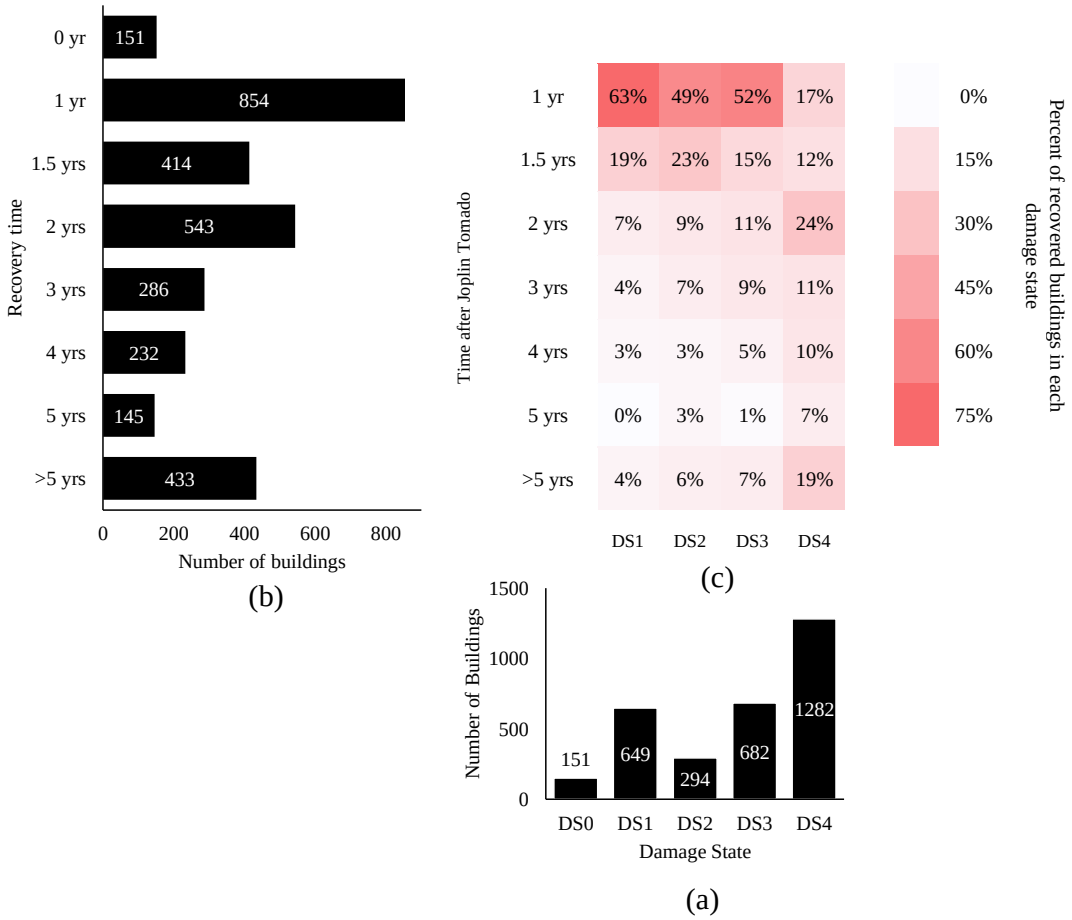

Figure 13: Distribution of: (a) buildings' initial damage state, (b) buildings' recovery time, and (c) percentage of recovered buildings at each year per their initial damage state.

3.4. Comparison of predicted and documented time-dependent repair recovery trajectory

In this section, the empirical results for the time-dependent repair recovery trajectory resulting from the longitudinal field study in the city of Joplin are compared to the analytical results from the work conducted by Koliou and van de Lindt (2019). A discussion is provided to explain discrepancies between the empirical and analytical results, and how to adjust analytical outcomes to more realistically capture the recovery

trajectory analytically accounting for the impeding factors. The analytical functionality fragility curves were generated for different archetypes using their analytical predictions with an example shown earlier in this chapter (Figure 11). These fragility curves quantify the probability of reaching specified functionality levels at a certain amount of time conditioned on the initial functionality level (and associated damage). In order to compare the results of the analytical study with the empirical results presented in the current study for a five-year period, empirical functionality fragilities were developed in the same manner. Fragility functions were developed for seven of the archetypes presented in Table 10, namely, residential wood buildings (T1-T5), business and retail buildings (T6), and office building (T19), which correspond to the archetypes included in the video datasets. The resulting fragility functions are tabulated in Table 13 along with their corresponding fragilities from the analytical study provided in parentheses. Fragility functions are defined by lognormal distributions with mean λ and standard deviation ξ, as presented in Table 13. Each fragility function in this table is defined for a building reaching a specified functionality level (second row of Table 13) conditioned on its initial functionality level (second column of Table 13). For example, the functionality fragility of residential wood buildings (T1-T5) with initial functionality level of FL4 that reaches functionality level of FL0 is described as a Lognormal (6.60, 0.53^2) using the empirical dataset in the current study, and is described as a Lognormal (5.19, 0.52^2) per the analytical study. A number of cells in Table 13 do not contain numbers, where dash ("—") indicates that this functionality fragility cannot be defined (e.g., there is no fragility with initial functionality of FL2 and reaching functionality of

FL3 since it means getting worse), and "N/A" indicates that there were not enough data points in the empirical dataset to develop an appropriate fragility (such data were not captured over the five-year longitudinal field study).

Table 13: Fragility function distributions for archetypes T1-T5 (residential wood building), T6 (business and retail building (strip mall)), and T19 (office building) for reaching different functionality levels (FL3 to FL0) conditional on their initial functionality level (FL4 to FL1)

	Reached functionality level	*FL3*		*FL2*		*FL1*		*FL0*	
Archetype ID	**Initial Functionality**	λ^*	ζ^*	λ^*	ζ^*	λ^*	ζ^*	λ^*	ζ^*
T1-T5	**FL4**	6.13 (2.71)	0.33 (0.52)	6.49 (3.42)	0.60 (0.52)	6.39 (4.78)	0.48 (0.52)	6.60 (5.19)	0.53 (0.52)
	FL3	—	—	5.56 (3.10)	0.46 (0.55)	5.74 (3.79)	0.55 (0.55)	5.90 (4.62)	0.60 (0.55)
	FL2	—	—	—	—	5.87 (2.89)	0.35 (0.55)	6.06 (3.52)	0.32 (0.55)
	FL1	—	—	—	—	—	—	5.90 (3.09)	0.50 (0.51)
T6	**FL4**	N/A	N/A	N/A	N/A	N/A	N/A	6.64 (5.05)	0.50 (0.60)
	FL3	—	—	N/A	N/A	N/A	N/A	5.82 (4.51)	0.46 (0.55)
	FL2	—	—	—	—	N/A	N/A	N/A	N/A
	FL1	—	—	—	—	—	—	N/A	N/A
T19	**FL4**	N/A	N/A	N/A	N/A	N/A	N/A	6.45 (5.32)	0.51 (0.55)
	FL3	—	—	N/A	N/A	N/A	N/A	N/A	N/A
	FL2	—	—	—	—	N/A	N/A	N/A	N/A
	FL1	—	—	—	—	—	—	6.40 (1.45)	0.50 (0.55)

*Units: ln(days) [e^{λ} = days]

There are moderate to significant differences between the empirical and analytical results for all fragility functions presented in Table 13. Further examination reveals that all empirical fragilities have larger mean values compared to the analytical fragilities, which indicates that it takes longer time for the buildings to recover from a functionality level to a higher level in "living communities". Reasons causing such differences are discussed in detail in the next section followed by methods to calibrate the analytical results.

Figure 14a-d present fragility functions of residential buildings (T1-T5) for reaching higher functionality levels conditioned on four initial functionality levels namely FL4, FL3, FL2, and FL1, respectively. Three types of curves are shown to compare analytical and empirical results: (i) empirical cumulative distribution function (CDF) of the time that took for the buildings in Joplin to recover from the initial functionality levels to higher functionality levels, (ii) empirical functionality fragilities developed using the dataset developed herein, and (iii) analytical fragility curves developed by Koliou and van de Lindt (2019).

(a)

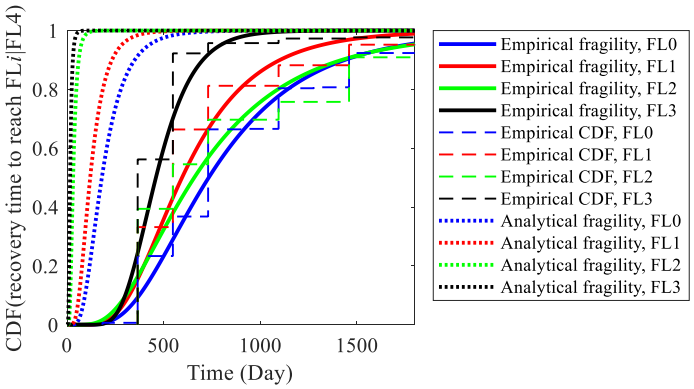

(b)

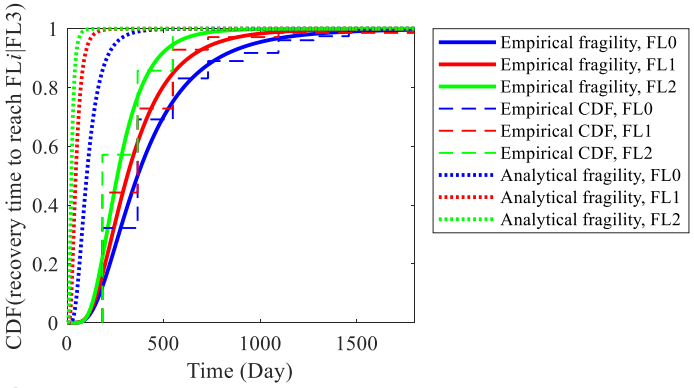

(c)

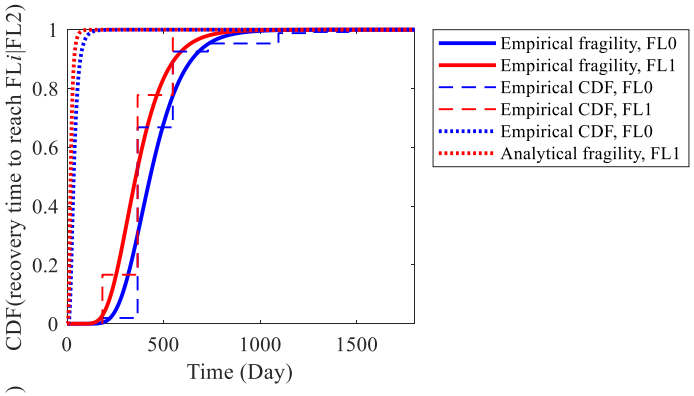

(d)

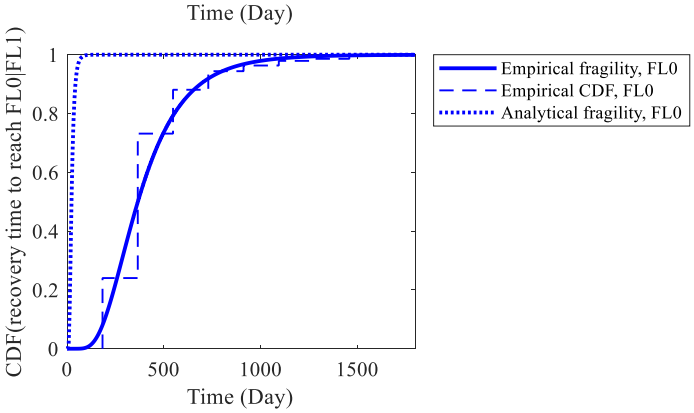

Figure 14: Functionality fragility curves to reach various levels of functionality from starting functionality level of (a) FL4, (b) FL3, (c) FL2, and (d) FL1.

Figure 14a demonstrates the abovementioned curves for the cases that the residential building archetypes start with functionality level FL4 associated with tornado-induced damages. Note that the number of data points available to develop each one of the empirical fragilities for reaching FL0, FL1, FL2, and FL3 are 1,846, 424, 32, and 258, respectively. Although it is expected that fragility curves for reaching higher functionality levels would appear below lower functionality levels (since they are reached faster, e.g., reaching FL3 is expected to be faster and easier than reaching FL0 assuming that the starting functionality level is FL4), in Figure 14a it is shown that the empirical fragility for reaching FL2 (green) is lower than the one for reaching FL1 (red). This may be attributed to the fact that a low number of data points (32 building samples) were available to develop the FL2 fragility which increases its uncertainty. It should be noted that the relatively small number of time intervals may also cause an undesirable fit for the fragility functions regardless of the number of the data points, and hence, it could also be a reason for such unexpected behavior. The analytical fragilities are presented in this figure for comparison purposes with the same colors used for empirical curves but with dashed lines. It is observed that the analytical curves are shifted to the left side of the figure which means that there is a considerable "gap"/difference between the analytical curves with their corresponding empirical ones, as also identified in Table 13 and discussed earlier in this chapter. Figure 15 depicts the differences between the mean value of the empirical and analytical fragilities in the unit of days ($\mu_{\text{empirical}}$-$\mu_{\text{analytical}}$ [days]). This figure indicates that for the fragility functions presented in Figure 14a, the

largest gap between the empirical and analytical fragilities is observed in FL2 (with 628 days) fragilities, followed by FL0 (with 556 days) fragilities.

Figure 14b demonstrates the functionality fragility curves for the residential buildings with an FL3 initial functionality level after the tornado happens. The number of data points used here to develop the empirical fragility curves for reaching FL0, FL1, and FL2 are 509, 70, and 7, respectively. Again, there are moderate differences between the empirical and analytical fragilities as Figure 14b demonstrates, while these differences are considerably less than what was observed in Figure 14a for the cases with starting functionality of FL4. This is confirmed by Figure 15 showing that all fragilities have differences less than a year with the largest (267 days) for FL1 fragility.

Figure 14c presents the functionality fragility curves for the residential buildings with the initial functionality level of FL2. The number of data points used here to develop the empirical fragility curves for reaching FL0 and FL1 are 256 and 18, respectively. As this figure indicates, there are considerable differences between the analytical and empirical curves, while as shown in Figure 15, this gap is around one year with the largest difference for FL2 fragility (395 days).

Finally, the fragility curve for residential building archetypes associated with an initial functionality of FL1 that reach the full functionality level of FL0 is shown in Figure 14d. The number of data points used to develop the empirical fragility was 570. As Figure 15 also indicates, the difference between the mean value of the empirical and analytical fragilities was around a year (343 days). Note that the number of available data points for developing the empirical CDF and fragility curves are provided because a

small sample number can adversely affect the integrity of the CDF curves as well as their fitted fragilities and therefore the associated findings for this study.

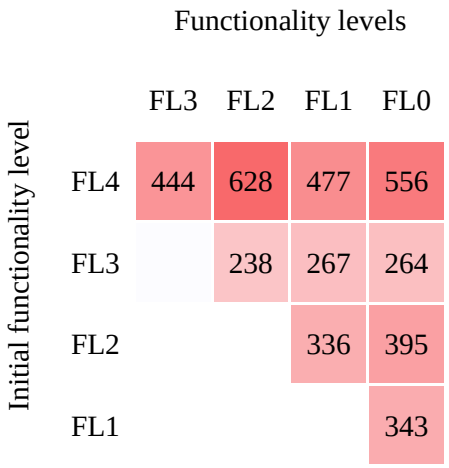

Figure 15: Difference between mean values of the empirical and analytical functionality fragilities in the unit of days.

3.4.1. Discussion and proposed updates

In this section, the reasons causing the differences between the analytical and empirical results presented in the previous section are discussed along with the proposed modifications to calibrate the analytical framework in order to converge its results closer to the real-world empirical data collected after the Joplin Tornado.

The analytical fragilities were developed considering the perfect restoration and reconstruction conditions with sufficient financial, material, and labor-work resources without any form of delays (associated impeding factors). However, this may not be a realistic case following major disasters. Various post-disaster data reconnaissance studies have reported major delays before initiating the repair and restoration of the damaged infrastructure systems (Mohammad Aghababaei et al., 2018; Chang, Wilkinson, Potangaroa, & Seville, 2010), while the construction/project management

literature also emphasizes that there are delays even during the construction phase (Fugar & Agyakwah-Baah, 2010; Kazaz, Ulubeyli, & Tuncbilekli, 2012; Odeh & Battaineh, 2002). The extent of the delays for repair/reconstruction may not be uniform throughout the community and a wide range of factors affect such delays, such as the building occupancy (e.g., residential, different types of businesses, and governmental facilities), building characteristics (e.g., age, distance from the hazard source, and construction type), available financial resources (e.g., financial aid and family resources), loss mitigation actions pre-disaster (e.g., purchasing insurance policies), the overall status of the community after the disaster (e.g., level of income, education, and socio-demographic characteristics), etc.

Lin and Wang (2017) proposed a building portfolio recovery model to predict the recovery trajectory of buildings after major disasters where the waiting time of a building reaching a higher functionality state was computed accounting for the initial delays, the repair time to reach that functionality state, and the utility disruption. Lin and Wang (2017) proposed the following equation to calculate the delay time to initiate the repair:

$$T_{delay} = T_{\text{insp}} + Max\{T_{\text{fina}}, T_{\text{conm}}, T_{\text{engm}}\} + T_{\text{perm}} \quad (16)$$

where, T_{insp}=time needed to inspect the building, T_{fina}=time to collect sufficient financial resources for conducting the repair (based on the building's access to various financial resources, including the Small Business Administration (SBA) loans, insurance payouts, private loans, and also if the building has no coverage), T_{conm}=time to employ

engineers/architects/contractors and for the bidding process, T_{engm}=time to design/redesign and planning, and T_{perm}=time to get permit. The method utilized by Lin and Wang (2017) to estimate and compute the delays was captured from the REDi^{TM} framework (Almufti & Willford, 2013a), which is a framework to estimate the impeding factors after earthquake events. In addition, the probability distributions for each of the aforementioned delays in Equation (16) were adopted from the REDi^{TM} framework (Almufti & Willford, 2013b).

In this chapter, in order to fill the gaps between the analytical and empirical fragilities presented in the previous section and calibrate the analytical fragilities, a number of alternative methods to include the delays in generating analytical fragilities are examined and the results are compared. For so doing, these delays are added to the computed building-level repair times generated using the analytical approach proposed by Koliou and van de Lindt (2019) in a probabilistic manner, and the updated functionality fragilities are generated afterwards. The extent of the delay caused by a number of these impeding factor (e.g., delays due to permitting, inspection, and engineering/redesigning) is dependent on the damage level of the building, and hence, different delay distributions are considered depending on the building damage state. Using the method proposed by Lin and Wang (2017) and the delay distributions employed from REDi^{TM} framework (Almufti & Willford, 2013b), per Equation (16) to include the delays in the analytical fragilities, resulted in large discrepancies with the empirical fragilities. As an example, the resulting analytical fragilities for residential buildings conditioned on the initial functionality level of FL4 are demonstrated in Figure

16 along with the empirical fragilities developed in the current study. The analytical fragilities in this figure clearly indicate overestimation of the recovery time compared to the empirical ones.

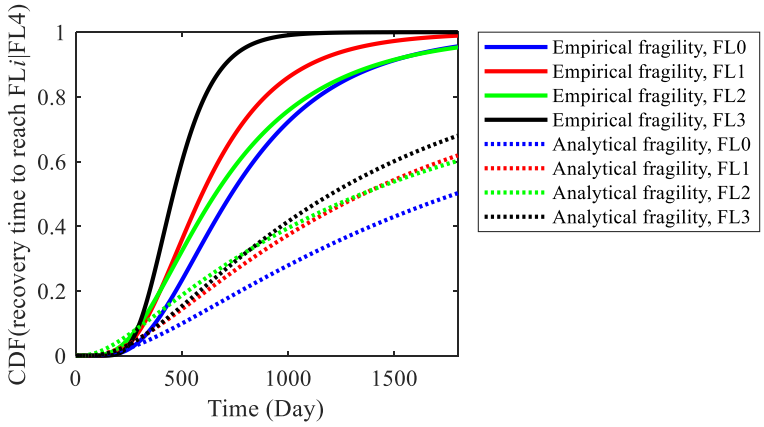

Figure 16: Functionality fragility of residential buildings to reach various functionality levels with initial functionality level of FL4 (this figure includes the empirical fragilities developed in this study and the updated analytical fragilities using Equation (16))

In order to modify the results for the purpose of this study, two approaches are considered: (i) modifying Equation (16) to be closer to the reality, and specially to be more appropriate for the weather-related events (both approaches by Lin and Wang (2017) and the REDi^{TM} framework (Almufti & Willford, 2013b) were developed for earthquakes), and (ii) using real-world data to have more representing probability distributions for different types of delay. As a result, the following equation was proposed to include the delays into the analytical functionality fragilities:

$$T_{delay} = T_{\text{insp}} + Max\{T_{\text{fina}}, T_{\text{conm}}\} + T_{\text{perm}} \quad (17)$$

where, T_{engm} is eliminated in Equation (17) due to reasoning that, for low-rise wood residential buildings in the U.S. (which represents the majority of the dataset in the

current study), there is no need to employ an engineer, and usually the whole process is conducted by the contractor, and hence, there is no need to consider it as a separate delay. It should be noted that this assumption may differ for communities outside the U.S. and regions in the U.S. with high seismic hazard (such as California), and there might be requirements to hire an engineer in order to redesign and repair the building. In addition, according to the previous weather-related disasters, there are much smaller portion of buildings experiencing major structural damage compared to earthquake events, and as a result, there is less need to redesign the building. The second modification/adjustment adopted in the current study is related with the use of data collected in prior disasters. More specifically, a dataset collected in Galveston, TX, after Hurricane Ike related to delays associated with SBA loans and permitting time was considered. Although this study focused on a wind related event, the SBA loan and permitting distribution data should be somewhat representative of conditions in a typical community impacted by a natural hazard. The distributions of the time to receive an SBA loan disbursement and the time to the first construction permit are updated as presented in Table 14 and Table 15, respectively, using the real-world administrative data collected after Hurricane Ike in Galveston, TX, conditioned on the initial damage state (Dustin, 2010; Watson, 2019).

Table 14: Number of days to SBA loan disbursement.

Damage State	mean	median	standard deviation	min	max
DS1	128.0	125	58.8	45	299
DS2	123.1	109	62.9	44	303
DS3	140.3	115	93.8	37	752
DS4	177.4	136	138.8	33	1,053

Table 15: Number of days to first permit (any).

Damage State	mean	median	standard deviation	min	max
DS1	123.9	67	122.2	10	502
DS2	136.1	93.5	120.2	10	503
DS3	111.0	67	105.3	10	503
DS4	111.4	67	101.5	10	502

All of the analytical fragilities presented in Table 13 and Figure 14 were updated using the modification method proposed here, and the updated results are summarized in Table 16 and Figure 17. Table 16 is generated similarly to Table 13 but with the updated statistics of the analytical fragilities provided in parentheses instead of the ones from Koliou and van de Lindt (2019). The statistics of the updated analytical fragilities in this table are much closer to the statistics of the empirical ones with a few exceptions. To better illustrate, the comparison between the updated/revised analytical fragilities accounting for impeding factors and the empirical ones for residential buildings is graphically shown in Figure 17. As shown in this figure, the updated analytical fragilities are now closer to the real-world empirical fragilities compared to the ones presented in Figure 14. The updated analytical fragilities in this figure are more accurate approximations of the empirical ones, and hence, the analytical method proposed by Koliou and van de Lindt (2019) to develop repair time fragilities are better representations of the real-world aftermath conditions when combined with the modification method proposed in this study.

Figure 17a shows the functionality fragilities for the residential buildings with the initial functionality level of FL4. It is observed that the analytical fragilities reaching functionality levels of FL0 and FL1 are good approximations of the empirical ones.

However, this is not the case for the fragilities of reaching FL2 and FL3. As mentioned previously in this chapter, the empirical fragility for reaching FL2 may not be accurate due to lack of sufficient data (small sample size) which may explain its discrepancy with the analytical fragility in Figure 17. Figure 17b presents the functionality fragilities for the cases with the initial functionality level of FL3 where it is shown that analytical fragilities overestimate the empirical fragilities by 67% on average. Figure 17c demonstrates the functionality fragilities for the cases with the initial functionality level of FL2, where the pattern of overestimating analytically the recovery is observed again but in a much smaller range, 22% on average. Finally, as Figure 17d represents, the analytical fragility well captures the results of the empirical fragility for residential buildings with an initial functionality level of FL1 (associated with slight damage). Although the updated/revised analytical fragility curves slightly overestimate the recovery time of the building stock in Joplin in most cases, they can be further employed in other studies related to tornado-induced damage for realistically predicting time-dependent repair recovery process and inform models associated with pre-disaster preparedness or post-disaster resource allocation.

(a)

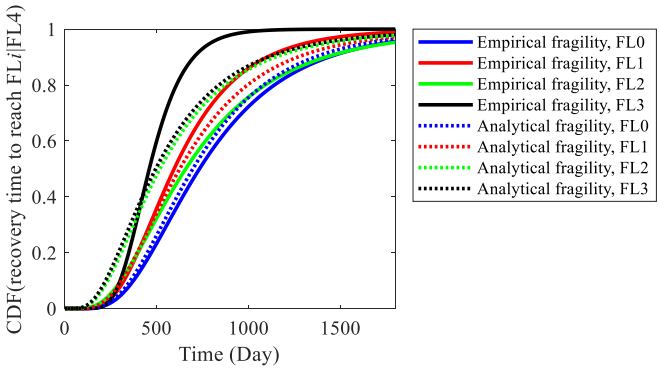

(b)

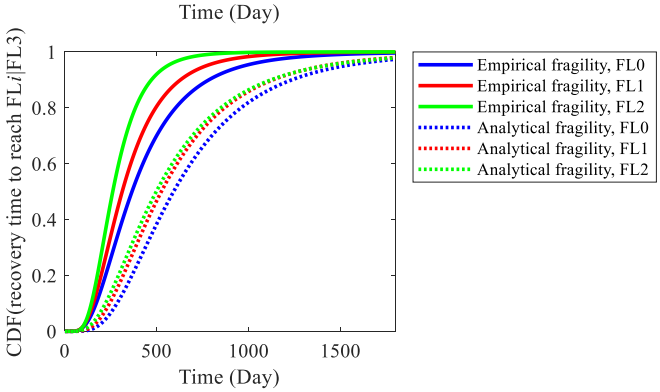

(c)

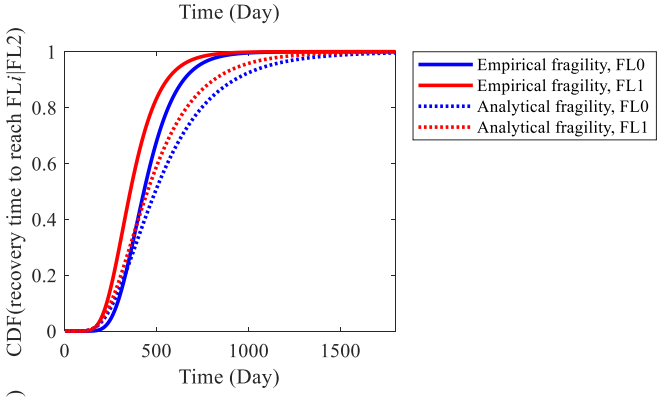

(d)

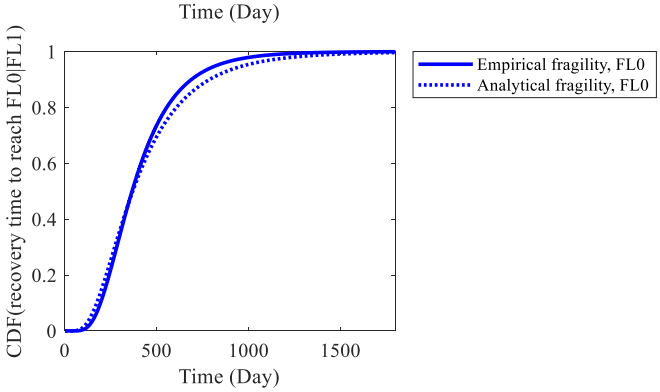

Figure 17: Functionality fragility curves to reach various levels of functionality from starting functionality level of (a) FL4, (b) FL3, (c) FL2, and (d) FL1 (these plots include the empirical fragility functions and the updated analytical fragilities using the method presented in this study).

Table 16: Distributions of the functionality fragilities (empirical and updated analytical) for archetypes T1-T5 (residential wood building), T6 (business and retail building (strip mall)), and T19 (office building) for reaching different functionality levels (FL3 to FL0) conditional on their initial functionality level (FL4 to FL1).

	Reached functionality level	*FL3*		*FL2*		*FL1*		*FL0*	
Archetype ID	**Initial Functionality**	λ^*	ζ^*	λ^*	ζ^*	λ^*	ζ^*	λ^*	ζ^*
T1-T5	**FL4**	6.13 (6.18)	0.33 (0.58)	6.49 (6.21)	0.60 (0.56)	6.39 (6.41)	0.48 (0.50)	6.60 (6.52)	0.53 (0.48)
	FL3	—	—	5.56 (6.18)	0.46 (0.58)	5.74 (6.24)	0.55 (0.56)	5.90 (6.35)	0.60 (0.51)
	FL2	—	—	—	—	5.87 (6.11)	0.35 (0.46)	6.06 (6.20)	0.32 (0.50)
	FL1	—	—	—	—	—	—	5.90 (5.90)	0.50 (0.54)
T6	**FL4**	N/A	N/A	N/A	N/A	N/A	N/A	6.64 (6.50)	0.50 (0.49)
	FL3	—	—	N/A	N/A	N/A	N/A	5.82 (6.37)	0.46 (0.52)
	FL2	—	—	—	—	N/A	N/A	N/A	N/A
	FL1	—	—	—	—	—	—	N/A	N/A
T19	**FL4**	N/A	N/A	N/A	N/A	N/A	N/A	6.45 (6.56)	0.51 (0.51)
	FL3	—	—	N/A	N/A	N/A	N/A	N/A	N/A
	FL2	—	—	—	—	N/A	N/A	N/A	N/A
	FL1	—	—	—	—	—	—	6.40 (5.81)	0.50 (0.63)

*Units: ln (days) [e^{λ} = days]

3.5. Summary and Conclusions

This chapter assesses and then calibrates the analytical repair time fragilities available in the literature for buildings subject to tornado events with empirical fragilities developed in this study using the restoration data of a five-year field study in the city of Joplin after the catastrophic 2011 Joplin tornado. In this longitudinal field study, a method utilizing spatial videos was employed to efficiently collect the visual recovery observations along with geospatial information. The collected dataset was later post-processed to assign an appropriate functionality level to each building at each of the six time intervals of this study (1, 1.5, 2, 3, 4, and 5 years after the tornado). Findings concerning the recovery trajectory of the community extracted from this longitudinal study showed that from 3,058 inspected buildings in Joplin, only 151 buildings were fully functional immediately after the tornado, while 64% of the buildings completely recovered within the first two years from the event. It was also observed that the recovery pace is related to the initial damage of the building, such that the buildings experienced the highest damage state (DS4) had a considerably slower recovery rate compared to the other buildings, and 19% of them did not recover within the first five years after the tornado.

Empirical functionality fragilities were also generated in this study using the post-processed dataset of the Joplin Tornado longitudinal study. The resulting empirical fragilities were compared with the analytical repair time fragilities developed by an existing study, which showed considerable differences. The main cause of the differences between the analytical and empirical fragilities highlighted herein were that the analytical fragilities did not account for the effect of impeding factors (such as delays

associated with inspection of the damaged buildings, acquisition of construction permit and adequate financial resources, as well as identification of available contractor crews) in the recovery process. To address that, a method was proposed herein to modify the analytical results by including various types of delays that happen after major disasters, including the delays due to the post-disaster inspections, delays to prepare the necessary financial resources, delays due to high demand on the construction industry (such as hiring contractors and repair crew), and time to get the reconstruction permit. Since all of these delays do not occur in sequences or in parallel, a method to aggregate them in an appropriate way to be consistent with the real-world conditions is proposed in this study. Based on the results presented, it was shown that the updated analytical functionality fragilities using the proposed modification method resulted in more realistic recovery predictions and captured more accurately the empirical fragilities developed from the longitudinal study.

The functionality fragility models developed in this study may be further applicable in risk-based resilience assessment of communities subject to the tornado hazards, but it is recognized that there may be some limitations not accounted for such as local governance factors. Adjustments based on such factors may be needed for a broad geographical generalization, but the calibration provided in this study brings the predictive fragilities for building restoration one major step closer to being used for modeling of other communities. Similarly, to the PBE framework that accumulates the hazard loads, building responses, as well as direct and indirect impacts to conduct a risk analysis, it is feasible to utilize the generated functionality fragilities in this study to

conduct a risk analysis with the target of functionality instead of damage. The outcomes of such an analysis may be strategies to decrease the impacts and help communities recover faster.

4. THRUST C: AN AGENT-BASED MODELING APPROACH FOR COMMUNITY RESILIENCE ASSESSMENT ACCOUNTING FOR SYSTEM INTERDEPENDENCIES

In this chapter, an agent-based modeling approach to develop a quantitative model of a community is proposed. This framework accounts for the system of interconnected systems within a community, i.e., components/infrastructures within a community and their interactions. This chapter represents two consecutive steps performed during this study separated in two subchapters, called Thrust C-A and Thrust C-B herein. In the first step, Thrust C-A, a broad literature review was conducted, the conceptual framework was developed, and it was implemented for the virtual community of Centerville to study the resilience of education system in this community. To accomplish the objectives of this step, the proposed ABM framework characterized the players making a role in the operation and performance of the education system, namely, schools, households, electric power network, water supply network, school district, construction companies, and utility companies. Using the implemented community model, resilience of the education system in Centerville subject to tornado threats was evaluated. The second step of this chapter, Thrust C-B, is actually an extension to the community model developed in the first step to account for more infrastructures/players within the community. The objective is to assess and quantify the resilience of the community as a whole to the tornado threats, identify the most vulnerable components, and develop a decision-making platform to establish mitigation plans to enhance the community resilience. Hence, the ABM framework is proposed in the first subchapter, while the

second subchapter extends the comprehensiveness of the community model of the first step for the purpose of community resilience assessment and decision-making. These two steps are presented in two separate subchapters below, called Thrust C-A and C-B.

4.1. Thrust C-A: ABM approach and its application on the education system[†]

This subchapter introduces an agent-based modeling (ABM) approach to model a community as a system of interdependent systems for studying education systems resilience, one of the least-studied components of communities in the quantitative disaster literature. In this ABM approach, autonomous entities, called agents, simulate the components of a system, while internal interactions among them shape the system and external interactions among systems shape the community. To study the education system resilience subject to tornado hazard, a library of agents is proposed including school, household, electric power network, water supply network, and construction companies agents. The proposed ABM approach is applied on the virtual Centerville community. A Monte Carlo sampling analysis for various tornado intensities is conducted to account for and quantify the inherent uncertainties. Moreover, an education system resilience measure based on the education quality and quantity is proposed and computed for the virtual community of Centerville. The probabilities of the education system falling in different resilience levels are also computed for different tornado intensities. Taking advantage of the comprehensive quantitative model proposed,

[†] This chapter is submitted to the "Journal of Engineering Structures" as an individual paper (Aghababaei, M. and Koliou, 2021. An Agent-Based Modeling Approach for Community Resilience Assessment Accounting for System Interdependencies: Application on Education System. *Engineering Structures* (under review)

decisions for enhancing the education system resilience can be evaluated, which is demonstrated by assessing the effect of providing backup utilities for schools on the education system resilience.

4.1.1. Introduction

This subchapter presents the modeling approach based on ABM proposed in the current study to develop a community and its components, including schools, households, electric power network, and water supply network, along with decision makers in the community, with interdependencies between their performance and recovery. The proposed modeling approach is utilized in this subchapter to study the resilience of the education system within the community under its threatening hazards. Education system in this study refers to schools, students, school employees, and the quality of education within the community. When it comes to the quantitative community resilience studies, schools are among the least studied components of a community. Hassan et al. (2020) proposed a framework to study the resilience of a school system after massive earthquake disasters. This framework accounted for the quantity and quality of education service provided in the aftermath to describe the functionality and resilience of the school system. However, most of the education system literature focused on the effect of past natural disasters on the operation of schools, their recovery, and financial and mental health issues students and school employees face in the aftermath (Abramson & Garfield, 2006; Nastasi, Overstreet, & Summerville, 2011). Although such studies are of great importance to protect students and their families by knowing the vulnerabilities and health-related issues that may occur in the aftermath, still there is a need to

quantitatively model schools and their interactions with students when a major disaster occurs within the context of community resilience. By modeling the response of schools in the face of major disasters along with other systems of the community (e.g., power and water networks, households, government, etc.) in a comprehensive framework, it is feasible to evaluate the resilience of the education system in the community in its current condition. In addition, the quantitative community model enables decision making by implementing various strategies and selecting the most effective ones among all. The proposed ABM approach in this chapter is capable of modeling all systems within a community, including schools, and their interactions in the desired level of details, starting from the moment that the community is initially impacted by the disaster until when the community is recovering in the aftermath. It should be noted that the proposed ABM approach is generic, meaning that it can incorporate other sectors of a community not discussed in this section, and can be used to study other systems within a community than education system or multiple systems in the community at the same time. Since the focus of this subchapter is on the education system, a broad literature review about it is provided in the next section.

A large number of studies in the literature focused on the direct consequences of disaster loads on the physical infrastructures and how to mitigate those consequences (Mohammad Aghababaei & Mahsuli, 2019; Ayyub, Foster, McGill, & Jones, 2009; Brennan & Koliou, 2020; Kakareko, Jung, & Vanli, 2020; Y. Li & Ellingwood, 2006; Mahsuli & Haukaas, 2012; O. M. Nofal & van de Lindt, 2020). These studies conventionally utilized risk analysis methods to quantify the current state of the

infrastructures as well as make mitigation actions to enhance their condition. Two prominent risk analysis approaches for this purpose are the ones based on the concept of Performance Based Earthquake Engineering (PBEE) (Cornell & Krawinkler, 2000; Moehle & Deierlein, 2004) and the ones based on the structural reliability methods (e.g., Monte Carlo sampling, First-Order Reliability Method (FORM)) (Mohammad Aghababaei & Mahsuli, 2018; Mahsuli & Haukaas, 2013b). These studies conducted in various levels of refinement (i.e., regional, building, and component levels) and for various hazards (e.g., seismic, hurricane, flooding, etc.).

Disaster resilience studies typically account for the recovery of the system in the aftermath in addition to the direct losses when a disaster happens. Bruneau et al. (Bruneau et al., 2003) proposed a generic framework to quantify the resilience of the communities subject to seismic hazards, with emphasis on impact reduction, rapid recovery, and decreasing the communities vulnerability to future disturbances through social learning and adaption. In a recent study, Nasrazadani and Mahsuli (2020) proposed a probabilistic framework accounting for both direct losses and losses during the recovery stage of a community impacted by an earthquake, and accumulated all losses in terms of monetary loss using risk analysis methods.

Among studies on the disaster resilience, some studies focused on one component/system of the community because of their critical role in the aftermath, such as transportation networks (Adams et al., 2012), Electrical Power Networks (EPN) (Ouyang & Dueñas-Osorio, 2012), and hospitals and healthcare facilities (Gian Paolo Cimellaro et al., 2010b). Outcomes of such studies were finding vulnerabilities and

making decisions to make the system more robust, or developing algorithms to recover the system faster when it is disrupted. On the other hand, when conducting a resilience study in the community-level, it is essential to take into account the interdependencies between different systems interacting with one another. For example, households need access to drinking water through water supply network after a disaster, while water network itself typically requires access to electric power to function. Such dependencies create a complex system of systems forming the community where the performance of each system not only depends on its own operability but also on the performance of other interconnected systems. One common method in the literature to include such dependencies is considering the recovery as a Markov Chain of events to ultimately restore the performance of buildings. Lin & Wang (2017b), for instance, proposed a stochastic process for the recovery of building portfolio as a continuous time Markov Chain accounting for their interdependencies with utility accessibility. Simplicity of such methods facilitates their application, but they are not capable of modeling complex interconnected system of systems.

The proposed ABM approach in this study can quantitatively model a community and all of its interdependent components comprehensively. This study presents the application of the proposed modeling approach in the virtual community of Centerville (Ellingwood et al., 2016), illustrated in Figure 18, to model schools, households (and students in the household), along with other infrastructures and decision makers involved in the recovery of schools and students' education in the community. More details about Centerville are presented in the Simulation section of this subchapter. In

the remainder of this subchapter, to better demonstrate the proposed ABM approach, it is presented together with its application on Centerville.

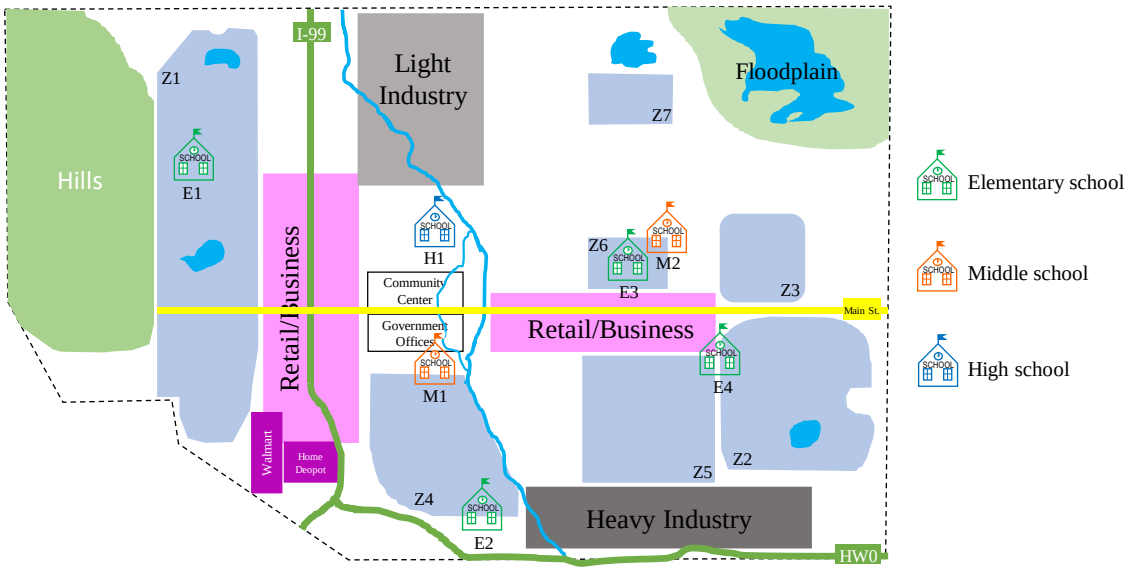

Figure 18: Centerville virtual community.

4.1.2. Education system

This section presents a literature review on the education system in communities impacted by major natural disasters. A wide range of attributes related to the education systems in communities hit by major natural disasters are studied in the literature. These include the physical damage schools incurred, displacement of students, issues school employees faced in the aftermath, and students' mental health issues related to the disaster.

Various articles and reports after major disasters outlined significant student displacements. According to a report by The Boston Consulting Group (2012) after Hurricane Katrina in New Orleans, Louisiana (LA), 64,000 students in public schools were displaced, while 4,000 public school teachers were laid off which itself caused

extra financial consequences for them and their families. A notable report (RAND, 2006) by the RAND Corporation studied the student displacement in Louisiana when Hurricanes Katrina and Rita happened in 2005. Based on this report, around 200,000 public school students were displaced. When Hurricane Katrina made landfall, an immediate drop occurred in the number of students kept enrolling in their original schools and this drop intensified as Hurricane Rita arrived.

A large number of studies reported disruptions in education of students due to school closure or student's family relocation which caused students miss days to weeks of school. According to the Boston Consulting Group report (The Boston Consulting Group, 2012), 85% of the 128 school buildings in New Orleans experienced some damage, while 35% of them experienced severe damage. Based on this report, by January 2006, only nine parochial schools and 17 public schools initiated their operation in New Orleans. According to the report by the National Public Radio (NPR) (NPR, 2017), following Hurricanes Harvey and Irma, students missed from one day to several weeks of school. For instance, in Corpus Christi, Texas (TX), students missed several weeks of school due to hurricane, and in Aransas Pass, TX, 1,800 students missed 34 days of school, while it was 10 days in Houston. In Puerto Rico after Hurricane Maria, approximately 345,000 students missed several weeks of school and a considerable portion of them left their parents to live with their relatives outside Puerto Rico and attend schools there, especially in Florida and New York. According to a report by the Children at Risk organization (Children At Risk, n.d.), around 1.4 million students of public schools in the affected areas after Hurricane Harvey started their school at least

one week later, while in the Greater Houston area around 216,000 students did not start school until September 11th.

A large portion of students enrolled in schools other than their original school either because their families were displaced to another place or the original school was closed. According to Webb (2018), of students who were living from Corpus Christi, TX, to the Louisiana border, around 46,500 did not have any other choice but enrolling in different schools after the event. This report revealed that the number of enrollments decreased moderately to significantly in the affected campuses, while less impacted campuses enrolled more students than before the disaster. According to the report by RAND (RAND, 2006), a large percentage of students in LA after the hurricanes of 2005 did not enroll in their original schools at all during this school year, and a large percentage of them did not enroll in any LA public school. The latter included students who enrolled outside LA or in private schools, and the ones who did not enroll in any school during that school year. Around 38% of displaced students returned back to their original school after not enrolling in any other school for a while. Around 7% relocated temporary and returned back to their original school, while around 24% did not return to their original school for the remainder of 2005-2006 school year. Finally, 31% of displaced students did not enroll in any LA public school, either enrolled outside LA, or in private schools, or did not enroll in any school.

In some cases, when damage was not severe, schools decided to make some adjustments and modifications to start school in their original campus as soon as possible. According to Webb (2018), after hurricane Harvey, a number of schools started

their operation by the available not-severely-damaged spaces of their schools. For example, they used blue tarps to divide undamaged spaces to better use them as learning spaces, or divided them using wood plywood. In addition, school teachers were forced to travel long hours to get to their jobs or they stayed in hotels using FEMA funding. In a damaged school in Texas after hurricane Harvey, called Orangefield high school, the school was opened on September 25 by providing temporary walls in the undamaged spaces in the corners of the gym and in the lobby. Teachers used methods like co-teaching whenever possible to combine classrooms with similar subjects by removing the tarps to avoid the extra distractions caused by conducting multiple separate classrooms in the same area. When damage was severe, some schools decided to operate their school in a temporary location. According to a report (Fay, 2018) after Hurricane Harvey, most of the school districts were repairing the damaged schools, while the Houston Independent School District decided to rebuild four damaged schools and in meanwhile students (2,800 students) attended temporary schools until January 2020. According to Webb (2018), two schools in Little Cypress-Mauriceville Consolidated Independent School District (CISD), TX, started their 2018-2019 school year in portable classrooms. These temporary campuses were built in February after the disaster.

Studies after natural disasters indicate that students suffered mental health issues and long-term consequences due to disruption in their education. According to a survey of 665 randomly selected residents, 44% of children suffered from new mental health issues, depression, and anxiety (Abramson & Garfield, 2006). These issues were intensified due to a major decrease in the access to the mental health services during the

aftermath caused by abrupt decrease in the number of psychiatrists and phycologists in the impacted area. In the Houston area, after Hurricane Harvey, about 22,000 students were homeless which made their life and education facing more severe issues compared to others. Statistics of displaced students also revealed that a larger percentage of displaced students belonged to socially vulnerable groups, such as racial/ethnic minorities groups. In Louisiana in 2005, around 65% of displaced students were among racial/ethnic minorities groups, compared to 59% in the affected parishes and 52% statewide. Blacks were the majority, with 58% in the displaced students, 53% in the affected parishes, and 48% statewide (RAND, 2006).

A summary of findings and insights from this review section utilized in this study are as follows:

i. Schools are typically vulnerable in natural disasters and major disruptions occur in the education system of a community when it is hit by a disaster.

ii. Students in the impacted areas miss days to weeks of school because of a number of reasons. Typically, all students miss at least one day to a few days in massive disasters because of evacuation orders and going into emergency shelters. However, two other reasons cause longer periods of being out of school. First, families being displaced due to damage to their housing, and as a consequence, students may not have access to their original school due to their displacement. The second reason is the original school closure to be repaired or to make adjustments in order to initiate the operation.

iii. A large portion of students change school multiple times in the aftermath, and a considerable percentage of them do not return back to their original school.

iv. Social vulnerability increases the likelihood of student displacement.

v. Schools in the impacted areas select different recovery trajectories depending on the damage they incurred and other factors in their community. Schools with minor and moderate damage start the repair and they go back to operation in a few days or weeks. Severely damaged schools may decide to make some adjustments, such as reorganizing classrooms in safe spaces of their campus, to not delay reopening long to repair the whole campus. In some cases, these schools decide to start school in temporary places or in portable classrooms.

This section discussed the importance of studying resilience of education systems in areas with high hazard threats to avoid and mitigate short- and long-term adverse effects on students' lives. In addition, this section provided a good insight about the recovery trends of schools and student displacement which are used later in this subchapter to develop appropriate agents in the proposed ABM approach.

4.1.3. Agent-based modeling approach

In ABM, a system is modeled as a set of decentralized entities (called agents) functioning all together, while specific relationships among them form and govern the response of the system (Nasrazadani & Mahsuli, 2020; Rasoulkhani & Mostafavi, 2018). In the current study, a modeling approach based on ABM is proposed to model a community as a system

of interdependent systems, as illustrated in Figure 19. In this approach, each system is modeled as a population of agents with similar attributes. A number of systems included in the community model considered herein to study the resilience of the education systems are shown in Figure 19. In the system level, agents of the same type, such as EPN agents, may have *internal interactions* to achieve the performance goals of the system. This can be a complex interaction between all agents (e.g., WSN or EPN agents), or there may be interactions between clusters of agents (e.g., elementary schools interact with one another but not with other schools), or there may be minor direct interactions (e.g., household agents). In addition to the population of agents, two single agents which are responsible of decision-making actions to recover specific systems in the community are included in the proposed model.

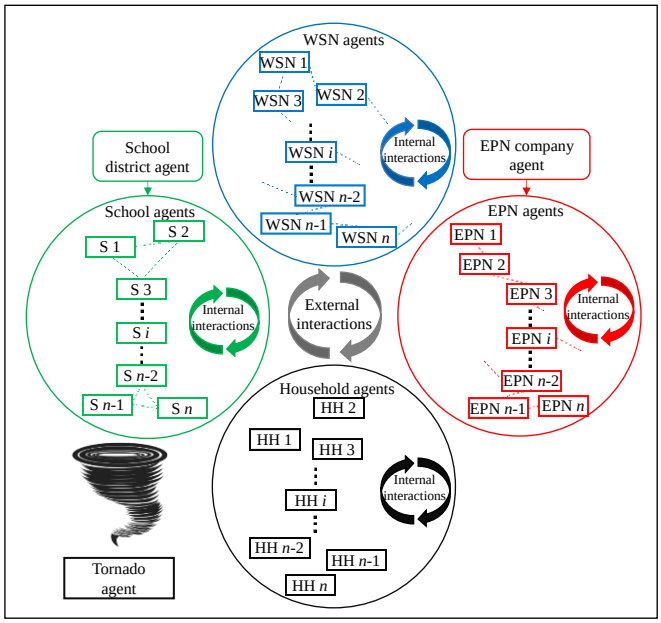

Figure 19: Schematic overview of modeling a community using ABM.

Except for internal interactions in each system, different systems also may have *external interactions*. For example, the WSN is dependent on having power access

through the EPN, while schools are dependent on both the EPN and WSN to operate. In ABM, these interactions are implemented using micro-behaviors defined between interacting systems, such that performance of a system has a certain level of dependency on performance of the other system. After defining these external dependencies, the system of systems forming the community is developed.

When a tornado hits the community, all wind-vulnerable components, including the EPN elements (e.g., power substations, towers, poles, etc.), housing units, and schools, are prone to damage. In addition, although the WSN is typically not directly damaged by tornado, its performance is dependent on access to the electricity through the EPN. In the aftermath, all components simultaneously start recovering to return back to the normal condition, and although they act independently, their recovery has a dynamic cascading effect on the rest of the interacting components (e.g., recovery of specific nodes in EPN enables recovery of WSN). In addition to the physical infrastructures, there exist some decision-making entities, such as power company and school district management, which make decisions related to the recovery prioritizations and resource allocations. In the schematic overview presented in Figure 19, the EPN company is in charge of allocating its labor and monetary resources to recover the EPN based on a number of specific criteria (e.g., prioritizing critical facilities and populated neighborhoods). School district in this community has the role of inspecting damaged schools, planning for their repair and recovery, distributing students from severely damaged schools to other operable schools, and in the overall decision making to restore all schools in the community.

It should be noted that the ABM approach in this study is not limited to the systems presented in Figure 19, and the extent of details and number of components included in the model depends on the purpose of the study.

4.1.4. Agents

In this section, agents and their attributes to model the community shown in Figure 19 are provided. For each agent, a number of models are required which are either adopted from the literature or developed in this study. First, a brief review of the models used in the literature is discussed for each agent type, and then, the adopted or proposed models in this study are presented. Figure 20 demonstrates the Unified Modeling Language (UML) class diagram of the community-level quantitative model in this study. This figure summarizes the attributes of each agent type and their operators defining their behavior. In addition, the functionality of a number of systems depends on the functionality or decision of another system or agent, which is depicted using arrows entering the dependent agent type. Various operators in Figure 20 are highlighted with different colors indicating that they receive inputs from other agent types in the community (identified with the same color), which simply shows their interactions. The computational community framework in this study is implemented in an object-oriented modeling platform called AnyLogic 8. AnyLogic is a java-based simulation platform with various libraries for agent-based modeling, discrete event simulation, and system dynamics analysis (“AnyLogic Software,” 2021).

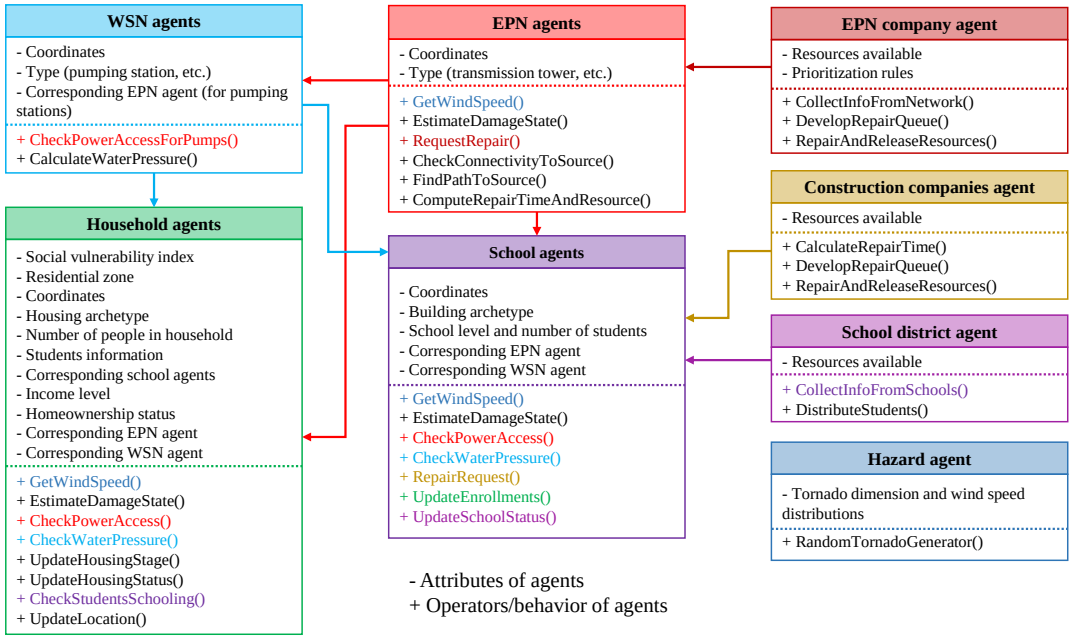

Figure 20: Unified Modeling Language (UML) class diagram of the model, showing the attributes and functions of agents in the community model as well as their interactions.

4.1.4.1. Hazard agent

The hazard agent simulates the disaster, its magnitude and extent throughout the city, and informs other affected agents of the intensity of the disaster in the agent's location. A large number of hazard models exist in the literature, especially in the disaster risk analysis literature, for earthquake (Mahsuli & Haukaas, 2013a; Tamhidi et al., 2021; Tamhidi, Kuehn, Ghahari, Taciroglu, & Bozorgnia, 2020), flooding (O. Nofal, van de Lindt, & Do, 2020), and tornado (Standohar-Alfano & Van De Lindt, 2015), among others.

In the current study, the Centerville community is subjected to tornado events. This study adopted and implemented the probabilistic tornado hazard model proposed by Standohar-Alfano and Van De Lindt (2015) to simulate tornado disasters. This method uses the Enhanced Fujita (EF) scale to rate the intensity of tornado based on the degree

of damage observed after the tornado. This scale ranges from EF0, minor or no damage, to EF5 that represents total destruction, and indicates the highest intensity of a tornado, while there is variation in its intensity along both its width and length. For each EF scale, the associated 3-second gust wind speed is presented in the second column of Table 17. Standohar-Alfano and Van De Lindt (2015) proposed an idealized tornado path represented by rectangles such that the highest intensity occurs at the center and it decreases gradually moving outward. Figure 21 illustrates an example EF5 tornado path in Centerville simulated using the method proposed by Standohar-Alfano and Van De Lindt (2015). Using the empirical dataset of tornados occurred between 1973 and 2014, Masoomi and van de Lindt (2018) generated marginal Weibull probability distributions for tornado width and length as tabulated in Table 17. In this table, λ and k are respectively scale and shape parameters for Weibull distributions, and ρ is the correlation coefficient for the marginal distribution. In addition, Standohar-Alfano and Van De Lindt (2015) used observations from a number of detailed surveys after major tornado outbreaks to estimate the percentage of width for each tornado intensity along tornado path width, and similarly, the percentage of length for each intensity along tornado path length. These deterministic values are presented in Table 18 for each tornado intensity.

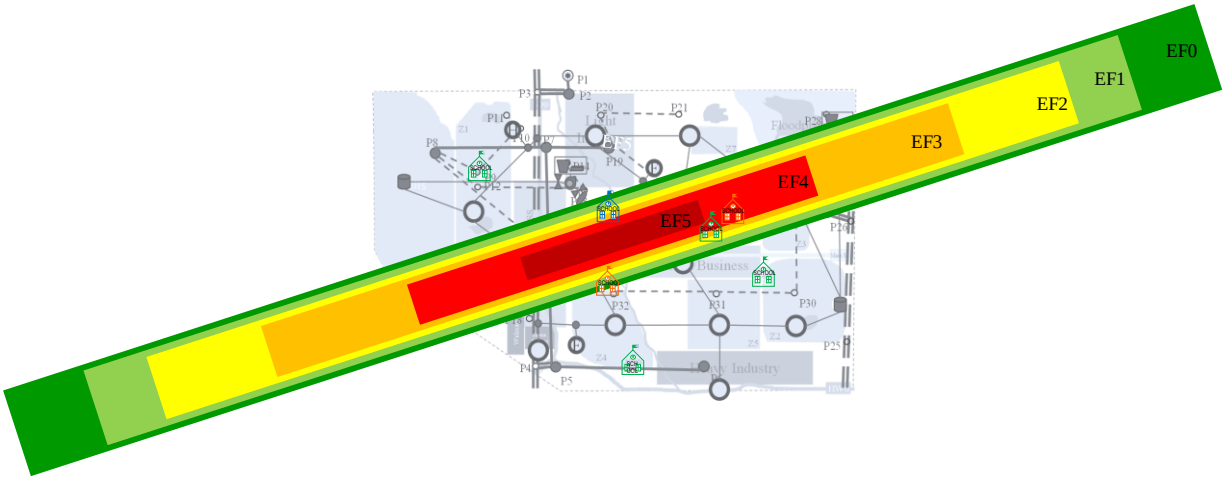

Figure 21: A sample of simulated EF5 tornado in Centerville.

Table 17: 3-*s* gust wind speed of each EF scale and marginal Weibull distribution parameters for tornado length and width (Masoomi & van de Lindt, 2018b)**.**

		Length		Width		
EF scale	3 *s* gust (m/s (mph))	λ	k	λ	k	ρ
EF0	29-38 (65-85)	0.718	0.675	0.025	1.043	0.225
EF1	39-49 (86-110)	2.671	0.727	0.058	0.943	0.250
EF2	50-60 (111-135)	6.514	0.796	0.117	0.912	0.253
EF3	61-74 (136-165)	15.865	1.031	0.261	1.004	0.180
EF4	75-89 (166-200)	26.997	1.117	0.437	1.150	0.307
EF5	90+ (200+)	38.074	1.291	0.572	1.423	0.367

Table 18: percentage of width and length of each sub-EF category along tornado path width and length, respectively (Standohar-Alfano & Van De Lindt, 2015)**.**

EF category	Width percentage (%)	Length percentage (%)
EF5 tornado path		
EF5	27.3	14.9
EF4	19.9	18.5
EF3	13.6	24.2
EF2	13.8	18.9
EF1	12.7	10.3
EF0	12.7	13.2
Total	100	100
EF4 tornado path		
EF4	27.3	21.2
EF3	18.7	21.0
EF2	19.0	27.8
EF1	17.5	15.8
EF0	17.5	14.2
Total	100	100
EF3 tornado path		
EF3	33.8	32.1
EF2	20.2	31.8
EF1	26.2	24.4
EF0	19.8	11.7
Total	100	100
EF2 tornado path		
EF2	47.5	36.7
EF1	31.4	35.2
EF0	21.1	28.1
Total	100	100
EF1 tornado path		
EF1	62.5	42.6
EF0	37.5	57.4
Total	100	100

In summary, to generate a tornado path using this model, the hazard agent first determines the EF scale of the tornado. Using the Weibull distributions of this EF scale in Table 17, the hazard agent generates random width and length, and afterward, using percentages extracted from Table 18 for this EF scale, calculates width and length of each sub-EF intensity (e.g., sub-EF intensities for an EF2 tornado are EF2, EF1, and EF0).

4.1.4.2. Electrical power network agents

There are a large number of studies in the literature focusing on the performance, recovery, and resilience of power systems in severe disasters (Brennan & Koliou, 2020; Unnikrishnan & van de Lindt, 2016; Winkler, Duenas-Osorio, Stein, & Subramanian, 2010). Ouyang and Dueñas-Osorio (2012) proposed a probabilistic approach to assess the resilience of EPN, with an application for the Harris County, Texas, USA. The simulation approach presented in this work initiates with the hazard model, followed by component fragility model, power system response model, and restoration model. Five main components of EPN included in this study were transmission substations, transmission lines, distribution nodes, distribution lines, and local distribution circuits, which deliver electricity from distribution node to customers at each node.

In the current study, an approach similar to the one proposed by Ouyang and Dueñas-Osorio (2012) was adopted to model the response of the EPN to the tornado loads and its restoration in the aftermath. Figure 22 presents the EPN in Centerville. Although not shown in this figure, it is assumed that there are distribution poles in the distribution and sub-distribution lines every 38 meters (124.7 ft), and similarly, there are transmission towers in the transmission lines every 450 meters (1476.4 ft). This assumption is close to the real-world practices and was captured from study by Unnikrishnan and van de Lindt (2016) on Centerville EPN.

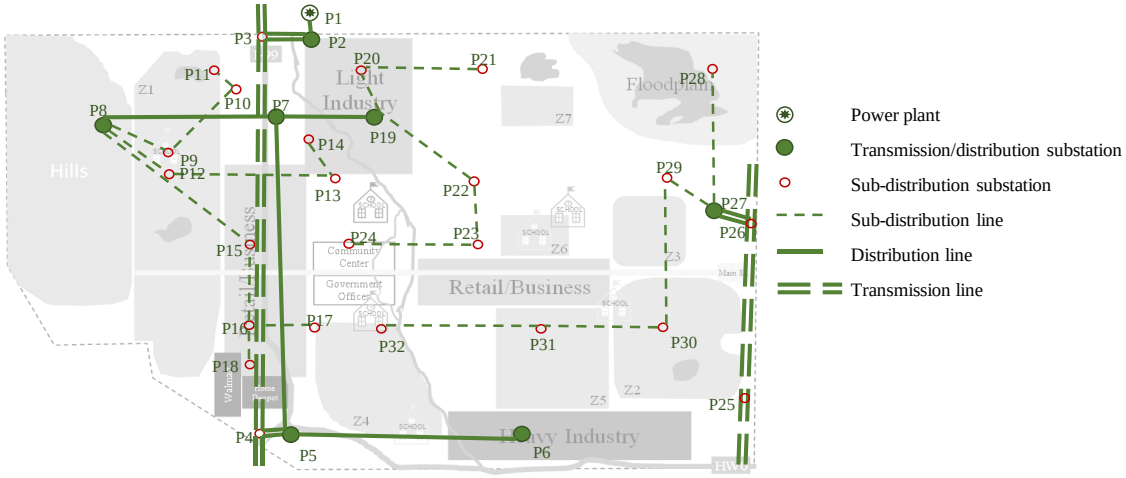

Figure 22: Electrical power network in Centerville.

In the ABM approach proposed in this study, each component contributing to the response and recovery of the EPN in a tornado event is assumed as an agent. In this chapter, all nodes, including transmission, distribution, and sub-distribution substations, electric poles, and transmission towers, are considered as agents. A single agent called EPN company is also defined which is responsible for managing the network in normal circumstances and repairing it when it is disrupted. Figure 23 illustrates the attributes and behavior of each agent in the population of EPN agents and its interactions with the EPN company agent in cases of disruption. All agents are in the Normal state prior to a tornado event in the case of Centerville. According to Figure 23, after the tornado occurrence, all agents (i.e., all EPN components) exit the Normal state. In the next step, each agent from the population of EPN agents (EPN agent i, i=1,…, n; n=total number of agents in the population) inquires the tornado hazard agent about the wind speed at its specific location. Using the acquired wind speed ($v_{EN,i}$) and damage fragilities for each component type, a damage state (DS) is estimated for the agent. In this study, damage fragility functions for electric poles developed by HAZUS were explored from IN-

CORE Web Tool, and fragilities for the rest of EPN components were adopted from Masoomi and van de Lindt (2018), as presented in Table 19. Per Figure 23, after the damage state of the agent is estimated, it is checked if it needs repair or not. If not, its connectivity to the power source is checked repeatedly during the simulation until all other EPN agents in its path towards source are repaired. The symbol "  " in this figure indicates a process that repeats periodically, and in this case, it means that the connectivity check function repeats periodically until the agent is connected to the source and goes back to the Normal state. If the agent needs repair, it goes to the repair queue of the EPN company, and after it is repaired, it similarly goes to the periodic connectivity check until it is connected to the source and goes back to the Normal state.

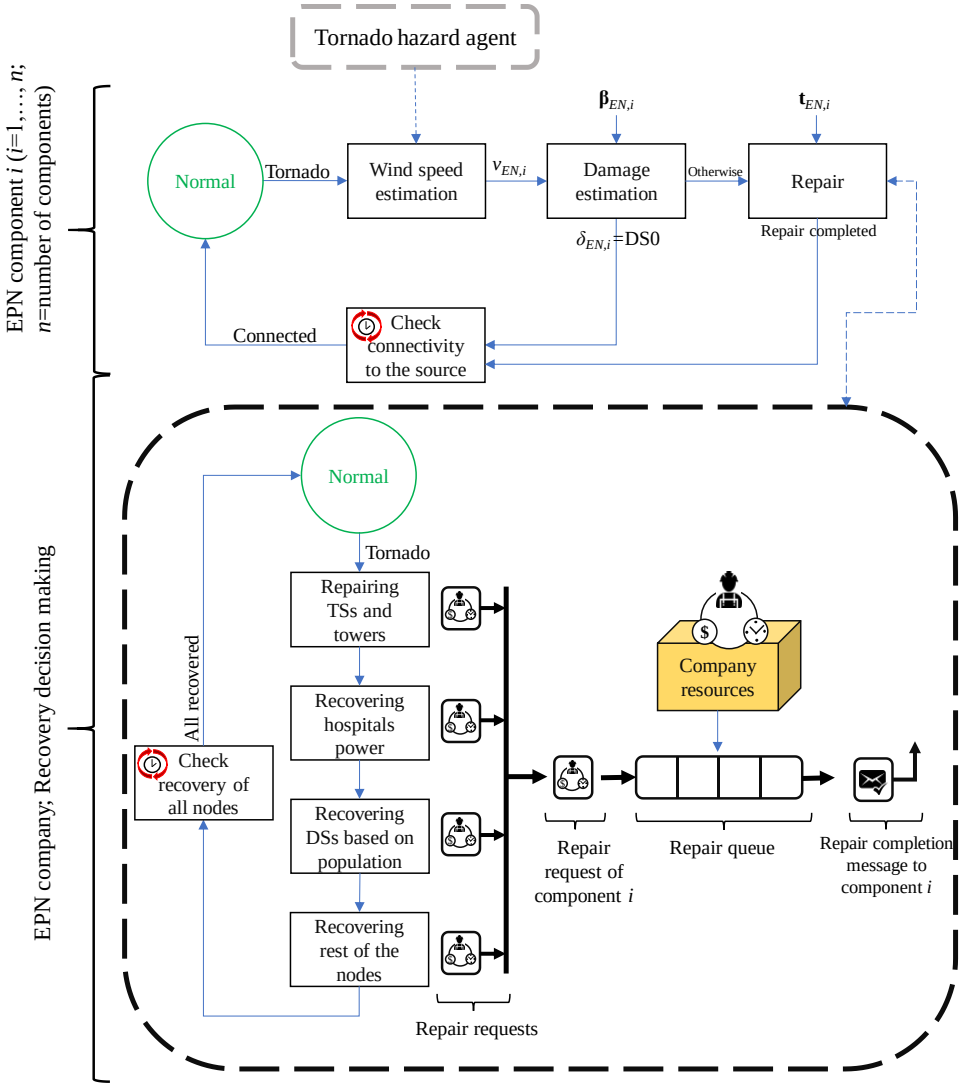

Figure 23: EPN agents attributes and their interactions with tornado hazard agent and EPN company.

Table 19: Damage fragilities for EPN components (medians are in m/s with their equivalent mph values in parentheses).

	DS1		DS2		DS3		DS4	
Component	Median	Log-std	Median	Log-std	Median	Log-std	Median	Log-std
Transmission, distribution, and sub-distribution substation	33.4 (74.8)	0.2	39.5 (88.4)	0.2	48.6 (108.8)	0.2	60.8 (136.0)	0.2
Transmission tower	—	—	—	—	—	—	60.8 (136.0)	0.12
Electric poles	—	—	—	—	—	—	51.9 (116.1)	0.15

As Figure 23 indicates, the EPN company plays the role of decision making to repair the EPN components and provide electric power service to the consumers. Per Figure 23, the EPN company agent exits the Normal state after a tornado takes place. After receiving requests from all EPN agents asking for repair, the EPN company agent puts their requests in a queue of repair based on some prioritization rules. In the current study, as presented in Figure 23, priority rules in order are: (i) repairing transmission substations and towers because they are essential to transmit electric power to the city, (ii) recovering power service to the hospitals, (iii) providing power to the distribution and sub-distribution substations which provide electricity to the most populated areas, and finally (iv) repairing the remainder of the nodes in the network. Based on these rules, a repair queue of damaged EPN agents is prepared, and after each EPN agent is repaired, the EPN company agent communicates with that agent regarding its repair completion. After all of the EPN agents are connected to the electric power sources, the EPN company agent goes back to the Normal state.

4.1.4.3. Water supply network agents

A large number of studies on water supply network (WSN) performance and resilience exist in the literature. Choi, Yoo, & Kang (2018) proposed a simulation approach to develop restoration curves for water networks after earthquakes. This approach has six main steps starting from simulation of the network damage, hydraulic analysis to measure the extent of damage on the network, calculate the necessary repair resources, set some priority rules for recovery, generate a list of prioritizations and compute the serviceability of the network over time, and finally generate the restoration curve using

the resulting recovery data. Rasoulkhani & Mostafavi (2018) used multi-agent simulation, which is a category of ABM, to model the response of a water distribution network to internal and external stressors within an extended horizon to detect regime shifts to assess the long-term resilience of the network.

The WSN typically is not damaged in tornado events, but still there is a possibility of disruption in providing service due to power outage. There exist three water pumping stations in the WSN of Centerville which are dependent on power accessibility. Figure 24 demonstrates the interdependencies between three infrastructures in Centerville, namely, EPN, WSN, and schools. As indicated by black arrows, water pumps in the WSN depend on electric power service on specific nodes in the EPN.

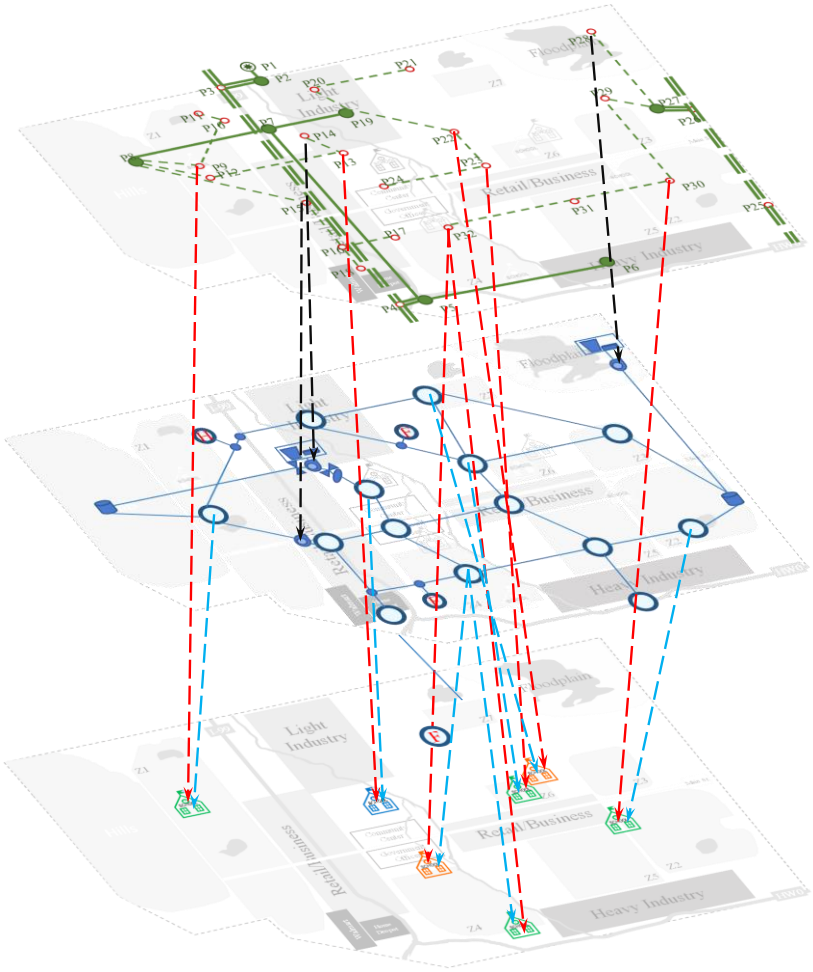

Figure 24: Interdependency of WSN on EPN as well as schools on both EPN and WSN.

Figure 25 presents details of the WSN in Centerville. In the ABM approach of this study, all nodes in this figure are represented by a population of WSN agents. Because this WSN is an interconnected system, it is assumed that water supply in each demand node is dependent on a number of suppliers in the network and not only on one supplier. These suppliers are two tanks and three pumping stations as presented in Figure 25. In order to avoid computationally-expensive hydraulic analysis, it is assumed that each of these five suppliers provide a certain percentage of the full supply of each

demand node. These percentages for each demand node were assigned based on its proximity to the supplier nodes. It should be noted that the ABM approach in this study is not limited to the models used in this study, and in the case of WSN, any other hydraulic model can be substituted with the model used in here. In the proposed ABM approach, as shown in Figure 24, there are interactions between certain agents in the EPN and WSN. In this framework, accessibility of the pumping station agents to power through their supplier agents in the EPN is checked periodically, such that whenever the supplier agent in the EPN returns back to the Normal state, the interconnected pumping agent also goes back to the Normal state. By so doing, the supply network is recalculated to update the provided supply in each demand node agent. This continues until all pumping station agents return back to their normal state, and accordingly, the whole WSN returns back to its normal service.

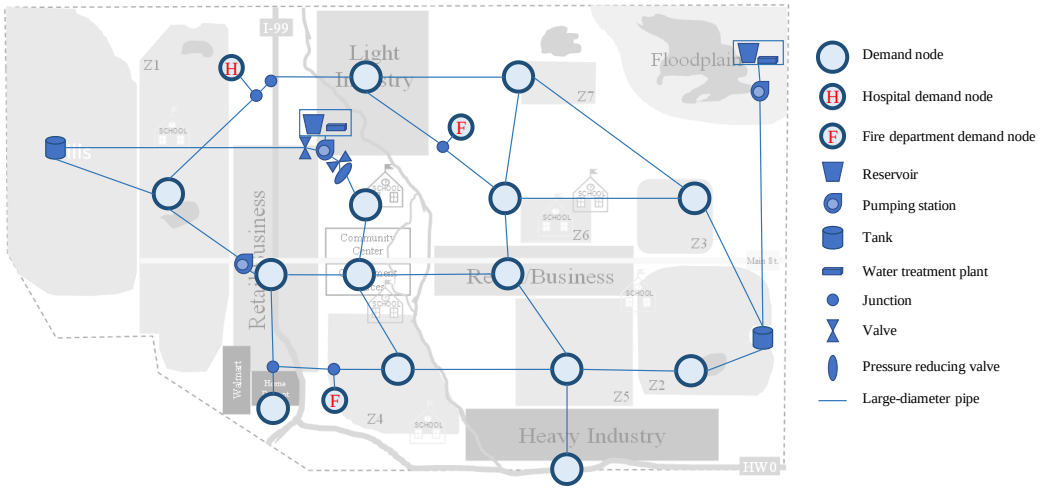

Figure 25: Water supply system in Centerville.

4.1.4.4. School agents

A broad review of literature on the effect of natural disasters on the education system in a community, including schools, students, and quality of education, was presented in the second section of this subchapter. A few studies in the literature studied schools in the quantitative disaster resilience context. Masoomi and van de Lindt (2018) developed a model of a community including WSN, EPN, residential buildings, schools, and businesses with their dependencies to investigate the restoration of the community subject to tornado events.

In the proposed ABM approach, all schools presented in Figure 18 were modeled as a population of school agents, while one agent was defined, named school district, which is responsible for managing schools in the community in the aftermath. This included making decisions about severely damaged schools to either send their students to other nearby operable schools, called host schools, or prepare a temporary location for them to start their operation. The school agents have interactions with other agents in the community. As Figure 24 illustrates, each school is dependent on having access to power and water through specific nodes in these networks. These dependencies are shown by red and blue arrows respectively for the dependency of schools on the EPN and WSN. In addition, damaged schools depend on the construction companies (which will be defined as an agent later in this subchapter) to repair them to their undamaged state.

Figure 26 illustrates the attributes of each school agent within the population of school agents in the proposed ABM framework and their interactions with other agents in the community model. A school agent is in the Normal state before the tornado event,

and when a tornado occurs it communicates with the tornado agent to calculate the wind speed in its location. Afterwards, the damage model estimates the damage state (DS) of the school agent using the resulting wind speed in its location. In the case of Centerville, damage fragility models from Memari et al. (2018) were employed which are tabulated in Table 20. As Figure 26 shows, the school agent goes through different recovery trajectories depending on the estimated damage:

i. If the school incurs no damage (DS0), it communicates with the school district agent, and it goes to the list of agents which are capable of hosting students from affected schools. In addition to the physical performance, the school agent depends on the access to power and water to operate. Hence, this agent exchanges information with its corresponding EPN and WSN agents (each school agent depends on specific predetermined EPN and WSN agents as indicated in Figure 24) periodically to check if its access to them is back to normal. After the utility is back, the school agent communicates with the school district agent to see if it has to host students from other affected schools, and if yes it goes to the Extra Enrollment state. The school agent continues the communication with the school district agent periodically until it hosts no additional students, and in that case, it goes back to the Normal state.

ii. If the school incurs minor damage (DS1), it needs some minor repair and preparations prior to going back to full operation. In addition, since no considerable damage is incurred by this agent, it goes to the list of agents

which are capable of hosting students from affected schools. After its minor repair and preparation is completed in a few days, it goes to the same procedure as agents with DS0 go (i.e., checking for utility connection and checking if they have to host additional students, see Figure 26).

iii. If the school incurs moderate damage (DS2), its recovery trajectory is similar to the agents with damage state DS1. The only difference is that repair and preparation for this agent takes a longer time.

iv. If the school incurs considerable damage (DS3), but some parts of the campus are not severely damaged, the school agent adopts some modifications in order to start school in dense condition as soon as possible. This is in line with the review of the recovery of schools in the US after weather disasters as discussed earlier in this subchapter. It takes days to a few weeks to complete and implement the adopted modifications through remodeling and dividing spaces and conduct repair actions. Afterwards, the school goes to the Initiation in Dense Condition state as Figure 26 indicates. This school agent communicates with the construction companies agent and goes to the repair queue of the construction companies agent. This agent communicates with the construction companies agent periodically until it receives the message of repair completion of the campus. Afterwards, access to the utility is checked, and if it has access, the school agent goes directly to the Normal state.

v. If the school experiences extensive damage (DS4), its campus needs to be reconstructed, and hence, it communicates with the construction companies agent to go to the repair queue. Additionally, this school agent communicates with the school district agent to see if there is any host school available within the district. If there exist host schools within the community, all students of this school enroll in the host schools, and this agent goes to a state named In Host Schools. If there exist no host, school looks for a temporary place or portable schools to initiate the school operation as soon as possible. In both cases, the school agent communicates with the construction companies agent periodically until it receives the repair completion message. Afterwards, the agent checks for the utility access, and if it has access, it directly goes to the Normal state. Students who did not relocate to other cities and are currently enrolled in host schools return back to their original school after it goes back to the Normal state.

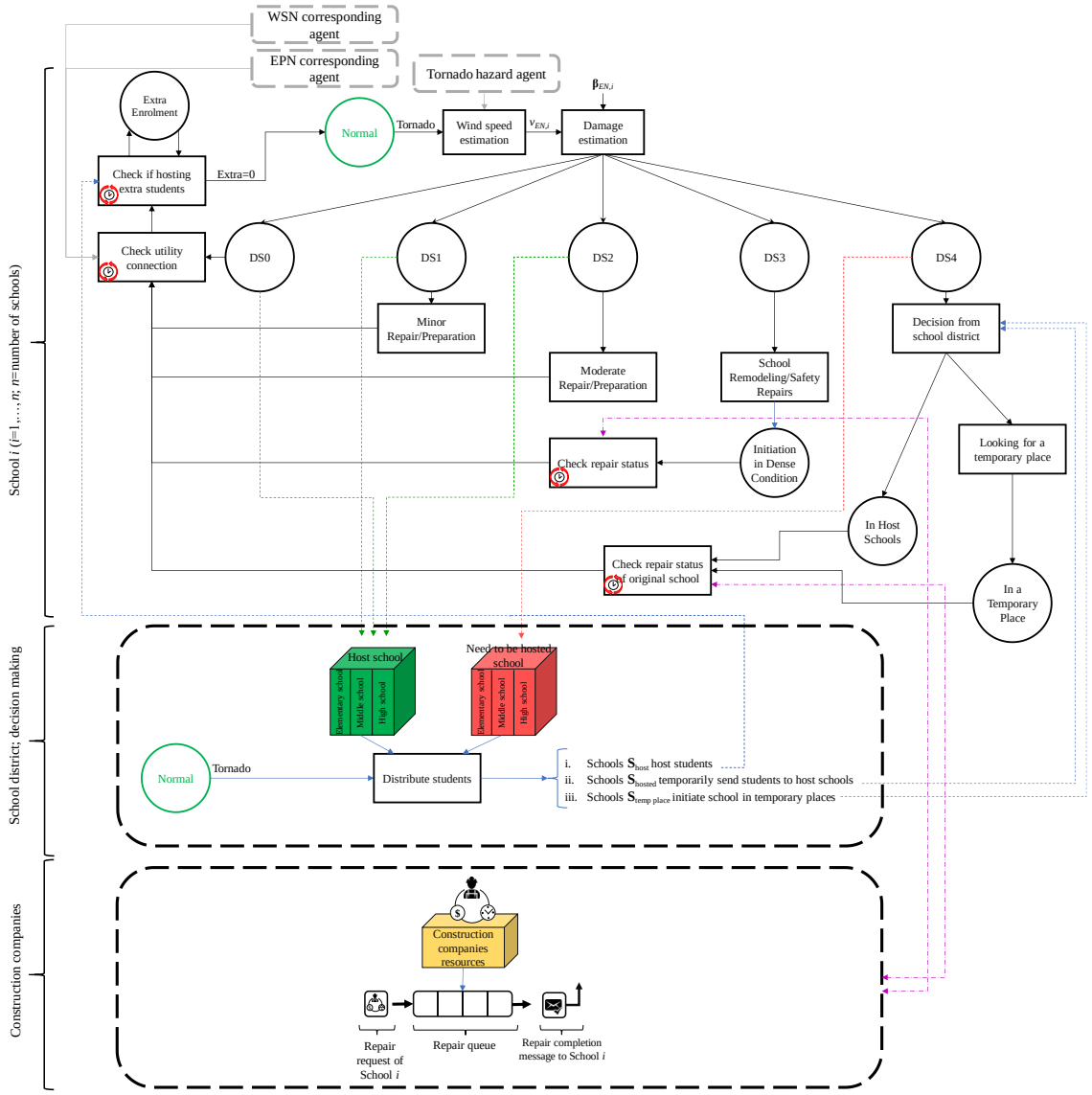

Figure 26: School agent attributes and its interactions with other agents in the community.

Table 20: Damage fragilities for schools in Centerville (medians are in m/s with their equivalent mph values in parentheses).

School level	Archetype in Memari et al.(Memari et al., 2018)	DS1		DS2		DS3		DS4	
		Median	Log-std	Median	Log-std	Median	Log-std	Median	Log-std
Middle school	T9a	33.6 (75.2)	0.12	42.3 (94.6)	0.11	49.2 (110.1)	0.10	65.0 (145.4)	0.12
Elementary school	T9b	32.6 (72.9)	0.12	42.7 (95.5)	0.11	47.2 (105.6)	0.11	61.9 (138.5)	0.16
High school	T10	34.0 (76.1)	0.12	41.9 (93.7)	0.11	49.2 (110.1)	0.11	71.2 (159.3)	0.12

4.1.4.5. Construction companies agent

The construction companies agent represents the resources available in the community in terms of the number of construction companies, their crew, material, equipment, etc. After massive natural disasters, communities typically face shortage in construction resources due to the high demand caused by severe damage to the infrastructure. In the proposed ABM framework, such limitations and shortages are modeled in the construction companies agent by defining a repair queue and a resource pool with limited capacity. As illustrated in Figure 26, the construction companies agent receives repair requests from agents damaged due to tornado loads and put them in a repair queue. Whenever an agent (e.g., damaged school agent) in the repair queue reaches to the point where its repair starts, depending on the extent of damage and characteristics of the damaged agent, a certain amount of construction resources is allocated from the resource pool to the repair of that damaged agent. These allocated resources are occupied for the period of repair (repair time), and they are released whenever repair completes. The released resources return back to the resource pool to be employed for the next damaged agent in the repair queue.

4.1.4.6. Household agents

Households play a significant role in recovering an impacted community. They have interactions with almost all sectors in a community, including businesses, schools, lifelines, critical facilities, and government facilities/systems. One important aspect of household recovery is housing recovery. Households recover when they reach permanent housing and they start their routine life as before the disaster. Peacock et al. (2007)

gathered a broad review of the literature on the sheltering and housing recovery after disasters. This review paper pulled together the research that utilized Quarantelli's sheltering and housing typology. Quarantelli (1982) suggested four forms of sheltering and housing following a disaster: emergency sheltering, temporary sheltering, temporary housing, and permanent housing. Sutley and Hamideh (2020) added a fifth stage, representing households having unstable housing and oscillating between different stages. In this study, a Markov Chain model was proposed to simulate the post-disaster housing recovery of households accounting for uncertainties in this process. In this Markov Chain model, the transition of households between different housing stages was computed using a transition probability matrix (TPM). Sutley and Hamideh (2020) proposed a number of transition probability models which were functions of social vulnerability of the household. These models were used to compute the TPM to be used in the Markov Chain model.

Figure 27 presents the housing attribute of each agent from the population of household agents in the proposed ABM framework. The Markov Chain model proposed by Sutley and Hamideh (2020) was adopted for the household agent to probabilistically simulate the movement of households between different housing stages in the aftermath of a disaster. As Figure 27 shows, a household agent is in Normal state just before the disaster takes place (t=0). After a disaster occurs (tornado event in the case of Centerville), it exits the Normal state, while it communicates with the tornado agent to calculate the wind speed in its location, and consequently, this agent estimates its damage based on the resulting wind speed. The initial housing stage of the agent is

determined by mapping the damage it incurred and the condition in the aftermath. After the initial stage is determined, the household agent enters the Markov Chain process adopted from Sutley and Hamideh (2020), with the TPM calculated based on the agent's social vulnerability. Social vulnerability in this study is quantified with a number between 0 and 1, such that vulnerability closer to 0 indicates low social vulnerability and vulnerability close to 1 indicates high social vulnerability. Details on the elements of the TPM calculations are included in the study by Sutley and Hamideh (2020). The household agent initiates its housing with its initial housing stage, and after the Markov Chain process is formed using the calculated TPM, its stage is updated every month until it reaches Stage 4 or fails to Stage 5. As Figure 27 presents, the household agent can move from its current stage to other stages at each time step (one month), or it can stay in the same stage. This is randomly generated using the Markov chain model, and the ABM framework asks each household agent to update its housing stage based on its TPM. The oscillation between stages stops whenever the agent enters a permanent housing (Stage 4) or failure (Stage 5). Sutley and Hamideh (2020) proposed explicit definition for housing failure. Based on their definition, a household fails if it takes more than seven years (i.e., 84 time steps) for the household to reach Stage 4. Another rule for failure is that the household experiences more than four regressive steps in one year (12 time steps), seven regressive steps in two years (24 time steps), or 10 regressive steps during the simulation. In the ABM framework in this study, a household agent enters Stage 5 whenever any of these failure rules are met.

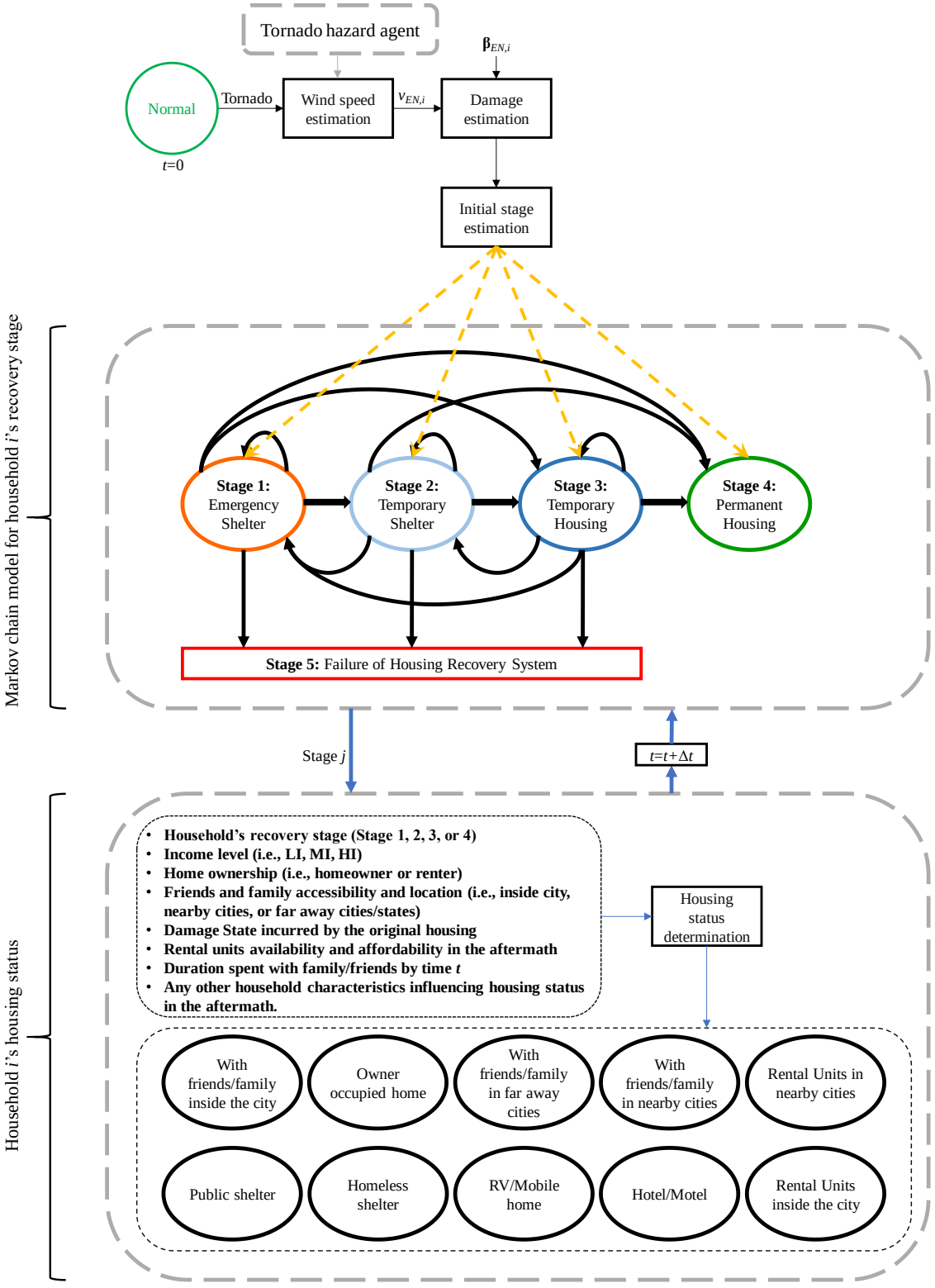

Figure 27: Housing stage and housing status of the household agent.

In order to account for the student displacement in the ABM framework, knowing the location of each household agent during the simulation time is essential. The Markov Chain model used in this study simulates the housing stages, but these stages should be correlated with housing statuses expressing the location and type of the housing more clearly. For this purpose, in the current study, the resulting housing stage at each time step is mapped into a housing status selected among 10 different statuses presented in Figure 27. As Figure 27 demonstrates, at each time step, as a random housing stage is generated, the household agent adopts a housing status based on a number of factors, including the current housing stage, income level, home ownership, access to family and friends and their location, damage state of the original housing, availability and affordability of rental units in the aftermath, duration spent with friends/family by the time of simulation, *t*, and any other household characteristics influencing the housing status of the household in the aftermath. By doing so, the location of the household agent and whether it is inside or outside the city is determined. After this step, if there are students in a household agent, it is known where they are located in the aftermath. This information is used to calculate the enrollment count of each school in the aftermath.

In order to account for the student displacement in the current study, knowing the location of each household agent during the simulation time is essential. The Markov Chain model used in this study simulates the housing stages, but these stages should be correlated with housing statuses expressing the location and type of the housing more clearly. For this purpose, in the current study, the resulting housing stage at each time

step is mapped into a housing status selected among 10 different statuses presented in Figure 27, where at each time step, as a random housing stage is generated, the household agent adopts a housing status based on a number of factors, including the current housing stage, income level, home ownership, access to family and friends and their location, damage state of the original housing, availability and affordability of rental units in the aftermath, duration spent with friends/family by the time of simulation, *t*, and any other household characteristics influencing the housing status of the household in the aftermath. By so doing, the location of the household agent and its students (if any) is determined.

After the location of the students and status of the school agents in the community are known, the schooling status of students within each household can be determined. The school status of students within each household is updated periodically using the process demonstrated in Figure 28, where for each student within Household Agent *i*, first, based on the agent's housing status, it is determined whether the household is located inside or outside the city. If outside, students are not living in this community for that timeframe, and hence, they will enroll in schools outside the city. If the household agent is located inside the city, for each student within the household, this agent communicates with the original school agent (i.e., school before the disaster), to check if it is operational. If yes, based on the operation level of the school agent, student's schooling status falls within one of the five categories demonstrated by green boxes in Figure 28. On the other hand, if the original school agent is not operational due to complete damage (see schools experiencing DS4 in Figure 26), the original school

agent looks for a host school through the school district agent (discussed in Section 4.1.4.4). If no suitable host is found inside the community, the original school looks for a temporary place to initiate the school, and hence, the student goes back to the original school, but in a temporary location as shown by an orange box in Figure 28. If host school agents are available, the student goes to the selected host school, and the student's schooling status depends on the host school's operation status, as presented by blue boxes in Figure 28.

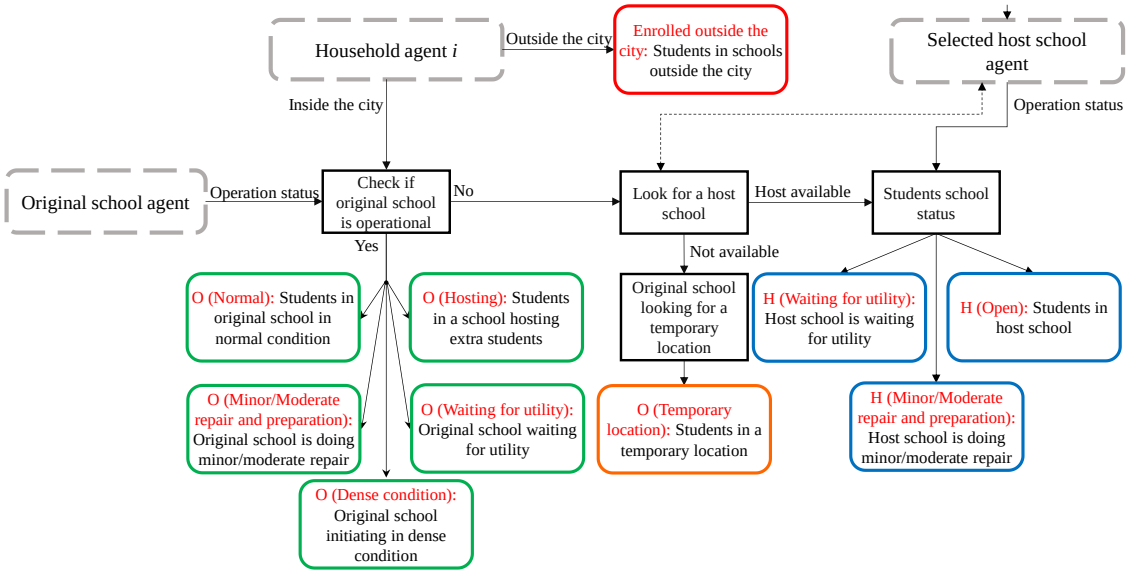

Figure 28: School status of students of a household based on the household's location, and operation status of the original school and other schools within the community.

4.1.5. Simulation

The proposed ABM framework in this subchapter was discussed together with its application on the virtual community of Centerville. In this section, first, more information about the Centerville testbed is provided, and second, the implementation of the proposed ABM framework in this community is discussed.

4.1.5.1. Centerville testbed

The virtual community of Centerville, presented in Figure 18, was introduced by Ellingwood et al. (2016) to facilitate fundamental resilience algorithms and tools to be initiated, tested, coded, and modified. The Centerville testbed is a city of 50,000, located in the Midwestern parts of the US. The median household income in this city is close to the US average. As Figure 18 presents, there exist seven residential zones in this community, and each zone is described by Ellingwood et al. (2016) by their income level (i.e., low-income (LI), middle-income (MI), or high-income (HI)) and population density (i.e., low-density (LD) or high-density (HD)). In the current study, since information was needed in the household level, such general descriptions about each zone were broken down into household level information while maintaining the overall characteristics consistent with Ellingwood et al. (2016). Table 21 summarizes the resulting characteristics at each zone, including the average income level and population density, population, number of households, as well as distributions of income level, homeownership, and location of families/friends available in case of a disastrous event. For more information about the overall characteristics of each zone, readers can refer to Ellingwood et al. (2016).

Table 21: Seven residential zones in Centerville testbed and summary of their characteristics.

Zone		Z1	Z2	Z3	Z4	Z5	Z6	Z7
Income/Density		HI/LD	MI/LD	MI/LD	MI/HD	LI/LD	LI/HD	Mobile home park
Population		10,875	5,758	2,032	12,109	4,714	11,166	3,434
Number of households		4,246	2,267	800	4,767	1,856	4,396	1,352
Income level (%)	HI	95	20	5	0	0	0	0
	MI	2.5	60	55	50	20	5	0
	LI	2.5	20	40	50	80	95	100
Homeownership (%)	Owner	70	70	10	30	30	30	0
	Renter	30	30	90	70	70	70	0
	Mobile/RV	0	0	0	0	0	0	100
Friends/family location (%)	IC	30	25	15	30	30	20	20
	NC	40	30	40	40	40	30	20
	FC	30	45	45	30	30	50	60

Another important piece of information needed in the household level for the purpose of this study was the number and level of students within each household, which was not provided by Ellingwood et al. (2016). In the current study, the total number of students in the testbed was calculated to be consistent with the US statistics on the percentage of students in each education level (e.g., elementary school, middle school, high school, or college/university) provided by U.S. Department of Education, National Center for Education Statistics ("Digest of Education Statistics," 2020). Table 22 summarizes the resulting number of students within each residential zone and their distribution between different levels of school. As presented in Figure 18, there are seven schools in total in Centerville, including four elementary schools, two middle schools, and one high school. In the current study, depending on the location of each household, its students were assigned to the nearest available schools.

Table 22: Details of number and level of students in household located in residential zones.

Zone	Total number of students	Elementary school students	Middle school students	High school students	College/university students
Z1	2000	658	327	438	577
Z2	1093	360	179	239	315
Z3	400	132	65	88	115
Z4	2700	889	441	591	779
Z5	1050	346	172	230	302
Z6	2630	866	430	575	759
Z7	900	296	147	197	260

Now, all necessary information to be used in the proposed ABM framework are available in the household level. It means that for each household their location, archetype of their house, their homeownership, income level, number of household members, number of students in each school level, students' schools, and social vulnerabilities are known. At this stage, the ABM framework is implemented for the Centerville testbed and the number of each agent type is tabulated in Table 23.

Table 23: Number of agents defined in Centerville.

Agent type	Number of agents
Hazard	1
EPN	1,452
Utility company	1
WSN	32
School	7
School district	1
Construction companies	1
Household	19,648

4.1.5.2. Verification and validation

Verification and validation tasks were performed in the current study in a systemic process to ensure the credibility and quality of the simulation outcomes. To conduct verification, various tests were performed on each agent type by changing their attributes and their exposure to the hazard and tracing their behavior to ensure they behave consistent with the grounded theories and logic which were used to develop them (Sargent, 2010). In

addition to the agent-by-agent assessment, an external verification was performed by assessing various outputs of the community model by changing the hazard characteristics and identify any unusual pattern. Examples of such outputs are visual representations for housing recovery and school enrollments, similarly to the example results presented in Figure 30 and Figure 31 in the next section of this subchapter.

Various validation techniques (e.g., predictive validation, operational graphics, extreme condition tests, and internal validity (Sargent, 2010)) were also performed to ensure the credibility of the outcomes of the model. The ranges of variables input to the model were examined to be consistent with the available empirical data, information available about the Centerville community and the existing literature. Furthermore, it was ensured that the models employed from the literature to simulate the behavior of the agents were validated previously, such as the housing recovery model (Sutley & Hamideh, 2020) and damage fragility models (Mohammad Aghababaei, Koliou, Pilkington, et al., 2020; Masoomi & van de Lindt, 2018b; Memari et al., 2018; Vickery, Lin, Skerlj, Jr, & Huang, 2006). In order to assess the credibility of the model in the community level, predictive validation technique (Sargent, 2010; Xiang, Dame, & Cabaniss, 2005) was selected and outputs of the model under different tornados were compared to the actual observations from previous tornado events in the US. For this purpose, various outputs of the model, such as maximum drop in school enrollments and population dislocation rates, were compared to the similar events. Examples of such order-of-magnitude comparisons made with the 2011 Joplin tornado are presented in the next section, where the tornado and the affected population in the scenario presented

were similar to the 2011 Joplin tornado. Additionally, the model was tested under extreme conditions to check if the results are plausible for unlikely events. Multiple graphs were dynamically plotted during the simulation in order to trace the dynamic behavior of the model, identify errors, and evaluate the accuracy.

4.1.5.3. Single scenario sample

In order to better demonstrate the results of the proposed ABM approach on Centerville and the recovery dynamics in the city after a strong tornado occurs, first, a single realization of this model is presented in this section. In this realization, a strong EF5 tornado, demonstrated in Figure 21, with the maximum 3-sec gust speed of 105 m/s (235 mph), width of 1.5 miles and length of 21 miles happened with center located close to the center of Centerville. As Figure 21 shows, this tornado damages a large portion of the EPN components, including the transition towers, and as a consequence, all parts of the city experienced electric power outage right after the tornado. Figure 29 presents the number of households without access to electric power and full water service in the aftermath of the EF5 tornado in this realization. As this figure indicates, all households (19,648) lost their electric power access for one whole week, while all households experienced lower-than-normal water pressure for 25 days. According to Figure 29, more than 70% of the households did not have power access for 37 days, while recovery sped up afterwards and in day 45 all households had power access. Additionally, after 27 days from the tornado occurrence, water pressure in all supply nodes in WSN returned back to normal. As seen, the WSN recovered faster than the EPN and this is due to the

fact that WSN goes back to normal when only its electric power supply nodes (see Figure 23) recover, and not necessarily all EPN.

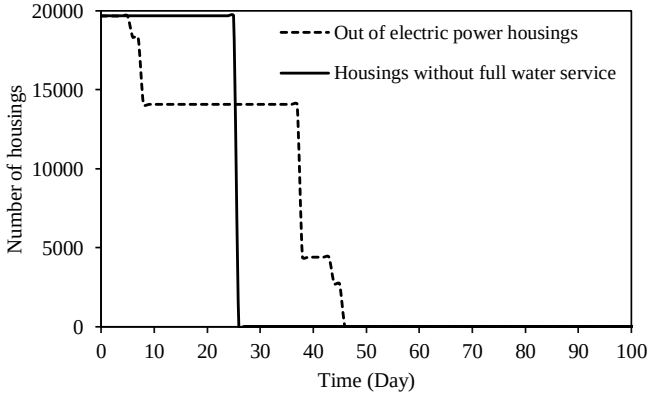

Figure 29: Number of households without access to electric power and full water service during the post-tornado period.

In order to thoroughly capture the recovery of the community in the aftermath, the simulation time was set to eight years (2,922 days), and the ABM framework captured the recovery of all sectors within the community up to this time after the tornado occurrence. A total of 7,437 households were located within the tornado path illustrated in Figure 21, and they experienced a wide range of damage states depending on the tornado intensity in their location and the housing archetype.

Figure 30a presents the percentage of households in each housing stage during the simulation time (2,922 days). According to this figure, of 7,437 households in the tornado path, only 31% were in Stage 4 (permanent housing) right after the tornado took place, while 67%, 1%, and 1% were in Stages 1, 2, and 3, respectively. One month after the disaster, 44% were in Stage 4, while 25% were still in Stage 1 (e.g., public shelters (if available), hotel/motel with financial assistance from various agencies, homeless shelter, family/friends, etc.), 9% were in Stage 3 (temporary housing), and 21% were in

Stage 2 (temporary shelters). Afterwards, the recovery continued smoothly, and some households were experiencing unstable housing by transitioning between different stages frequently, and as a consequence, as Figure 30a indicates, some households experienced housing failure (Stage 5) starting from eight months (240 days) after the disaster. The number of households in Stages 4 and 5 increased continuously, while four years after the tornado, only 1% of the households were in other three stages. At this instance of time, of all 7,437 households in the tornado path, approximately, 83.96% were in Stage 4, 0.01% in Stage 3, 0.47% in stage 2, 0.62% in Stage 1, and 14.94% in Stage 5. After this point, very small variations in these numbers happened, and at the end of the simulation (eight years), 84.19% were in Stage 4 and 15.81% were in Stage 5.

According to the reports from the 2011 EF5 Joplin tornado (Stewart, n.d.), around 7,500 buildings (mainly residential units) in the tornado path experienced damage, out of which 4,000 were completely damaged, and 9,200 people were displaced. As discussed above, in Centerville which has similar population density and building archetypes, 7,437 households were in the path, out of which 5,000 households (approximately 12,000 people) were initially displaced, which is close to the observations after the 2011 Joplin tornado.

(a)

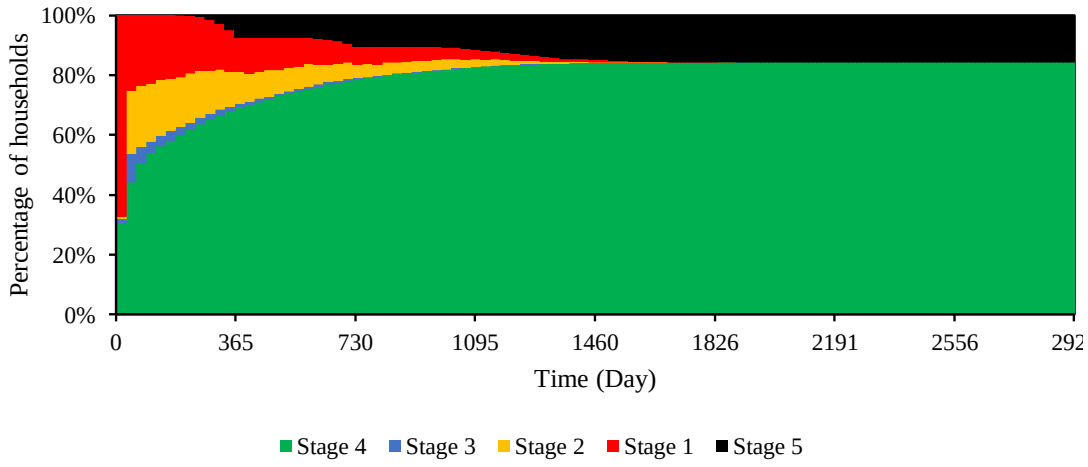

(b)

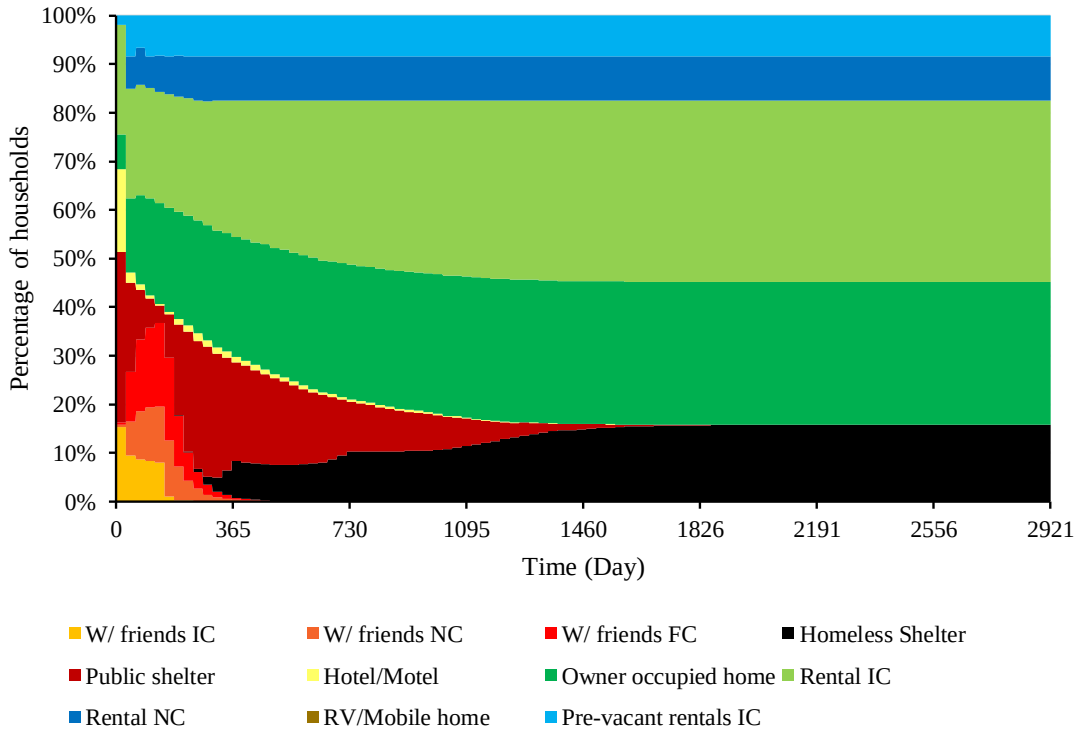

Figure 30: (a) Housing stage and (b) housing status of households located in the tornado path during the simulation time after the tornado occurrence (2,922 days).

Figure 30b presents the housing status of households determined based on assumptions made in the current study to map housing stage to housing status as discussed in the Household agents section and demonstrated in Figure 27. This information was used later to determine the location of students in the aftermath. Based

on Figure 30b, a large portion of the displaced households stayed with their friends and family during the first six months, while they moved to different types of public sheltering provided afterwards, and after one year, less than 1% were living with their friends and family. In the current study, it is assumed that 625 vacant rental units existed before the disaster (which is in line with average vacancy in the US), and as Figure 30b shows, these rental units absorbed a portion of needs for rental units during the first year due to damage to other rental units after the tornado. However, due to the extent of damage, these pre-vacant rental units were not sufficient and some households did not have any other choice but to leave the community and living in nearby cities. This situation was though alleviated as the damaged rental units were repaired and went back to the housing market. At the end of eight years, 8.9% of the 7,437 households relocated to the nearby cities, 29.2% lived in their own housings, 37.7% lived in the undamaged/repaired rental units, 8.4% lived in rental units vacant before the tornado, and 15.8% were experiencing housing failure which is defined as living in homeless shelters.

Figure 31a to Figure 31g present the number of enrollments of students in each of the seven schools in Centerville during time in the aftermath of the EF5 tornado up to two years (730 days). In addition, Figure 31h presents the number of students at each level of school (i.e., elementary, middle, and high school) who enrolled in schools outside the city because of the temporary or permanent displacement of their households.

Figure 31a and Figure 31b present Elementary Schools E1 and E2, respectively. As these figures indicate, the drop in enrollment of these schools was not significant

with a maximum drop of 4.3% and 2.5% respectively, while their enrollments increased continuously through time, but did not reach the pre-disaster enrollment during the first two years. As Figure 21 illustrates, Elementary School E3 was located at EF4 zone of the tornado, and hence, was significantly damaged which caused school closure to reconstruct its campus. As a consequence, as Figure 31c shows, its enrollment dropped to zero and all of its students enrolled in host schools and especially in School E4 which was the nearest one. Figure 31d shows that enrollment in this school increased by around 180% at the beginning, while it dropped through time by displacement of students to outside the city. This increase declined to 160% one year after the disaster. Finally, after 678 days, School E3 was completely repaired and all students went back to their original school, and as a result, the number of enrollments in School E4 dropped immediately. Middle Schools M1 and M2 had a similar recovery trajectory to Elementary Schools E3 and E4. School M2 was located at the EF4 zone of the tornado, shown in Figure 21, and experienced extensive damage. As a consequence, all of its students were enrolled in the only other available middle school M1, and it started its reconstruction right away. Per Figure 31e, at the beginning, School M1 experienced an increase of 84% in its enrollment, which was declined smoothly in the first five months as a result of student displacements outside the city, while it was reversed as some other households started moving back to the city. Finally, after the construction of School M2 was completed about 602 days after the tornado, students were enrolled back to their original school as Figure 31e and Figure 31f also indicate. As Figure 31f shows, although students were back from the host School M1, a drop of 8.6% remained in the enrollment of M2 due to

household permanent displacements. Figure 31g presents enrollments in the only high school in Centerville through post-disaster time. High School H1 was located in the tornado path and experienced DS3, and students started their school in dense condition until repair was completed and school went back to its normal state. As Figure 31g shows, a maximum drop of 14.4% occurred in the number of enrollments in this school, which was later recovered to 3.5% drop after one year from the tornado occurrence. Ultimately, Figure 31h demonstrates the number of students at each school level enrolled in schools outside the city. As this figure shows, these numbers increased during the first six months, while they decreased afterwards as some households started to return back to the community. This figure though shows a residual number which represents students whose families permanently displaced to other communities, and hence, they kept enrolling in schools not in Centerville. According to the report on the condition of schools after the 2011 Joplin tornado (Sulzberger, 2011), a drop of approximately 10% occurred in the number of enrollments in Joplin schools compared to the previous school year. According to Figure 31h, a maximum drop of around 14% occurred in the total student enrollments in Centerville schools, which is an acceptable drop approximate compared to the Joplin school system (4% more than Joplin) considering that housing disruption was more severe in Centerville. This drop also decreased gradually through time by returning of a portion of households.

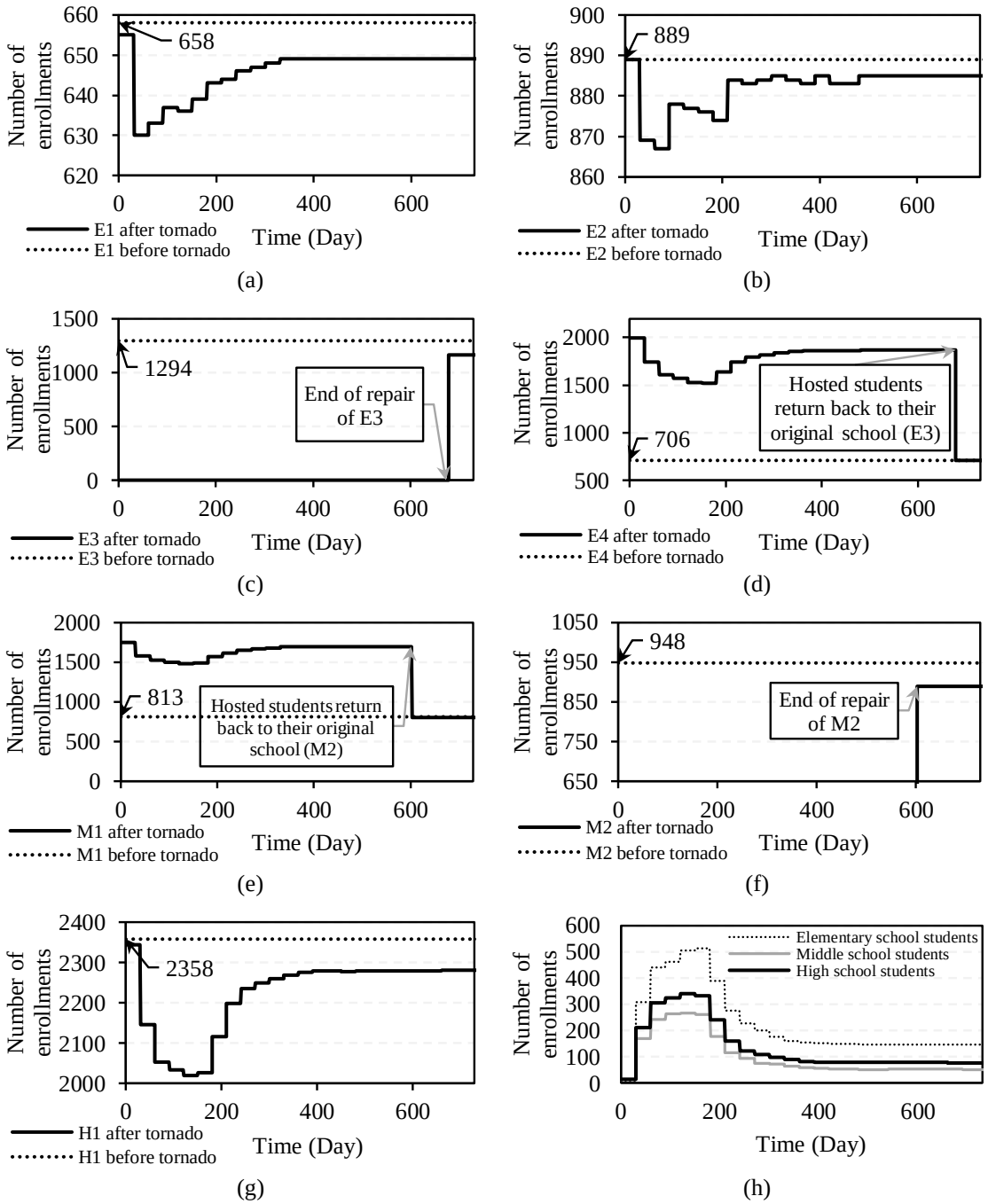

Figure 31: Number of student enrollments in the aftermath of tornado in schools (a) E1, (b) E2, (c) E3, (d) E4, (e) M1, (f) M2, and (g) H1, and (h) number of students enrolled in schools outside the city.

Figure 32 presents the school status of students who were living in Centerville prior to the EF5 tornado, determined using categories defined in Figure 28. In Figure 32,

"O" indicates student who enrolled in their original school, while "H" indicates students who enrolled in schools in the community other than their pre-disaster school (host schools). In the parentheses, the operation status of the school at which the student was enrolled is described based on categories in Figure 28. Per Figure 32, all students missed at least 22 days of school with the largest percentage (68.9%) due to electric power outage and the rest due to school repair and preparations. This includes schools which did not incur any damage, but the lack of utility postponed their reopening. Students are in Normal schooling only if they are enrolled in their original school and school is fully operational (i.e., O (Normal)). Due to closure of two schools in the city after tornado (E3 and M2), a major disruption happened in the education of schools which continued for 680 days. A large portion of students were enrolled in host schools, while a considerable percentage of students did not have their normal schooling since their school was hosting extra students from damaged schools. When School M2 was repaired on day 602, a jump is observed in the number of students in normal school status, while another jump occurred in day 678 when School E3 was completely repaired. According to this figure, 3.6% of students were still enrolling in schools outside Centerville even after two years from the disaster.

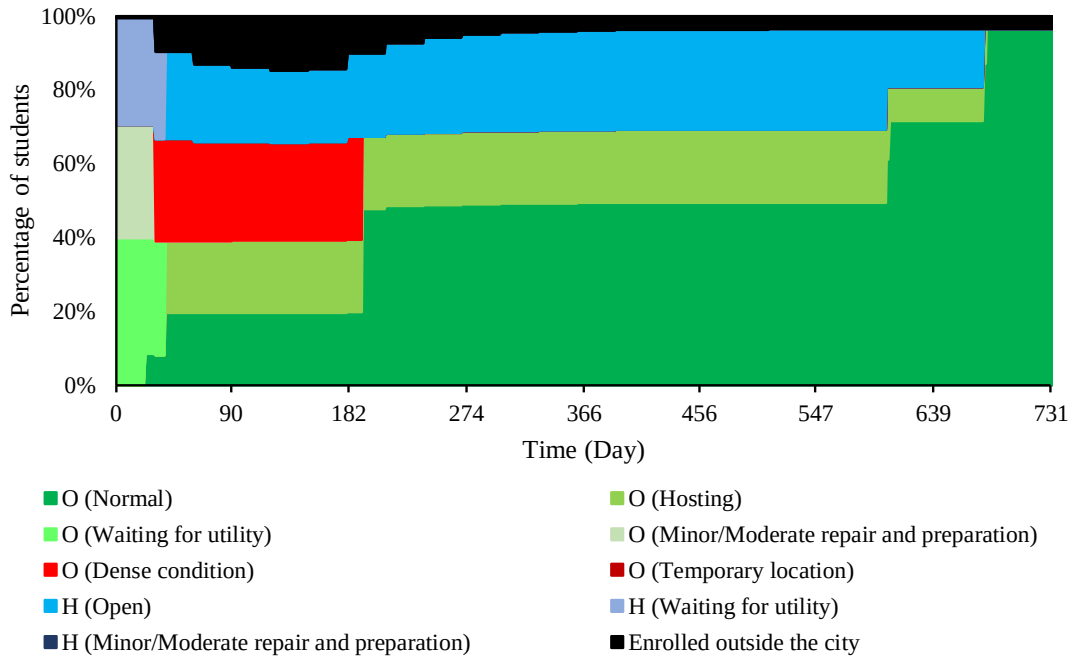

Figure 32: School status of students in Centerville through time up to two years after tornado.

4.1.5.4. Monte Carlo Sampling

One essential component to be accounted for in quantitative community resilience studies is the uncertainties in the response of the community to a disaster and its recovery trajectory. The proposed ABM framework is fully capable of capturing such uncertainties through randomness included in the model. In order to quantify the uncertainties in the consequences and recovery of the community, this study utilized Monte Carlo sampling. Each sample represents a scenario starting from the disaster occurrence and ending at a certain time in the aftermath (i.e., simulation duration). In the Centerville application of this study, for each sample, first, a tornado realization with random location, wind speed, width, and length is generated. Then, for each infrastructure agent (e.g., EPN agents, WSN agents, school agents, and household

agents), depending on the wind speed at the agent's location, random damage state based on its specific fragility model is generated. Based on their characteristics and initial state, agents follow different recovery trajectories. Uncertainties in these recovery trajectories are accounted for using a wide range of random variables input to each part of the model, such as random variables for repair time and impeding factors during the restoration. These uncertainties in each agent can significantly change the restoration of the community when aggregated together, and hence, this study utilized Monte Carlo sampling to account for the uncertainties.

For the application of this study, Monte Carlo sampling is conducted for tornados with intensities ranging from EF1 to EF5 with center randomly located within the boundaries of Centerville, and with random width, length, EF zone sizes, wind speed at each zone, and angle to the north pole. In addition, the simulation time is set to two years (730 days), and the reason for this selection is that the focus of this study is on the education system of Centerville and two years is considered a long enough period for such a purpose. It should be noted that the proposed ABM framework is capable of simulating long-term recovery of the community in the aftermath as well.

Figure 33 presents various example results of the Monte Carlo sampling analysis (100,000 samples) for EF5 tornado scenarios in Centerville. It should be noted that the randomly generated EF5 tornados located within the Centerville boundaries, but there is a chance that a portion of them did not hit the infrastructures in the city (e.g., tornado occurred near the boundaries and its path did not cross the city physical infrastructures). Figure 33a presents the mean values for number of households without access to electric

power, number of households experiencing less than normal water pressure, and water service percentage (i.e., water service compared to before the event averaged throughout the demand nodes) against time after the EF5 tornado occurrence, averaged over 100,000 sample scenarios resulted from Monte Carlo. One advantage of Monte Carlo sampling analysis is accounting for the uncertainties in the outcomes of the model. The mean values presented in Figure 33a are associated with a moderate to high level of uncertainty. To demonstrate this, the coefficient of variation (CoV), minimum, and maximum of the resulting curves in this figure at two time instances of one and three weeks after the tornado are tabulated in Table 24 along with the mean values from Figure 33a. Per Table 24, the population of households without power and full water service was highly uncertain at times one and three weeks after the event, all having CoV of over 100%. In addition, minimum and maximum values at these two times were 0 and 19,684 (all households). This means that in 100,000 realizations of the Monte Carlo analysis, there were cases that no household experienced power or water outage at these times, and there were cases that all households had no access to power and water services at these times. The latter means that in at least one realization, all city did not have power and water for at least three weeks. Table 24 also indicates that the water service percentage values at these two times were moderately uncertain with CoVs below 50%. As another representation of the effect of the EF5 tornados on EPN and WSN, Figure 33b presents the exceedance probability curves for full recovery time of these two infrastructures in Centerville. For each point on these curves, the corresponding value on the vertical axis indicates the probability that recovery period exceeds the corresponding value on the

horizontal axis. For example, as indicated in Figure 33b, there are respectively 0.45 and 0.24 chance that recovery of EPN and WSN exceed one month, if Centerville is struck by an EF5 tornado.

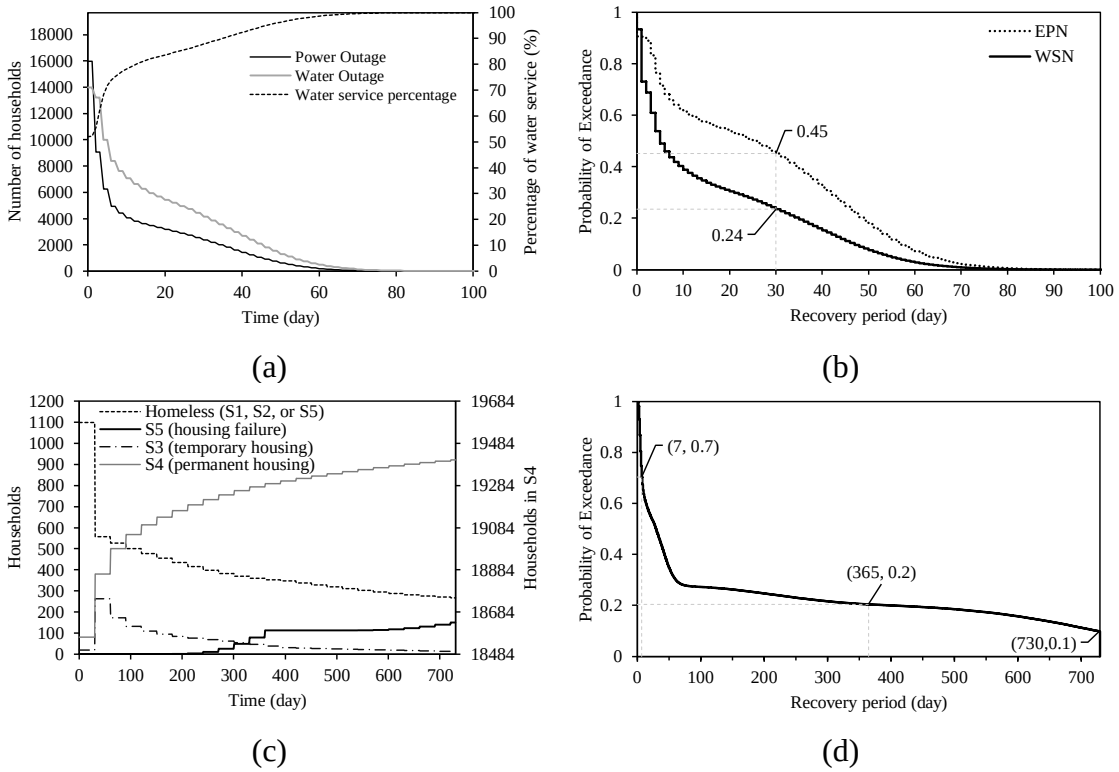

Figure 33: Example results of EF5 tornado scenarios: (a) mean of number of households experiencing water and power outage and water service percentage over time, (b) EPN and WSN recovery time exceedance probability curve, (c) mean of number of households at each housing stage over time, and (d) exceedance probability curve of education system restoration period.

Table 24: examples of uncertainties associated with mean values presented in Figure 33a and Figure 33c.

Variable	Mean	CoV (%)	Minimum	Maximum
Population without power 1 week after tornado	4,953	110.7	0	19,684
Population without power 3 weeks after tornado	3,184	144.5	0	19,684
Population without full water service 1 week after tornado	8,400	110.7	0	19,684
Population without full water service 3 weeks after tornado	5,443	156.1	0	19,684
Water service percentage (%) 1 week after tornado	75.3	40.7	0	100
Water service percentage (%) 3 weeks after tornado	84.0	31.5	0	100
Number of households in S1 3 months after tornado	260	183.7	0	3,869
Number of households in S1 18 months after tornado	107	189.9	0	1,631
Number of households in S2 3 months after tornado	267	163.5	0	3,991
Number of households in S2 18 months after tornado	92	173.2	0	1,437
Number of households in S3 3 months after tornado	172	144.7	0	2,208
Number of households in S3 18 months after tornado	23	166.4	0	339
Number of households in S4 3 months after tornado	18,984	4.7	11,509	19,684
Number of households in S4 18 months after tornado	19,350	6.6	14,552	19,684
Number of households in S5 18 months after tornado	113	162.1	0	1,725

Figure 33c presents the mean values resulted from 100,000 realizations for number of homeless households (i.e., households in S1, S2, or S5) against time after tornado up to two years, as well as number of households in temporary housing (S2), and number of households experienced housing failure (S5). In addition, on the secondary vertical axis, mean number of households with permanent housing is presented through time. In accordance with Figure 33c, right after an EF5 tornado happens within Centerville boundaries, on average 1,100 households (5.5% of all households in Centerville) lost their housing and temporarily become homeless. A rapid recovery initiated at the beginning of the restoration in the aftermath, while it decelerated afterwards. Per this figure, 267 households (1.35% of all households) on average remained homeless two years after the tornado, a large portion of which experienced housing failure. Similarly to Figure 33a, the mean values in Figure 33c are associated with significant uncertainties. Table 24 summarizes the statistics of the number of households experiencing each housing stage three and 18 months after the tornado, resulted from 100,000 realization in Monte Carlo analysis. According to this table, the

mean values presented in Figure 33c are associated with significant uncertainties with CoVs above 100% with the exception of number of households in S4. The reason for this exception is that a large portion of households were not located within the tornado path, and hence, remained in S4 in the aftermath, which increases the mean value and decreases CoV accordingly.

Attention now is turned into the education system in Centerville and its resilience against EF5 tornado scenarios. Figure 33d presents the exceedance probability curve for the recovery time of the education system in Centerville. Recovery of the education system here was defined as the time when all schools are recovered back to their normal state. Two examples are pointed out in this figure at time instances of one week and one year after the tornado occurrence. As indicated, there is 0.7 probability that recovery of the education system takes more than one week following an EF5 tornado occurring within boundaries of Centerville, while there is 0.2 probability that full recovery is not achieved within the first year in the aftermath. In addition, there is 0.1 probability that recovery of all schools takes more than two years after an EF5 tornado. Such long recovery durations are attributed to long reconstruction time when one or more schools are extensively damaged. This not only affects the students of the damaged school, but also the whole education system to absorb the lack of that school during the reconstruction phase. In the next step, a resilience measure to quantify education system resilience is proposed. Furthermore, more findings and insights will be provided based on the results of different tornado intensities resulted from Monte Carlo sampling analysis.

The Exceedance Probability (EP) curves of the recovery period for the education system in Centerville are presented in Figure 34 for tornado intensities ranging from EF1 to EF5. The disaggregated EP curves for system of schools in the same level, including elementary, middle, and high school systems (including four, two, and one schools, respectively) are also presented. For each point on curves in Figure 34, the corresponding value on the vertical axis indicates the probability that recovery period exceeds the corresponding value on the horizontal axis. Since probabilities of exceedance vary significantly for the EP curves of different tornado intensities, the ordinate in Figure 34 is shown in logarithmic scale. As an example of the results that can be obtained from Figure 34, exceedance probabilities for recovery periods of 30 days and 365 days are tabulated in Table 25 where red highlights are used to demonstrate the results, such that higher probabilities are shown with darker red color. As indicated by the results of Table 25 and Figure 34, the exceedance probabilities are much higher for stronger tornados, while exceedance probabilities are lower for the only high school in the city compared to the elementary and middle school systems. Moreover, exceedance probabilities are lower for the system of middle schools (two schools) in Centerville compared to the system of elementary schools (four schools). This may be attributed to the fact that as the number of schools in a system (e.g., elementary school system) increases, the likelihood of at least one of them to be damaged in a tornado event increases causing potential disruptions in all other schools of the same system in addition to the damaged school itself. It should be noted that although the likelihood of disruption for systems with more schools is higher due to their exposure to the tornado hazard, they

have more resources to absorb the adverse effects of the tornado compared to simpler systems. In the case of the only high school in Centerville, although there is a lower probability of damage to the school in a tornado event, the consequences on the quality of education received by students is significantly affected in the cases of damage to this high school.

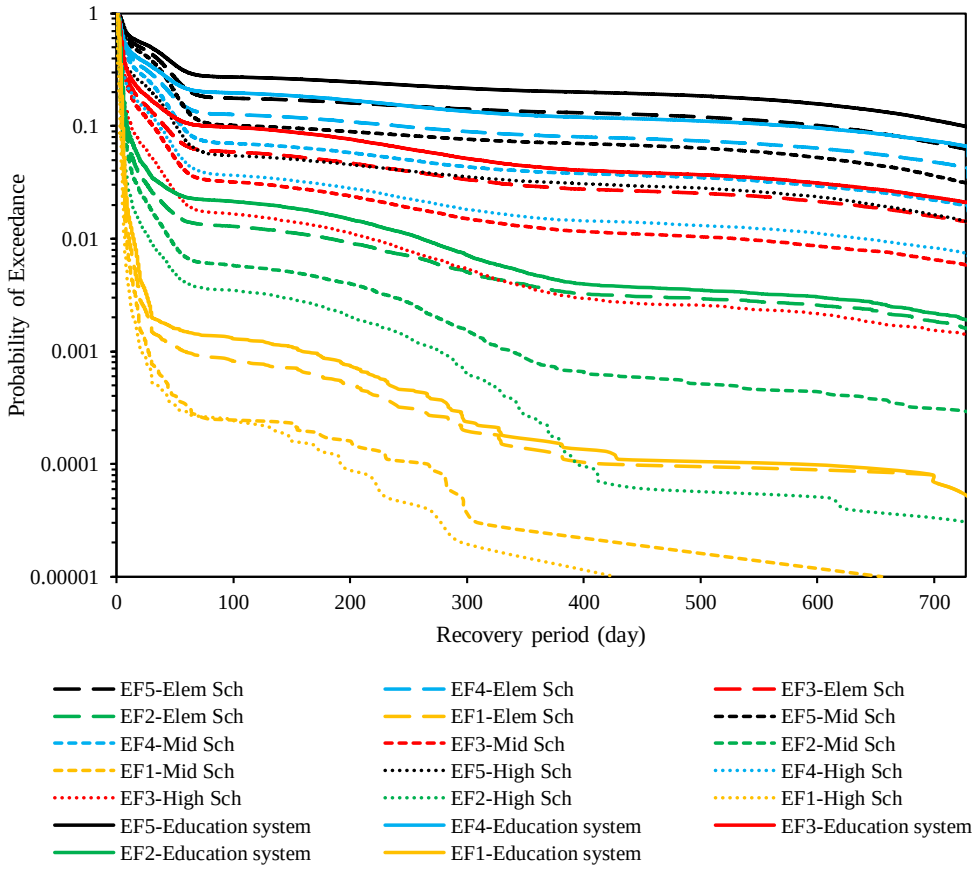

Figure 34: EP curves for the recovery period of the education system in Centerville and its disaggregation into three levels of elementary, middle, and high school for different tornado intensities.

Table 25: probability of exceedance of recovery period of the education system in Centerville from 30 days and 365 days for different tornado intensities.

Recovery period	Tornado intensity	Education system	Elementary school system	Middle school system	High school system
30 days	EF1	0.00222	0.00162	0.00082	0.00063
	EF2	0.03631	0.02681	0.01812	0.00950
	EF3	0.17062	0.13611	0.10579	0.05354
	EF4	0.34066	0.29198	0.24035	0.12488
	EF5	0.50130	0.44097	0.38721	0.20602
365 days	EF1	0.00016	0.00013	0.00002	0.00001
	EF2	0.00462	0.00367	0.00076	0.00022
	EF3	0.04282	0.02882	0.01234	0.00341
	EF4	0.12285	0.08223	0.03902	0.01511
	EF5	0.20407	0.13372	0.07148	0.03191

4.1.5.5. Education system resilience measure

In this section, a measure indicating the resilience of the education system is defined. Studies in the literature defined and utilized various measures to describe the resilience of a system. Figure 35 schematically demonstrates the functionality function, $Q(t)$, of a system over time after a disruption takes place, where 100% functionality indicates full functionality and 0% means total loss of functionality.

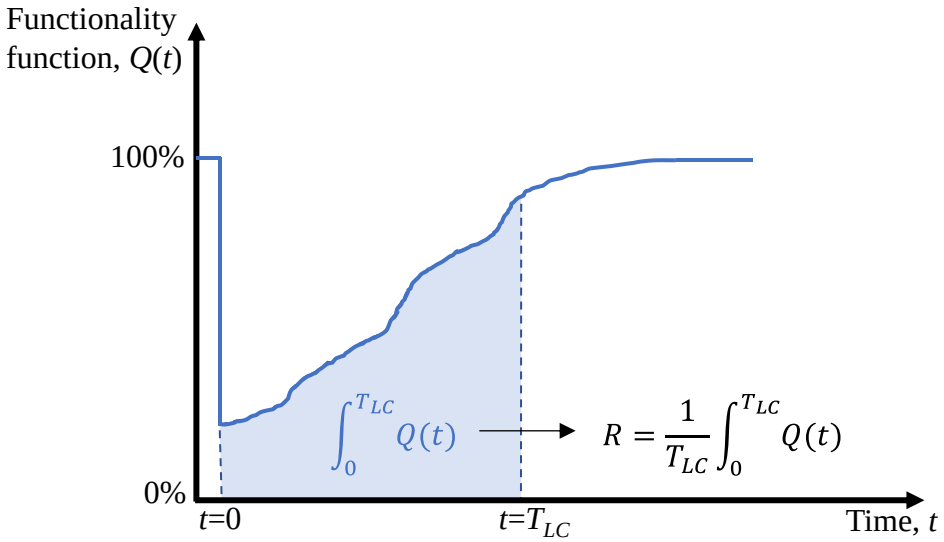

Figure 35: Schematic overview of resilience of a system.

A common method to quantify the resilience of a system is using the following equation (Bruneau et al., 2003; Gian Paolo Cimellaro et al., 2010b):

$$R = \frac{1}{T_{LC}} \int_0^{T_{LC}} Q(t)\, \mathrm{d}t \quad (18)$$

where R is the resilience measure of the system, T_{LC} is the control time, and $Q(t)$ is the functionality function of the system which is a dimensionless (percentage) function of time, t. The graphical representation of the resilience measure calculated using this equation is the normalized area underneath the functionality function in Figure 35 from time zero to T_{LC}. Various studies in the literature utilized Eq. (18) to quantify the resilience of a system, such as hospitals (Gian Paolo Cimellaro, Reinhorn, & Bruneau, 2010a), electric power network (Ouyang & Dueñas-Osorio, 2014), and water network (G. P. Cimellaro, Tinebra, Renschler, & Fragiadakis, 2016). The key elements in Eq. (18) are appropriate functionality function and the control time, T_{CL}. This equation is adopted in the current study to quantify and measure the resilience of the education system.

The functionality/performance of the education system in this study is described using Figure 32 which presents the schooling status of students over time in the aftermath. More specifically, the quantity and quality of the education that students receive in the aftermath is presented by indicating the percentage of students out of school, the percentage of students in each of the categories describing the quality of schooling, and the duration of students being in each of these categories. In addition, the functionality function in this figure is dimensionless which is suitable to be used in Eq. (18). One method to calculate the area underneath Figure 32 is to calculate only the area

under “O(Normal)” category since it is the same as the schooling before the disaster (i.e., students are in their original school, and school is in normal operation). However, this method does not capture the full functionality of the system, underestimates the resilience of the education system, and ignores its coping capacity to absorb the adverse effects of the tornado damages on the system. Therefore, the areas underneath schooling categories other than “*O(Normal)*” are added to the area resulted from *O(Normal)* but with coefficients between 0 and 1 resulting to computing the resilience of the education system as follows:

$$R = \left(A_{O,N} + \alpha_{O,H} \cdot A_{O,H} + \alpha_{O,WU} \cdot A_{O,WU} + \alpha_{O,RP} \cdot A_{O,RP} + \alpha_{O,DC} \cdot A_{O,DC} + \alpha_{O,TL} \cdot A_{O,TL} + \alpha_{H,O} \cdot A_{H,O} + \alpha_{H,WU} \cdot A_{H,WU} + \alpha_{H,RP} \cdot A_{H,RP} + \alpha_{\text{Outside}} \cdot A_{\text{Outside}}\right)/T_{LC} \quad (19)$$

where $A_{O,N}$ is the area underneath *O(Normal)* schooling category, and similarly $A_{O,H}$, $A_{O,WU}$, $A_{O,RP}$, $A_{O,DC}$, $A_{O,TL}$, $A_{H,O}$, $A_{H,WU}$, $A_{H,RP}$, and A_{Outside} are respectively the areas underneath *O(Hosting)*, *O(Waiting for utility)*, *O(Minor/moderate repair and preparation)*, *O(Dense condition)*, *O(Temporary location)*, *H(Open)*, *H(Waiting for utility)*, *H(Minor/moderate repair and preparation)*, and *enrolled outside the city* categories in Figure 32. The α-variables in this equation are the coefficients with values between 0 and 1 indicating the quality of the schooling compared to the *O(Normal)* schooling status, such that the closer the quality of the schooling to the pre-disaster status (i.e., *O(Normal)*), the higher the coefficient.

The values for the α-variables should be selected by decision makers based on their judgement about the quality of schooling students are receiving in each schooling status compared to the normal status prior to the disaster, which also depends on the policies, sociodemographic, economic, and other characteristics of a community. For the

application of this study, $\alpha_{O,WU}$, $\alpha_{O,RP}$, $\alpha_{H,WU}$, and $\alpha_{H,RP}$ are set to zero since they represent cases that students were missing school, and are assumed the worst schooling statuses, while, values for $\alpha_{O,H}$, $\alpha_{O,DC}$, $\alpha_{O,TL}$, $\alpha_{H,O}$, and α_{Outside} are set to 0.9, 0.5, 0.6, 0.7 and 0.3, respectively. After applying Eq. (19) on the results of the single EF5 scenario presented in this section, Figure 32 is transformed into Figure 36 presenting the functionality function of the education system in Centerville. The resilience measure can then be calculated using Eq. (18) by computing the area underneath this figure (i.e., sum of colored areas in this figure) divided by the control time. The resilience measure using this method for the particular tornado scenario when considering control time to be 730 days, 365 days, or 180 days, is 0.802, 0.704, and 0.554, respectively. The calculated resilience measure varies by changing the control time in Eq. (18), and it should be selected by the decision makers based on their desirable timeframe in the aftermath (Ouyang & Dueñas-Osorio, 2012).

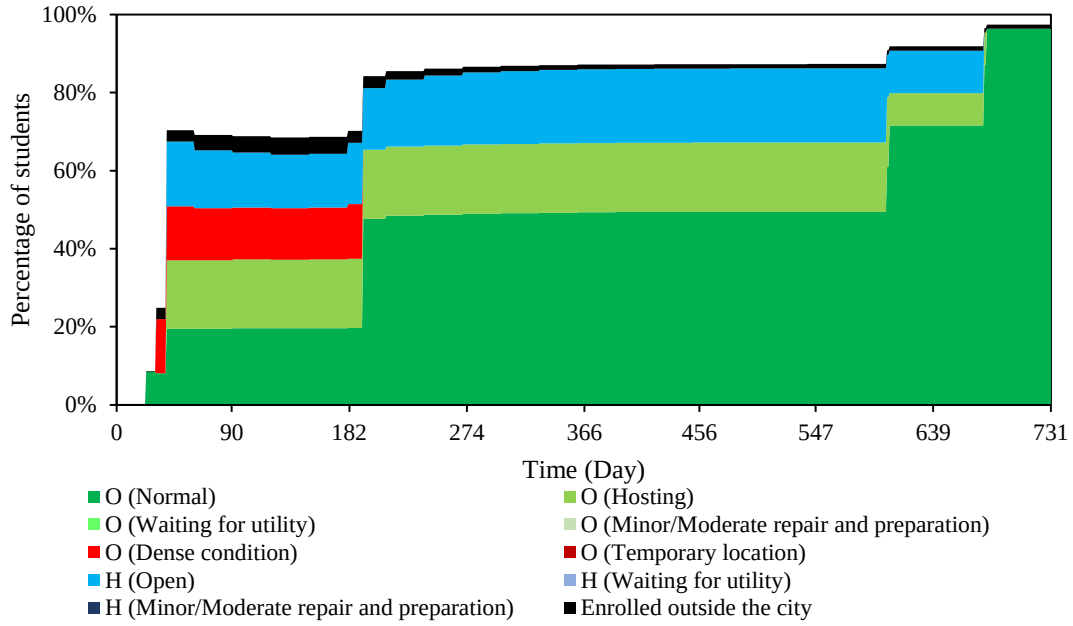

Figure 36: transformation of Figure 32 using Eq. (19) for the purpose of resilience quantification.

In the current study, for each tornado intensity (e.g., EF5), the resilience measure of the education system was computed by averaging the resilience measures of 100,000 random scenarios generated in the Monte Carlo analysis. In order to show the effect of control time, T_{CL}, in Eq. (18), the mean education system resilience measure is presented in Figure 37 for control times ranging from 1 day to 730 days indicating the significance of choosing control time on the resulting resilience measures.

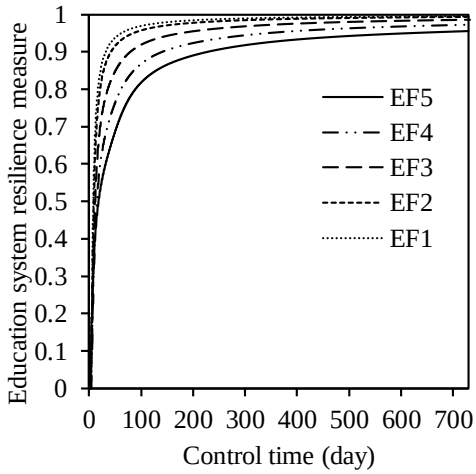

Figure 37: education system resilience measure versus control time for different tornado intensities.

Figure 37 presents the mean values of the resilience measure calculated in this study, while using the Monte Carlo sampling results, it is feasible to gain insights related to the randomness in the nature of this problem. In this study, four quantitative resilience levels describing the resilience of the education system were defined, namely, highly resilient, moderately resilient, slightly resilient, and non-resilient. To address the uncertainties, the probability mass function of the resilience measure of the education system resulted from Monte Carlo sampling assuming the control time to be 180 days was discretized in accordance with the defined resilience levels, and results are presented in Figure 38a. According to Figure 37, the average resilience measure of the education system against EF5 tornado scenarios is 0.88 when control time is 180 days, while Figure 38a indicates that out of 100,000 random EF5 tornados in Centerville, in 21% of the cases the education system was highly resilient, in 34% of the cases it was moderately resilient, in 37% of the cases it was slightly resilient, and in 8% of the cases it was non-resilient.

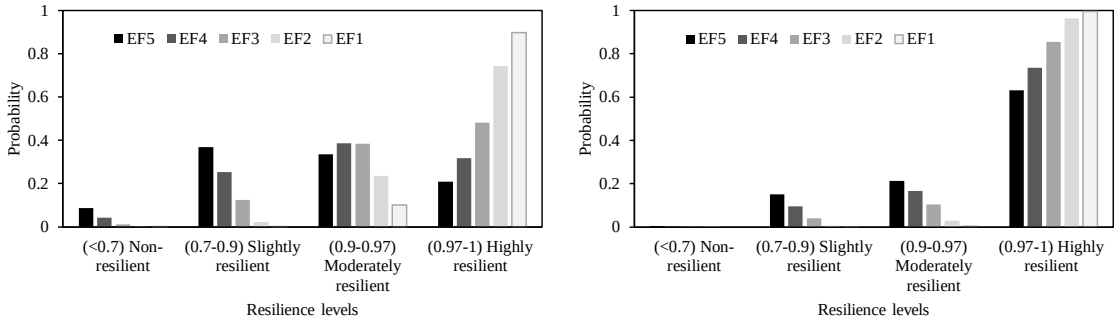

Figure 38: Probability mass function of resilience level of education system in Centerville given the tornado intensity (a) in its original condition, and (b) when backup utilities are provided.

Using the community model developed in this study and the quantified education system resilience measure, it is possible to make decisions for enhancing the resilience of the system by implementing various strategies on the community model and examining their outcomes/efficiency. The results of the analyses on Centerville revealed the significant effect of utility disruptions on the operability of schools, and as a result, on the education system. Hence, one potential strategy to enhance the resilience of the education system in Centerville is providing backup utilities for schools. This decision was implemented in the Centerville community model and Figure 38b illustrates the effectiveness of this decision on the calculated resilience measure. By comparing Figure 38a and Figure 38b, significant increase in the resilience of the education system in Centerville is observed when backup utilities are provided for schools prior to the disaster. The backup utilities can be electric power generators and water supplies. The reason for such significant increase in the resilience of the education system is that tornado events unlike hurricanes have a small area of impact, and hence, there is a

considerable chance that schools are not directly damaged by the tornado loads. However, because the EPN is typically spread throughout the city, there is a high chance of being disrupted by tornados causing parts or all of the city, including schools, to lose electric power access and this was one of the main factors affecting the resilience of the education system of Centerville. By having alternative utility resources, a higher level of redundancy is built in the education system, and the adverse effects of the EPN disruption on schools are absorbed. Other methods may also be considered to increase the redundancy of the EPN to restrict the area with power outage when one or a number of nodes are failed. This can be implemented in the community model in this study to see its effects on the education system resilience, and then compare the costs and benefits with the previous decision and select the best among all. In addition, other strategies, such as changing the restoration protocol by the school district, may be implemented and compared with one another.

4.1.6. Concluding Remarks

This study puts forward a modeling approach based on agent-based modeling (ABM) to model a community as a system of interdependent systems. In this study, components in each system are defined as autonomous entities (agents), while internal interactions among them shape the system and external interactions among different systems shape the community. The response and recovery of each agent is defined using a chain of probabilistic models, such as damage fragility model, repair model, and functionality recovery model, while internal and external interactions are defined by micro-behaviors implemented between interacting agents. Such interactions cause cascading consequences

when the community is impacted by a disaster, and account for interdependencies in the restoration of different agents during the recovery phase.

The developed community model is utilized to study the education system resilience of the communities, which is one of the least studied components of the communities in the quantitative disaster literature. A review of a number of past disasters and their effects on schools and students is used to identify the consequences as well as the restoration strategies adopted by schools and decision makers with the goal to recover the education system. A library of agents that encompass components/infrastructures and decision makers of a community involved in the response and recovery of the education system, including schools, households, EPN, WSN, school district, EPN company, and construction companies are implemented in the proposed agent-based model of the community subject to tornado hazard. For each agent type in the library, its response, recovery, and interactions with other agents are accounted for and presented in this subchapter.

The proposed ABM approach is applied to the virtual community of Centerville for evaluating the resilience of the education system through a series of probabilistic simulations. Uncertainty in the response of the model is accounted for using parameters input to the model, such as parameters describing tornado characteristics, damage fragilities, and repair time distributions. To demonstrate the results, first, a single strong EF5 tornado scenario is simulated and the results for various infrastructures in the community as well as education system are illustrated. Second, to account for and quantify the inherent uncertainties in the problem, a Monte Carlo sampling analysis is

performed for tornado intensities ranging from EF1 to EF5. A measure to quantify the education system resilience is also proposed in this study accounting for the quantity and quality of schooling students receive during the aftermath, while this measure is computed for the education system in Centerville subject to tornados with different intensities. Using the Monte Carlo analysis results, the probability of education system falling within different resilience levels, ranging from non-resilient to highly resilient, is computed for each tornado intensity. One advantage of quantitative study of the resilience of a community is enabling decision making by implementing various strategies on the community model and compare the quantified outcomes while selecting the best among all at the end. This subchapter demonstrated this capability by recalculating the education system resilience measure when backup utilities are provided to the schools as a pre-disaster mitigation action. The results showed a significant increase in the resilience measure of the education system of Centerville, and this is attributed to the vulnerability of the EPN to the tornado loads and the dependence of schools on the utilities to operate.

4.2. Thrust C-B: Community resilience assessment and decision-making platform based on the ABM framework

4.2.1. Introduction

This subchapter is an extension to the previous subchapter to account for additional sectors within the community. This study aims to assess the resilience of the community through proposing a resilience measure and developing a decision-making platform to compare various mitigation strategies. Using this platform and the calculated resilience measure, it is possible to apply different mitigation strategies on the agent-based model of the community, quantitatively compare the results on the community and its sectors, and ultimately, select the most effective among all. The focus of the previous subchapter was on the education system accounting for the community components influencing its performance and resilience, while this subchapter extends those components to have a more comprehensive overview of the community.

Various resilience measures were adopted in the literature to represent the resilience of a community or an individual system in a community. Several measures of resilience exist in the literature that are suitable for the scope of each work. Panteli and Mancarella (2015) proposed two measures, loss of load expectation (LOLE) and loss of load frequency (LOLF) indicating the average number of hours that some customers are disconnected due to events on the transmission network and the number of occurrences of such disconnections per week, respectively, to evaluate the resilience in different scenarios. Adams et al. (2012) described the resilience of transportation networks using two measurements, called reduction and recovery, showing the rate of decrease in the

system performance after the disaster and the rate of recovery in the performance after the system starts to recover, respectively. In this study, performance was quantified using the speed and counts of trucks in a highway section before and after the disaster. Ouyang and Dueñas-Osorio (2012) expressed the performance of power grids using the total amount of flow delivered, while they utilized this performance metric to calculate the resilience measure of the grid. Cimellaro et al. (2010) utilized the percentage of healthy population compared to pre-disaster status as a measure of performance to quantify the hospitals resilience in the community level. Zhang et al. (2009) measured the resilience of businesses in terms of capital vulnerability, labor vulnerability, supplier vulnerability, and customer vulnerability. In the studies of household resilience against disasters, a large portion of studies used welfare flow of the household as a recovery metrics and an indicator of the resilience of households. Various indicators for the welfare of households are identified in the literature. Kurosaki (2010) utilized the consumption changes as an indicator, while Rodriguez-Oreggia et al. (2013) and Carter et al. (2007) studied poverty rate of households as indicators of welfare change after major disasters. Arouri et al. (2015) employed different welfare indicators, including per capita income, per capita expenditure, household poverty status, and income share of different sources. Navrud et al. (2012) proposed a novel approach to estimate the welfare loss of the households based on their willingness-to-contribute labor to the flood prevention programs.

The aforementioned measures describe the resilience of a component/system of the community (e.g., lifelines, businesses, or households) against disturbances. However,

there is a need to aggregate all of these components/systems and the measures describing their resilience to comprehend the resilience of the whole community as a system of systems to disasters. To address this, various studies in the literature combined the nondimensionalized consequences of different systems within the community using a weighted approach to define a community resilience measure (Gian Paolo Cimellaro et al., 2010a; Didier, Broccardo, Esposito, & Stojadinovic, 2018; Vugrin, Warren, Ehlen, & Camphouse, 2010). These weights were typically selected through expert judgment and qualitative methods, which may have the disadvantage of being subjective. To address this, Nasrazadani and Mahsuli (2020) integrated risk methods and agent-based simulation to introduce a new resilience measure based on the monetary loss accumulated through different systems in the community impacted by seismic loads. They utilized several loss models in the literature to quantify the monetary loss of each sector, accounting for physical, economic, and social consequences. This method results in a unified resilience measure without the subjective relationships used in other studies. However, monetizing all consequences in the aftermath, especially social losses, is a challenging task and requires specific research for each community.

In the next sections of this subchapter, first, the newly added agents, including business agents, person agents, unemployed labor pool agents, and hospital agents, are introduced. Thereafter, using the developed community model for Centerville, various outcomes of the newly added agents when the community is subject to a strong EF5 tornado are discussed. In the next step, resilience measures are proposed to quantify resilience of the community and its systems, while the application of these measures to

assess the community resilience and conduct decision making are discussed with an application on Centerville.

4.2.2. Agents

In the previous subchapter, a modeling approach based on agent-based modeling (ABM) was proposed to develop a system of systems (SoS) model of a community accounting for various systems, including electric power network (EPN), water supply network (WSN), schools, households, and construction companies. This subchapter utilizes this approach and develops a comprehensive model of a community by adding more systems into it, including businesses and the healthcare system. For this purpose, various agent types and their interactions are defined in this subchapter. These agents which are described in this section are business agents, person agents, unemployed labor pool (ULP) agents, and hospital agent.

4.2.2.1. Business agents

Each business unit in this study is modeled as a separate agent, the behavior of which is defined using statecharts presented in Figure 39. As this figure indicates, the functionality of a business depends on its physical functionality as well as employee availability. The blue box in Figure 39 demonstrates the physical recovery of a business if it is damaged. According to this figure, physical recovery of a business is a function of various impeding factors typically observed in the aftermath of major disasters as well as a number of mitigation factors that accelerate the physical recovery. Impeding factors in

this study are calculated based on Chapter 3, where the REDi (Almufti & Willford, 2013b) framework for calculating impeding factors was modified to better represent reconstruction delays due to weather-related hazards. Impeding factors in this study account for delays due to safety inspections (T_{insp}), securing finances to initiate the repair process (T_{fina}), finding and hiring a contractor (T_{conm}), and getting a construction permit (T_{perm}). Delays due to securing finances depend significantly on the attributes of a business, including its insurance coverage, size, capital, and access to other resources which may help business to secure its necessary finances as soon as possible. In this study, to reflect this, different delay distributions are adopted from REDi (Almufti & Willford, 2013b) depending on the insurance coverage of the business. According to Cremen et al. (2020), there are also some mitigation factors that may shorten the restoration time, such as management effect and ability of the business to relocate. This concept is adopted in the current study, and a business, if feasible, relocates temporarily or permanently when relocation is a better option in short- or long-term. In Figure 39, when relocation is an option (i.e., $MF_{R,i} = 1$) for a business agent, it relocates to a new place and starts its full or partial functionality in $t_{reloc,i}$ days after the decision to relocate is made. If relocation is not an option, still an effective management can reduce the delays in repair. In this study, using the concept by Cremen et al. (2020), it is assumed that the management mitigation factor can accelerate securing the finances, finding and hiring a contractor, and getting a construction permit. The formula used in Chapter 3 to calculate delays of reconstruction ($T_{I,i}$) after weather disasters is modified in the current study to account for the mitigation factors (e.g., management mitigation ($MF_{m,i}$)):

$$T_{I,i} = T_{\text{insp},i} + \left(1 - MF_{m,i}\right) \cdot \left(\max\{T_{\text{fina},i}, T_{\text{conm},i}\} + T_{\text{perm},i}\right) \quad (20)$$

Similarly, other mitigation factors, such as hastening recovery and backup utilities, can also be included to calculate the delay in repair due to impeding factors, similarly to the mitigation factors considered in Cremen et al. (2020). On the contrary to the mitigation factors, there are some factors that may worsen the situation and even cause permanent closure of the business. For example, in previous disasters, it was observed that small businesses with owners who were near retirement are likely to close permanently if they were significantly damaged (Smith & Sutter, 2013a). In the ABM approach in this study, such rules can be reflected into the decisions made by the business agents by defining a set of micro-behaviors for them. After starting the repair, the repair time to achieve a certain physical functionality level depending on the initial damage state of the building is estimated using repair time distributions generated by Koliou and van de Lindt (2020) for various building archetypes. The time distributions provided by Koliou and van de Lindt (2020) are used to estimate the time that takes for a building after its repair initiation to reach partial (FL1) or full functionality (FL0) depending on the initial damage it incurred. As shown in Figure 39, business can reach partial physical functionality, and thereafter it reaches full physical functionality by the repair completion.

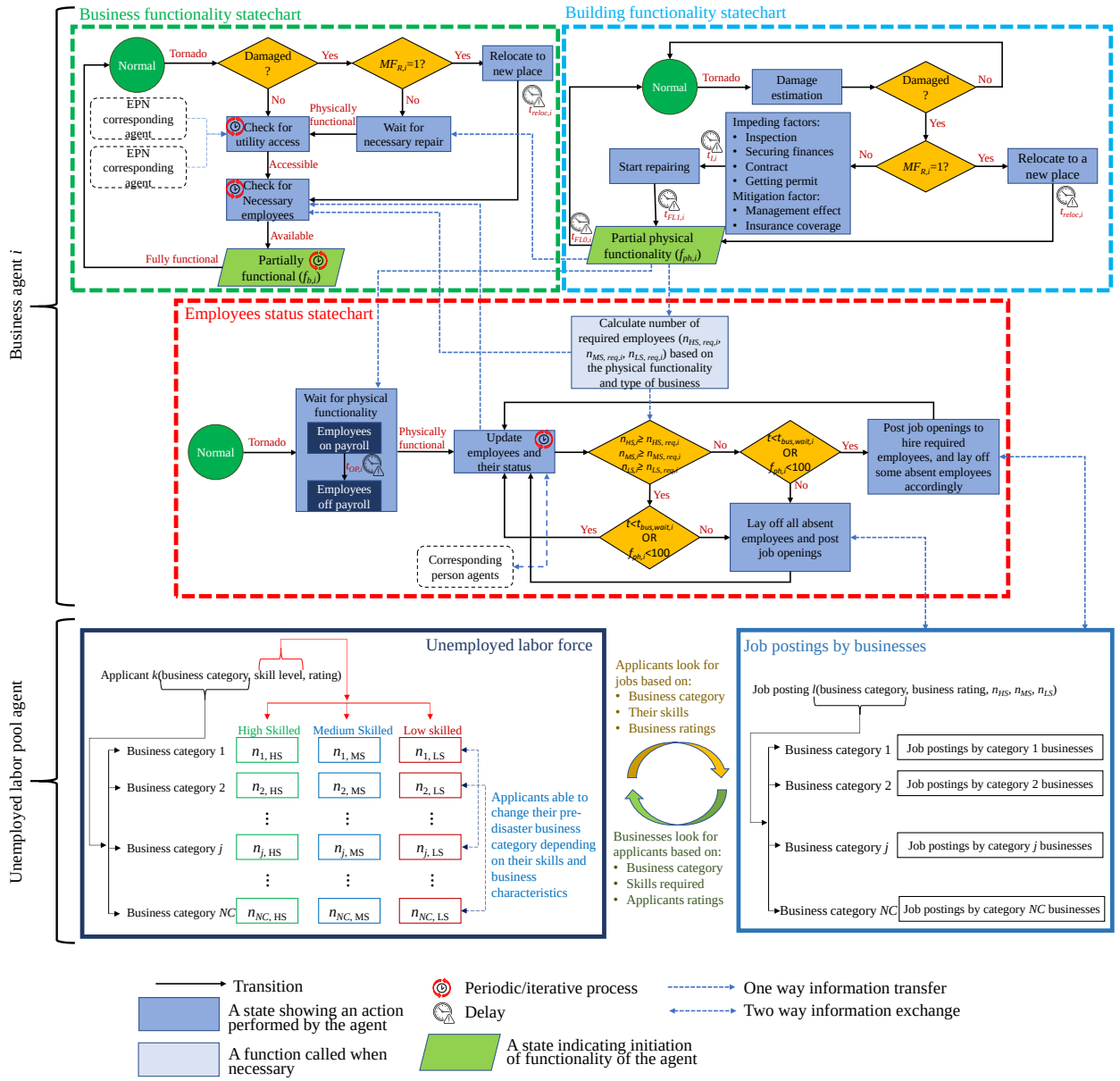

Figure 39: Business agents and unemployed labor pool agent.

As shown in the green box in Figure 39, whenever the business reaches partial or full physical functionality, the business agent checks for access to the necessary utilities (e.g., water and power). Each business depends on specific nodes in the EPN and WSN to provide its necessary electricity and water. The next requirement to resume the business in the aftermath is retaining the necessary employees. In this study, the level of

skills of an employee in each business category is defined as low, medium, or high, and each business agent requires a certain number of low-skilled ($n_{LS,req,i}$), medium-skilled ($n_{MS,req,i}$), and high-skilled ($n_{HS,req,i}$) employees to be able to operate. These numbers depend on the characteristics of the business as well as the level of its physical functionality.

The red box in Figure 39 demonstrates the statechart simulating the process of updating employees of the business agent, their working status, as well as decisions to lay off absent employees or hire new ones. According to this figure, during the time that the business is awaiting physical functionality recovery, employees may be on or off the payroll depending on the resources to which the business has access. If the business has business interruption insurance, depending on the policy details, the insurance may pay for the salary of the employees up to a certain time in the aftermath, which typically ranges from two weeks to one year. Additionally, businesses may keep their employees on the payroll using resources other than interruption insurance, such as the business capital and loans. Large businesses typically have more resources to keep their employees on the payroll, which is evident from previous disasters (Smith & Sutter, 2013b). In addition, franchise businesses may transfer their employees to other branches temporarily to keep them on the payroll. After a business agent gains its physical functionality, it periodically updates the list of employees and their status. Employees may also leave a business before it gets back to physical functionality because of various reasons, such as not being on the payroll. The status of the employees shows whether they are available to work, which depends on their location in the aftermath (i.e., inside

or outside the city), their injury level, and their household status (i.e., whether or not they need to take care of a family member due to injury or home schooling). In the past tornado disasters, it was observed that businesses assist employees to address their issues in the aftermath, including providing them with temporary housing, essential needs, and financial support to repair their housing, while the businesses typically let their employees be absent for a certain amount of time in the aftermath, $t_{wait,bus,i}$. After this time, businesses may start replacing the absent employees with new ones. These are accounted for in developing the employee status statechart in Figure 39. Each time the statechart updates the employees and their status, it is evaluated if the business has enough employees to operate depending on the level of its physical functionality. If the business does not have enough employees and the time did not pass $t_{wait,bus,i}$ or the business did not reach full physical functionality, the business agent posts job openings to hire only required employees and lays off some absent employees accordingly. If the business does not have enough employees and the time passed $t_{wait,bus,i}$ and the business is back to full physical functionality, the business agent lays off all absent employees and posts new job openings accordingly. If the business has enough employees to initiate its operation, but the time passed $t_{wait,bus,i}$ and the business is back to full physical functionality, the business lays of all absent employees and posts job openings to go back to full functionality. This process of updating employees and their status, laying off absent employees, and hiring new ones continues during the simulation periodically, and the information about the employees is communicated with the business functionality statechart (green box in Figure 39) to update the functionality status and the level of

functionality, f_b. To hire new employees, the business agent communicates with the unemployed labor pool agent through posting job openings, and the business agent can retain new employees depending on the availability of unemployed people with the desired skill level and business category. This process is further discussed later about the unemployed labor pool agent.

4.2.2.2. Person agents

Each person in the population of the community (called people herein) is modeled as a separate person agent, which defines the behavior of the person and contains various attributes of the agent. Two main attributes of the person agents which are periodically updated during the simulation are the health condition (injury level of the agent and its treatment process) and their occupation. The latter applies to the agents who are considered as labor force. In the following, first, the method used in this study to estimate the injury level of each person agent due to tornado events is discussed, and second, details of the person agent are presented.

4.2.2.2.1. Injury level estimation

Various methods exist in the literature to predict the casualties due to natural hazards. For tornados, different models exist that predict the number of injuries and fatalities at the regional level as a function of a number of predictors, such as tornado intensity, tornado length, and population within the tornado path (Masoomi & van de Lindt, 2018a). However, these models do not distinguish between different levels of injury and they work at the regional level, which is not suitable in the current study. A model is required in this study to predict the injury level of each person agent depending on the

building archetype where the agent was during the event as well as the damage state of that building. To address this, a casualty model is proposed here that predicts injury level (IL) of a person agent based on the building archetype where the agent was during the event and the damage state of the building. Injury levels are adopted from Hazus 4.2 and their descriptions are provided in Table 26.

Table 26: Injury levels and their definition, adopted from Hazus 4.2.

Injury Severity Level	Injury Description
Severity 1 (IL1)	Injuries requiring basic medical aid that could be administered by paraprofessionals. These Types of injuries would require bandages or observation. Some examples are a sprain, severe cut requiring stiches, a minor burn (first-degree or second-degree on a small part of the body), or a bump on the head without loss of consciousness. Injuries of lesser severity that could be self-treated are not accounted for in here.
Severity 2 (IL2)	Injuries requiring a greater degree of medical care and use of medical technology such as x-rays or surgery, but not expected to progress to a life-threatening status. Some examples are third-degree burns on the head that causes loss of consciousness, or fractured bone.
Severity 3 (IL3)	Injuries that pose an immediate life-threatening condition if not treated adequately and expeditiously. Some examples are uncontrolled bleeding, punctured organ, other internal injuries, spinal column injuries, or crush syndrome.
Severity 4 (IL4)	Instantaneously killed or mortally injured.

A fault tree analysis is used in this study to predict the injury level of a person in a building which incurred a certain damage state during the event. This fault tree is schematically demonstrated in Figure 40 for a person agent inside an Archetype T_i. Damage state (DS) of the building is determined using damage fragility functions available in the literature for the 19 archetypes defined by Memari et al. (2018). In this figure, $P_{j,k}$ indicates the probability that a person incurs Injury Level j (ILj) when he/she is in a building damaged to DSk due to tornado loads. For example, $P_{2,1}$ indicates the probability that a person agent incurs IL2 when the agent is in a building damaged to DS1. The mathematical formulation of the probabilities in Figure 40 is as follows:

$$P_{j,k} = P(\mathrm{IL} = \mathrm{IL}j | \mathrm{DS} = \mathrm{DS}k) \quad (21)$$

$$P_{1,k} + P_{2,k} + P_{3,k} + P_{4,k} \leq 1 \quad (22)$$

The probability that a person in a building with DS*k* incurs no injury is:

$$P_{0,k} = P(\text{No injury}|\text{DS} = \text{DS}k) = 1 - P_{1,k} - P_{2,k} - P_{3,k} - P_{4,k} \quad (23)$$

An expert solicitation was conducted to estimate the $P_{j,k}$ probabilities for all 19 archetypes. An online questionnaire was distributed between experts with a deep knowledge of damage and casualty estimations after massive tornado events. For each Archetype T_i, the experts were provided with the construction details of the archetype as well as its damage state descriptions. Using these information and injury level descriptions in Table 26, the experts were able to provide their estimations for $P_{j,k}$ probabilities. The estimations of the $P_{j,k}$ probabilities provided by the experts for Archetypes T_1, T_2, T_3, T_4, and T_5, which represent all residential archetypes per Memari et al. (2018), are tabulated in Table 27. Using the resulting fault tree, it is possible to randomly estimate the IL of a person agent when DS of the building where the agent was during the event is known.

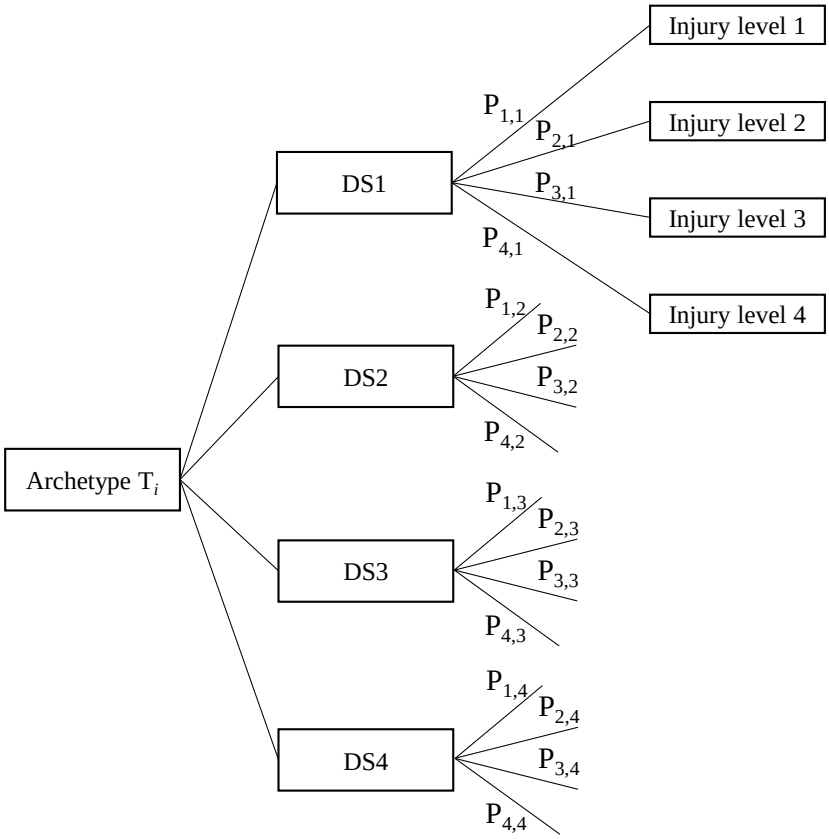

Figure 40: fault tree used to estimate injury level of person agents.

Table 27: Probability estimations provided by the experts to define the fault tree of Archetypes T_1, T_2, T_3, T_4, and T_5.

Probability	T1 and T3	T_2, T_4, and T_5
$P_{0,1}$	0.99489	0.99239
$P_{1,1}$	5E-3	7.5E-3
$P_{2,1}$	1E-4	1E-4
$P_{3,1}$	1E-5	1E-5
$P_{4,1}$	0	0
$P_{0,2}$	0.974895	0.97489
$P_{1,2}$	2E-2	2E-2
$P_{2,2}$	5E-3	5E-3
$P_{3,2}$	1E-4	1E-4
$P_{4,2}$	5E-6	1E-5
$P_{0,3}$	0.93895	0.9389
$P_{1,3}$	5E-2	5E-2
$P_{2,3}$	1E-2	1E-2
$P_{3,3}$	1E-3	1E-3
$P_{4,3}$	5E-5	1E-4
$P_{0,4}$	0.795	0.7575
$P_{1,4}$	0.1	0.12
$P_{2,4}$	7.5E-2	0.085
$P_{3,4}$	2.5E-2	3E-2
$P_{4,4}$	5E-3	7.5E-3

4.2.2.2.2. Person agent details

If the person agent is considered as labor force (employed or unemployed), this agent contains information about its ability to work, whether or not the agent is unemployed, and the business where the person works at each time during the simulation (if employed). The statechart presented in Figure 41 simulates the health and occupation status of the person agents who are in the labor force. The IL of the agent is determined probabilistically using the method presented in the previous section (Section 4.2.2.2.1). If the agent incurs injury level 4 (IL4), the agent is assumed dead and this information is conveyed to the business where the agent worked before the disaster (if the agent was employed). If the person agent incurs an injury level except IL4 (i.e., IL1, IL2, or IL3), the agent needs treatment, and hence, goes to the healthcare system agent. Depending on the severity of the injury and access to the healthcare service, the agent recovers after some time and becomes able to work. As shown in Figure 41, the ability of a person agent to work depends on various contributors, including the health condition of the agent, the location of the agent, the health condition of the household members and whether or not they need assistance, and if there are any children in the household needing homeschooling. If the agent is able to work and was unemployed before the disaster, it looks for a job by sending an application to the unemployed labor pool (ULP) agent. As shown in Figure 39, each application sent to the ULP agent contains information about the business category which applies to the applicant, as well as the skill level and rating of the applicant. Whenever the applicant is selected by a business which is looking to hire new employees, a message is sent to the person agent

(applicant) that it is employed. On the other hand, as illustrated in Figure 41, if the person agent was employed before the disaster, the agent periodically updates its job status by communicating with its corresponding business agent (i.e., the business where the person agent was working prior to the disaster). The person agent may be laid off by the business agent after a while when the agent is absent (see Section 4.2.2.1), or may chose to leave a business if the business is closed and the person is not being paid for more than a tolerable period, $t_{wait,emp,i}$. In either of these cases, the agent is unemployed and sends an application to the unemployed labor pool agent, if the agent is able to work.

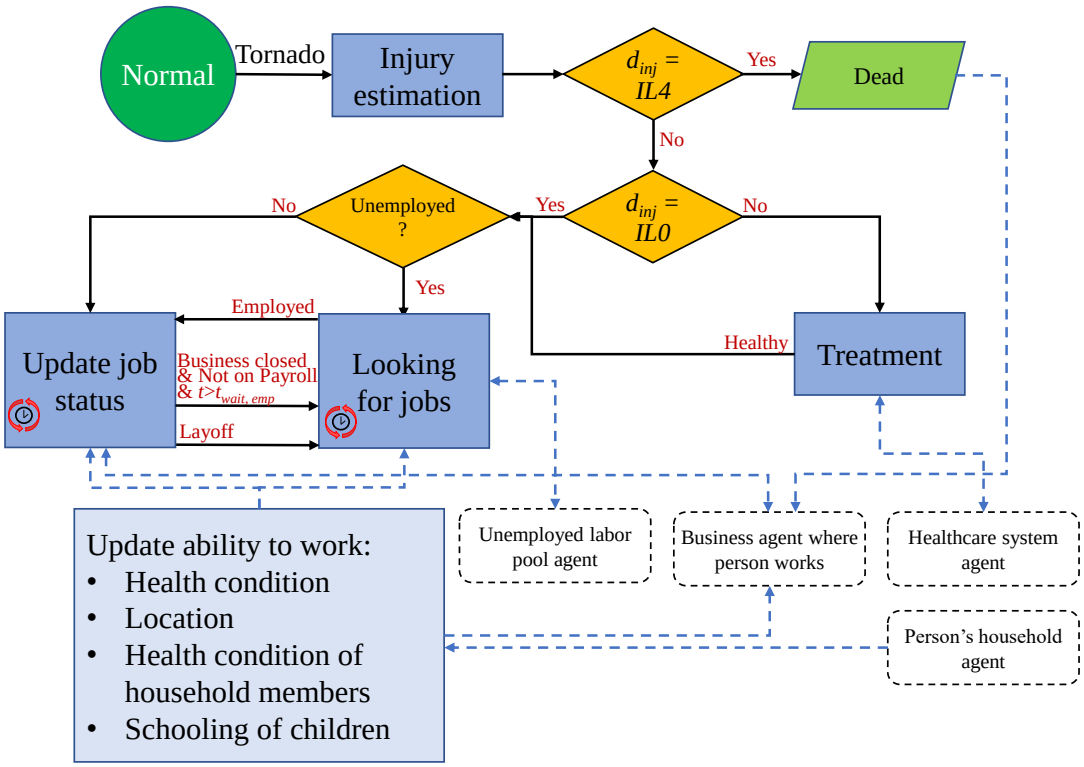

Figure 41: Person agents in the labor force.

If a person agent is not in the labor force (e.g., children, stay-at-home parents, above 65 people not working, etc.), a statechart simpler than the one presented in Figure 41 is used, where the injury and recovery of a person is simulated. If the person agent

incurs injury, it goes to the healthcare system agent to be treated, and returns back to normal after the treatment is completed.

4.2.2.3. Unemployed labor pool agent

A single agent, named unemployed labor pool (ULP) agent, is defined in this study and illustrated in Figure 39, which models the dynamics between businesses looking for employees and the unemployed person agents looking for jobs. According to the U.S. Bureau of Labor Statistics (2021), unemployed population can be grouped based on the business category they are looking for opportunities. In the current study, job applicants are classified into different groups based on their business category, while job postings by the businesses are also classified into different groups depending on their category. The business categories adopted in this study for Centerville are: (i) retail, (ii) manufacturing, (iii) services, (iv) construction, (v) healthcare, (vi) education, (vii) professional services, (viii) utility, and (ix) government. The services category is also divided into four subcategories of information, financial activity, leisure, and other services. According to Figure 39, applicants are able to change their pre-disaster business category depending on their skills and business category. For example, in the current study, it is assumed that low-skilled persons can move between businesses in certain categories, such as retail, services, healthcare, and professional services.

In accordance with Figure 39, each applicant (person agent) is placed in a group of unemployed persons based on its business category and skill level (i.e., low-, medium-, or high-skilled). Each applicant has a rating between 0 and 1 which indicates

the desirability of that person to be employed based on the person's years of experience, education, etc. Each job posting by the business agents is also placed in a certain group based on the business's category. Each job posting contains information about the number of low-skilled (n_{LS}), medium-skilled (n_{MS}), and high-skilled (n_{HS}) employees the business is looking to hire, while the business rating, which is a number between 0 and 1, indicates how desirable the business is for a person to be hired at. The business rating can indicate the job compensations, the business values, the working environment, hardship of work, etc. The higher the business rating, the more desirable the business is for people agents looking for jobs. The dynamics between groups of applicants and job postings is such that businesses look to find their employees in each skill level in order to hire candidates with the highest rating (i.e., the most desirable ones). On the other hand, applicants prioritize businesses with higher ratings when applying for jobs. Whenever a person agent finds a job, the agent is removed from the ULP agent, while a message ("Employed") is sent to the person agent (see Figure 41). According to Figure 39, whenever a business agent posts a job opening to the ULP agent, it is checked if there are any suitable applicants in the pool, and if all or a portion of the needed employees are hired through this process, this information is conveyed to the business agent and the list of employees is updated. If more employees are needed, the business agent posts a new job opening to the ULP agent, and this process is repeated until all necessary employees are hired.

4.2.2.4. Hospital agent

Healthcare system in a community is responsible for providing injured people with outpatient and inpatient services in hospitals and healthcare providers inside the city or transferring them to hospitals outside the city when demand exceeds the capacity inside the city. In addition to the mission of the healthcare system in the urgent phase after the disaster, it addresses healthcare needs of the people in the long-run after the disaster as well. The healthcare system includes large hospitals and other healthcare providers (e.g., clinics and urgent care services) inside the city. In this section, a type of agent called hospital agent is defined which simulates the functionality of a hospital in the aftermath. In the current study, other healthcare providers, such as clinics, are defined as businesses (see Section 4.2.2.1), the restoration of which depends on the decision of the owners, physical functionality of the healthcare provider, and employee availability in the aftermath. It should be noted that due to limitations inside a community to treat all injuries after a massive event, the urgent response of the healthcare system significantly depends on outside resources, such as rescue teams, ambulances, and supplies, while transferring patients to other nearby city hospitals may also be needed. However, in the long-run, typically people prefer to address most of their medical needs inside their community.

As demonstrated in Figure 42, the capacity of a hospital in the aftermath is governed by the physical functionality of the building itself, as well as the percentages of physicians, nurses, and other staff available. The physical functionality of the hospital is determined by estimating damage to different buildings of the hospital and access of the

building to essential utilities (e.g., electric power and water). To estimate the percentage of hospital personnel available, their ability to work is collected from the corresponding person agents. Per Figure 42, by aggregating the information about the operability of the buildings, as well as the number of physicians, nurses, and other staff who are able to work, it is possible to estimate the percentage of emergency and inpatient beds available. During the recovery phase, the number of available beds may increase gradually by the return of the personnel back to work and repair of the buildings or temporary buildings options. In addition, in the aftermath, personnel, supply, and building may be managed between the emergency and inpatient departments in order to maximize the utilization of the hospital. This is especially important because of the surge demand on the emergency room right after the disaster, while the need for inpatient beds increases gradually by transferring some patients to the inpatient departments.

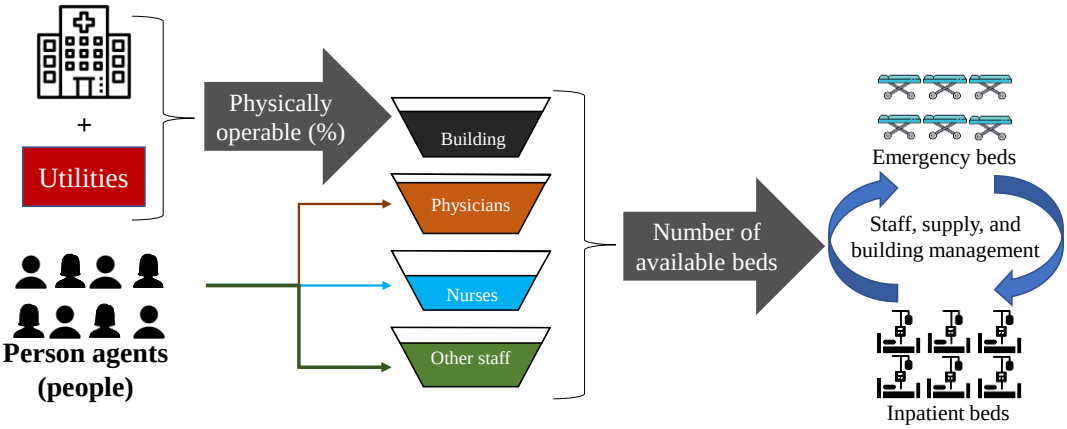

Figure 42: Number of available beds in a hospital after a disaster.

In the current study, a discrete event simulation (DES) is adopted to model the process of rescuing injuries, transferring them to the hospitals inside or outside the city, providing them with service in the emergency department, and if needed, in the inpatient

department, and finally discharging them after the treatment. There are limitations in the healthcare system when severe events happen, including limitations in the number of ambulances, while waiting time may increase in the emergency and inpatient departments due to large number of patients in the queue for receiving service. DES effectively simulates this process accounting for delays and limitations in the aftermath and has been used in the literature to model the rescue and treatment process after natural disasters (Favier, Poulos, Vásquez, Aguirre, & De La Llera, 2019).

In the Centerville testbed, only one hospital exists, while there are a number of healthcare facilities which provide medical services. Person agents incurring injury level IL1 do not need hospitalization and it is assumed that they may go to smaller clinics and healthcare facilities to receive treatment, while person agents incurring injury levels IL2 and IL3 will need to visit a hospital due to their injury severity. Figure 43 demonstrates the patient handling process in Centerville after a tornado event takes place. The process of rescuing is dependent on the number of active ambulances which may decrease due to direct damage to them during the tornado, or may increase by receiving help from nearby hospitals. Since the only hospital in Centerville has a limited capacity, depending on the severity of the tornado, it may be necessary to transfer patients to nearby hospitals in other communities, or in some cases, in other states. For example, according to the report by the Center for Preparedness and Response (2017), the Missouri Department of Health and Senior Services (DHSS) evacuated 713 individuals injured during the 2011 Joplin tornado to 42 hospitals in four neighboring states.

In the current study, it is assumed that if a patient with IL3 is admitted to the hospital, there will be no waiting time because of the urgent care needed, and hence, the patient is admitted to the emergency room. However, patients with IL2 may need to stay in a waiting queue to receive medical treatment in the emergency department. After treatment in the emergency department, depending on the severity of their injury, it may be necessary to transfer the patient to the inpatient department, or if not, the patient is discharged to complete the treatment at home. Patients in the inpatient department will stay depending on their treatment time, and then will be discharged from the hospital. Because the inpatient department has a limited capacity, some patients may be transferred to other hospitals to continue their treatment. Additionally, after the demand on the emergency room department is declined after a few days from the tornado, some resources may be transferred from the emergency room to increase the inpatient capacity. As shown in Figure 41, person agents, when injured, are in close contact with the healthcare system agent to receive treatment, and whenever discharged from the hospital, they may spend some more time in their home to complete their treatment and be ready to continue their routine life. For example, for agents in the labor force, per Figure 41, after the agent is discharged from the hospital and completed the appropriate treatment at home, the agent is classified as “healthy” and may be able to continue routine life.

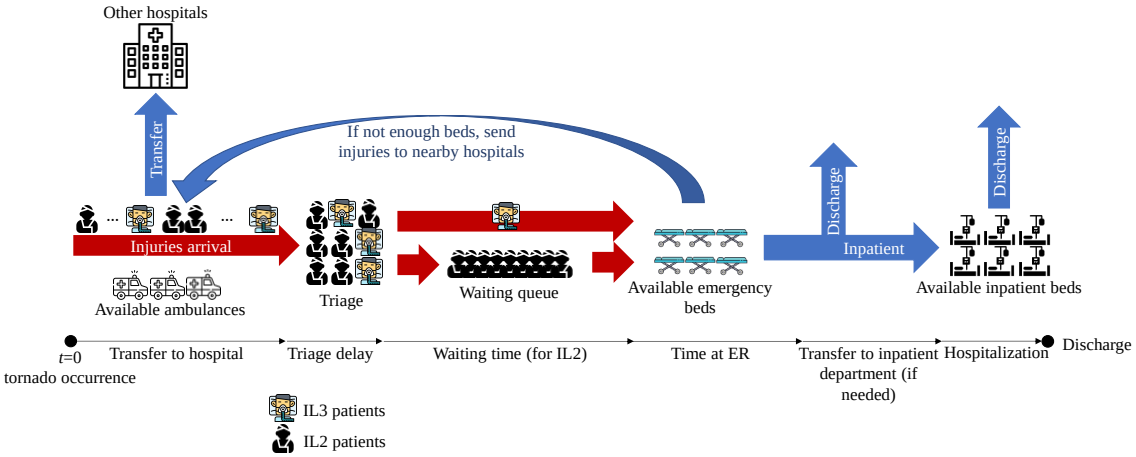

Figure 43: Patient handling process in Centerville healthcare system agent.

4.2.3. Verification and validation

The verification and validation (V&V) task is an essential component of a simulation study to ensure the credibility and quality of the outcomes. The community model presented in this subchapter is an extension to the model presented in Thrust C-A of this dissertation. The verification and validation task was conducted for most of the systems in the community model in Thrust C-A, while it is necessary to perform it for the newly added systems and also in the community level. To perform the verification first, various tests were conducted on each agent type by exposing them to different hazard intensities (including extreme conditions) and changing their attributes to ensure the consistency of their behavior with the grounded theories and rules utilized to define each of them. Additionally, an external verification was conducted by evaluating the outputs of the model by changing the hazard characteristics. If any unusual patterns were detected, a closer investigation was performed to identify and address possible issues. Example of the outputs used at this stage are time series of unemployment rate and number of

functional businesses.

Various internal and external validation techniques similarly to Thrust C-A were utilized to ensure the credibility of the outputs considering the newly added systems/agents. The range of variables input to each agent type was examined to make sure they are within an acceptable range in accordance with the information available about Centerville, empirical data from past events, and the literature. Furthermore, it was checked if the models utilized in the agent (e.g., damage fragility and restoration models) from the literature were validated previously. A predictive validation (Sargent, 2010; Xiang et al., 2005) was conducted in the current study by comparing various outputs of the model under different hazard scenarios with the actual observations from past similar events in the US. Multiple outputs from the model were utilized for this purpose, such as unemployment rate at certain times in the aftermath, number of injured people treated inside or outside the community, number of closed businesses, and cease operation days of businesses. In Thrust C-A, to better demonstrate the comparisons performed for the V&V task, various outputs of the model under an EF5 tornado scenario were compared to the observations after the 2011 Joplin tornado because of the similarities between the events and their impact. In the current subchapter, this is continued by comparing outputs of the model considering the newly added components to the observations from Joplin.

4.2.4. Application

A model of the community of Centerville was developed in Thrust C-A using the ABM approach, and various outcomes of the developed community model were presented for

different systems, such as EPN, WSN, households, and education system. This section presents various example outcomes of the systems added to the community model, including businesses and healthcare, while discussing the effects of the disaster on the labor force.

Thrust C-A presented the model outcomes for an EF5 tornado scenario shown in Figure 44, which is a strong tornado with the maximum 3-sec gust wind speed of 105 m/s (235 mph), width of 2.4 km (1.5 miles) and length of 33.8 km (21 miles) with its center located approximately at the center of Centerville. In this section, results are presented for the businesses, labor force changes, and the single hospital in Centerville subject to that scenario.

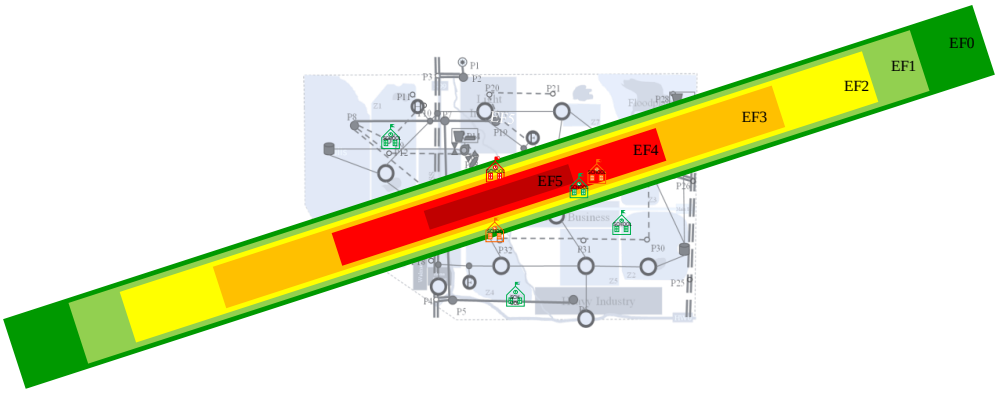

Figure 44: A sample of simulated EF5 tornado in Centerville.

4.2.4.1. Businesses

Businesses were significantly impacted in this EF5 tornado because 576 of the 1,093 businesses in Centerville were within the tornado path. Their operation was severely affected due to the damage to their buildings, loss of utilities, and absence or shortage of employees. As Figure 39 demonstrates, a business agent gets back to operation as it

recovers its building functionality, gets access to the necessary utilities, and have required employees present at work. Figure 45a presents the histogram of cease operation days for businesses in Centerville after the disaster, while Figure 45b presents the histogram of the time took for businesses to recover their building functionality. After the business recovers its building functionality, it may wait for a period of time for access to the utilities to return to physical functionality. Figure 45c shows the histogram of this waiting period for businesses with functional buildings. After the utilities were restored, the business has physical functionality, but it may still not be able to reopen for a period of time because of the absence of employees. The histogram of this waiting time for having the required employees is presented in Figure 45d.

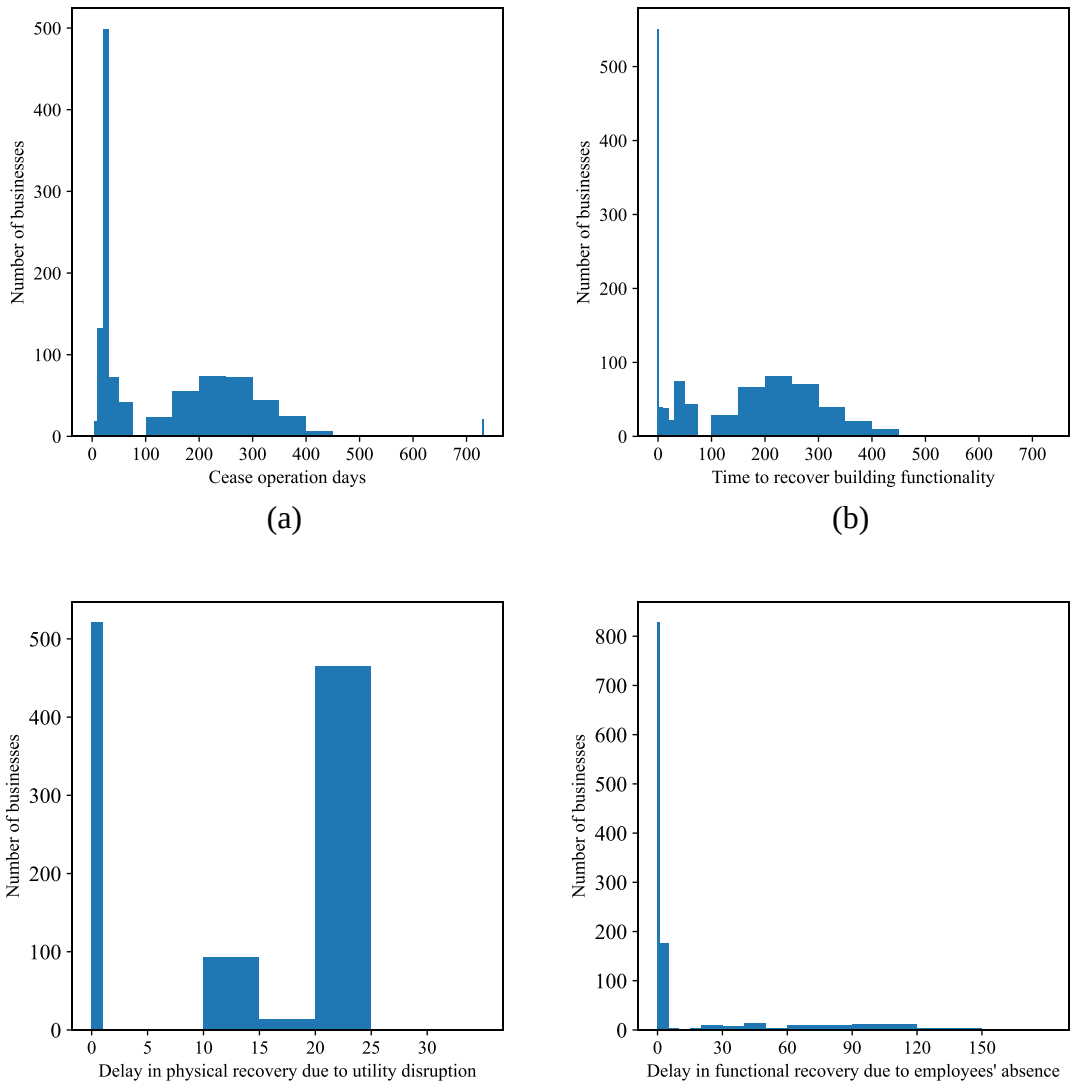

Figure 45: Functional recovery of the businesses after the EF5 tornado: (a) histogram of cease operation days, (b) histogram of time to recover building functionality, (c) delay in physical functionality due to utility disruption, and (d) delay in business functionality due to employees' absence.

As Figure 45b shows, the time to recover building functionality of 529 businesses was zero, meaning that their buildings were not damaged. However, as Figure 45a indicates, only a few businesses were able to operate right after the tornado and the reason was the dependency of most of the businesses on access to the utilities, and

hence, they could not get back to operation until after utilities were restored, as shown in Figure 45c. There were delays in reopening of some of the businesses even after they were physically functional, and this was due to their employees absence or shortage in the required employees. Figure 45d shows the histogram of the delay in the reopening of a business after it is physically functional, where around 800 of the businesses did not have any issues in retaining their required employees, while there were a few businesses that delayed their reopening even after physical functionality recovery for an additional four months because of lack of required employees. Overall, these figures indicate that the short-time utility disruption can delay the reopening significantly, while building damage can have both short- and long-run effects on the reopening.

4.2.4.2. Labor forces

Major disruptions happened to the labor forces in Centerville because more than half of the community's businesses were within the tornado path and most incurred some levels of damage. As indicated in Figure 39, a closed business may keep the employees on the payroll for the duration of closure or a portion of it depending on its attributes, including its business interruption insurance, size of the business, etc. However, not all of the businesses have the resources to keep their employees on the payroll during the closure, similarly to the observations in Joplin after the 2011 Joplin tornado, where approximately 60% of the employees of the 553 destroyed or damaged businesses were kept on the payroll during the closure time (The Joplin Globe, 2021). In addition, when a closed business plans to reopen, the absent employees may be laid off, and hence, they

are removed from the payroll of the business. Figure 46a presents the status of employees of 576 businesses in Centerville located in the tornado path until two years after the event occurrence. As this figure indicates, some businesses kept their employees on the payroll for a certain period of time, while they could not continue it after a while because of the long closure time, or laid them off because of their absence. Figure 46a shows also that around 59% of the employees of the businesses in the tornado path were kept on the payroll for the whole recovery time, which is similar to the observations after 2011 Joplin tornado. It is also observed that employees started moving to other businesses after they were off the payroll, while a portion of them were unemployed for a period of time with the maximum of 15% around seven months after the tornado. Additionally, a percentage of employees of these businesses lost their job because they moved to other communities/cities, while most of them found jobs in other businesses inside the city when they returned back to the city.

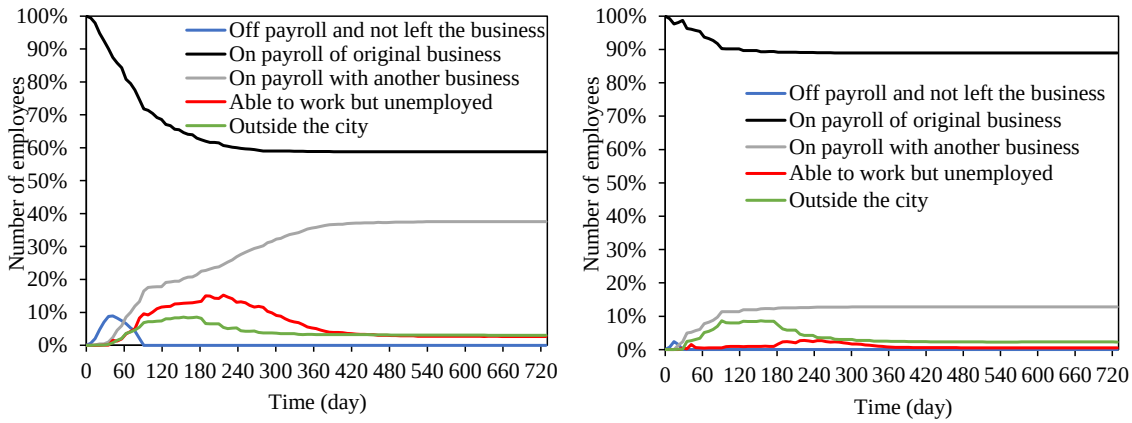

Figure 46: employees of businesses located (a) inside and (b) outside the tornado path in Centerville.

Although about half of the city's businesses were outside the tornado path, some of them still suffered from the consequences, such as injured or dead business owner, absent employees, and lack of utilities. These caused short-term and in a number of cases long-term closure of the businesses, and it is evident in Figure 46b, where the status of employees of the businesses located outside the tornado path is presented. According to this figure, around 89% of the employees were kept on payroll for the total duration meaning that they either were being paid during the closure time or the business was fully functional and employees were working. The main reason for 11% decrease in the number of employees on the payroll was the absence of the employees due to their displacement to other cities, which caused them to be laid off. In a few cases, employees were removed from the payroll because of the business closure due to various reasons, such as death of the owner of a small business, long utility disruption, and significant employee disruption. As shown in Figure 46b, unemployment between the employees of the businesses outside the tornado path reached a maximum of 2.7% which is much less compared to the unemployment rate of employees of the businesses within the path (15%). The comparison of Figure 46a and b indicates that although all of the labor force were somehow affected by this disaster, the consequences were much more severe for the ones who were employed in the businesses located in the tornado path.

Figure 47 presents the unemployment rate in Centerville in the first year after the tornado, where it is shown that the unemployment rate did not increase in the first month because employees were on the payroll, but when a portion of the affected businesses decided to stop keeping them on the payroll, a sudden jump occurred with the

unemployment rate increasing to more than 6% (with maximum of 8.3%) for a period of six months, while it decreased rapidly afterwards reaching 3.06% one year after the disaster (1.4% increase compared to the pre-disaster state).

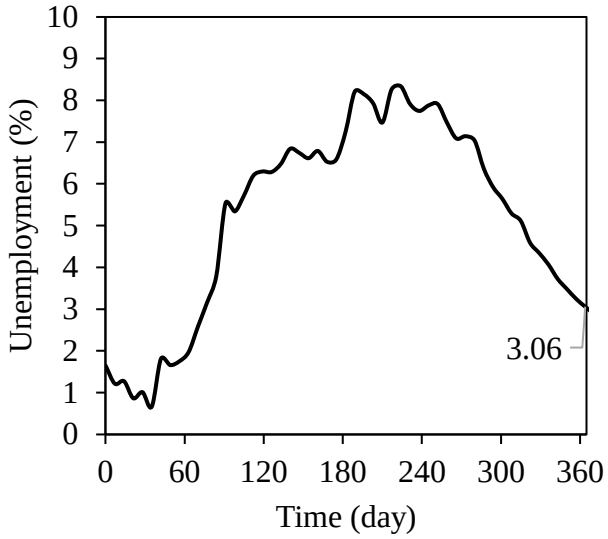

Figure 47: Unemployment rate in Centerville after the EF5 tornado.

Employees may be absent after a disaster due to various reasons, including injuries to the employee, need to take care of an injured family member, need to take care of children at home because of school closure, and relocation to other cities. Figure 48 presents the number of absentees at work and the reasons of their absence over time. In the first month following the disaster, the main reasons of absence at work were childcare and injury of the employee or need to take care of an injured family member. However, in the later months, the main reason of absentees at work was relocation outside the city, which was caused because of damage to the building stock and unavailability of alternative housing inside the city.

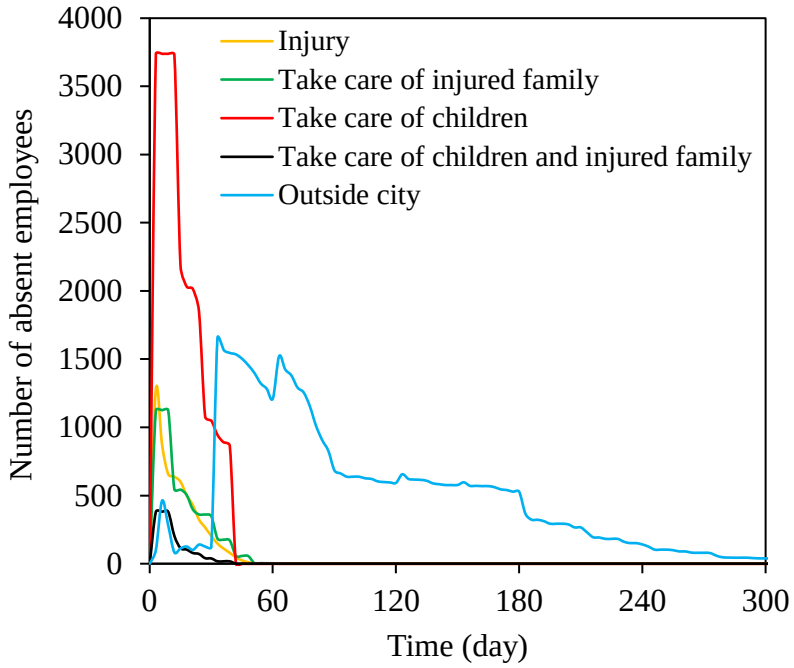

Figure 48: Absent employees and reasons for their absence.

4.2.5. Community resilience quantification

The purpose of this section is to present a community resilience measure which accounts for the resilience of all the systems within a community. For this purpose, first, for each system, a resilience measure is proposed to quantify its resilience, and then a community resilience measure is calculated by combining the resulting resilience measures for the systems.

4.2.5.1. EPN resilience measure

The resilience measure of the EPN subject to a tornado scenario is calculated using the approach proposed by Ouyang and Dueñas-Osorio (2012). A well-known method to quantify resilience of a system is using the following equation (Bruneau et al., 2003):

$$R = \frac{1}{T_{LC}} \int_0^{T_{LC}} Q(t)\, \mathrm{d}t \quad (24)$$

where R is the resilience measure of the system, T_{CL} is the control time, and $Q(t)$ is the functionality function of the system which is a dimensionless function of time, t. The performance metric utilized in the current study to define the functionality function is the number of consumers being served through time, which is normalized by the total number of customers to calculate the functionality function $Q(t)$. Resilience measure of the EPN, R_{EPN}, to tornado hazard is computed in this study assuming the control time to be 45 days. This control time is suitable for evaluating the resilience of the EPN because electric power is essential to all activities in the city and a resilient EPN should restore fast after a disruption. Calculating the EPN resilience measure with a large control time may not be able to effectively represent disruptions in the EPN in short term after the tornado. Additionally, a very short control time may fail to capture major disruptions in the EPN after the control time.

4.2.5.2. WSN resilience measure

The resilience measure for the WSN is calculated similarly to the method used for the EPN. The performance metric selected in this study to compute a resilience measure for WSN is the average water pressure consumers have access to compared to the normal water pressure. Using Eq. (24), the resilience measure of the WSN, R_{WSN}, can be computed, and the control time in the case of Centerville is assumed to be 45 days. The reasoning for selecting this control time is similar to the EPN resilience measure.

4.2.5.3. Education system resilience measure

A resilience measure for education system accounting for the quality and quantity of education in the aftermath was proposed in Thrust C-A of this dissertation and is adopted in here to compute the resilience measure of education system subject to tornado events. The control time is selected to be 90 days in computing education system resilience measure.

4.2.5.4. Healthcare system resilience measure

There is only one hospital in Centerville, while there are multiple small healthcare providers throughout the city. As mentioned previously, only patients with injury levels IL2 and IL3 need to be treated at a hospital, and patients with injury level IL1 can be treated in smaller healthcare providers. When number of injuries is high, the only hospital in Centerville cannot provide service to all injuries, and hence, injured people are transferred to other hospitals in the nearby cities, which in turn increases the waiting time to receive treatment. Other studies (Gian Paolo Cimellaro et al., 2010b; Hassan & Mahmoud, 2020) in the literature utilized waiting time as a measure of quality of healthcare service people receive in the aftermath, which is adopted in the current study to evaluate the quality of service received by each injured person in the aftermath. For Injured Person *i*, the quality of health service received, Q_i, is calculated using Eq. (25) which is adopted from (Gian Paolo Cimellaro et al., 2010b; Hassan & Mahmoud, 2020).

$$Q_i = \max\left(0, \frac{WT_{max} - WT_i}{WT_{max} - WT_0}\right) \leq 1 \quad (25)$$

Where WT_{max} is the maximum allowable waiting time, WT_0 is the waiting time in the normal pre-disaster condition, and WT_i is the waiting time for Injured Person *i* to receive treatment. This equation gives a number between 0 and 1, where quality equal to 0 means that the waiting time was more than the allowable time, and quality equal to 1 means that the waiting time was less than or equal to the normal pre-disaster waiting time. The performance of the healthcare system of the community and the nearby region in providing urgent healthcare service to the people in short time, R_{urgent}, can be calculated as the average Q_i values computed for all injured persons per Eq. (26).

$$R_{\text{urgent}} = \frac{\sum_{i=1}^{i=n_{inj}} Q_i}{n_{inj}} \tag{26}$$

Where n_{inj} is the total number of injuries due to tornado event. Although R_{urgent} can be a proper indicator of the performance of the healthcare system in providing urgent care, the long-term performance of the system depends on the accessibility of healthcare service in the city, which depends on the performance of the hospital and other healthcare providers inside the city. In the current study, the long-term performance of the healthcare system is assessed by the number of hospital beds available and the number of smaller healthcare providers which are providing service. This performance can be adversely affected in the aftermath by reduced number of beds in the hospital or closure of the small healthcare providers due to damage to their buildings, absence of employees, lack of utilities, etc. The functionality function of the hospital, $Q_h(t)$, is calculated as the weighted geometric mean of the number of emergency beds ($n_{er}(t)$) and

inpatient beds ($n_{in}(t)$) available normalized by the number of beds before the disaster, using Eq. (27).

$$Q_h(t) = \left(\frac{n_{er}(t)}{n_{er,b}}\right)^{w_{er}} \cdot \left(\frac{n_{in}(t)}{n_{in,b}}\right)^{1-w_{er}} \leq 1 \qquad , w_{er} \leq 1 \tag{27}$$

Where $n_{er,b}$ and $n_{in,b}$ are the number of emergency and inpatient beds prior to the disaster and w_{er} is the weighting factor of the emergency bed availability compared to the inpatient bed availability, such that w_{er}=0.5 indicates that the same weight is assigned to both inpatient and emergency beds, while w_{er}>0.5 indicates a higher weight for, and hence, a higher relative importance of the emergency bed availability compared to the inpatient bed availability. In this study, the same weight is assigned to both emergency and inpatient departments (w_{er}=0.5).

The functionality of other smaller healthcare providers in the city can be described based on their operation level and whether or not they are open. In the current study, the macro-level functionality of non-hospital healthcare providers, $Q_{nh}(t)$, is calculated as the weighted average of the functionality rate of the individual units weighted based on their size.

$$Q_{nh}(t) = \frac{\sum_{i=1}^{n_{nh}} w_i Q_{hb,i}(t)}{\sum_{i=1}^{n_{nh}} w_i} \tag{28}$$

Where n_{nh} is the number of healthcare providers in the community, $Q_{hb,i}(t)$ is the functionality of the healthcare provider i, and w_i is the weighting factor for healthcare provider i, which is an indicator of its size. In the current study, the total number of employees before the disaster are used as the indicators of the size of the healthcare provider.

A comprehensive resilience measure for the healthcare system should encompass the long-term resilience of the hospitals and other types of healthcare providers, and additionally, account for the capability of the system to cope with the surge in demand for medical assistance in the face of a tornado event. R_{urgent} in Eq. (26) indicates the resilience of the healthcare system in terms of providing urgent care to injuries, while the overall long-term resilience of the hospitals (R_h) and other healthcare facilities (R_{nh}) can be calculated using Eqs. (29) and (30), respectively, where $T_{LC,h}$ and $T_{LC,nh}$ are the selected control times for hospitals and other types of healthcare providers, respectively. The overall resilience of the healthcare system in the community, $R_{\text{healthcare}}$, is calculated as a weighted geometric mean of these resilience metrics using Eq. (31), where the corresponding weights, w_u, w_h, and w_{nh}, can be selected based on their importance in a community. In the current study, these weights are set to be 1, meaning that all have the same contribution to the calculated resilience metric, while $T_{LC,h}$ and $T_{LC,nh}$ are both set to 6 months.

$$R_h = \frac{1}{T_{LC,h}} \int_0^{T_{LC,h}} Q_h(t)\, \mathrm{d}t \tag{29}$$

$$R_{nh} = \frac{1}{T_{LC,nh}} \int_0^{T_{LC,nh}} Q_{nh}(t)\, \mathrm{d}t \tag{30}$$

$$R_{\text{healthcare}} = \left({R_{\text{urgent}}}^{w_u} \cdot {R_h}^{w_h} \cdot {R_{nh}}^{w_{nh}}\right)^{\frac{1}{w_u + w_h + w_{nh}}} \tag{31}$$

4.2.5.5. Resilience measure for businesses

Resilience of each Business Agent i, $R_{b,i}$, subject to the tornado event is calculated using Eq. (24) by defining the functionality function to be equal to $f_{b,i}(t)$ per Figure 39 and assuming control time to be one year. It is expected that control time of one year enables

capturing both short- and long-term disruptions in business operations. This study calculates a single resilience measure for the businesses in the community, $R_{\text{businesses}}$, using Eq. (32), as follows:

$$R_{\text{businesses}} = \frac{\sum_{i=1}^{n_b} w_i R_{b,i}}{\sum_{i=1}^{n_b} w_i} \quad (32)$$

Where n_b is the number of businesses in the community and w_i is an indicator of the size of the business, which in this study is assumed to be equal to the number of employees of a business.

4.2.5.6. Community resilience measure

In this study, a resilience measure for the community, $R_{\text{community}}$, is calculated by aggregating the resilience measure of different systems in the community using Eq. (33) as their weighted geometric average:

$$R_{\text{community}} = \left(\prod_{i=1}^{N_s} {R_i}^{w_i}\right)^{1/\sum_{i=1}^{N_s} w_i} \quad (33)$$

Where N_s is the number of systems accounted for in calculating the community resilience measure, R_i is the resilience measure calculated for system *i* of the community (e.g., R_{EPN}), and w_i is the weight factor for system *i*. The decision maker in the community can adjust weight factors depending on the significance of the resilience of each system on the resilience of the community.

At this stage, using the resilience measures introduced in this section for various systems as well as the community resilience measure calculated using Eq. (33), the resilience of Centerville community subject to the EF5 tornado presented in Figure 44 is assessed. To account for the uncertainties in the response of the community to this event,

a Monte Carlo sampling analysis is conducted. Figure 49 presents the histogram of the computed resilience measures for the community and its systems separately. In addition, the mean value of the computed resilience measure is shown in each histogram. As Figure 49a shows, the resulting community resilience measure ranges from 0.74 to 0.82 with mean value of 0.77. This can be used as a measure for decision making by comparing the resulting resilience measure after applying different mitigation strategies.

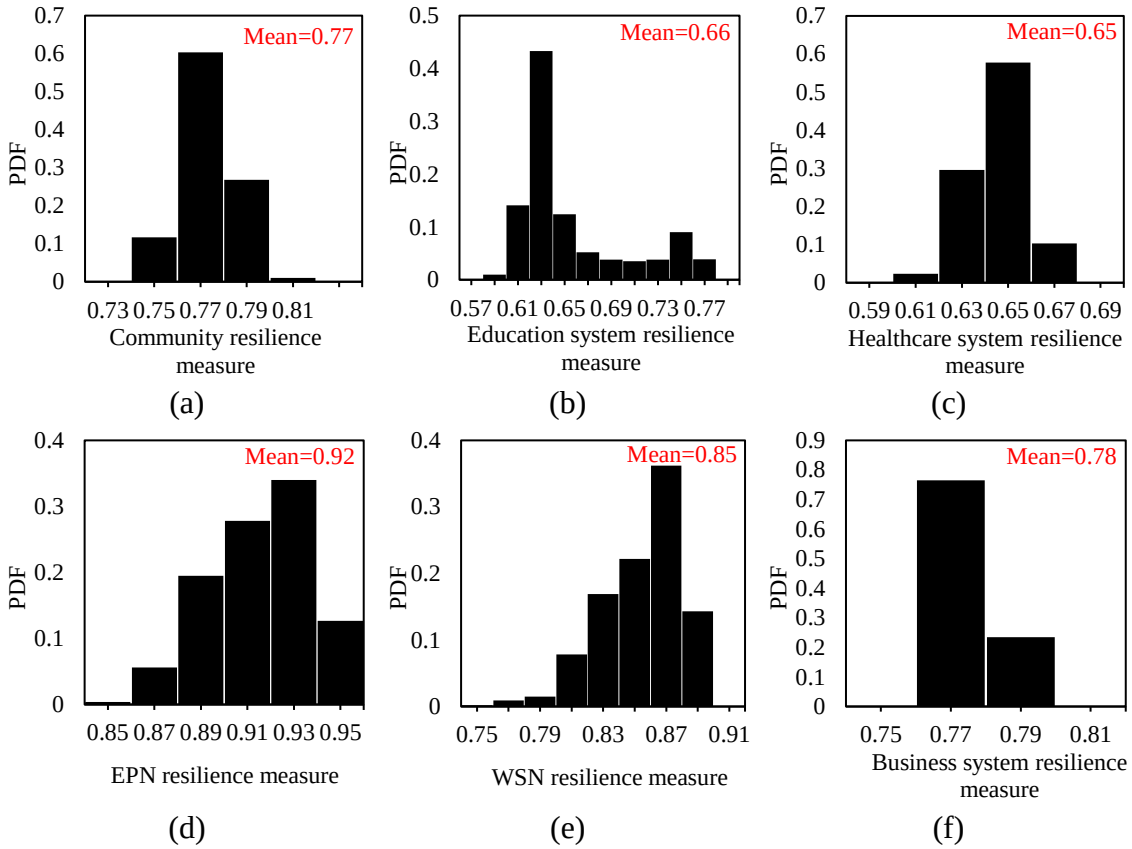

Figure 49: Histogram of computed resilience measures for: (a) the community and its systems, including (b) education system, (c) healthcare system, (d) EPN, (e) WSN, and (f) businesses.

4.2.6. Decision making

This section aims in presenting the application of the quantitative model developed using

ABM and the proposed community resilience measure for quantitative decision making. Previous studies utilized various resilience measures to investigate the effect of different decisions, such as building retrofit decisions (W. Wang et al., 2021), pre- and post-disaster policies (N.L. Dehghani, Darestani, & Shafieezadeh, 2020; Esmalian et al., 2021; Khanmohammadi, Farahmand, & Kashani, 2018; W. L. Wang & van de Lindt, 2021), on the resilience of the community and its systems. Using the community model, it is possible to implement various mitigation strategies and compute the community resilience measure accordingly. According to the calculated resilience measures and the cost associated with each considered strategy, the effectiveness of that strategy can be evaluated, and ultimately, one or a combination of the strategies may be selected. Although not discussed in this study, it is possible to evaluate the effect of any decision on the community resilience, and not necessarily mitigation strategies. For instance, the decision makers may want to see the effect of an urban development plan on the resilience of the community. It is possible to implement such changes into the model and investigate the outcomes.

Since tornado events have a small area of impact compared to most of other natural hazards, such as earthquakes and hurricanes, it is necessary to evaluate the resilience of a community under multiple tornado scenarios impacting different locations of the community. To illustrate the application of the resilience measures presented in this chapter, a set of tornado scenarios with different directions and centers are considered to affect the Centerville community. The scenarios considered in this analysis include only EF5 tornado scenarios, but it is possible to conduct this analysis by

including any set of tornado events. The outcomes of this analysis will be investigating the effect of different mitigation strategies on the severe EF5 tornados that may happen in the future. In addition, a Monte Carlo sampling analysis is conducted to account for the uncertainties in the exposure and response of the community to such an event. Table 28 presents the characteristics of the 10 different EF5 tornado scenarios considered. This table provides information about the intensity of each tornado scenario, its maximum 3-sec gust wind speed, path dimensions, center coordinates, and angle to the north pole. The procedure discussed in Section 4.2.5 is utilized here to calculate the resilience measure of each system within the community and the community as a whole subject to each tornado scenario. To account for the uncertainties, a Monte Carlo sampling analysis is performed with 100 random realizations under each of the 10 tornado scenarios by randomly generating different variables input to different agents of the model. This gives 1,000 calculated resilience measures for the community and its systems, while an average resilience measure for the community under its current condition is resulted by averaging these calculated values. By implementing a mitigation strategy into the community model, this analysis can be repeated to calculate the resulting average community resilience measure. These average measures can be used to evaluate the effectiveness of each strategy and compare them. In the following, first, resilience measures of the community and its systems without any mitigation actions are computed and presented. Thereafter, a number of mitigation actions are implemented and their results on the computed resilience measures are presented and discussed.

Table 28: tornado scenarios considered for decision making in the case of Centerville.

Intensity	Maximum 3-sec gust wind speed (mph)	Length (mile)	Width (mile)	Center coordinates	Angle to north	Event ID
EF5	235	30	1	(215, 134)	72˚	1
					36˚	2
				(429, 268)	72˚	3
					36˚	4
				(644, 402.5)	72˚	5
					36˚	6
				(859, 536.7)	72˚	7
					36˚	8
				(1073, 670.8)	72˚	9
					36˚	10

4.2.6.1. No mitigation actions

Figure 50 presents the histogram of the calculated community resilience measure for Centerville under all tornado scenarios of Table 28, resulted from the Monte Carlo sampling analysis. As shown in this figure, the resilience measure of the community under all of the tornado scenarios ranges from 0.43 to 0.94 with a mean value of 0.76. In the next section, different strategies are implemented and are compared to the mean community resilience measure of 0.76.

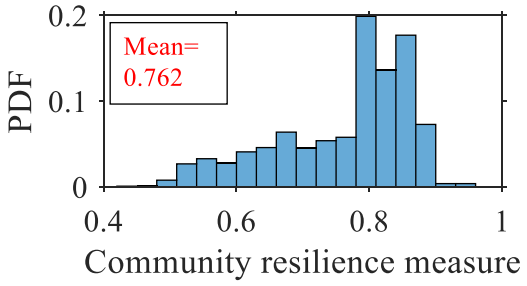

Figure 50: Histogram of average community resilience measure under tornado scenarios in Table 28.

4.2.6.2. Effect of mitigation actions

A set of mitigation strategies are implemented in the Centerville community model to investigate their effectiveness on the resilience measures calculated for the community

and its systems. A summary of each considered mitigation strategy and their expected effect is discussed below:

i. **Backup utilities for schools:** School disruption after natural disasters affects not only the education system, but also other systems in the community, such as households, businesses and the healthcare system. As discussed in Section 4.2.2.2, the ability of a person agent to work can be affected if that agent needs to take care of children needing homeschooling, which in turn causes absence of the employee at work. In addition, as discussed in Sections 4.2.2.1 and 4.2.2.4, the functionality of the businesses and hospitals is directly affected by the absence of the employees. As a result, enhancing the resilience of the education system can help increase/enhance the community resilience measure. As evaluated in Section 4.1.5.5, providing backup utilities for schools can significantly increase the resilience of education system subject to tornado hazard.

ii. **Mandating all businesses in Centerville to purchase insurance**: One of the most significant impeding factors delaying the recovery of the damaged businesses in the aftermath is the time to secure finances needed for the repair and reconstruction costs. This strategy seeks to investigate the effect of mandating insurance purchase for all businesses. The effect of purchasing insurance by the businesses in Centerville is evaluated by changing the attributes of the business agents such that all of them have insurance policies covering the repair costs.

iii. **All buildings have a tornado safe room**: Injuries after a natural disaster may put an unprecedented pressure on the healthcare system, while disruptions can

propagate to other systems of the community as well. Employees of the businesses, schools, and hospitals might not be able to get back to work immediately because of their own or their family member's injury. As a result, any method, such as safe rooms, which can decrease the number of injuries may help to improve the resilience of the community.

iv. **Increased resources for the EPN repair**: Access to electricity is essential in the operation of almost all systems within a community, including, the WSN, schools, healthcare system, businesses, etc. Since the EPN is widespread throughout the city, it is highly likely that it gets damaged in any tornado event. Hence, having an emergency plan to restore electricity would be a viable option to increase the resilience of the community by providing electricity as soon as possible. One method is having mutual emergency plans with nearby cities to share the resources in cases of a tornado. In this study, this strategy is reflected by increasing the repair resources and shortening the repair actions.

v. **Minor retrofit of housing units**: For the application of this study, it is assumed that damage fragilities are shifted equivalent to 30 mph, which means that the wind speed thresholds to cause each damage state are increased by 30 mph. This is done to assess the effect of more resistant housing units on the resilience of the community to EF5 tornados. Such retrofits can be more resistant roof covers and window shutters.

vi. **Moderate retrofit of school buildings**: This action is similar to Strategy v, but here it is assumed that this shift is 50 mph. This higher assumption is because there

are a few schools in the community and it is possible to have special design or retrofit for their buildings to improve their response.

vii. **Minor retrofit of businesses**: In this action, similarly to Strategy v, damage fragilities of the business buildings are shifted equivalent to 30 mph.

viii. **Increase in the construction resources**: One of the leading reasons for delay in the reconstruction process after massive natural disasters is the lack of sufficient construction resources and difficulty to find a contractor. In this strategy, it is assumed that there is no delay due to finding a construction contractor after the tornado event to assess its effectiveness on the resilience of the community. In the real world, this can be done by getting help from construction companies and contractors in other regions. This especially is practical because tornado events are local and other nearby communities are not damaged, and hence, there is no surge in construction demands in those communities.

ix. **Preventing late insurance payouts**: One of the leading reasons for delay in reconstruction is delays due to securing finances. Although some businesses may have insurance to cover their costs, there is a chance that the process of getting a payout from the insurers lasts long. This strategy seeks to evaluate the effect of preventing late insurance payouts on the resilience of the community. This strategy is implemented in the Centerville model by decreasing the uncertainty of the insurance payout time, which in turn, decreases the chance of late payouts.

For each mitigation strategy, the resilience measures of the community and its systems are computed by conducting a Monte Carlo sampling analysis on the modified

community model (i.e., original community model but with the strategy implemented in it). The average resilience measures computed using Monte Carlo sampling analysis considering the tornado scenarios of Table 28 are tabulated in Table 29. This table also includes the computed average resilience measures for the original Centerville model without any mitigation strategies implemented in order to easier assess the effectiveness of each strategy on the resilience of the community. Each column in Table 29 is colored separately with green such that the density of the green color indicates the level of the effectiveness of the associated strategy on that resilience measure.

Table 29: resilience measures calculated for the Centerville community and its systems in its current condition and when mitigation strategies are implemented.

Strategy	$R_{\text{community}}$	R_{EPN}	R_{WSN}	$R_{\text{businesses}}$	$R_{\text{healthcare}}$	$R_{\text{education}}$
No strategy	0.762	0.779	0.755	0.839	0.731	0.746
Strategy i: Backup utility for schools	0.797	0.779	0.755	0.844	0.737	0.922
Strategy ii: Insurance purchase requirement for businesses	0.765	0.779	0.755	0.841	0.732	0.748
Strategy iii: Saferooms in all buildings	0.796	0.779	0.755	0.843	0.908	0.746
Strategy iv: Increased resources for EPN repairs	0.841	0.895	0.881	0.863	0.746	0.839
Strategy v: Minor retrofit of housings	0.768	0.779	0.755	0.85	0.746	0.746
Strategy vi: Moderate retrofit of schools	0.772	0.779	0.755	0.841	0.732	0.783
Strategy vii: Minor retrofit of businesses	0.765	0.779	0.755	0.846	0.735	0.746
Strategy viii: Increase in construction resources	0.762	0.779	0.755	0.839	0.731	0.746
Strategy ix: Preventing late insurance payout	0.762	0.779	0.755	0.839	0.731	0.746
Combination of Strategy i and iv	0.858	0.895	0.881	0.866	0.748	0.923
Combination of Strategy ii, viii, and ix	0.765	0.779	0.755	0.851	0.733	0.746

By comparing the community resilience measures in Table 29 resulted after implementing each strategy with the community resilience measure computed for Centerville without any strategy, the effectiveness of each strategy can be assessed. According to the results presented in this table, the community resilience measure was improved by implementing some of the strategies, but a number of them were more effective compared to others. For instance, Strategy iv, which indicates the increase in repair resources for the EPN, can significantly increase the resilience of the community and different systems within it. This indicates that enhancing the resilience of the EPN

helps increasing resilience of all systems, including the WSN, businesses, education, and healthcare. Some other strategies have less widespread impact on the resilience of different systems, but still can improve the resilience of the community. For example, Strategy i, which is providing backup utilities for schools, significantly improves the resilience of the education system, while its effect on the resilience of other systems is not very significant. This strategy improves the resilience of the business and healthcare systems as well, which is devoted to the fact that closed schools cause parents to take care of children doing homeschooling, which in turn, causes their absence at work. When the education system become more resilient, such disruptions become less frequent, and hence, less disruptions happen in the labor force in the community. Strategy iii, which is securing saferooms in every building, increases the resilience of the healthcare system significantly, while it slightly increases the resilience of the businesses. Strategy v, which is minor retrofit of the housing units, slightly enhances the resilience of the community, businesses, and healthcare system. This is due to decrease in the number of casualties and number of households needing to relocate, which in turn decreases the disruption in the labor force and hence businesses and healthcare providers. Strategy vi, which is slight retrofit of school buildings, enhances the resilience of the community, education system, businesses, and healthcare system. By comparing this strategy with Strategy i, which was also related to schools with providing backup utilities, it is clear that Strategy i has a more significant impact on the resilience of the community and its systems. The main reason is the vulnerability of the EPN in tornado events and its effect on school operations, while this can be addressed by providing

backup utilities. Strategy vii, which is minor retrofit of businesses, slightly increases the resilience of the businesses, while its effect on the community is negligible. This is because minor retrofit only prevents damage subject to low-intensity tornados and it cannot help a building to stand against an EF5 tornado. Strategies vii and ix are related to increasing construction resources and preventing late insurance payouts, respectfully. Both of these strategies could not increase the resilience measure calculated for the community. The reason is that even though construction resources are increased, still construction is delayed to secure the finances. Similarly, when insurance payouts are faster, still construction can be delayed due to the lack of enough construction resources. By combining Strategies ii, vii, and ix, the resilience measure calculated for the businesses increases slightly. The reason for this insignificant effect can be attributed to the fact that businesses are significantly damaged in EF5 tornados, and even though these strategies accelerate securing finances and finding contractors to repair, still it takes a long time for severely damaged businesses to be reconstructed/repaired. This long closure affects the businesses, business owners, and labor forces, and hence, still the resilience measure of the businesses is not improved significantly. Based on these observations, one can conclude that a strategy which can significantly strengthen business buildings subject to tornado loads can help improving their resilience the most. The other strategy may be pre-disaster preparations by business owners/managers to relocate immediately when their building is severely damaged.

According to Table 29, increasing resilience of the EPN (Strategy i) and providing backup utilities for schools (Strategy iv) have considerable effect on the

resilience of all systems in the community and increase the community resilience measure significantly. Per Table 29, combining these two strategies increases the community resilience measure from 0.762 to 0.858, which is a considerable improvement. Similarly, it is possible to combine various mitigation strategies to achieve the desirable resilience measure for the community.

4.2.7. Concluding Remarks

This subchapter extended the community model developed in Thrust C-A by adding more systems into the model. Business agents are created to represent individual businesses in the community, while their functionality is defined based on their physical functionality as well as access to the required employees. The physical functionality is also dependent on the building functionality as well as access to the required utilities. Person agents are created in this study to simulate the health condition and occupation of people in the community in the cases of disaster occurrence. A fault tree analysis is designed in this chapter to predict the injury level of each person agent depending on the impact of the tornado on the building housing the agent in the onset of disaster. Additionally, the occupation status of person agents who are in the labor force is updated during the simulation depending on their ability to work as well as the functionality status and attributes of the business agents where they were working before the disaster. Hospital agents are defined to model the response of the hospitals in short-term when there is a surge in demand due to injuries as well as in the long-term to provide regular service to the patients inside the city. Functionality of the hospital is defined based on its available inpatient and outpatient beds, which depends on its physical functionality and

availability of the personnel. Discrete Event Simulation (DES) is adopted in this study to model the rescue and treatment process in the aftermath.

Different outputs of the community model related to the newly added systems were discussed in this subchapter. The disruption incurred by the businesses and the labor force in the community of Centerville due to a strong EF5 tornado scenario were discussed. Based on the outcomes, 576 of the 1,093 businesses in Centerville were within the tornado path. According to the histograms of the functionality recovery time of the businesses, it took from one day to more than two years for the businesses to reopen, while around 4% of the businesses in Centerville were permanently closed. Furthermore, it was observed that utility disruption in the short-run and building repair in the long-run governed the reopening of the businesses in Centerville. Moreover, around 800 of the businesses did not have any issues in retaining their required employees, while for other businesses it took up to four months after they gained their physical functionality to retain their required employees and reopen. The model outcome indicated severe disruptions in the labor forces in the community with the most effect on the employees of the businesses which were within the tornado path. Around 59% of the employees of the businesses in the tornado path were kept on the payroll for the whole closure time. Employees who were not on the payroll started moving to other businesses in the city, while some of them were unemployed for a period of time with a maximum of 15% around seven months after the tornado occurrence. On the other hand, disruptions were less severe for the employees of the businesses which were located outside the tornado path. Around 89% of these employees were kept on the payroll for

the whole duration meaning that they either were being paid during the closure time or the business was fully functional and employees were working. The main reason for the 11% decrease in the number of employees of the businesses outside the tornado path who were on the payroll was their absence at work because of displacement to outside the city. The results showed a maximum of 2.7% unemployment between employees of the businesses outside the tornado path, which is much less compared to the unemployment of the employees of the businesses inside the tornado path. The overall results of Centerville indicated an unemployment rate of 3.06% one year after the tornado which was 1.4% more than the unemployment rate just before the tornado occurred.

In the next step of this subchapter, resilience measures were proposed to quantify the resilience of the community and its systems. These measures can be used to assess the resilience of the community, while they can be used to evaluate the effectiveness of different mitigation strategies on the resilience of the community. A Monte Carlo sampling analysis was performed to calculate the resilience measure of the Centerville community subject to the EF5 tornado scenario accounting for the uncertainties in the response of the community. The histogram of the results indicated that the calculated community resilience measure ranges from 0.74 to 0.82 with the mean value of 0.77. In the last step, the Centerville community model and the proposed resilience measures were utilized to assess and compare the effectiveness of various mitigation strategies on the resilience of the community. For this purpose, each strategy was implemented in the community model and the resilience measures of the community and its systems were

calculated under a set of predefined EF5 tornados by conducting a Monte Carlo sampling analysis. The mitigation strategies included strategies to enhance the resilience of the EPN, schools, healthcare system, and businesses. According to the outcomes, having emergency plans and sufficient resources to rapidly recover the EPN can significantly increase the resilience of the community and all systems within it under tornado threats. Furthermore, having backup utilities for schools can considerably increase the resilience of the education system as well as businesses and healthcare system. Moreover, having saferooms in all buildings can potentially increase the resilience of the healthcare system and businesses. As discussed in this chapter, a combination of different mitigation strategies can be employed to increase the community resilience measure to the desired level. This was illustrated by combining Strategies i and iv, which represent increasing the EPN repair resources and providing backup utility for schools respectively, and the results indicated increase in the community resilience measure from 0.762 to 0.858. Strategy i is related to having emergency management plans and mutual restoration plans with nearby communities to restore the EPN rapidly and Strategy ii is providing backup utilities for seven schools in the community. Both of these strategies, although not very costly, can significantly increase the resilience of the community. Other strategies discussed in this chapter can also be combined with these two strategies, but there are challenges in implementing them in the real world because of different reasons, such as their high associated cost.

This study concludes that lifelines play a significant role in both short- and long-term performance of a community and all of its systems, and vulnerability of these

infrastructure to disaster loads can adversely affect all parts of the community. Different actions can be taken in order to address these vulnerabilities, such as pre-disaster mitigation actions by strengthening the lifelines and having emergency plans to restore them quickly in cases of disruption, as well as decreasing the dependence of critical systems to lifelines by providing backup utilities for hospitals, schools, etc. As another conclusion in this study, there are various obstacles in the restoration of the building infrastructure in a community, some of the most important of which are delays due to difficulties in securing the finances, construction resource limitations, and time to take a reconstruction/repair permit. This study showed that although having access to insurance and fast insurance payout can help securing the finances to repair faster, other impeding factors can still be obstacles in the recovery of the buildings. This study also revealed that a community should make efforts to address all of these impeding factors at the same time in order to have an effective and rapid restoration. Furthermore, addressing all impeding factors can help initiating the recovery of the building infrastructure faster, but still powerful disasters, such as high-intensity tornados, can cause the community to suffer long period of recovery because of the extensive damage to the infrastructure in the city, and hence, long repair period. This indicates the importance of decreasing the vulnerability of the buildings prior to an event occurring by retrofit actions or design improvements.

5. SUMMARY AND FUTURE WORK

Chapter 1 of this dissertation presented a summary of original contributions of this study to the disaster resilience literature. The current chapter presents a summary of this dissertation, the modeling approach, and observations from a broader perspective. In addition, multiple directions for the future research of this study are presented.

5.1. Summary of the research approach

This dissertation targets the area of quantitative disaster resilience by developing models and frameworks required to model a community in the desired level of details and utilizing the developed model for resilience assessment and decision making. Developing a quantitative community model requires various types of models to simulate the response and behavior of each system, while an approach is required to model a community as a system of interdependent systems. This dissertation contributed to the former by developing models for predicting the business recovery and restoration of residential buildings after they are damaged. Additionally, this study contributed to the latter by utilizing the ABM approach to model different systems of the community accounting for their interactions and interdependencies. For illustration purposes, the modeling approach in this study is presented along with its application for the virtual community of Centerville subjected to tornado hazard. Different agent types are defined to model systems and decision maker entities within the community, including schools, electric power network, water supply network, businesses, households, healthcare facilities, and construction companies. A comprehensive review of the literature was conducted to define agents which can simulate the response of the components in the

community from the onset of the hazard occurrence to the restoration and full recovery of the community. Additionally, a broad review of the literature as well as past natural disasters was utilized to define internal interactions between agents forming a system and external interactions between different systems forming the community. By so doing, a quantitative model of the community is developed as a system of interdependent systems, capable of simulating the response and recovery of the community from the event occurrence to the desired time in the aftermath. A verification task was performed to ensure that the model behaves as expected per grounded rules, while a validation task was further conducted to ensure the credibility of the outcomes. This dissertation also proposed resilience measures to quantify the resilience of the community and its respective systems. These measures can be used to not only assess the resilience of the community in its current condition, but also to conduct decision making by implementing various mitigation strategies and comparing them using the computed resilience measures. The application of these measures for resilience assessment and decision making is presented for the case of Centerville. The modeling approach in this dissertation offers various advantages some of which are listed below:

i. It is possible to study less-studied components of the communities in the quantitative disaster literature, such as the education system. Although the response of the education system in past disasters was broadly studied, most of the studies were qualitative and the purpose was to identify the effect of different factors on the recovery of schools. However, similarly to other systems of the community, such as the EPN, quantitative studies are required to assess the

resilience of the education system in a community, and ultimately, make quantitative decisions to enhance its resilience. This advantage of the ABM approach in this dissertation is showcased by studying resilience of education system in Centerville.

ii. The ABM approach can take advantage of the disperse studies in the literature to model a community. There are a large number of studies in the disaster literature focusing on different systems of the communities under different perils. The modeling approach in this study provides the opportunity to utilize these studies to model a community as a system of systems accounting for their interdependencies. In the application of this, multiple models and findings were adopted from the literature to define agents and their interactions to develop a community model for Centerville. These included damage fragility models, restoration models, as well as findings from past literature which were used to define micro-behaviors describing the behavior of an agent and its interactions with other agents.

iii. There are no certain requirements about the models which are utilized in this modeling approach. This makes the community model development more feasible considering that models in the literature are developed using various modeling techniques and have their specific characteristics.

iv. The response and restoration of communities after major disasters is uncertain, and it is possible to include such uncertainties into the community model through randomness in the behavior of the agents and their interactions. The simplest type of randomness included in the case of Centerville was through random variables

input to different agents of the community. However, other types of randomness, such as random realizations from a Random Forest model, can also quantify the uncertainties in the response of the community.

v. The application of this dissertation presented a detailed model of a community by modeling its systems and their detailed components. However, the ABM approach is fully capable of modeling a community with less refinement/resolution. This is especially important when modeling a large region or in the cases that enough information is not available to model the community in detail. There are a large number of models in the literature focusing on a region or a large infrastructure (e.g., EPN of a city) without going into details of their buildings or components. Examples of such models are models predicting damage to a neighborhood without looking into its individual buildings, or models simulating the response of the EPN to an event using a Markov Chain model without going into details of the network's components or the available resources. It is possible to utilize and integrate these existing models using the ABM approach to develop a quantitative model of a community with less resolution.

vi. The decision-making platform developed in this study is not community-specific. Quantifying resilience of a community using the method proposed in this study needs input from decision makers of a community. These inputs include their judgement about control times used to compute resilience measure of each system, quality of each schooling category compared to the normal condition, and weight factors used to combine resilience measures of different systems into the

community resilience measure. This is particularly important because in communities with different socioeconomic characteristics and priorities, their decision makers may assign different weights to each system of the community or may weight quality of education differently.

5.2. Future work

A number of potential research topics are identified as future research directions of this study. As also discussed in this dissertation, one essential component in developing a quantitative model of a community is having appropriate models to define agents and their behavior. This study developed a number of models for business recovery and residential building recovery, while most of the models were adopted from the literature. Still, efforts are needed to extend the library of existing probabilistic models for various systems of the community, while some improvements are needed to the existing models. In particular, this study identified the following areas that require further research:

i. Casualty models for tornado events are limited to the regional level, and no model existed in the literature estimating casualties at the building level. To address this, the current study proposed a method similar to the method used by HAZUS for earthquake hazard, while performed an expert solicitation to estimate the probability of different injury levels for a person in a building damaged due to tornado. Future research is needed to calibrate this model to the data from real-world tornado events.

ii. The housing recovery model utilized in this study predicts the housing stages of a household through time based on their social vulnerability. However, in order to

study the population dislocation and its effects on the community, it is necessary to have information about the housing status and location of the households. In the ABM approach, this enables providing such information into other agents of the community model, such as businesses, to include their effect on other sectors of the community. In the current study, assumptions are made based on the characteristics of the household to map housing stages into housing statuses. However, future research is needed to generalize this model to be applicable into other communities.

iii. The application of the ABM approach was presented for the community of Centerville by modeling this community with high resolution (i.e., households, businesses, and other components were modeled as individual agents). Future research is needed to implement this modeling approach on a larger community but with decreased level of details. In such a model, the modeler might define agents by grouping community entities. For example, one agent might be defined for each residential neighborhood, or less agents might be defined to model the EPN only using its distribution substations. There would be challenges and also benefits by decreasing the details particularly for large metropolitan areas.

iv. This study proposed different resilience measures for the community and its systems. These measures, in order to be computed, need input from decision makers in a community. Future research is needed to get such inputs from decision makers of a real community and identify challenges in doing so. The possible outcome of this research would be a generalized approach to get input from

decision makers, which not only facilitates its utilization, but also generalizes it to be used for other communities.

v. The community model developed using the ABM approach has the capability of being used in optimization studies to make quantitative decisions targeting to maximize the resilience measure of the community. The constraints of such optimization studies would be the amount of resources available, particularly monetary resources, as well as environmental or political restrictions. Future research is needed to study the challenges of such optimization studies and application to real communities for various scales and socioeconomic characteristics.

6. REFERENCES

Abramson, D. M., & Garfield, R. M. (2006). On the edge: Children and families displaced by Hurricanes Katrina and Rita face a looming medical and mental health crisis.

Adams, T. M., Bekkem, K. R., & Toledo-Durán, E. J. (2012). Freight Resilience Measures. *Journal of Transportation Engineering*, *138*(11), 1403–1409. https://doi.org/10.1061/(asce)te.1943-5436.0000415

Aghababaei, M., & Mahsuli, M. (2019). Component damage models for detailed seismic risk analysis using structural reliability methods. *Structural Safety*, *76*. https://doi.org/10.1016/j.strusafe.2018.08.004

Aghababaei, Mohammad. (2017). Probabilistic damage models for detailed risk analysis of buildings with reliability methods (Master's thesis). Department of Civil Engineering, Sharif University of Technology, Tehran, Iran.

Aghababaei, Mohammad, Koliou, M., & German Paal, S. (2018). Performance Assessment of Building Infrastructure Impacted by the 2017 Hurricane Harvey in the Port Aransas Region. *Journal of Performance of Constructed Facilities*, *32*(5). https://doi.org/10.1061/(ASCE)CF.1943-5509.0001215

Aghababaei, Mohammad, Koliou, M., Pilkington, S., Mahmoud, H., Van De Lindt, J. W., Curtis, A., … Watson, M. (2020). Validation of Time-Dependent Repair Recovery of the Building Stock following the 2011 Joplin Tornado. *Natural Hazards Review*, *21*(4), 1–12. https://doi.org/10.1061/(ASCE)NH.1527-6996.0000408

Aghababaei, Mohammad, Koliou, M., Watson, M., & Xiao, Y. (2020). Quantifying post-disaster business recovery through Bayesian methods. *Structure and Infrastructure Engineering*, *0*(0), 1–19. https://doi.org/10.1080/15732479.2020.1777569

Aghababaei, Mohammad, & Mahsuli, M. (2018). Detailed Seismic Risk Analysis of Buildings Using Structural Reliability Methods. *Probabilistic Engineering Mechanics*, *53*, 23–38. https://doi.org/10.1016/j.probengmech.2018.04.001

Aghababaei, Mohammad, & Mahsuli, M. (2019). Component damage models for detailed seismic risk analysis using structural reliability methods. *Structural Safety*, *76*, 108–122. https://doi.org/10.1016/j.strusafe.2018.08.004

Ajayakumar, J., Curtis, A., Smith, S., & Curtis, J. (2019). The Use of Geonarratives to Add Context to Fine Scale Geospatial Research. *International Journal of Environmental Research and Public Health*, *16*(3), 515.

Alesch, D. J., Holly, J. N., Mittler, E., & Nagy, R. (2001). Organizations at risk: What happens when small businesses and not-for-profits encounter natural disasters.

Almufti, I., & Willford, M. (2013a). REDi™ Rating System: Resilience-based Earthquake Design Initiative for the Next Generation of Buildings, (October).

Almufti, I., & Willford, M. (2013b). The resilience-based earthquake design initiative (REDi™) rating system, (October).

AnyLogic Software. (2021). Retrieved September 6, 2021, from https://www.anylogic.com/

Arouri, M., Nguyen, C., & Youssef, A. Ben. (2015). Natural Disasters, Household Welfare, and Resilience: Evidence from Rural Vietnam. *World Development*, *70*,

59–77. https://doi.org/10.1016/j.worlddev.2014.12.017

Asgary, A., Anjum, M. I., & Azimi, N. (2012). Disaster recovery and business continuity after the 2010 flood in Pakistan: Case of small businesses. *International Journal of Disaster Risk Reduction*, *2*, 46–56.

Attary, N., Unnikrishnan, V. U., van de Lindt, J. W., Cox, D. T., & Barbosa, A. R. (2017). Performance-Based Tsunami Engineering methodology for risk assessment of structures. *Engineering Structures*, *141*, 676–686. https://doi.org/10.1016/j.engstruct.2017.03.071

Attary, N., van de Lindt, J. W., Mahmoud, H., & Smith, S. (2019). Hindcasting Community-Level Damage to the Interdependent Buildings and Electric Power Network after the 2011 Joplin, Missouri, Tornado. *Natural Hazards Review*, *20*(1), 4018027.

Attary, N., van de Lindt, J. W., Mahmoud, H., Smith, S., Navarro, C. M., Kim, Y. W., & Lee, J. S. (2018). Hindcasting community-level building damage for the 2011 Joplin EF5 tornado. *Natural Hazards*, *93*(3), 1295–1316.

Ayyub, B. M., Foster, J., McGill, W. L., & Jones, H. W. (2009). Risk analysis of a protected hurricane-prone region. II: Computations and illustrations. *Natural Hazards Review*, *10*(2), 54–67.

Barton, D., Eidson, E., Schoenwald, D. A., Stamber, K. L., & Reinert, R. K. (2000). Aspen-ee: An agent-based model of infrastructure interdependency. *Sandia Report*. Retrieved from http://prod.sandia.gov/techlib/access-control.cgi/2000/002925.pdf

Basu, N., Pryor, R., & Quint, T. (1998). ASPEN: A Microsimulation Model of the

Economy. *Computational Economics*, *12*(3), 223–241. https://doi.org/10.1023/A:1008691115079

Bazli, M., Ashra, H., Jafari, A., Zhao, X., & Gholipour, H. (2019). E ff ect of thickness and reinforcement con fi guration on fl exural and impact behaviour of GFRP laminates after exposure to elevated temperatures, *157*(August 2018), 76–99. https://doi.org/10.1016/j.compositesb.2018.08.054

Box, G. E. P., & Tiao, G. C. (1992). *Bayesian inference in statistical analysis*. *Wiley-Interscience*. NJ: John Wiley & Sons. Retrieved from http://doi.wiley.com/10.1002/9781118033197

Brennan, A. L., & Koliou, M. (2020). Probabilistic loss assessment of a seismic retrofit technique for medium-and high-voltage transformer bushing systems in high seismicity regions. *Structure and Infrastructure Engineering*, 1–10.

Brown, C., Seville, E., & Vargo, J. (2017). Efficacy of insurance for organisational disaster recovery: case study of the 2010 and 2011 Canterbury earthquakes. *Disasters*, *41*(2), 388–408.

Bruneau, M., Chang, S. E., Eguchi, R. T., Lee, G. C., O'Rourke, T. D., Reinhorn, A. M., … Von Winterfeldt, D. (2003). A framework to quantitatively assess and enhance the seismic resilience of communities. *Earthquake Spectra*, *19*(4), 733–752.

Carter, M. R., Little, P. D., Mogues, T., & Negatu, W. (2007). Poverty traps and natural disasters in Ethiopia and Honduras. *World Development*, *35*(5), 835–856.

Center for Preparedness and Response. (2017). *Public Health Emergency Preparedness (PHEP) Program-Stories from the Field*.

Centers for Disease Control and Prevention. (2018). Flooding from Hurricane Matthew in North Carolina. (2019). Retrieved from https://www.cdc.gov/phpr/readiness/stories/nc.htm

Chang, Y., Wilkinson, S., Potangaroa, R., & Seville, E. (2010). Resourcing challenges for post-disaster housing reconstruction: A comparative analysis. *Building Research and Information*, *38*(3), 247–264. https://doi.org/10.1080/09613211003693945

Children At Risk. (n.d.). Hurricane Harvey keeps 1.4 million students out of public schools for at least a week. Retrieved June 10, 2020, from https://childrenatrisk.org/hurricane-harvey-keeps-1-4-million-students-out-of-public-schools-for-at-least-a-week/

Choi, J., Yoo, D. G., & Kang, D. (2018). Post-earthquake restoration simulation model for water supply networks. *Sustainability (Switzerland)*, *10*(10), 1–17. https://doi.org/10.3390/su10103618

Cimellaro, G. P., Tinebra, A., Renschler, C., & Fragiadakis, M. (2016). New Resilience Index for Urban Water Distribution Networks. *Journal of Structural Engineering*, *142*(8), 1–13. https://doi.org/10.1061/(asce)st.1943-541x.0001433

Cimellaro, Gian Paolo, Reinhorn, A. M., & Bruneau, M. (2010a). Framework for analytical quantification of disaster resilience. *Engineering Structures*, *32*(11), 3639–3649. https://doi.org/10.1016/j.engstruct.2010.08.008

Cimellaro, Gian Paolo, Reinhorn, A. M., & Bruneau, M. (2010b). Seismic resilience of a hospital system. *Structure and Infrastructure Engineering*, *6*(1–2), 127–144. https://doi.org/10.1080/15732470802663847

Corey, C. M., & Deitch, E. A. (2011). Factors affecting business recovery immediately after Hurricane Katrina. *Journal of Contingencies and Crisis Management*, *19*(3), 169–181. https://doi.org/10.1111/j.1468-5973.2011.00642.x

Cornell, C. A., & Krawinkler, H. (2000). Progress and challenges in seismic performance assessment. *PEER Center News*, *3*(2), 1–4.

Cremen, G., Seville, E., & Baker, J. W. (2020). Modeling post-earthquake business recovery time: An analytical framework. *International Journal of Disaster Risk Reduction*, *42*, 101328. https://doi.org/10.1016/j.ijdrr.2019.101328

Curtis, A., Curtis, J. W., Shook, E., Smith, S., Jefferis, E., Porter, L., … Kerndt, P. R. (2015). Spatial video geonarratives and health: Case studies in post-disaster recovery, crime, mosquito control and tuberculosis in the homeless. *International Journal of Health Geographics*, *14*(1), 22.

Curtis, A., & Fagan, W. F. (2013). Capturing damage assessment with a spatial video: An example of a building and street-scale analysis of tornado-related mortality in Joplin, Missouri, 2011. *Annals of the Association of American Geographers*, *103*(6), 1522–1538.

Curtis, A., & Mills, J. W. (2012). Spatial video data collection in a post-disaster landscape: The Tuscaloosa Tornado of April 27th 2011. *Applied Geography*, *32*(2), 393–400.

Dahlhamer, J. M., & Tierney, K. J. (1996). Winners and losers: predicting business disaster recovery outcomes following the Northridge earthquake.

Dahlhamer, J. M., & Tierney, K. J. (1998). Rebounding from disruptive events: Business

recovery following the northridge earthquake. *Sociological Spectrum*, *18*(2), 121–141. https://doi.org/10.1080/02732173.1998.9982189

Dehghani, N.L., Darestani, Y. M., & Shafieezadeh, A. (2020). Optimal Life-Cycle Resilience Enhancement of Aging Power Distribution Systems: A MINLP-Based Preventive Maintennce Planning. *IEEE Access*, (In Press).

Dehghani, Nariman L, Fereshtehnejad, E., & Shafieezadeh, A. (2020). A Markovian approach to infrastructure life-cycle analysis: Modeling the interplay of hazard effects and recovery. *Earthquake Engineering & Structural Dynamics*.

Der Kiureghian, A. (2005). First- and second-order reliability methods. In E. Nikolaidis, D. M. Ghiocel, & S. Singhal (Eds.), *Engineering design reliability handbook*. Boca Raton, FL: CRC Press.

Didier, M., Broccardo, M., Esposito, S., & Stojadinovic, B. (2018). A compositional demand/supply framework to quantify the resilience of civil infrastructure systems (Re-CoDeS). *Sustainable and Resilient Infrastructure*, *3*(2), 86–102. https://doi.org/10.1080/23789689.2017.1364560

Digest of Education Statistics. (2020). Retrieved from https://nces.ed.gov/programs/digest/d18/tables/dt18_203.10.asp

Durkin, M. E. (1984). *The economic recovery of small businesses after earthquakes: the Coalinga experience*. Vigyan Bhavan (Government House).

Dustin, H. (2010). *Patterns of Post-Disaster Housing Recovery*. Texas A&M University.

Eid, M. S., & El-adaway, I. H. (2017). Integrating the Social Vulnerability of Host Communities and the Objective Functions of Associated Stakeholders during

Disaster Recovery Processes Using Agent-Based Modeling. *Journal of Computing in Civil Engineering*, *31*(5), 04017030. https://doi.org/10.1061/(asce)cp.1943-5487.0000680

Ellingwood, B. R., Cutler, H., Gardoni, P., Peacock, W. G., van de Lindt, J. W., & Wang, N. (2016). The Centerville Virtual Community: a fully integrated decision model of interacting physical and social infrastructure systems. *Sustainable and Resilient Infrastructure*, *1*(3–4), 95–107. https://doi.org/10.1080/23789689.2016.1255000

Esmalian, A., Wang, W., & Mostafavi, A. (2021). Multi-agent Modeling of Hazard-Household-Infrastructure Nexus for Equitable Resilience Assessment. Retrieved from http://arxiv.org/abs/2106.03160

Farokhnia, K. ., van de Lindt, J. W., & Koliou, M. (2020). Selection of Residential Building Design Requirements for Tornado Based Community Functionality Goals. *ASCE Journal of Practice Periodical on Structural Design and Construction*, *25*(1). https://doi.org/10.1061/(ASCE)SC.1943-5576.0000464

Favier, P., Poulos, A., Vásquez, J. A., Aguirre, P., & De La Llera, J. C. (2019). Seismic risk assessment of an emergency department of a Chilean hospital using a patient-oriented performance model. *Earthquake Spectra*, *35*(2), 489–512. https://doi.org/10.1193/103017EQS224M

Fay, L. (2018). Texas Schools Face Long Road to Recovery After Hurricane Harvey. Retrieved June 10, 2020, from https://www.the74million.org/texas-schools-face-long-road-to-recovery-after-hurricane-harvey/

Fugar, F. D. K., & Agyakwah-Baah, A. B. (2010). Delays in building construction projects in Ghana. *Construction Economics and Building*, *10*(1–2), 103–116.

Ganji, H. T., Alembagheri, M., & Khaneghahi, M. H. (2019). Evaluation of seismic reliability of gravity dam-reservoirinhomogeneous foundation coupled system. *Frontiers of Structural and Civil Engineering*, 1–15.

Gardoni, P., Der Kiureghian, A., & Mosalam, K. M. (2002). Probabilistic capacity models and fragility estimates for reinforced concrete columns based on experimental observations. *Journal of Engineering Mechanics*.

Gissing, A., & Blong, R. (2004). Accounting for variability in commercial flood damage estimation. *Australian Geographer*, *35*(2), 209–222.

Han, R., Li, Y., & Van De Lindt, J. (2017). Probabilistic assessment and cost-benefit analysis of nonductile reinforced concrete buildings retrofitted with base isolation: Considering mainshock-aftershock hazards. *ASCE-ASME Journal of Risk and Uncertainty in Engineering Systems, Part A: Civil Engineering*, *3*(4), 1–15. https://doi.org/10.1061/AJRUA6.0000928

Hassan, E. M., & Mahmoud, H. (2020). An integrated socio-technical approach for post-earthquake recovery of interdependent healthcare system. *Reliability Engineering and System Safety*, *201*(March), 106953. https://doi.org/10.1016/j.ress.2020.106953

Hassan, E. M., Mahmoud, H. N., & Ellingwood, B. R. (2020). Resilience of School Systems Following Severe Earthquakes. *Earth's Future*, *8*(10). https://doi.org/10.1029/2020ef001518

Hazus 4.2. (2020). *Hazus Earthquake Model Technical Manual*. Retrieved from

https://www.fema.gov/

Holling, C. S. (1973). RESILIENCE AND S1i\BILI1-'Y .:. 4050 OF ECOLOGICAL SYS1-'EMS. *Annu.Rev.Ecol.Syst.*, *4*, 1–23. https://doi.org/10.1146/annurev.es.04.110173.000245

Kakareko, G., Jung, S., & Vanli, O. A. (2020). Hurricane risk analysis of the residential structures located in Florida. *Sustainable and Resilient Infrastructure*, *5*(6), 395–409.

Kammouh, O., Cimellaro, G. P., & Mahin, S. A. (2018). Downtime estimation and analysis of lifelines after an earthquake. *Engineering Structures*, *173*, 393–403. https://doi.org/10.1016/j.engstruct.2018.06.093

Karatani, Y., & Hayashi, H. (2007). Quantitative evaluation of recovery process in disaster-stricken areas using statistical data. *Journal of Disaster Research*, *2*(6), 453–464.

Kates, R. W., Colten, C. E., Laska, S., & Leatherman, S. P. (2006). Reconstruction of New Orleans after Hurricane Katrina: a research perspective. *Proceedings of the National Academy of Sciences of the United States of America*, *103*(40), 14653–14660. https://doi.org/10.1073/pnas.0605726103

Kazaz, A., Ulubeyli, S., & Tuncbilekli, N. A. (2012). Causes of delays in construction projects in Turkey. *Journal of Civil Engineering and Management*, *18*(3), 426–435.

Khan, M. A. U., & Sayem, M. A. (2013). Understanding recovery of small enterprises from natural disaster. *Environmental Hazards*, *12*(3–4), 218–239.

Khaneghahi, M. H., Alembagheri, M., & Soltani, N. (2019). Reliability and variance-

based sensitivity analysis of arch dams during construction and reservoir impoundment. *Frontiers of Structural and Civil Engineering*, *13*(3), 526–541.

Khanmohammadi, S., Farahmand, H., & Kashani, H. (2018). A system dynamics approach to the seismic resilience enhancement of hospitals. *International Journal of Disaster Risk Reduction*, *31*, 220–233.

Kikitsu, H., & Sarkar, P. P. (2014). Building damage, wind speed estimation, and post disaster recovery in an EF5 Tornado. *Natural Hazards Review*, *16*(2), 4014019.

King, L. J. (1985). Central place theory. *Regional Research Institute, West Virginia University Book Chapters*, 1–52.

Koliou, M., Masoomi, H., & van de Lindt, J. W. (2017). Performance Assessment of Tilt-Up Big-Box Buildings Subjected to Extreme Hazards: Tornadoes and Earthquakes. *Journal of Performance of Constructed Facilities*, *31*(5), 04017060. https://doi.org/10.1061/(asce)cf.1943-5509.0001059

Koliou, M., & van de Lindt, J. W. (2020). Development of Building Restoration Functions for use in Community Recovery Planning to Tornadoes. *ASCE Natural Hazards Review*. https://doi.org/10.1061/(ASCE)NH.1527-6996.0000361

Koliou, M., van de Lindt, J. W., & Filiatrault, A. (2016). Evaluation of an alternative seismic design approach for rigid wall flexible wood roof diaphragm buildings through probabilistic loss estimation and disaggregation. *Engineering Structures*, *127*, 31–39.

Koliou, M., van de Lindt, J. W., McAllister, T. P., Ellingwood, B. R., Dillard, M., & Cutler, H. (2018). State of the research in community resilience: progress and

challenges. *Sustainable and Resilient Infrastructure*, *9689*, 1–21. https://doi.org/10.1080/23789689.2017.1418547

Kroll, C. A., Landis, J. D., Shen, Q., & Stryker, S. (1991). Economic impacts of the Loma Prieta earthquake: a focus on small business.

Kuligowski, E. D., Lombardo, F. T., Phan, L. T., Levitan, M. L., & Jorgensen, D. P. (2014). *Final report, National Institute of Standards and Technology (NIST) technical investigation of the May 22, 2011, tornado in Joplin, Missouri*.

Kurosaki, T. (2010). „Vulnerability of Household Consumption to Natural Disasters in Rural Pakistan".

Li, J., Spencer Jr, B. F., & Elnashai, A. S. (2012). Bayesian updating of fragility functions using hybrid simulation. *Journal of Structural Engineering*, *139*(7), 1160–1171.

Li, Y., & Ellingwood, B. R. (2006). Hurricane damage to residential construction in the US: Importance of uncertainty modeling in risk assessment. *Engineering Structures*, *28*(7), 1009–1018. https://doi.org/10.1016/j.engstruct.2005.11.005

Lin, P., & Wang, N. (2017a). Stochastic post-disaster functionality recovery of community building portfolios I: Modeling. *Structural Safety*, *69*, 106–117. https://doi.org/10.1016/j.strusafe.2017.05.004

Lin, P., & Wang, N. (2017b). Stochastic post-disaster functionality recovery of community building portfolios II: Application. *Structural Safety*, *69*, 106–117. https://doi.org/10.1016/j.strusafe.2017.05.004

Liu, C., Black, W. C., Lawrence, F. C., & Garrison, M. E. B. (2012). Post-disaster

coping and recovery: The role of perceived changes in the retail facilities. *Journal of Business Research, 65*(5), 641–647.

Lounis, Z., & McAllister, T. P. (2016). Risk-Based Decision Making for Sustainable and Resilient Infrastructure Systems. *Journal of Structural Engineering, 142*(9), F4016005. https://doi.org/10.1061/(ASCE)ST.1943-541X.0001545

Mahsuli, M., & Haukaas, T. (2012). Computer program for multi-model reliability and optimization analysis. *Journal of Computing in Civil Engineering*, *27*(1), 87–98.

Mahsuli, M., & Haukaas, T. (2013a). Seismic risk analysis with reliability methods, part I: Models. *Structural Safety*, *42*, 54–62.

Mahsuli, M., & Haukaas, T. (2013b). Seismic risk analysis with reliability methods, part II: Analysis. *Structural Safety*, *42*, 63–74. Retrieved from http://dx.doi.org/10.1016/j.strusafe.2013.01.004

Marshall, M. I., & Schrank, H. L. (2014). Small business disaster recovery: A research framework. *Natural Hazards*, *72*(2), 597–616. https://doi.org/10.1007/s11069-013-1025-z

Masoomi, H., Ameri, M. R., & van de Lindt, J. W. (2018). Wind Performance Enhancement Strategies for Residential Wood-Frame Buildings. *Journal of Performance of Constructed Facilities*, *32*(3), 04018024. https://doi.org/10.1061/(asce)cf.1943-5509.0001172

Masoomi, H., & van de Lindt, J. W. (2016). Tornado fragility and risk assessment of an archetype masonry school building. *Engineering Structures*, *128*, 26–43.

Masoomi, H., & van de Lindt, J. W. (2018a). Fatality and Injury Prediction Model for

Tornadoes. *Natural Hazards Review*, *19*(3), 04018009. https://doi.org/10.1061/(asce)nh.1527-6996.0000295

Masoomi, H., & van de Lindt, J. W. (2018b). Restoration and functionality assessment of a community subjected to tornado hazard. *Structure and Infrastructure Engineering*, *14*(3), 275–291. https://doi.org/10.1080/15732479.2017.1354030

Memari, M., Ameri, M. R., Pilkington, S. F., Mahmoud, H., Attary, N., van de Lindt, J. W., & Masoomi, H. (2018). Minimal Building Fragility Portfolio for Damage Assessment of Communities Subjected to Tornadoes. *Journal of Structural Engineering*, *144*(7), 04018072. https://doi.org/10.1061/(asce)st.1943-541x.0002047

Mills, J. W., Curtis, A., Kennedy, B., Kennedy, S. W., & Edwards, J. D. (2010). Geospatial video for field data collection. *Applied Geography*, *30*(4), 533–547.

Mishra, S., Vanli, O. A., Alduse, B. P., & Jung, S. (2017). Hurricane loss estimation in wood-frame buildings using Bayesian model updating: Assessing uncertainty in fragility and reliability analyses. *Engineering Structures*, *135*, 81–94.

Moehle, J., & Deierlein, G. G. (2004). A framework methodology for performance-based earthquake engineering. In *13th world conference on earthquake engineering* (pp. 3812–3814).

Murphy, R. E. (2017). *The central business district: a study in urban geography*. Routledge.

Najafabadi, E. P., Khaneghahi, M. H., Amiri, H. A., Estekanchi, H. E., & Ozbakkaloglu, T. (2019). Experimental investigation and probabilistic models for residual

mechanical properties of GFRP pultruded profiles exposed to elevated temperatures. *Composite Structures*, *211*, 610–629.

Nasrazadani, H., & Mahsuli, M. (2020). Probabilistic Framework for Evaluating Community Resilience: Integration of Risk Models and Agent-Based Simulation. *Journal of Structural Engineering (United States)*, *146*(11), 1–20. https://doi.org/10.1061/(ASCE)ST.1943-541X.0002810

Nastasi, B. K., Overstreet, S., & Summerville, M. (2011). School-based mental health services in post-disaster contexts: A public health framework. *School Psychology International*, *32*(5), 533–552. https://doi.org/10.1177/0143034311402926

Navrud, S., Tuan, T. H., & Tinh, B. D. (2012). Estimating the welfare loss to households from natural disasters in developing countries: A contingent valuation study of flooding in Vietnam. *Global Health Action*, *5*(1), 0–11. https://doi.org/10.3402/gha.v5i0.17609

Nejat, A., & Damnjanovic, I. (2012). Agent-Based Modeling of Behavioral Housing Recovery Following Disasters. *Computer-Aided Civil and Infrastructure Engineering*, *27*(10), 748–763. https://doi.org/10.1111/j.1467-8667.2012.00787.x

NIST. (2015). *Community Resilience Planning Guide for Buildings and Infrastructure Systems*. Gaithersburg, MD.

NOAA. (2019). U.S. Tornado Climatology. Retrieved February 8, 2019, from https://www.ncdc.noaa.gov/climate-information/extreme-events/us-tornado-climatology

NOAA. (2020). Billion-Dollar Weather and Climate Disasters: Time Series.

Nofal, O. M., & van de Lindt, J. W. (2020). Probabilistic Flood Loss Assessment at the Community Scale: Case Study of 2016 Flooding in Lumberton, North Carolina. *ASCE-ASME Journal of Risk and Uncertainty in Engineering Systems, Part A: Civil Engineering*, *6*(2), 5020001.

Nofal, O., van de Lindt, J. W., & Do, T. Q. (2020). Multi-variate and Single-variable Flood Fragility and Loss Approaches for Wood Frame Buildings. *Reliability Engineering & System Safety*, 106971.

North Carolina Emergency Management. (2017). Hurricane Matthew Resilient Redevelopment Plan: Robeson County. (n.d.). Retrieved from https://files.nc.gov/rebuildnc/documents/matthew/rebuildnc_robeson_plan_combined.pdf

NPR. (2017). Natural Disasters And The Implications Of Missing So Much School.

Odeh, A. M., & Battaineh, H. T. (2002). Causes of construction delay: Traditional contracts. *International Journal of Project Management*, *20*(1), 67–73. https://doi.org/10.1016/S0263-7863(00)00037-5

Orhan, E. (2016). Lessons Learned from Businesses to Ensure Community Level Recovery in a Postdisaster Period: Case from Adapazari, Turkey. *Natural Hazards Review*, *17*(1), 1–12. https://doi.org/10.1061/(ASCE)NH.1527-6996.0000191

Ouyang, M. (2014). Review on modeling and simulation of interdependent critical infrastructure systems. *Reliability Engineering and System Safety*, *121*, 43–60. https://doi.org/10.1016/j.ress.2013.06.040

Ouyang, M., & Dueñas-Osorio, L. (2012). Time-dependent resilience assessment and

improvement of urban infrastructure systems. *Chaos*, *22*(3). https://doi.org/10.1063/1.4737204

Ouyang, M., & Dueñas-Osorio, L. (2014). Multi-dimensional hurricane resilience assessment of electric power systems. *Structural Safety*, *48*, 15–24. https://doi.org/10.1016/j.strusafe.2014.01.001

Panteli, M., & Mancarella, P. (2015). Modeling and Evaluating the Resilience of Critical Electrical Power Infrastructure to Extreme Weather Events Resilience of electric power systems to earthquakes and tsunamis View project DIMMER View project. *Article in IEEE Systems Journal*, *11*(3), 1733–1742. https://doi.org/10.1109/JSYST.2015.2389272

Peacock, W. G., Dash, N., & Zhang, Y. (2007). Sheltering and housing recovery following disaster. In *Handbook of disaster research* (pp. 258–274). Springer.

Pilkington, S. F., Curtis, A., Mahmoud, H. N., van de Lindt, J. W., Smith, S., & Ajayakumar, J. (2019). Documented Recovery Patterns and Conclusions from Video Cataloged Data of the 2011 Joplin Tornado. *ASCE Natural Hazards Review*.

PPD 21. (2013). *Presidential Policy Directive (PPD) 21*. *Critical Infrastructure Security and Resilience (Washington, DC: White House*.

Prevatt, D. O., Coulbourne, W., Graettinger, A. J., Pei, S., Gupta, R., & Grau, D. (2012). Joplin, Missouri, tornado of May 22, 2011: Structural damage survey and case for tornado-resilient building codes. American Society of Civil Engineers.

Quarantelli, E. L. (1982). General and particular observations on sheltering and housing in American disasters. *Disasters*, *6*(4), 277–281.

Ramachandran, V., Long, S. K., Shoberg, T., Corns, S., & Carlo, H. J. (2015). Framework for modeling urban restoration resilience time in the aftermath of an extreme event. *Natural Hazards Review*, *16*(4), 4015005.

RAND. (2006). *Student Displacement in Louisiana After the Hurricanes of 2005*. https://doi.org/10.1080/07448481.1987.9939004

Rasoulkhani, K., & Mostafavi, A. (2018). Resilience as an emergent property of human-infrastructure dynamics: A multi-agent simulation model for characterizing regime shifts and tipping point behaviors in infrastructure systems. *PLoS ONE*, *13*(11), 1–24. https://doi.org/10.1371/journal.pone.0207674

Rasoulkhani, K., Mostafavi, A., Reyes, M. P., & Batouli, M. (2020). Resilience planning in hazards-humans-infrastructure nexus: A multi-agent simulation for exploratory assessment of coastal water supply infrastructure adaptation to sea-level rise. *Environmental Modelling and Software*, *125*(August 2019), 104636. https://doi.org/10.1016/j.envsoft.2020.104636

Rodriguez-Oreggia, E., De La Fuente, A., De La Torre, R., & Moreno, H. A. (2013). Natural disasters, human development and poverty at the municipal level in Mexico. *The Journal of Development Studies*, *49*(3), 442–455.

Rose, A., Benavides, J., Chang, S. E., Szczesniak, P., & Lim, D. (1997). The regional economic impact of an earthquake: Direct and indirect effects of electricity lifeline disruptions. *Journal of Regional Science*, *37*(3), 437–458.

Runyan, R. C. (2006). Small business in the face of crisis. *Journal of Contingencies and Crisis Management*, *14*(1), 12–26. https://doi.org/http://dx.doi.org/10.1111/j.1468-

5973.2006.00477.x

Runyan, R. C., & Huddleston, P. (2006). Getting customers downtown: the role of branding in achieving success for central business districts. *Journal of Product & Brand Management*, *15*(1), 48–61.

Sargent, R. G. (2010). Verification and validation of simulation models. *Proceedings - Winter Simulation Conference*, (January 2011), 166–183. https://doi.org/10.1109/WSC.2010.5679166

Smith, D. J., & Sutter, D. (2013a). Response and recovery after the joplin tornado lessons applied and lessons learned. *Independent Review*, *18*(2), 165–188. https://doi.org/10.2139/ssrn.2261353

Smith, D. J., & Sutter, D. (2013b). Response and Recovery Lessons Applied and Lessons Learned. *Independent Review*, *18*(5), 165–188.

Standohar-Alfano, C. D., & Van De Lindt, J. W. (2015). Empirically based probabilistic tornado hazard analysis of the United States using 1973-2011 data. *Natural Hazards Review*, *16*(1), 1–13. https://doi.org/10.1061/(ASCE)NH.1527-6996.0000138

Stewart, R. (n.d.). Facts and Figures from the Joplin Tornado: What Did It Cost? Retrieved July 6, 2021, from https://www.ksmu.org/post/facts-and-figures-joplin-tornado-what-did-it-cost#stream/0

Sulzberger, A. G. (2011). Joplin Defies Odds, Just by Opening Schools. Retrieved July 6, 2021, from https://www.nytimes.com/2011/08/18/us/18joplin.html

Sun, L., Stojadinovic, B., & Sansavini, G. (2019). Resilience Evaluation Framework for

Integrated Civil Infrastructure-Community Systems under Seismic Hazard. *Journal of Infrastructure Systems*, *25*(2), 1–11. https://doi.org/10.1061/(ASCE)IS.1943-555X.0000492

Sutley, E. J., & Hamideh, S. (2020). Postdisaster Housing Stages: A Markov Chain Approach to Model Sequences and Duration Based on Social Vulnerability. *Risk Analysis*. https://doi.org/10.1111/risa.13576

Tamhidi, A., Kuehn, N., Ghahari, S. F., Rodgers, A. J., Kohler, M. D., Taciroglu, E., & Bozorgnia, Y. (2021). Conditioned Simulation of Ground-Motion Time Series at Uninstrumented Sites Using Gaussian Process Regression. *Bulletin of the Seismological Society of America*.

Tamhidi, A., Kuehn, N., Ghahari, S. F., Taciroglu, E., & Bozorgnia, Y. (2020). Conditioned Simulation of Ground Motion Time Series using Gaussian Process Regression.

The Boston Consulting Group. (2012). The State of Public Education in New Orleans, (June), 1–48. Retrieved from papers3://publication/uuid/45333E3F-7C26-4049-8C61-C55E22EE162F

The Joplin Globe. (2021). Joplin tornado by the numbers. Retrieved from https://www.joplinglobe.com/news/local_news/joplin-tornado-by-the-numbers/article_5bd98ce2-ba68-11eb-bfe1-9fb2325fe9a0.html

Tierney, K. J. (1997a). Business impacts of the Northridge earthquake. *Journal of Contingencies and Crisis Management*, *5*(2), 87–97.

Tierney, K. J. (1997b). Impacts of recent disasters on businesses: the 1993 Midwest

floods and the 1994 Northridge earthquake. *Economic Consequences of Earthquakes: Preparing for the Unexpected*, 189–222.

Tierney, K. J., & Nigg, J. M. (1995). Business vulnerability to disaster-related lifeline disruption.

U.S. Bureau of Labor Statistics. (2021). Table A-14. Unemployed persons by industry and class of worker, not seasonally adjusted. Retrieved January 5, 2021, from https://www.bls.gov/news.release/empsit.t14.htm

U.S. Geological Survey. (2018). National Water Information System: Web Interface (USGS 02134170 LUMBER RIVER AT LUMBERTON, NC). (n.d.). Retrieved from https://nwis.waterdata.usgs.gov/nc/nwis/uv?format=gif_default&site_no=02134170&period=&begin_date=2016-10-01&end_date=2016-10-16

Unnikrishnan, V. U., & van de Lindt, J. W. (2016). Probabilistic framework for performance assessment of electrical power networks to tornadoes. *Sustainable and Resilient Infrastructure*, *1*(3–4), 137–152. https://doi.org/10.1080/23789689.2016.1254998

van de Lindt, J.W., W. G. Peacock, J. Mitrani-Reiser, N. Rosenheim, D. Deniz, M. Dillard, T. Tomiczek, M. Koliou, A. Graettinger, S. Crawford, K. Harrison, A. Barbosa, J. Tobin, J. Helgeson, L. Peek, M. Memari, E. Sutley, D. Gu, S. Cauffman, J. F. (2018). *Community Resilience-Focused Technical Investigation of the 2016 Lumberton, North Carolina Flood: Multi-Disciplinary Approach*. *National Institute of Standards and Technology (NIST SP 1230)*.

Vickery, P. J., Lin, J., Skerlj, P. F., Jr, L. A. T., & Huang, K. (2006). HAZUS-MH Hurricane Model Methodology . I : Hurricane Hazard , Terrain , and Wind Load Modeling, *7*(May), 82–93. https://doi.org/10.1061/(ASCE)1527-6988(2006)7

Vugrin, E. D., Warren, D. E., Ehlen, M. A., & Camphouse, R. C. (2010). A framework for assessing the resilience of infrastructure and economic systems. In *Sustainable and resilient critical infrastructure systems* (pp. 77–116). Springer.

Wang, W. L., & van de Lindt, J. W. (2021). Quantitative modeling of residential building disaster recovery and effects of pre-and post-event policies. *International Journal of Disaster Risk Reduction*, *59*, 102259.

Wang, W., Van De Lindt, J. W., Rosenheim, N., Cutler, H., Hartman, B., Sung Lee, J., & Calderon, D. (2021). Effect of Residential Building Wind Retrofits on Social and Economic Community-Level Resilience Metrics. *Journal of Infrastructure Systems*, *27*(4), 4021034.

Wasileski, G., Rodríguez, H., & Diaz, W. (2011). Business closure and relocation: A comparative analysis of the Loma Prieta earthquake and Hurricane Andrew. *Disasters*, *35*(1), 102–129. https://doi.org/10.1111/j.1467-7717.2010.01195.x

Watson, M. (2019). *The Influence of Disaster Loans on Long-Term Business Survival in Galveston, TX after Hurricane Ike*. Texas A&M University.

Webb, G. R., Tierney, K. J., & Dahlhamer, J. M. (2000). Businesses and disasters: Empirical patterns and unanswered questions. *Natural Hazards Review*, *1*(2), 83–90.

Webb, G. R., Tierney, K. J., & Dahlhamer, J. M. (2002). Predicting long-term business

recovery from disaster: A comparison of the Loma Prieta earthquake and Hurricane Andrew. *Environmental Hazards*, *4*(2–3), 45–58. https://doi.org/10.1016/S1464-2867(03)00005-6

Webb, S. (2018). Harvey One Year Later-Gulf Coast Schools get a lesson in perseverance. Retrieved June 10, 2020, from https://www.houstonchronicle.com/news/houston-weather/hurricaneharvey/article/Gulf-Coast-schools-get-a-lesson-in-perseverance-13169699.php

Winkler, J., Duenas-Osorio, L., Stein, R., & Subramanian, D. (2010). Performance assessment of topologically diverse power systems subjected to hurricane events. *Reliability Engineering & System Safety*, *95*(4), 323–336.

Xiang, X., Dame, N., & Cabaniss, S. (2005). Verification and Validation of Agent-based Scientific Simulation Models, 47–55.

Xiao, Y., & Nilawar, U. (2013). Winners and losers: analysing post-disaster spatial economic demand shift. *Disasters*, *37*(4), 646–668.

Xiao, Y., & Peacock, W. G. (2014). Do hazard mitigation and preparedness reduce physical damage to businesses in disasters? Critical role of business disaster planning. *Natural Hazards Review*, *15*(3), 4014007.

Xiao, Y., & van Zandt, S. (2012). Building Community Resiliency: Spatial Links between Household and Business Post-disaster Return. *Urban Studies*, *49*(11), 2523–2542. https://doi.org/10.1177/0042098011428178

Yazdi-Samadi, M. R., & Mahsuli, M. (2018). Time-Variant Seismic Risk Analysis of

Transportation Networks Considering Economic and Socioeconomic Impacts. *Journal of Earthquake Engineering*, *00*(00), 1–29. https://doi.org/10.1080/13632469.2018.1453401

Zhang, W., Lin, P., Wang, N., Nicholson, C., & Xue, X. (2018). Probabilistic Prediction of Postdisaster Functionality Loss of Community Building Portfolios Considering Utility Disruptions. *Journal of Structural Engineering*, *144*(2001), 1–13. https://doi.org/10.1061/(ASCE)ST.1943-541X.0001984

Zhang, Y., Lindell, M. K., & Prater, C. S. (2004). Modeling and managing the vulnerability of community businesses to Environmental Disasters. *Disasters*, *33*(1), 38–57. https://doi.org/10.1111/j.1467-7717.2008.01061.x

Zhang, Y., Lindell, M. K., & Prater, C. S. (2009). Vulnerability of community businesses to environmental disasters, *33*(1), 38–57.